ABSTRACT

Title of Document: **ONE-AND-TWO-LEVEL NATURAL GAS EQUILIBRIUM MODELS AND ALGORITHMS**

Seksun Moryadee
Civil Systems Program
Department of Civil & Environmental Engineering
University of Maryland, College Park, MD USA

Directed By: **Professor Steven A. Gabriel**
Department of Civil and Environmental Engineering/Applied Mathematics, Statistics, and Scientific Computation Program

This dissertation consists of three parts; Part 1 provides two applied studies for the current issue of the global natural gas market, Part 2 presents the World Gas Model (WGM) 2014 version-a significant extension of WGM 2012, and Part 3 develops a novel Benders decomposition procedure with SOS1 reformulation to solve mathematical programs with equilibrium constraints (MPECs) and then is applied to several applications in natural gas and additional test problems.

Part 1 presents two applied studies related to the impacts of U.S. liquefied natural gas (LNG) exports on global gas markets as well as the influence of the Panama Canal tariff selection on global gas trade. The first study within Part 1 investigates the effect

of the U.S. LNG exports on the global gas markets using the WGM 2012 (Gabriel et. al., 2012), a market equilibrium model for global LNG markets based on a mixed complementarity problem (MCP) format. The second study within Part 1 focuses on the influence of the Panama Canal tariffs on global trade using WGM 2012 as well. After a planned expansion, the Panama Canal waterway will accommodate more than eighty percent of LNG tankers, providing significant potential time and cost savings for LNG buyers and producers. The aim of the second applied study is to address how the Panama Canal tariffs affect global gas trades

In Part 2, a significant extension of the World Gas Model 2012 is developed. This new version called WGM 2014, distinguishes itself from the previous version in the sense of more detail for LNG markets including more market participants e.g., liquefiers, regasifiers, LNG shipping operators, and a canal operator as new players with separate optimization problems and market-clearing conditions. Moreover, the LNG shipping costs and congestion tariffs for canal transit fees are endogenously determined inside the model as opposed to being exogenously determined before. Also, WGM 2014 has flexible LNG routes. In particular, there are three route options for each LNG shipping operator: 1. Sending LNG via the Panama Canal, 2. the Suez Canal, or using a regular route without a canal. Moreover, WGM 2014 takes into account the limitations of maritime transportation by limiting the size of the LNG tankers that can pass through the Panama and Suez canals which itself is a major improvement for natural gas policy study.

In part 3, the method we develop uses an SOS1 approach based on (Siddiqui and Gabriel, 2012) to replace complementarity in the lower-level problem's optimality conditions. Then, Benders algorithm decomposes the MPECs into a master and a subproblem and solves the overall problem iteratively. This methodology is applied to small, illustrative examples and a large-scale MPEC version of the World Gas Model where the Panama Canal operator is a Stackelberg leader with a reduced version of the rest of the global gas markets considered as followers.

ONE-AND-TWO-LEVEL NATURAL GAS EQUILIBRIUM MODELS AND ALGORITHMS.

By

Seksun Moryadee

Dissertation submitted to the Faculty of the Graduate School of the
University of Maryland, College Park, in partial fulfillment
of the requirements for the degree of
Doctor of Philosophy
2015

Advisory Committee:
Professor Steven A. Gabriel, Chair
Professor Lars Olson, Dean's representative
Professor Shapour Azarm
Dr. Andy Kydes
Dr. Jeremy Lin

Acknowledgements

This dissertation, like everything else I've created in my life, wouldn't have been possible without the help and support of the people around me. For that I extend my deepest gratitude and thanks to:

Dr. Steven A. Gabriel, my advisor, for all of his exceptional guidance, support, and inspiration during my academic life at the University of Maryland. He introduced me to the world of energy market modeling and optimization. He also encouraged and gave me opportunities to present our work at conferences and meetings, not only here in the United States but internationally as well. The knowledge and passion I gained from working with him will remain with me always.

The Research Council of Norway and Électricité de France (EDF) for their financial support and interesting research questions. A large part of the work presented in this dissertation was developed as a part of the LinkS project, which was supported by the Norwegian Research Council via the Norwegian University of Science and Technology and SINTEF. Without funding opportunities such as these my work would not have been possible.

My committee members for all of their advice on the work: Dr. Lars J. Olson, for graciously agreeing to serve as the Dean's representative; Dr. Andy Kydes, for his valuable feedback, which significantly improved my research; Dr. Shapour Azarm, for help in developing some key computational aspects; Dr. Jeremy Lin, for his valuable knowledge of energy markets and his agreeing to serve on my committee despite living in southeastern Pennsylvania. I appreciate each of their contributions a lot.

Tritana Supamusdisukul and Warangkana Rusitanonta, my housemates, who have often been a welcome distraction during my qualifying exams and other research stresses. I would also like to thank Kanoon, the dog, who kept me company for thousands of hours, sleeping next to my feet every day as I worked.

All of my fellow research assistants, my colleagues: Andrew Blohm, David Prentiss, Chalida U-Tapao, for their valuable comments, discussions and suggestions on my work.

Importantly, thanks to all my family for their unconditional love, support, and encouragement especially when I could not see the light at the end of the tunnel. Finally, thanks to my father, Phadungsak Moryadee, who has supported me always and given me great advice and guidance whenever I was stuck in work, love, or life.

Table of Contents

List of Tables

List of Figures

Chapter 1: Introduction and Motivation

1.1 Significance of Natural Gas

1.1.1 Overview of Global Gas Markets

Natural gas is a key fuel source for cooking, heating, industrial operations, and power generation. It is composed of methane and other elements and is found in underground rock formations or associated with other hydrocarbon reservoirs. It is produced from either onshore or offshore wells. Natural gas is delivered to the markets by pipelines in gaseous form or transported as liquefied natural gas (LNG) by tankers to destination globally. Natural gas is important to energy sectors due to many reasons. First, it is the cleanest-burning fossil fuel, producing the lowest greenhouse gas emissions as compared to other fossil fuels such as coal or oil. Second, natural gas is considered to be a major input fuel for electricity production. Third, still on the subject of energy, natural gas is used as a backup source for intermittent renewable energy sources e.g., wind and solar. For example, twenty five percent of the total power produced in the U.S. in 2012 came from natural gas (EIA, 2013). Fourth, natural is used as the feedstock for many consumer products such as plastics. Lastly, various countries use natural gas (e.g., compressed natural gas) as an alternative fuel source for transportation, especially in Asia.

Because more countries aim to use environmentally cleaner fuel to meet future economic growth, the global demand for natural gas is expected to expand significantly. According to EIA (2013a) the world natural gas consumption is projected to increase approximately 1.8% per year, see Figure 1-1. In terms of natural gas supply, European domestic production declined by approximately 10% from 2012 to 2011. However, North America and the Middle East increased their production by 1.9% (BP

Statistical Review, 2013). The ramped-up production in North America mostly came from U.S. shale gas climbing up by 29% compared to shale production in 2011 (EIA, 2014). Given advanced drilling techniques, EIA predicts that by 2040 shale gas production is estimated to account for 39% of the total U.S. gas production (EIA, 2013a). Many countries attempt to follow the U.S. shale gas development path. For example, China has recently begun to focus on shale gas as a potential new clean source of gas supply to meet growing demand. The government also announced its national shale gas policy and is targeting shale gas production of 6.5 Bcm by 2015 and 60 Bcm by 2020. The Ukraine is attempting to reduce dependence on Russia by exploring its own shale gas resources and signed a drilling deal with Shell in early 2013. For Europe, The shale exploration in Poland is slowing down after disappointing early attempts at extraction. Although Europe has large unconventional gas reserves, France, Bulgaria, and the Netherlands passed laws banning hydraulic fracturing (hydrofracking) procedures for environmental reasons (Scott, 2013).

The history of gas markets began in the 1960s. Two market models were created (Jensens, 2004). A hub pricing mechanism was developed in the U.S. and UK markets. In particular, natural gas prices are determined by supply and demand of natural gas itself. In contrast, a different pricing model, oil-indexation pricing, was developed in the rest of Europe. Gas prices are linked to the prices of substitute fuels, e.g., oil, to establish long-term supply contracts. Long-term contracts are agreed to ensure adequate amounts of off-take of gas during indicated time periods and to secure supply. In addition, long-term contracts are made to guarantee sufficient payments for large investments in natural gas operations e.g., pipelines, LNG terminals. However, natural

gas trades in Asia are conducted using a combination of these two market mechanisms. Historically, all pipeline-trade volumes of gas transported to Asia use oil indexation pricing while gas-to-gas pricing is used for LNG spot trade (EIA, 2013). Currently, the global gas markets are still divergent with the prices varying in different regions. During the middle of 2012, Henry Hub gas prices dropped to $2 per million British thermal units (MMBtu) – the lowest prices in a decade, while the average import prices in Japan reached $17 per MMBtu. German import and UK prices were between $8-10 per MMBTU (BP Statistical Review, 2013). The North American gas market is expected to remain isolated from other regional markets. This phenomenon is recognized by the gap between Japanese liquefied natural gas (LNG) prices and Henry Hub gas prices which rose from around about $7 per MMBtu in January, 2011 to over $14 per MMBtu in March, 2012.

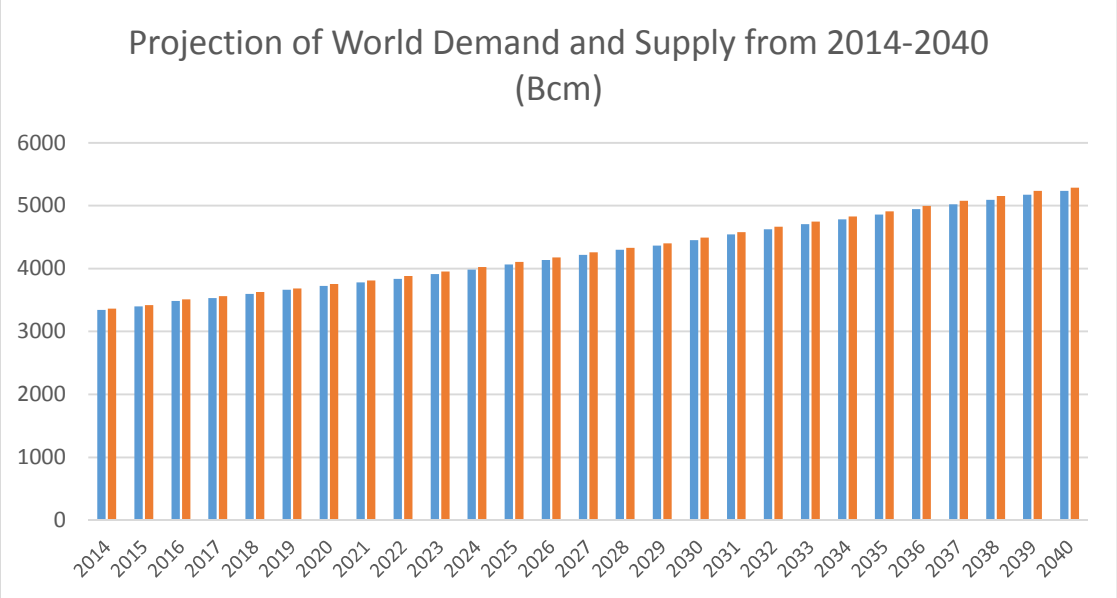

Fig.1-1 Projection of world demand (left) and supply (right) for natural gas 2014-2040 (Bcm) (EIA, 2013a)

1.1.2 The Development of U.S. LNG Exports

The United States became a main natural gas importer in the early 2000s and continued as such until the mid-2000s (EIA, 2012c). A number of regasification facilities were proposed so that domestic consumption never reached the total import capacity (Henderson, 2012). However, as a result of the shale gas revolution, the total natural gas production has gradually increased over time since 2006. Indeed, shale gas production has increased sevenfold from 2007 to 2012 and accounted for 34% of the total U.S. natural gas production in 2012 (EIA, 2014). Shale gas production in the U.S. is projected from 9.7 Tcf/y in 2012 to 19.8 Tcf/y by 2040, constituting 51% of the total U.S. production, see Figure 1-2.

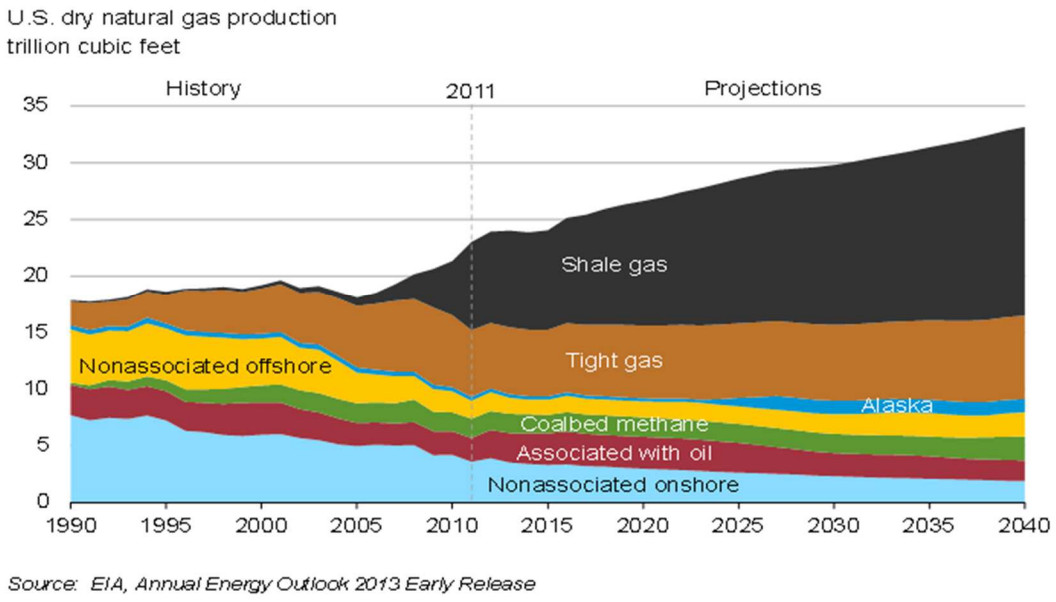

Figure 1-2 U.S. dry natural gas production (tcf) (EIA, 2013a)

The increased domestic shale gas production not only decreased the U.S. imports of natural gas but also has depressed natural gas wholesale prices from $10/MMBtu in

2008 to about $3 MMBtu in 2013. However, the gas prices in Asia and Europe remain the same so that this large price spread creates an arbitrage opportunity to U.S. natural gas exporters. As a result, a number of natural gas producers are eager to apply for natural gas export licenses (Ratner, 2011), as indicated in Table 1-1. However, the future of U.S. LNG exports is being questioned due to uncertain factors e.g., shale gas reserves, negative environmental externalities of hydrofracturing to produce shale gas and the global influence of exports on price and contracts.

Table 1-1 U.S. LNG exports as of March 5, 2014. (DOE, 2013)

	Total of all applications	**Approved**	**Pending**
FTA [1]application	38.50 Bcf/d (377.4Bcm/y)	37.80 Bcf/d (370.3 Bcm/y)	0.7 Bcf/d (7.1 Bcm/y)
Non-FTA application	35.58 Bcf/d (348.5 Bcm/y)	9.7 Bcf/d (95.03 Bcm/y)	25.88 Bcf/d (253.56 Bcm/y)

1.1.3 Problems and Research Questions

Although it is clear that the future of U.S. LNG exports will influence the global gas market over the next decade, the U.S. LNG will be only one element of the emerging global gas market. New supply from Australia, East Africa (e.g., Mozambique and Tanzania), and the Middle East will be supplied to the global market as well. Likewise Russian gas is competing with other suppliers in the European gas market since the Nord Stream and South Stream pipeline projects represent a long-term strategy for the

[1]FTA (Free Trade Area). FTA countries include Australia, Bahrain, Canada, Chile, Colombia, Dominican Republic, El Salvador, Guatemala, Honduras, Jordan, Mexico, Morocco, Nicaragua, Oman, Peru, Republic of Korea and Singapore.

European gas market. Also, future oil prices will also be important since traditional LNG trades are linked with oil indexation.

Despite these factors, U.S. LNG exports have merited special attention from the U.S. as these exports can have both negative and positive effects on the U.S. economy, environment, and employment level. Some experts believe that gas exports will result in a net benefit for the U.S. economy. Opponents argue that free trade in the LNG markets will harm U.S. consumers. Higher U.S. domestic gas prices could reduce a competitive advantage for the manufacturers who use natural gas to produce plastics and chemicals. Furthermore, some people are concerned that exporting LNG would lead to increased hydraulic fracturing activity, or "fracking," thus threatening the health of local residents and increasing water usage and contamination. As debates among various groups continue, the U.S. must ask how LNG exports will affect both the domestic and international markets and possibly the following key questions should be addressed:

- How could U.S. LNG exports affect prices in domestic and global markets?
- Which countries might benefit from U.S. LNG exports and which ones might be disadvantaged?
- How will the U.S. LNG exports compete with other supplies e.g., Qatari and Australian LNG?
- How will the U.S. LNG exports affect Russia given new pipeline projects completed in Europe?

Chapter 2 of this dissertation will investigate the future of global gas markets given an increase of U.S. LNG exports and answer the above questions using the World Gas

Model 2012. To do so, different levels of U.S. LNG exports have to be analyzed. In addition Chapter 2 considers hypotheses about how the various additional assumptions e.g., rapidly growing demands in Asia, competitiveness of LNG and pipeline supplies, future environmental policy, could impact future global gas markets.

1.2. Significance of Panama Canal Expansion on LNG Shipping

1.2.1 Global LNG Trade

Recently, the LNG market has just a few dominant exporters. In fact, one-third of LNG in 2012 was supplied from Qatar, see Figure 1-3. Qatar, Malaysia, Australia, and Nigeria contribute more than 75% of the total supplies. In the near future, more LNG supply is from Australia, the U.S. and East Africa. In fact, by 2016 Australia will become the largest LNG exporter after completion of several LNG terminals while the U.S. is aiming to start exporting LNG by 2016.

Figure 1-3 Overview of LNG market (MTPA) in 2012 and change related to 2011 (IGU,2013)

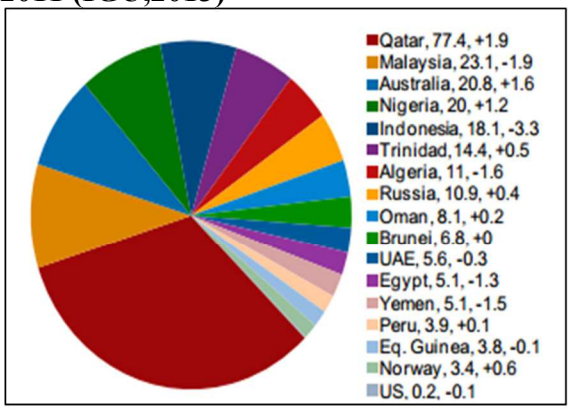

LNG Exports in MTPA by Countries

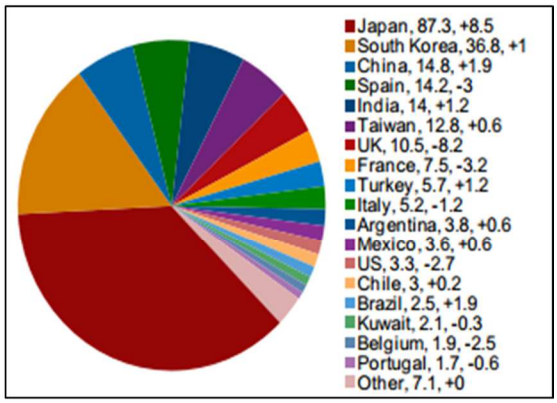

LNG Imports in MTPA by Countries

Asia is the largest LNG market and has the greatest growth prospects (IGU, 2013). Recently, Russia and China agreed on 30-year deal whereby Gazprom will deliver at least 1.3 trillion cubic feet of natural gas to China annually. This deal could potentially

have an impact on the volume of LNG that China needs to import and impact on the level of the spot price for LNG in Asia. However, Europe, South America, and North America are also LNG consumers. Over time, LNG trade has been divided into two basins, the Pacific and Atlantic Basins, and most LNG trade is confined within one basin (GIIGNL, 2013). Atlantic LNG producers such as Norway and Yemen supplied Atlantic consumers with approximately 75% of their LNG in 2012. Likewise, more than 98% of Pacific LNG production was sold to Asian consumers (GIIGNL, 2013). Before the 2010 nuclear disaster in Japan, LNG prices in these two basins were similar. According to the BP Statistical Review (2013), the LNG wholesale price averaged $9.06/MMBtu in Japan in 2009 compared to a German imported gas price of $8.52. Due to the similarity in prices, LNG trade between basins was unprofitable due to high shipping costs and financial disadvantages. The price gap between the basins has increased since mid-2010 due to strong demand in Asia, especially Japan. In 2012, LNG prices were $16.75/MMbtu in Japan but only $9.70 in Europe and $4.73 in the U.S. [2] Therefore, exporting LNG between basins became cost effective depending on the shipping costs.

1.2.2 LNG Shipping Cost

In general, LNG shipping costs involve three main elements: the LNG carrier's capital, the operating cost, and the voyage cost, i.e., marine fuel cost. The capital cost is considered a fixed cost, while the operating and voyage costs are variable. LNG projects require large investments. A new, standard-size LNG tanker (170,000 m^3)

[2] City gate prices: http://www.eia.gov/dnav/ng/ng_pri_sum_dcu_nus_a.htm

costs more than $200 million USD to build because it requires costly materials and sophisticated cargo-handling equipment (Petroleum Economist, 2011). The operating cost includes manning[3], maintenance, and insurance. Because LNG tankers are sophisticated ships, they require specialized crews. As a result, the manning costs are high, accounting for 35% of the operating cost (Petroleum Economist, 2011). The majority of the voyage cost is associated with fuel and port costs. The fuel cost is based on the speed and engine performance, whereas the port costs depend on the destination port; they can be complex and variable depending on the size and volume of the tanker. In addition, the voyage cost also includes transit fees, such as canal tolls. Because the capital cost is fixed, the main variable cost is the voyage cost, which depends on the distance of the trip. The shipping cost from the Atlantic Basin to Japan is three to four times higher than that for the Pacific Basin. However, the Panama Canal route (after canal expansion) will significantly reduce the time and shipping cost of transportation between the two basins.

1.2.3 Panama Canal expansion

The Panama Canal is currently restricted to vessels with beams[4] of less than 32 meters (Platt, 2012). Historically, no LNG tanker has passed the Panama Canal due to special structure of LNG fleets. The expansion of the Panama Canal will allow for the first time, large tankers with a maximum of 50-meter beams to pass, reducing the travel time from the U.S. Gulf Coast to Tokyo, Japan from 41 days to 25 days. Additionally,

[3] Wage costs.
[4] Beam - the greatest width of a nautical vessel.

the expansion will accommodate more than eighty percent of the existing LNG takers to pass through. The distance to transport U.S. LNG from Gulf of Mexico will decrease from 16,000 miles to approximately 9,000 miles.

Because a significant portion of the voyage costs depend on the fuel, which is a function of the distance, the use of the Panama Canal will greatly reduce the voyage costs from the Atlantic Ocean to the Pacific Ocean. IHS CERA (Reuter, 2013) estimated that the route via the Panama Canal will reduce the shipping cost from the Gulf of Mexico to Japan by approximately $1.50/MMBtu. However, at the time of this thesis research, the Panama Canal Authority has not determined what transit fee is it will charge LNG tankers to pass through the canal, so the final toll is unknown. IHS CERA assumed a toll of $0.30/MMBtu based on a $1 million round-trip fee for a medium-sized LNG tanker, which leaves a significant savings of $1.20/MMBtu. Regardless of the toll, the larger canal will likely improve the economics of LNG shipping between the two basins and will create incentives to exploit pricing differences between the Pacific and Atlantic markets. The price difference between the basins might be narrowed and may benefit Asian consumers as well as North American, East Coast suppliers.

1.2.4 Problems, Research Questions, and Modeling

Although using the Panama Canal can save time (approximately 14 days to Japan from the U.S. East Coast) and transportation costs, the canal fee is still uncertain thus motivating the research in Chapter 3 of this dissertation and related project work. Expansion of the Panama Canal expansion brings about several important questions. First, how will the Panama Canal tariffs affect the decision of LNG exporters and LNG shippers? Second, will more U.S. gas go to Asia (assuming it flows) given a shorter

distance or go to Europe? The initial question centers on U.S. exports: a parametric study in Chapter 3 focusing on canal fees and transportation costs for LNG Shipping are performed using the WGM 2012. In this study, the canal tariffs on U.S. LNG exports were varied. The canal tariff was exogenously given for specific LNG routes. Several scenarios were compared against those from a Base Case. The initial research questions related to that study are:

1. How will the Panama Canal expansion affect LNG shipping and trades?
2. What will be the effects of the Canal fee on natural gas prices?
3. How will the natural gas flow pattern change given different tariff regimes?
4. How will the U.S. gas trade affect other producers given the expansion of the Panama Canal?

Moreover, the issue of influence of the Panama Canal is dealt with in two different ways. Chapter 3 applied the existing WGM 2012 in a parametric study related to the Panama Canal tariff selection and its influence on global gas markets. By contrast, Chapter 4 presents the new WGM 2014 where the Canal operator is modeled by a separate optimization problem and interacts with LNG transporters. The advantage of modeling the Canal operator as the separate player is that the model can take into account canal limitations e.g., size of the tankers and congested tariff to endogenously determine tariffs and other key factors.

1.3 Mathematical Programs with Equilibrium Constraints (MPEC)

1.3.1 MPECs Overview

The mixed-complementarity form of the WGM represents the global gas market with all market players at the same level and making their decisions simultaneously. The

WGM allows for market power of the global gas market with Nash-Cournot behavior for the traders, the export arm of the producers. By contrast, in Chapter 5, a Stackelberg leader-follower game version of WGM is formulated with the Canal operator as the leader having an unequal influence on the other market players. The Canal operator anticipates the reactions of these other market participants in making its own decisions, especially the canal tariff. The leader's objective function is a profit maximization with constraints for the canal operator consistent with WGM 2014 but also the KKT conditions of the other market players' optimization problems taken in to consideration. The resulting model is a mathematical programs with equilibrium constraints (MPEC) (Gabriel et al., 2013).

MPECs are challenging problems to solve on a large-scale. In general, in order to find a solution to an MPEC, a two-level optimization needs to be solved. The computational complexity arises mostly from the equilibrium conditions at the lower level imposed as non-closed-form, non-convex constraints in the upper-level problem. These equilibrium conditions can arise from a single optimization problem, more than one, or more generally equilibrium problems such as mixed complemenarity problems (MCP) or variational inequalities (VI) to name a few examples (Facchini and Pang, 2003)

The MPEC formulation is as follows:

$$\begin{aligned} &\min f(x,y) \\ &s.t.\,(x,y) \in \Omega \\ &y \in S(x) \end{aligned} \qquad (1.1)$$

where the continuous variables $x \in R^n, y \in R^m$ are the vector of upper-level and lower-level variables, respectively, $f(x,y)$ is the objective function and Ω is the joint feasible region between theses two sets of the variables. Lastly, $S(x)$ is the solution set of the

lower-level problem parametrically defined as a function of the upper-level variables *x*. The structure of an MPEC expressed as a two-level problem is depicted in Figure 1-4.

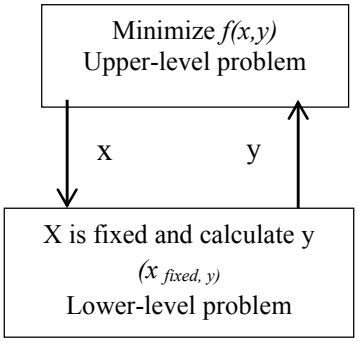

Figure 1-4 the structure of a general two-level problem (MPEC)

MPECs can be solved in a variety of ways such as: by a commercial solver (i.e., NLPEC), piecewise sequential quadratic programming (Kojima and Shindo, 1986), penalty interior point algorithms (Luo et al., 1996), an implicit function-based approach (Outrata et al., 1998), disjunctive-constraints (Fortuny-Amat and McCarl, 1981), and special ordered sets of type 1 (SOS1) variables methods, (Siddiqui and Gabriel, 2012) to name several examples. However, the disjunctive-constraints method is computationally expensive for large models (Luo et. al, 1996) due to the large number of binary variables that are needed to replace the complementarity conditions from the lower-level problem (or problems) while the SOS1 approach requires a good starting point with a heuristic approach for solving a large problem. In addition, other methods, for example, a relaxation scheme (Steffensen and Ulbrich 2010) and exact penalty functions with nonlinear perturbations (Uderzo 2010) also exist but have not been shown to work for large-scale models. Larger problems of MPEC are more difficult to solve (Siddiqui and Gabriel, 2012) due to non-convexity of MPECs. One particular

example of large-scale MPEC can be found in Chen et al. (2006). Chen et al. (2006) found that no single NLP solver could solve their large-scale electricity model, but they needed several solvers, SNOPT and FILTER, to obtain a solution. More details for MPECs will be discussed in Chapter 5. In this dissertation, we propose a new method based on Benders decomposition combined with the SOS1 approach (Siddiqui and Gabriel, 2012) that so far is promising to solve large-scale instances of MPECs. Besides some smaller test problems, we have successfully implemented this new approach on a large-scale natural gas market model.

1.3.2 Benders Decomposition

Benders Decomposition (Benders, 1962) is a classical solution algorithm for optimization problems, based on the ideas of partitioning of the variables into "complicating" and "non-complicating" ones as well as constraint generation. The constraints are generated on the fly to better approximate the optimal value function describing a subproblem when the complicating variables are fixed. In particular, the method partitions the model to be solved into two simpler problems, namely a master and one or more subproblems. The master problem is a relaxed version of the original problem, containing only a subset of the original variables and the associated constraints that approximate the optimal value function mentioned above. The subproblem is the original problem with the variables obtained in the master problem fixed and is therefore a more-constrained version of the original problem. Later, Geoffrion (1972) extended Benders algorithm and proposed a Generalized Benders decomposition (GBD) for a broader class of problems using nonlinear convex duality theory to drive optimality cut generation.

1.3.3 Research Questions and Algorithm Development

The objective in this part of the dissertation is to provide alternative solution procedures for solving MPECs. In particular, a Benders Decomposition approach for MPECs is proposed. The advantage of this method over traditional ones is that the computational time is much lower for larger problems discussed in Chapter 5.

1.4 Contribution of This Dissertation

There are three main contribution of the dissertation:

The first contribution is to provide two insightful policy studies. The first study (Chapter 2) is related to U.S. LNG exports using the existing World Gas Model (WGM 2012 version). The proposed study not only investigated the effects of U.S. LNG exports on the domestic markets but also the European and Asian gas markets as well. Ten scenarios related to U.S. LNG exports are presented in this study. Also, the scenario related to fast growing demands in Asia and the new pipeline project in Europe e.g. Nord Stream, South Stream, and Southern Corridor projects are investigated. These results offer a better understanding for energy system stakeholders, policy makers, decision makers, and government organizations. The second applied study (Chapter 3) also used WGM 2012 to gauge the impact of exogenous Panama Canal tariffs on global gas markets.

A second contribution of this research is the significant extension of the World Gas Model to include much more detail on LNG markets. The novel features of the World Gas Model 2014 (WGM 2014) are:

- The level of detail wherein the LNG transportation routes are incorporated: WGM 2014 has more than one possible route from the origin LNG export terminal to the destination LNG receiving terminal.
- The limitations of maritime transportation e.g., availability of tanker and Canal maximum tanker size allowance are considered.
- The LNG transportation cost is endogenously determined.
- The level of details for LNG shipping e.g., size of LNG tanker, average speed, and investment cost.

The main difference between these two versions are depicted in Table 1-3. This improvement in the model allows analyses of detailed policy implications, e.g., U.S. LNG exports.

Table 1-3. Differences between WGM 2012 and WGM 2014

	WGM 2012	**WGM 2014**
Market players with separate optimization problems	Producers Traders Pipeline operator Storage operator Marketers	Producers Traders Pipeline operator Storage operator Marketers Liquefier Regasifiers LNG shipping operator Canal operators
LNG shipping cost	$8 kcm/1000 nautical miles	Endogenous
Investment for producers	Exogenous	Endogenous
Investment for LNG tanker	No	Yes
Limitation on LNG shipping	No limit	Constraint on LNG Shipping operator

LNG routes	Only1 route origin-destination	Flexible up to 3 routes
Number of variables	~ 60,000 vars	~ 110,000 vars

A third contribution is the development and implementation of a new Benders-type decomposition approach (Benders-SOS1 method) for MPECs on a variety of test problems as well as a large-scale natural gas model as discussed in Chapter 5. This model has the Panama Canal operator as a leader with the rest of the market (using a modified form of the World Gas Model) as followers.

This dissertation is organized as follows. Chapter 2 and 3 deliberate two applied studies for the current issue of the global natural gas market and dedicate the first contribution. Chapter 2 is the policy analyses on the issue of U.S. LNG exports using the World Gas Model 2012. Chapter 3 considers a study on the impact of Panama Canal tariffs on global gas markets using the World Gas Model 2012. Chapter 4 discusses the second contribution and presents the World Gas Model 2014 with the issue of the effects of the Panama Canal capacity level for LNG shipping and LNG exports from the Gulf of Mexico. In Chapter 5, the Benders-SOS1 method for MPECs is presented and solves the MPEC version of WGM where the Panama Canal operator is the leader. Lastly, Chapter 6 provides conclusions and future directions of research.

Chapter 2: Investigating the potential effects of U.S. LNG exports on global natural gas markets

In the mid-2000s a revolution of shale gas production in the U.S. depressed the domestic natural gas prices so that they reach the lowest level in decade, leading to the emergence of U.S. LNG export era. Chapter 2[5] analyzes the effects on both U.S. domestic and global gas markets and presents the results with respect to domestic prices, production, and consumption. In addition, this chapter considers several possible scenarios related to U.S. exports, including the CO_2 reduction policy, increased demands for gas in Asia, and the new European pipeline projects, which are likely to influence global markets in the next decade.

2.1 Introduction

The United States became a large natural gas importer in the early 2000s and continued as such until the mid-2000s (EIA, 2012c). US gas imports have been increasing from 1988 to 2007 (to 4.6 tcf) and then began to decline. Most of US imports were from Canada. Many liquefied natural gas (LNG) import terminals and regasification terminals were built, but the demand never reached the total import capacity (Henderson, 2012). The import of natural gas in the United States began to decline after 2007 (EIA, 2010a) because of the development of unconventional domestic gas, particularly shale gas, of which the United States has abundant resources. According

[5] The analysis and results of this study have been published in S. Moryadee, S.A. Gabriel, H.G. Avetisyan, " Investigating the Potential Effects of U.S. LNG Exports on Global Natural Gas Markets, Energy Strategy Reviews 2(2014) 273-238

to the U.S. Energy Information Agency (EIA) (2011b), 862 trillion cubic feet (Tcf) or equivalently 24,411 billion cubic meters (Bcm) of technically recoverable shale gas resources—or approximately 40 times the annual U.S. consumption in 2010—are distributed throughout the contiguous 48 states. With advanced drilling technology, shale gas production has increased fivefold from 2006 to 2010 and accounted for 23% of the total U.S. natural gas production in 2010 (EIA, 2011a). Shale gas production in the U.S. is projected to reach 12 Tcf/y (339.84 Bcm/y) by 2030, constituting 46% of the total U.S. production (EIA, 2011a). The evolution of shale gas in the U.S. creates export opportunities for natural gas producers when the anticipated domestic production exceeds the domestic consumption requirement (EIA, 2012d).

The emergence of shale gas has shifted the U.S. from a natural gas importer to LNG exporters. U.S. natural gas companies are motivated to export for several reasons. First, natural gas prices in the U.S. are substantially lower than in other natural gas markets. The US natural gas prices peaked in 2008 and then collapsed thereafter due in part to the strong emergence of shale gas. Recently, the prices at Henry Hub were between $3-4 per million British thermal units (MMBtu) in 2012, which is relatively low compared with Asian prices ($15-16/MMBtu) and European prices ($9-11/MMBtu), as indicated in Figure 2-1 (BP Statistics, 2013). Asian natural gas prices continue to increase, particularly the LNG prices, which are among the highest prices in the world (Federal Energy Commission, 2012). Thus, the substantial price differences create arbitrage opportunities for natural gas exporters. As a result, a number of natural gas producers are eager to apply for natural gas export licenses (Ratner, 2011).

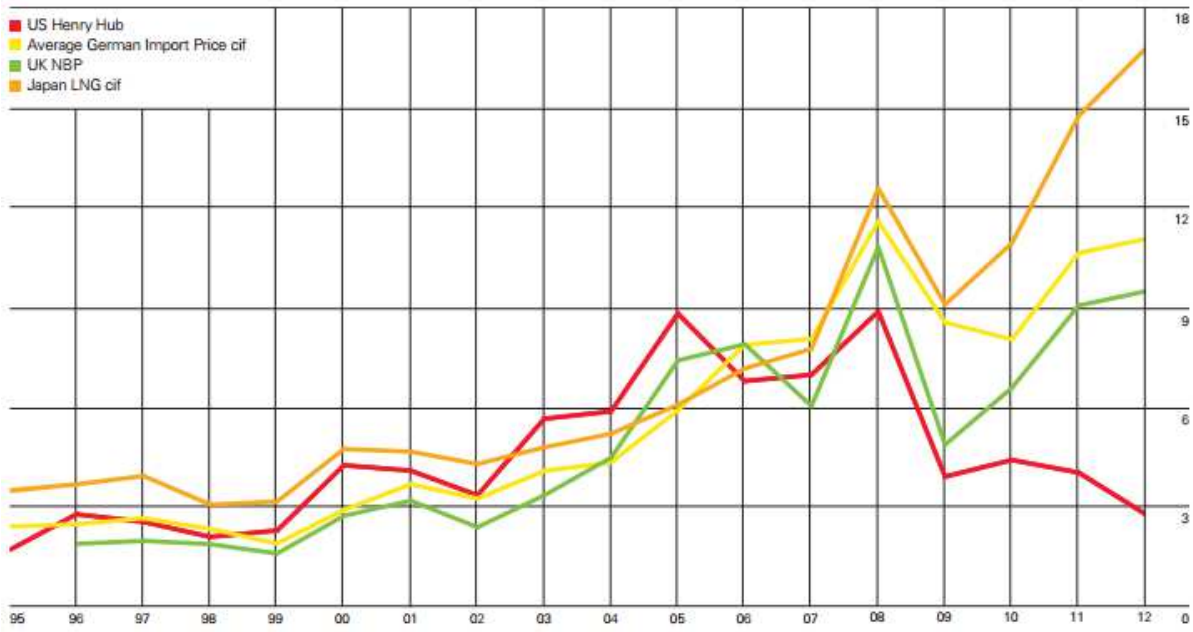

Figure 2-1 Comparison of prices from 1996 to 2012 ($/MMBtu), (BP Statistics, 2013).

Second, because natural gas is considered a key fuel source that exhibits the lowest carbon content among fossil fuels (EIA, 2011d), its demand is rapidly growing, especially in Asia due in part to current or anticipated environmental advantages over other fossil fuels (EIA,2010). Of these markets, Japan is the largest LNG importer. An upswing in LNG imports has been driven by the Fukushima nuclear disaster in 2011 since that country has required additional LNG to compensate for the lost nuclear power, leading to a 12% increase in natural gas consumption between 2010 and 2011 (EIA, 2012a). Likewise, the Chinese government aims to increase the use of natural gas as the country's primary source of energy by 8.3% by 2025 (IEA, 2011). According to forecasts from the China National Petroleum Cooperation (Zhaofang, 2010), the projected Chinese natural gas consumption based on its 12th five-year energy plan will reach 400 Bcm/year by 2030. Furthermore, the Chinese National Petroleum Cooperation has proposed promoting the use of natural gas in at least 200,000 vehicles

for the transportation sector by expanding LNG import terminals (Bai and Aizhu, 2012). Moreover, European natural gas usage is encouraged because of environmental considerations. Also, with the requirement for renewable portfolio standards in Europe, intermittent renewable power such as wind and solar, require natural gas as a thermal backup source since natural gas combined cycle turbines ramp up quickly and allow more flexible grid integration in addition to their environmental benefits. The International Energy Outlook (IEO) (EIA, 2011c) expects an average growth of 0.7% per year for OECD European natural gas consumption and the IEO projects reaching 23.2 Tcf (657 Bcm) in 2035 because of increasing demand in the power sectors of Europe. Although a small rate of demand growth is predicted, Europe will still require more imports because there is a considerable gap between the declining endogenous supply and the demand. Europe currently imports natural gas from five sources: Russia, Norway, Africa, Central Asia and overseas LNG imports. Therefore, U.S. LNG exports from the East Coast and the Gulf of Mexico would provide an alternative for Europe because of the close proximity, reliability, and political considerations.

A third reason for the emergence of the U.S. as an LNG exporter is that in the past many European countries have experienced negative consequences resulting from the Russia-Ukraine gas price disputes in 2006 and 2009 (Pirani et al., 2009). Supply security has led the European Union (EU) to try to mitigate these situations and to assist EU members in diversifying their natural gas suppliers by proposing a number of pipeline projects to deliver more gas to Europe (Ratner et al., 2012). Many rival European pipeline projects are competing with one another. The Southern Corridor project provides an option to import natural gas from the Caspian Sea area. Nord Steam

and South Stream are two underwater pipelines that will supply gas directly from Russia to Europe without requiring transit countries such as Ukraine. The total capacity of these two Russian projects is larger than the current volume of gas flowing through Ukraine into Europe. These projects should increase natural gas flows to Europe, but the market power of Russia over Europe cannot be underestimated. In addition to the aforementioned pipeline projects, numbers of large LNG import terminals are in the process of construction, such as the GATE Terminal in the Netherlands and the Polskie terminal in Poland. The routing of LNG cargoes not only provides flexibility, but also allows for rapid responses to uncertain demands (Hayes, 2006). Proposed LNG projects enable more LNG to be distributed throughout Europe as well as an export opportunity for LNG exporters. Any volumes of LNG exported from the U.S. potentially provide an additional option for European supply diversity to mitigate Russian market power.

Finally, U.S. LNG import facilities can be readily converted into LNG export terminals. Construction costs for LNG terminals have increased greatly due to the high price of steel. It costs approximately $1,000 per ton per annum (tpa) in 2012 as compared to $200 in the early 2000s to build a new liquefaction plant. However, the cost of converting an LNG import terminal to one that can export is approximately half of building a new terminal, at $625 per tpa, as indicated by the Sabine Pass project ($5 billion for a capacity of 8 Mtpa) (the Economist, 2012). There are twelve LNG import terminals in the United States, with a total capacity of 19.1 billion cubic feet per day (Bcfd) (Henderson, 2012). In the recent past, most of these terminals have been used for natural gas imports. After the great increase in shale gas resources, most LNG

import terminals have been redundant because of the rapid growth of the U.S. domestic shale gas production. To maintain their operation, there have been a number of re-export applications filed with the U.S. Department of Energy (DOE). In these cases, natural gas companies can use LNG import terminals to receive LNG cargo from different sources; they will then wait for higher prices and sell back to the LNG spot markets (Ratner, 2011). However, some of the terminals have also been developed to export domestic natural gas to import countries such as Sabine Pass Terminal. As of March 2012, the DOE had approved a total export capacity of 84 Bcm/y, accounting for approximately 15% of the total U.S. consumption in 2011. Seven export terminals will be fully operational by 2018. With this capacity, the U.S. will be the third largest exporter of LNG behind Qatar and Australia.

Although natural gas producers are considering exporting U.S. LNG for a number of reasons and in spite of already approved export licenses, this issue of U.S. LNG exports remains a subject of debate. The topic has gained special attention from Americans, as it has raised concerns regarding the influence of U.S. LNG exports on domestic gas prices and consumers, the U.S. economy, and the environment. Some experts believe that gas exports will result in a net benefit for the U.S. economy. Revenue from LNG exports can contribute to enhancing the U.S. trade balance (The Washington Post, 2012), taxes and royalty fees on natural gas producers increase state and local government revenue, and one LNG project can create 5,000 jobs (Folks, 2012). In addition, LNG exports could create revenue and jobs in upstream natural gas production. In 2010, the Pennsylvania State government received $1.1 billion in state and local tax revenues from Marcellus shale gas development; the project has created

140,000 jobs to date (Considine et al., 2011).

Opponents argue that free trade in the LNG markets will harm U.S. consumers. They claim that U.S. prices will increase as no gap between the global price and the domestic price exists (Olson, 2012). The higher domestic gas prices could reduce the competitive advantage for the manufacturers who use natural gas to produce plastics and chemicals (Dlouhy, A., Jennifer, 2013). Furthermore, some people are concerned that exporting LNG would lead to increased hydraulic fracturing activity, or "fracking," thus threatening the health of local residents and increasing water usage and contamination. Environmental groups would rather retain U.S. natural gas for domestic power generation to reduce carbon pollution in the power sector.

As debates among various groups continue, the U.S. must ask how exports will affect both the domestic and international markets. Several studies have been conducted to examine the influence of U.S. exports on domestic prices. The U.S. Energy Information Administration (EIA, 2012) has considered two different volumes of LNG exports (6 Bcfd and 12 Bcfd) in combination with other assumptions (e.g., shale estimated ultimate recovery (EUR) and economic growth) and found U.S. domestic prices will increase from 9.6% to 32% by 2025 under different assumptions. The Deloitte Center for Energy Solutions (Deloitte Center for Energy Solutions, 2011) assumed 6 Bcfd of LNG export using a dynamic model and calculated a 1.7% increase between 2016 and 2035. Navigant Consulting (Navigant Consulting Inc., 2012) investigated the effects of two export scenarios (3.6 Bcfd and 6.6 Bcfd) from three different export terminals and determined that LNG exports would result in a 6% increase compared to the reference case from 2015 to 2045. However, these studies assessed the domestic price influence

by assuming a particular volume of LNG exports from the U.S. but did not allow for global trade interactions. Medlock (2012) suggested that the impact of U.S. LNG exports should be done in the context of international trade and conducted an analysis using the Rice World Gas Trade Model. This study found that exporting U.S. LNG from the Gulf of Mexico is not profitable when land costs (the total cost of feed gas costs, liquefaction, and transportation) are compared with European and Asian market prices in the long term. Henderson (2012) concluded that the U.S. price, at $5/MMBtu, is no longer profitable in European markets in the short term. However, in Asian markets, U.S. gas prices can go up to $10/MMBtu before they become unprofitable. Although these two studies investigated the influence of U.S. gas exports in the context of international trade, there have been no attempts to numerically analyze the potential effects of U.S. LNG exports on global markets as well as market dynamics.

In contrast to previous studies, this study analyzes the effects on both U.S. domestic and global gas markets and presents the results with respect to domestic prices, production, and consumption. In addition, this study considers several possible scenarios related to U.S. exports, including the CO_2 reduction policy, increased demands for gas in Asia, and the new European pipeline projects, which are likely to influence global markets in the next decade. These results offer a better understanding for policy makers and decision makers.

Section 2.2 presents a discussion of the study methods and model calibration. Section 2.3 provides an overview of the study. Section 2.4 discusses the potential effects of U.S. LNG exports on the domestic and global markets. Section 2.5 analyzes the impact

of U.S. LNG exports on Asian markets. Finally, Section 2.6 summarizes the research and presents a list of recommendations for future work.

2.2 Study methods and model calibration

2.2.1 The World Gas Model

As a tool for studying the global influence of U.S. LNG exports, this study uses the World Gas Model (WGM), developed at the University of Maryland (UMD) with cooperation from DIW Berlin (Gabriel et al., 2012) and was originally based on the works by Gabriel et al. (2005a, 2005b). WGM is a large-scale mixed complementarity model of the global gas markets where agents include natural gas producers, traders, storage operators, an integrated pipeline and system operator, and marketers. The role of each market agent in WGM is summarized as follows:

- Producers supply natural gas to their dedicated traders and the producers are modeled as optimizing their profits subject to engineering bounds on daily and time-horizon production levels;
- Traders also are modeled as maximizing their profits and buy gas from either producers or storage operators during high-demand seasons and selling it to the local market or exporting it internationally via high-pressure pipelines and/or LNG vessels;
- Storage operators optimizing their profits by buying gas in low-demand seasons and selling it back to traders during high-demand seasons taking into account various engineering constraints on storage reservoirs;

- An integrated pipeline and system operator assigns the pipeline capacity to traders and makes decisions regarding the expansion of the pipeline capacity in order to maximize its profit;
- Marketers distribute gas to end users represented by an inverse demand curve.

Collecting the Karush-Kuhn-Tucker (KKT) conditions for all market agent optimization problems along with market-clearing conditions connecting among the players leads to the overall mixed complementarity problem. (Gabriel et al., 2012) provides more details regarding the mathematical formulation of the WGM. In the WGM, traders have a weighted combination of both price-taking and price-making behaviors. On one extreme, they can be price-takers with no market power consistent with perfect competition. Conversely, they can also be Nash-Cournot players who can manipulate market prices along with other traders or some weighted combination of these two extremes. The particular weight is determined by the node (country) in question and the calibration with historical values. Another feature of traders is that they consider long-term LNG contracts as lower-bound constraints in their optimization problems. Lastly, the WGM uses LNG transportation costs, and losses are taken as constant, distance-dependent values in terms of nautical miles. The application here differs from this previous paper by extending the time horizon to 2050 and including environmental considerations and other scenarios as described later in this study.

In the current version, the WGM takes into consideration environmental aspects. The WGM incorporates CO_2e emissions for each major player on the supply side of the

market. In addition, we can impose regional CO_2 prices ($/ton of CO_2e) as a cost on market participants. This new feature is a benefit for conducting CO_2 reduction policy analysis. Although natural gas produces the least carbon dioxide relative to other fossil fuels, the Energy Information Administration (EIA, 1999) stated that one million cubic meters (Mcm) of natural gas emits approximately 2.76 metric tons of carbon dioxide emission equivalent along the natural gas supply chain from the natural gas producers to consumers. The gas industry (INGAA, 2000) assumes that 27% of the carbon dioxide is emitted from the production process, 12% in the processing process, 28% in transmission, 24% from the distributing process, and 9% from storage. The shares of emissions for each market participant based on the proportion of CO_2 emissions are summarized in Table 2-1.

Table 2-1 Carbon dioxide equivalent emitted by market participants in metric tons (Mt) per million cubic meters (Mcm)

Market participants	CO2e (MT/MCM)
Producers	0.105
Traders	1.194
Storage operators	0.017
Transmission and system operators	0.249
Marketers	1.194
Total emissions	2.760

The inclusion of CO_2 emissions values allows for the analysis of carbon policy impacts on the global natural gas industry and measures the magnitude of the influence of policy at the country or regional level. To account for carbon dioxide equivalent emissions, a carbon cost term and adjusting factors are incorporated into the WGM. The carbon costs used in this study are obtained from the Global Change Assessment Model

(GCAM) developed by the Joint Global Change Research Institute (JGCRI); see Clarke et al. (2008) and Calvin et al. (2009). This cooperation between UMD and JGCRI is a part of the project "Linking Global and Regional Energy Strategies" (LinkS) (SINTEF, 2012). The purpose of this project is to analyze the impact of climate policy by linking the global climate model and the energy model. Therefore, the input data from GCAM for the carbon policy analyses includes carbon prices that are generated for each region modeled in the WGM. The carbon cost term was later extended to a newer version of the WGM, in which the effect of carbon costs can be applied to both the supplier side of the market and the consumer side but it was not used in this study; see Avetisyan (2013) for details.

In the current version, the WGM also characterizes three types of producers: conventional gas, shale gas, and non-shale unconventional gas in each region of the U.S. The production capacity is calibrated based on data from the U.S. Department of Energy's Annual Energy Outlook (2010). The U.S. contains a total of 24 natural gas producers, of which seven are shale gas and seven are unconventional. The rest of the U.S. producers are conventional producers. In addition, WGM also distinguishes between two types of natural gas producers in China: conventional gas and shale/coal bed methane producers. Finally, in the version of the WGM used in this study, U.S. shale gas exports to Asia and Europe were allowed different from previous versions of the model. This addition is an important feature that enables the analysis of the current state of the market.

2.2.2 Model calibration

The World Gas Model outcome is calibrated to fit global natural gas market trends in 2010 and incorporates natural gas market projections from multiple sources, such as the EC European Energy and Transport: Trends to 2030 (European Commission, 2008) and Natural Gas Information (IEA, 2007). Moreover, because of concerns regarding the dramatic growth in unconventional gas production in North America, the unconventional production reference from the forecast presented in the Annual Energy Outlook (AEO, 2009) is used. The model outcome for China considers the development of shale gas in China and the rapid growth of China's natural gas demand upon release of China's 12th five-year energy plan in 2011. China's natural gas consumption is specifically calibrated according to the forecast from China's Natural Gas Market Outlook (Zhaofang, 2010), and the work by Henderson (2011) is used as a reference for unconventional Chinese production.

2.3 Overview of the study

The organization of this study is divided into two parts due to different hypothetical U.S. LNG export scenarios and market assumptions that are likely to influence global gas markets in the next decade. The scenarios and assumptions are as follows;

- U.S. LNG export study part I: *"Domestic and Global Impacts"* uses the market assumptions in Section 2.2 and assumes contracts with minimum levels and specific destinations for the U.S. LNG exports to Asia and Europe. Part 1 includes a total of six scenarios discussed in Section 2.4.

- U.S. LNG export study part II: *"Asian LNG Focus"* includes three scenarios and assumes that the U.S. can export globally without restriction to the destinations in question. In addition, to capture strong demand growth in Asia, the WGM incorporates Asian demand projections from 2015-2035 based on the World Energy Outlook, 2011 New Policy Scenario (WEO, 2011) Section 2.5 discusses scenarios and results for Study Part II.

2.4. U.S. LNG export study part I:

2.4.1 Domestic and Global Impacts: scenario description

This section describes the six scenarios that assume a lower bound on the contracted gas volumes for U.S. LNG exports. In the Base Case, the U.S. has export contracts of 21.9 Bcm to Europe and Asia. This amount is minimum where the WGM determines any extra amount. We have defined two increased U.S. LNG export contract levels, 99.7 Bcm (Medium Exports) and123Bcm (High Exports), to examine the effect of increased U.S. LNG exports on domestic markets, as well as global markets. Then the Medium Export scenario is combined with three additional scenarios with alternative assumptions: first, Medium Exports with renewable policies gauges how the climate policy with CO_2 prices might affect natural gas markets. Second, Medium Exports with pipeline projects are used to observe the competition facing U.S. LNG exports and new European pipeline projects. Third, Medium Exports with low U.S. production focuses on how a ten percent reduction in U.S. production may affect the markets. Table 2-2 summarizes the scenarios that we consider in this study.

Table 2-2 Scenarios and description for Domestic and Global Impacts

Scenario Name	Abbreviation	Description
Base	Base	Reference Case: U.S. exports 21.9 Bcm/y from the Sabine Pass terminal to Asia and Europe
Medium Exports	Medium Exports	U.S. exports 99.7 Bcm/y to Asia and Europe
High Exports	High Exports	U.S. exports 123 Bcm/y to Asia and Europe
Medium Exports with Renewable Policy	Medium Exports/Renewable Policy	U.S. exports 99.7 Bcm/y with a Global 20/20/20 policy
Medium Exports with Pipeline Projects	Medium Exports/Pipeline Projects	U.S. exports 99.7 Bcm/y along with the development of the European pipeline projects (Nord Stream, South Stream, and Southern Corridor Projects)
Medium Exports with Low U.S. Production	Medium Exports/ Low U.S. Prod	U.S. exports 99.7 Bcm/y with a 10% decline in production beginning in 2035

2.4.2 U.S. LNG export scenarios

First, we consider the Base Case, which includes U.S. LNG contracts with Cheniere Energy (Cheniere Energy, 2012). The Base Case results are not intended as a forecast of natural gas production, consumption, prices, and other elements but rather as a point of comparison for the analysis. We investigate two LNG export scenarios based on two different volumes of U.S. LNG exports over the 2010-2040 periods. We assume that the U.S. begins exporting natural gas in 2015 based on long-term contracts between Cheniere Energy as shown in Table 2-3.

Table 2-3 Cheniere Energy long term take or pay contracts

	BG Group	Gas Natural Fenosa	GAIL	KOGAS
Annual contract (Bcm/y)	7.87	5.013	5.013	5.013
Annual Revenue	$723 Million	$454 Million	$548 Million	$548 Million
Revenue $/MMBtu	$2.25	$2.49	$3.00	$3.00
Term	20 years	20 years	20 years	20 years

(Source: Cheniere Energy, 2012)

The first scenario, namely Medium Exports, considers the global export of up to 99.7 Bcm/y of LNG. This scenario is based on one third of the total export capacity of the Non-FTA[6] export applications that were filed with the U.S. Department of Energy in August 2013, as indicated in Table 2-4. This fraction is based on an earlier total capacity when the study was initiated. In this analysis, we assume that the U.S. exports from three locations: the East Coast, the West Coast, and the Gulf of Mexico as indicated in Table 2-5. WGM uses port-to-port distances to calculate the transportation costs of LNG shipping. A longer distance increases transportation costs. Hence, we expect the LNG export behavior to involve shipping to closer consumers first, as indicated in Table 2-5. For the second export scenario, (e.g., High Export), we assume that the U.S. has an export capacity of up to 123 Bcm/y.

Table 2-4 Applications received by DOE to export domestically produced U.S. LNG as of August, 2013

[6]FTA with the U.S. requires national treatment for trade in natural gas, including Australia, Bahrain, Canada, Chile, Colombia, Dominican Republic, El Salvador, Guatemala, Honduras, Jordan, Mexico, Morocco, Nicaragua, Oman, Peru, Republic of Korea and Singapore (DOE, 2013).

	Total of all applications	Approved	Pending
FTA application	30.62 Bcf/d (316.51 Bcm/y)	29.93 Bcf/d (309.38 Bcm/y)	0.69 Bcf/d (7.13 Bcm/y)
Non-FTA application	29.21 Bcf/d (301.93 Bcm/y)	5.6 Bcf/d (57.88 Bcm/y)	23.61 Bcf/d (244.0 Bcm/y)

Table 2-5. WGM export terminals

WGM Terminal	Capacity	Actual Terminals	Export to
West Coast terminal	1.2 Bcf/d	Jordan Cove	Asia
East Coast terminal	1.0 Bcf/d	Cove Point	Europe
Gulf Coast terminal	7.3 Bcf/d	Sabine Pass Cameron LNG Free Port Lake Charles	Asia and Europe

In addition to the two considered LNG export volumes, the Medium Exports/LowU.S.Prod scenario represents the analysis of a reduced U.S. production due to a rapidly declining rate of unconventional production. To analyze the potential influence of U.S. LNG exports, we implement long-term contracts as a lower bound in a constraint in the U.S. trader optimization problem in WGM and then observe the dynamic changes in the global and domestic markets between the various scenarios outlined above.

2.4.3 Global 20-20-20 policy scenario

The third scenario (e.g., the Renewable Policy scenario) is the global 20-20-20 policy scenario obtained from JGCRI. The main policy assumptions are based on the EU 20-20-20 (The EU climate and policy package, 2012). The purpose of the EU 20-20-20 policy is to reduce 2020 greenhouse gas emissions by 20% relative to 1990 levels,

improve energy efficiency by 20%, and ensure the use of 20% renewable energy by 2020. The global 20-20-20 scenario from JGCRI differs from EU20-20-20 because it is expanded across the world, and new targets are established every fifteen years, as indicated in (Kalvin et al., 2014). The policy involves developed and developing countries. We assume that the policy is initiated in Europe in 2015. Subsequently, developed countries participate in 2030, and developing countries enter in 2045. However, there is no policy commitment for the least developed countries. Details regarding each target are provided in (Kalvin et al., 2014).

For the policy to be successful, regional CO_2 prices ($/ton of CO_2e) obtained from (Kalvin et al., 2014) appear in the natural gas supply chain. The higher costs are likely to force producers in the developing and developed countries to reduce their production, whereas lower-cost producers (e.g., producers in the least developed countries) will have production incentives. The countries that do not participate in the policy (e.g., Nigeria and Qatar) will increase their output and export levels. To determine impacts on U.S. LNG exports, we combine the Medium Export scenario (99.7 Bcm/y) and the global 20-20-20 policy to address the hypothesis pertaining to how a climate policy involving additional CO_2 cost will influence the natural gas market. It is important to note that the WGM only endogenously considers the natural gas markets across the world. Thus, the effects of increased carbon taxes from such a global 20-20-20 policy will only be reflected by spatially heterogeneous CO2 prices. However, these prices as determined by the integrated assessment model GCAM do in fact reflect many other sectors beyond gas.

2.4.4 European pipeline projects

In this scenario, we investigate the competition between U.S. LNG exports and selected pipeline projects that involve Europe and/or Russia. As shown in Table 6, the Nord Stream, South Stream, and Southern Corridor Projects have been incorporated into the WGM. The WGM allows new pipelines to be built and expanded as a function of the pipeline operator's investment decision in an endogenous manner. We set the maximum expansion per year according to the expected capacity as indicated in Table 2-6. Initially, the pipelines potentially have the capacities described in Table 2-6. However, the expected capacity or expansion will be determined through the pipeline operator's optimization problem. The pipeline operator considers expanding a particular pipeline endogenously if it is profitable. Some pipelines can be expanded every time period, but others may not be expanded at all if the pipeline operator finds that the expansion cost is higher than the anticipated benefits. The WGM considers the cost of pipeline expansion in terms of the length and type (on-shore or off-shore) of pipeline and distinguishes an initial cost for new construction and expansion. In this analysis, we largely focus on how new pipelines and increased LNG exports affect the markets, especially the flows from Russian pipelines into Europe, and observe future pipeline investments.

Table 2-6 European pipeline projects

Project	Connection	Capacity (Bcm/y)	Project Timeline, Starting Year Capacity (Bcm)
Nord Stream	Russia-Germany	55	2011 (27.5 Bcm) 2012 (55 Bcm)
South Stream	Russian-Bulgaria	63	2015 (15.5 Bcm) 2019 (63 Bcm)

Southern Corridor	Part 1: Turkey-Azerbaijan	16	2018 (16 Bcm)
	Part 2: Turkey-Romania	10	2018 (10 Bcm)

Sources: (Nord Stream, 2012), (South Stream, 2012), and (Berdikeeva, 2012)

2.4.5 Results and analysis of part I (Domestic and Global Impacts, scenarios 1-6)

2.4.5.1 Base case

To describe the Base Case, the projected regional production and consumption for 2020 are presented in Figure 2-2.The outcome presents the development of production and consumption in 2020. Remarkably, large differences can be observed between the production and consumption of Europe (350.9 Bcm) and China[7] (140.1 Bcm). The Middle East, the Former Soviet Union, and Africa are the main suppliers to Europe, Asia, and China. Production and consumption are nearly balanced in North America and South America.

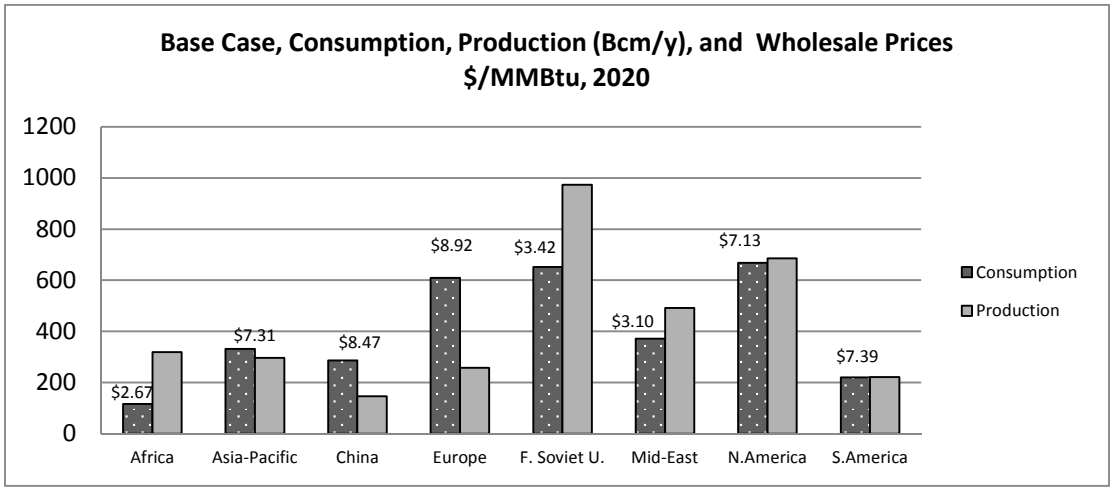

[7]In the current version of WGM we separated China from Asia Pacific because model output for China was recalibrated to specific sources. Also, we pay attention to the development of shale gas in China as well as the magnitude of increased demand due to new energy policies.

Figure 2-2 WGM production, consumption (Bcm/y), and wholesale prices ($/MMBtu)

In terms of regional price results[8], Figure 2-2 shows that in 2020, Europe and China will be in the highest range at $8.40-$8.90. N. America, S. America, and Asia-Pacific constitute the middle range at $7-$7.40. The producing regions, the Former Soviet Union, Africa, and the Middle East, represent the lowest range at $2.50-$3.50. Although the WGM accounts for the growth of unconventional production in North America, the price remains high because of a presumed increase in consumption for the Base Case in 2020.

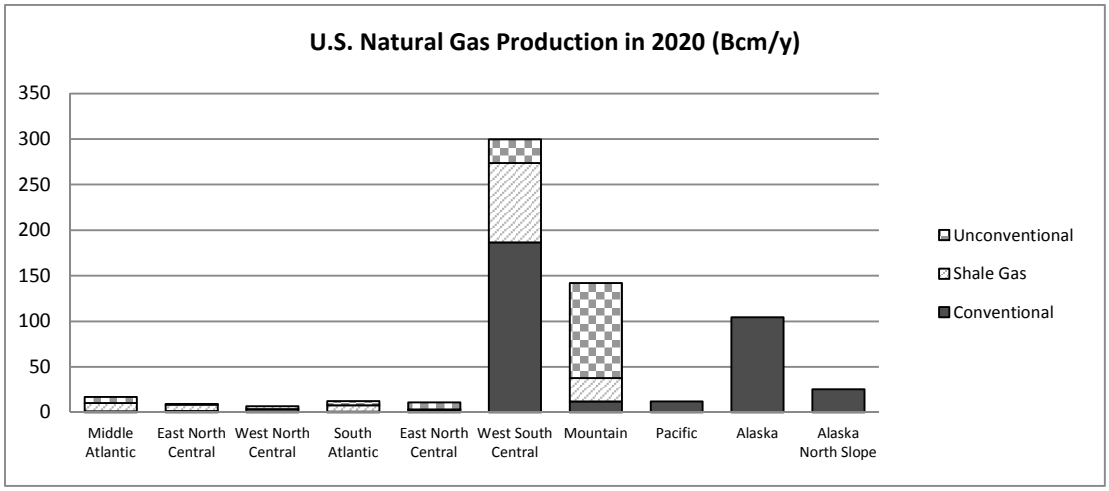

Figure 2-3 WGM Base Case, U.S. Natural Gas Production, Bcm

Figure 2-3 suggests that in 2020, the U.S. will produce a total of 640 Bcm, including 139.8 Bcm from shale gas production. In Figure 2-3, shale gas will account for 20%

[8]In terms of country prices, Japan is projected to have the highest estimated wholesale prices ($10.12) in 2020 for country level. Japan is included in the Asia-Pacific region.

of total production with the Barnett and Haynesville shale basins, located in the West South Central part of the country contributing approximately 60% of the total shale gas production (87.2 Bcm).

2.4.5.2 Domestic effects of U.S. LNG exports

To understand the influence of U.S. LNG exports on the domestic market, we investigate the hypothesis that these exports could affect the domestic markets. Each of the possible export volumes is compared with the Base Case and with one another to gauge the magnitude of exports' influence. Figure 2-4 shows the projected average U.S. price comparison from 2020 to 2040. The increased level of U.S. LNG exports will cause price increases of $0.70-$1 MMBtu in the Medium Exports and $1.03-$1.53 MMBtu in the High Exports from 2020 to 2040. The average price increase as a percentage over the time horizon is 8.4% under the Medium Exports and 10.9% under the High Exports.

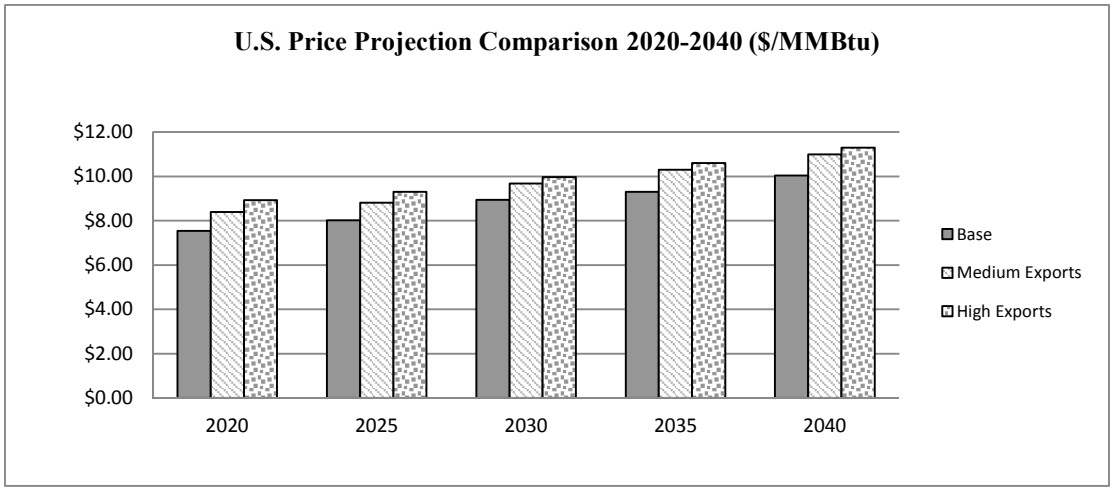

Figure 2-4 WGM Projected U.S. Natural Gas Prices from 2015 to 2040 in $/MMBtu

The maximum price effect is $1 for the Medium Exports and $1.30 for the High Exports. An explanation is that the U.S. is committed to exporting gas to Europe and Asia; thus, the total quantity produced becomes the domestic consumption plus the quantity exported and leads to increased domestic production levels. This change induces an increase in the logarithmic term in the Golombeck production cost function (Golombeck et al., 1995, 1998) used in the WGM, which reflects increasing marginal costs of production. Thus, less gas is available for domestic markets without higher prices. The Golombeck production cost function characterizes the nature of natural gas production because higher costs are expected when production is close to capacity.

In terms of U.S. natural gas production, commitment to LNG exports results in increased production in the U.S., especially in shale gas, because of the anticipation of domestic consumption and long-term contract requirements. Figure 2-5 shows that the total U.S. production increases considerably by 3.8% under the Medium Exports and 5.9% under the High Exports in 2020, and this effect appears to be more pronounced in 2040, with 4.5% growth under the Medium Exports and approximately a 7.3% increase under the High Exports (see Figure 2-6).

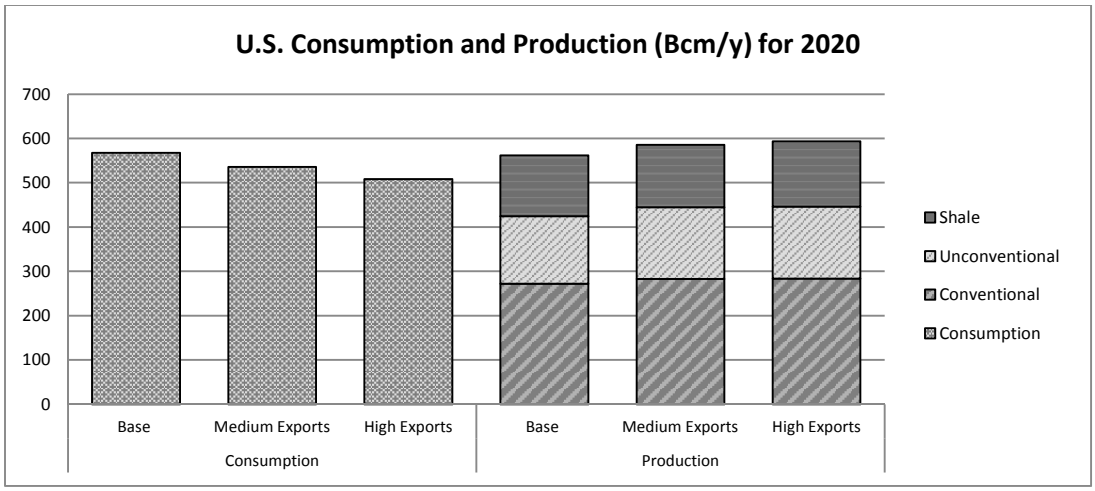

Figure 2-5 U.S. Production and Consumption (Bcm/y) for 2020

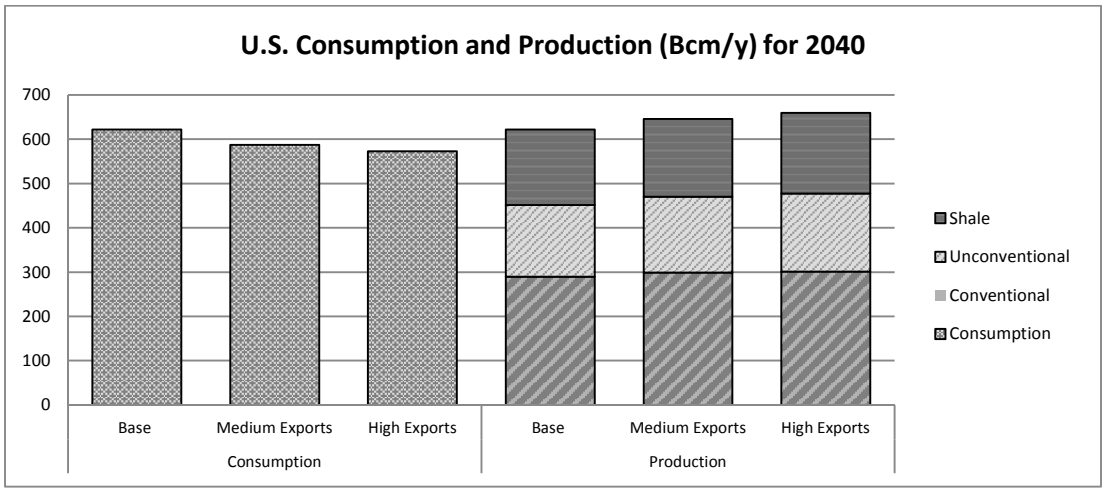

Figure 2-6 U.S. Production and Consumption (Bcm/y) for 2040

Next, we closely examine U.S. production in details. Shale gas production plays a key role to satisfy future natural gas demands even without increased LNG exports. Under the Base Case, shale gas production in 2040 will increase by approximately 24.9% relative to the 2020 level, and conventional production will increase by 6.2%. In 2040, shale gas production is projected to be higher in the Medium and High Exports (approximately 3-3.5% and 6.4-7.7%, respectively) compared with the Base Case.

Although we see only small percent increases in domestic production, the total production still satisfies domestic consumption and export requirements. This is how a new equilibrium, where demand and supply are met, is adjusted by small increases in production and diminishing demands due to higher prices.

The introduction of U.S. LNG exports will lead to reduced domestic consumption, presumably because of higher natural gas prices under two increased export scenarios. In 2020, U.S. consumption declines by 5.5% under the Medium Exports and by 7.9% under the High Exports relative to the Base Case, as indicated in Figure 2-6. Under the High Exports, the U.S. experiences the greatest effect of exporting LNG as domestic consumption declines nearly 60 Bcm in 2020 and approximately 50 Bcm by 2040. The difference in consumption between the export scenarios and the Base Case are smaller in subsequent years. Thus, the results may suggest that the long-term influence on consumption will recover if the supply is sufficiently elastic to respond to an increase in total production.

To determine the influence on increased export policies, we must observe the welfare changes from the market participants, namely the producers and consumers, to ascertain the extent to which they are affected. Since exporting LNG results in higher domestic prices, we compared a consumer surplus in the export scenario with the Base Case to examine the effect of increased prices on the domestic consumer. As indicated in Table 2-7, the increasing loss resulting from consumer surplus reaches 10.23% under the Medium Exports and 18.63% under the High Exports in 2020. However, the

difference in 2020 will be smaller in 2040 as it is only 6.81% under the Medium Exports and 11.21% under the High Exports.

Table 2-7 U.S. welfare in billions $ and percent difference

Welfare	Year	Billion $			Difference from Base Case	
		Base	Medium Exports	High Exports	Medium Exports	High Exports
Consumer Surplus	2020	182.003	163.383	148.102	-10.23%	-18.63%
	2040	301.502	280.959	267.704	-6.81%	-11.21%
Producer Surplus	2020	51.804	70.570	87.206	36.23%	68.34%
	2040	86.081	106.980	124.176	24.28%	44.25%
Social Welfare	2020	233.807	233.953	235.308	0.06%	0.64%
	2040	387.583	387.939	391.880	0.09%	1.11%

In contrast, because of an increase in export volume and higher domestic prices, the producer surplus will increase by approximately 36.23% under the Medium Exports and 68.34% under the High Exports in 2020 but will decrease in 2040. An increase in prices reduces the consumer surplus but increases the producer surplus. As a result, export policies increase social welfare by approximately 0.09% under the Medium Exports and 1.11% under the High Exports in 2040. Medium and High Exports have a positive influence on the economy in term of social welfare measurement, but the increase is relatively small.

Overall, the WGM results indicate that increased natural gas exports will lead to increased domestic natural gas production, higher domestic gas prices, and reduced domestic natural gas consumption. We may conclude that the major domestic effects are as follows:

- 99.7 Bcm in exports will lead to a $0.84-$1/MMBtu increase in domestic prices, a 23-33 Bcm decrease in consumption, and an 18-30 Bcm/y increase in production levels between 2020 and 2040
- Exporting 123 Bcm will lead to a $1.03-1.53/MMBtu increase in domestic prices, a 38-59 Bcm decrease in consumption, and a 31-50 Bcm/y increase in production levels between 2020 and 2040
- Only small social welfare increases in the U.S. economy will be observed

2.4.5.3 Global influence of U.S. LNG exports

This section analyzes the global effects of U.S. LNG exports. Table 2-8 depicts the WGM results for production of natural gas around the world by region for 2020 and 2040.

Table 2-8 Regional production for 2020 and 2040 (Bcm/y)

Regions	Year					
	2020			2040		
	Base	Medium Exports	High Exports	Base	Medium Exports	High Exports

Africa	319	314.7	312.7	432.5	427.2	426.3
Asia-Pacific	297	295	292.3	312.7	311.4	310.9
China	146.7	146.7	146.7	176.4	176.4	176.4
Europe	258.4	255.4	251.8	224.4	223.8	222.2
F. Soviet U.	973.2	962.2	955.2	1121.6	1117.2	1114
Mid-East	491.7	486	483.6	737.4	727.5	723.5
N.America[9]	686.1	711.9	724.7	754.3	780.5	795.1
S.America	221.7	222.1	222.1	315	314.8	315.3

It is important to note that N. America's production increases considerably under the export scenarios (especially the High Exports) compared with the Base Case. The difference between the Base Case and High Exports for N. American production will be approximately 38.6 Bcm/y in 2020 and 40.8 Bcm in 2040 as a result of the dramatic increase in U.S. LNG exports. Additionally, the production for the rest of the world is slightly affected by the increasing U.S. export volume. Due to an introduction of U.S. LNG, producing regions, such as Africa, the Middle East, and the Former Soviet Union, exhibit decreases in production of approximately 1.9%, 1.6%, and 1.8%, respectively, in 2020. In 2040, the production trends are similar to those for 2020, with little change relative to the Base Case. A significantly smaller effect on production is observed in 2040 relative to that in 2020. For example, the Former Soviet Union will reduce production by approximately 18 Bcm/y in 2020 but only by 7.6 Bcm/y in 2040 under High Exports. In terms of the global effect on

[9] The N. America node includes the United State of America, Canada, and Mexico.

consumption, Figure 2-7 and 2-8 present the selected region consumption by sources for 2020 and 2040.

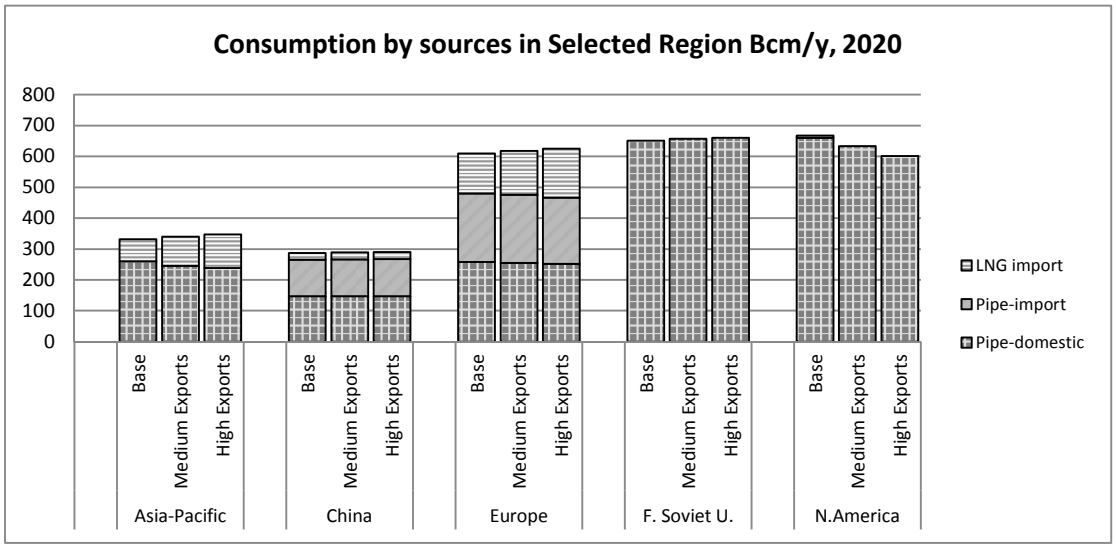

Figure 2-7 Regional consumption by sources (Bcm/y) for 2020

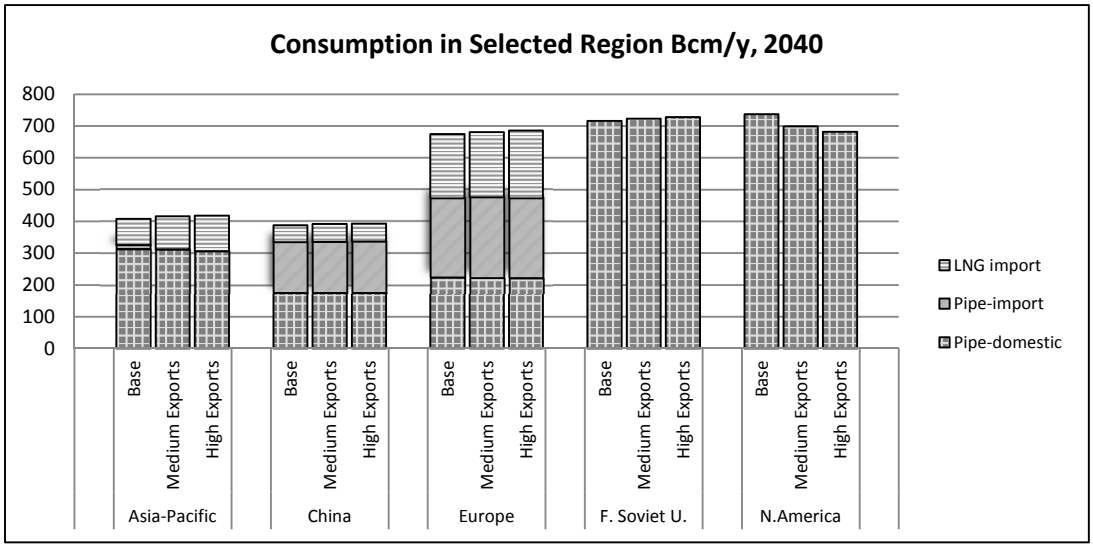

Figure 2-8 Regional consumption by sources (Bcm/y) for 2040

The most remarkable outcome is that N. American consumption declines by 4.2% in the Medium Exports and 8.9% in the High Exports as compared with the Base Case in

2020, presumably because of the decreased availability of inexpensive gas for domestic consumption as a result of increased exports. However, Asia-Pacific, Europe, and China exhibit a slight 2%-4% increase in consumption as a result of increased flows from U.S. LNG exports. Likewise, the domestic consumption in producing regions such as the Former Soviet Union exhibits slight increases although the U.S. does not export LNG to the producing regions. An explanation is that this phenomenon is a side effect of U.S. LNG exports because the U.S. displaces market shares from prominent suppliers in Asia and Europe. Thus, there is more inexpensive gas available for domestic consumption for the Former Soviet Union. Under the High Exports, in 2020, LNG imports increase significantly, by 50% for Asia and 23% for Europe, with reduced domestic flows and imports from pipelines, as indicated in Figure 2-7. In 2040, similar patterns of consumption are recapitulated in most regions, but China is less affected than in 2020 as shown in Figure 2-8. Total Chinese consumption reaches approximately 400 Bcm with increased pipeline imports. As a consequence of increased U.S. LNG exports, the consumption in importing regions exhibits a slight increase, and LNG simultaneously displaces gas importation from pipelines and domestic flows.

Table 2-9 Regional wholesale prices for 2020 and 2040 ($/MMBtu)

Regions	Year					
	2020			2040		
	Base	Medium Exports	High Exports	Base	Medium Exports	High Exports
Africa	$2.67	$2.56	$2.53	$3.56	$3.48	$3.47

Asia-Pacific	$7.31	$6.99	$6.70	$10.03	$9.72	$9.60
China	$8.47	$8.41	$8.37	$10.89	$10.77	$10.73
Europe	$8.92	$8.68	$8.46	$11.88	$11.66	$11.48
F. Soviet U.	$3.42	$3.36	$3.33	$5.36	$5.27	$5.22
Mid-East	$3.10	$3.05	$3.03	$4.28	$4.20	$4.17
N.America	$7.13	$8.03	$8.84	$9.39	$10.57	$11.10
S.America	$7.39	$7.64	$7.68	$8.81	$8.82	$8.88

Table 2-9 shows that the presence of increased U.S. LNG exports will lead to lower prices relative to the Base Case, particularly in Asia-Pacific and Europe. In 2020, Asia-Pacific wholesale prices are expected to be $0.33 and $0.61 less expensive under Medium Exports and High Exports, respectively. Likewise, using the same comparison, European wholesale prices are $0.24 and $0.46 lower than the Base Case. This effect will be less pronounced in 2040. The smaller price gap in later years reflects the elasticity of the supply in the long term. Because Asia-Pacific requires more supply to meet growing domestic consumption, production is adjusted by increasing production capacity in later years to form a new equilibrium. We can see this because under the High Exports scenario, Asia-Pacific prices as compared with the Base Case will decrease by 8.3 % in 2020, but only by 4.2 % in 2040. Nevertheless, the prices will increase greatly for North America. We see this because Table 2-9 shows higher prices relative to the Base Case for North America in 2020 (12.7% higher in the Medium Exports and 23% under the High Exports), and the same situation will repeat in 2040.

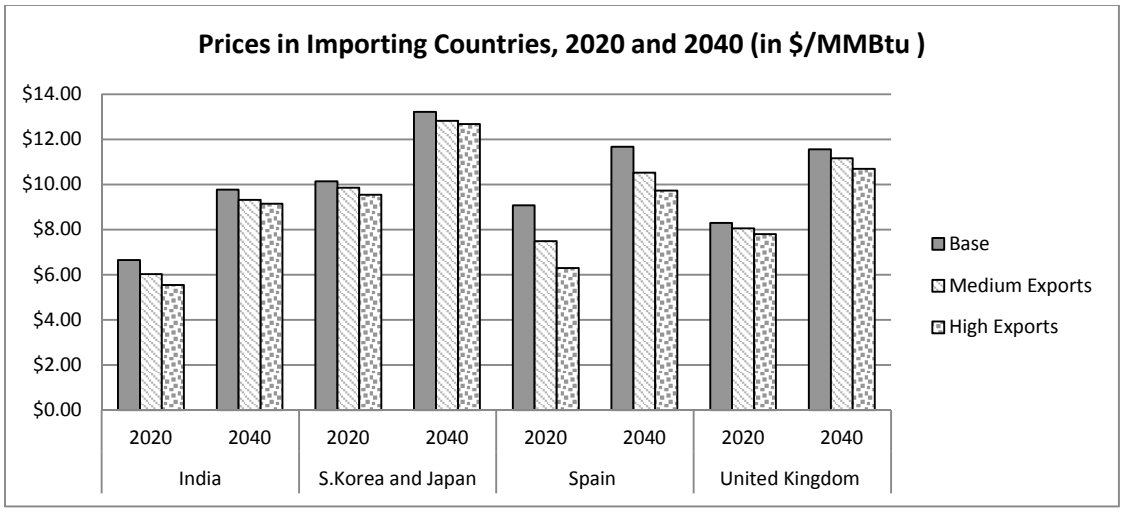

Figure 2-9 Prices in importing countries for 2020 and 2040 ($/MMBtu)

More precisely, Figure 2-9 allows us to investigate the importing countries in greater detail. Prices in the Medium and High Exports are lower than in the Base Case in both 2020 and 2040. Among the importing countries, Spain exhibits the largest differential for both export scenarios because in the WGM, Spain has almost no natural gas production and relies on imports nearly one hundred percent. With the presence of U.S. LNG, inexpensive gas from the U.S. displaces some of the prominent suppliers and diminishes prices. Although in this analysis, the U.S. supplies gas to only four countries, the pipeline system in the WGM allows gas from the receiving countries to be distributed to other countries. Hence, these four countries can transport gas to other countries in the region.

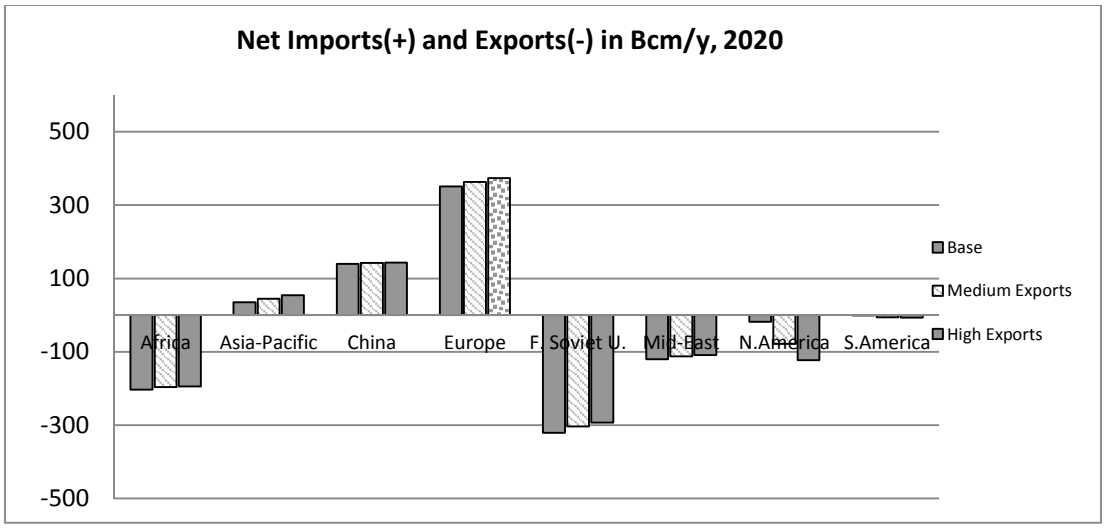

Figure 2-10 Imports (+) and exports (-) in Bcm/y, 2020

Figure 2-10 presents the trades in 2020. Exports from N. America substantially increase by 60.18 Bcm in the Medium Exports and 105.09 Bcm in the High Exports. Under the High Exports, Asian and European imports increase by 3% and 4.5%respectively as compared with the Base Case. However, the producing regions, namely, Africa, the F. Soviet U., and the Middle East, reduce their exports due to U.S.LNG exports. In 2020, Russia has the greatest effect on trade and exhibits the highest decrease (nearly 8.4 %) under the High Exports.

The effects on producer profits follow the natural gas trades discussed above. Figure 2-11 reveals that N. American producers generate 29.5% (45.9%) more profit in the Medium Exports (High Exports) than in the Base Case in 2040, but the profits for the remainder of the world are slightly lower (1-2% and 2-3% in the Medium and High Exports, respectively), likely because of an increase in U.S. LNG exports. The S. American profits are minimally affected by U.S. exports.

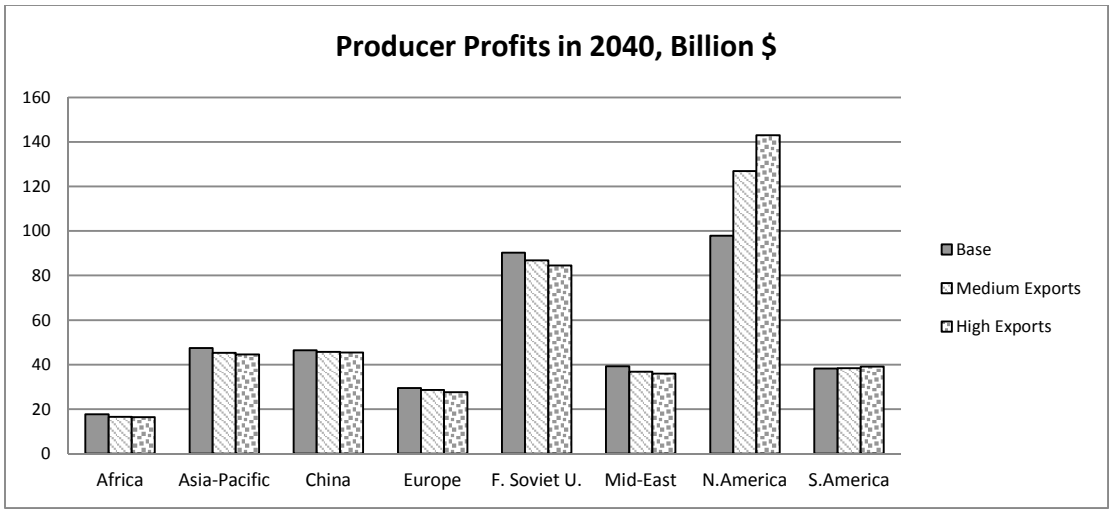

Figure 2-11 Producer profits in billions, 2040

We can conclude that a decrease in producer profits largely occurs in unbalanced trade regions[10], importing regions and exporting regions. This result occurs because inexpensive U.S. LNG replaces market shares from both domestic and international suppliers and results in losses for existing suppliers compared with the Base Case.

2.4.5.4 Other scenarios

In this section, we consider the significance of European pipeline projects, a sensitivity analysis scenario, and renewable policy to assess questions such as the following. How would lower U.S. production influence domestic and global prices if the U.S. is committed to supplying LNG globally under long-term contracts? What is the result of competition between European pipeline projects and U.S. gas exports? Finally, how will climate policy change the magnitude of the markets? Additional scenarios are compared with the Base Case and the Medium Exports to investigate the hypothesis that U.S. LNG exports and markets are affected by climate policy, the uncertainty

[10] An unbalanced trade region is one in which supply and demand are considerably different.

surrounding unconventional gas production, and the introduction of new pipeline projects that will bring more natural gas to Europe.

In the Medium Exports/Low U.S. Prod, we assume a decline in U.S. production to a level 10% lower than that of the Base Case in 2035 and 2040. This decreasing production is characterized by a higher rate of decline in shale gas production and possibly limited resources for other natural gas types by future regulations and energy policies. In particular, extraction from shale gas resources is depicted as decreasing rapidly in the long term as stated in (Cohen, 2009). Hence, the U.S. may confront shortfalls in maintaining the production that is necessary to meet growing domestic demands and LNG export commitments. The results are shown in Figure 2-12 to 2-17. Figure 2-12 indicates that with declining U.S. production in 2040, prices increase by $0.50 domestically and $2.16 for N. American prices (see Figure 2-13).

Moreover, N. American consumption decreases by 9.5%, as shown in Figure 2-14. Prices in Europe and Asia remain lower than the prices in the Base Case (Figure 2-13). Africa gains benefits from decreased U.S. production by increasing production (Figure 2-15) and LNG trading in 2040 (Figure 2-16). Moreover, Figure 2-16 suggests that N. America will reduce LNG trading by approximately 28% as a result of lower production. Thus, we may conclude that even a merely ten percent decrease in production can significantly affect exports, particularly in terms of prices and LNG trading.

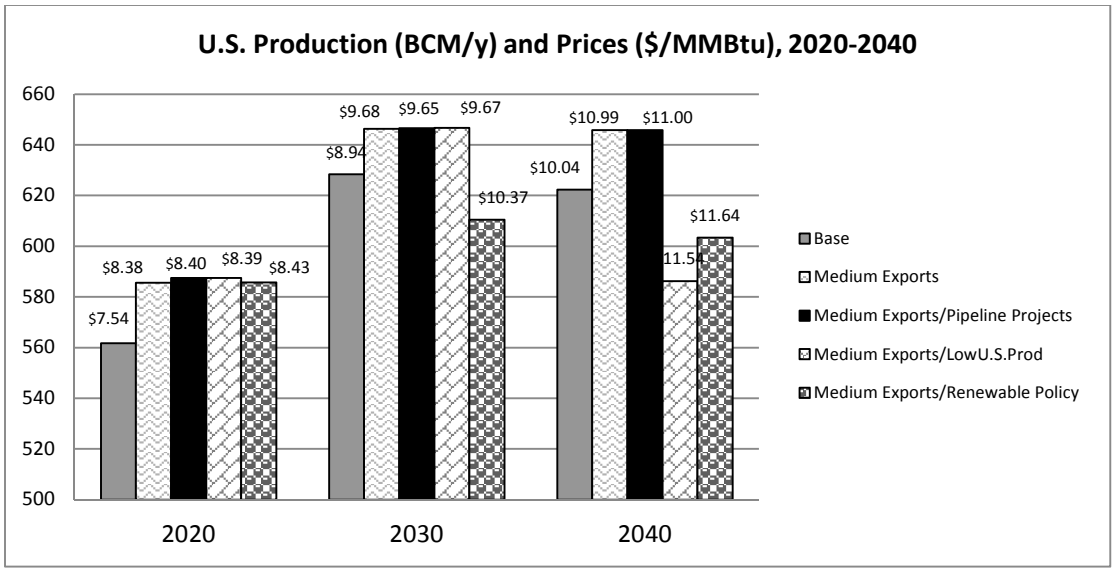

Figure 2-12 U.S. production in Bcm/y and prices in $/MMBtu from 2020 to 2040

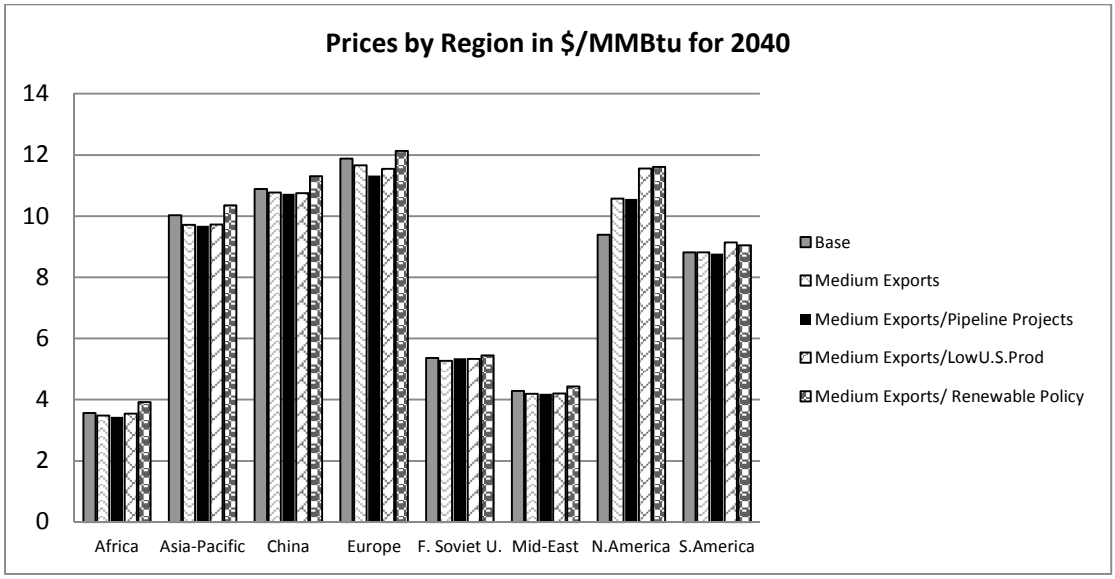

Figure 2-13 Prices by region $/MMBtu for 2040

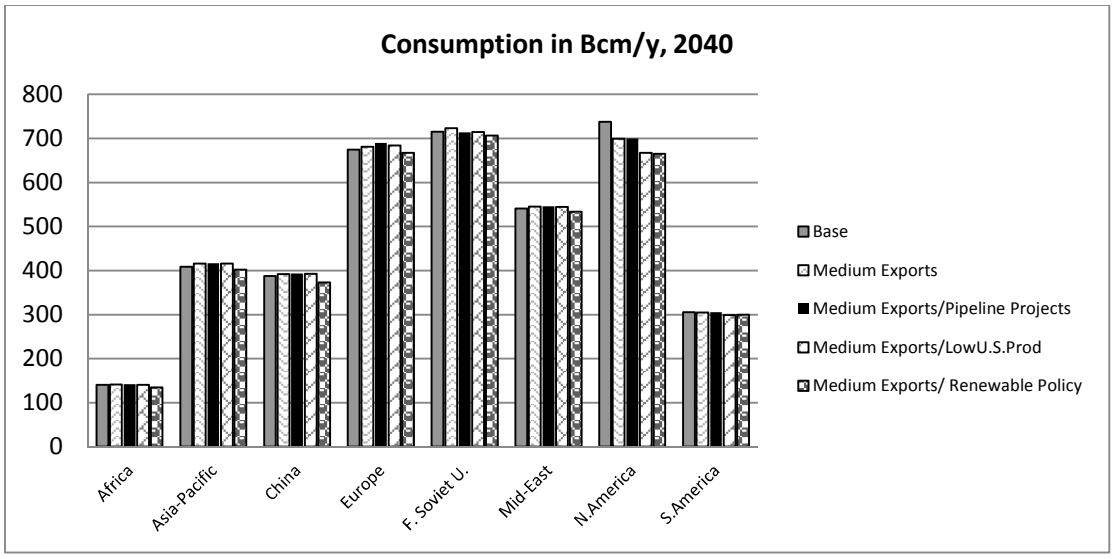

Figure 2-14 Consumption by region in 2040 Bcm/y

Efforts to reduce CO_2 emissions by establishing typical targets for regional policy are presented in (Kelvin et. al, 2009). Under the policy scenario abbreviated Medium Exports/ Renewable Policy the average prices are the most expensive relative to the other scenarios, particularly in N. America. Two reasons for this price disparity are the CO_2 prices, which represent an additional cost to the producers of $45.33 per ton of CO_2e in 2040, and the effect of exports. The prices in N. America are $2.21 higher than in the Base Case (Figure 2-13). Figure 2-13 indicates that prices in rapidly developing and developed regions, namely, Europe, Asia-Pacific, and China, exhibit an increase of $0.25-$0.55 because of increased CO_2 prices. However, the prices in the least developed regions, expressly Africa and the Middle East, continue to increase for a different reason. Because no renewable policy has been implemented in Africa or the Middle-East, producers in these regions increase production output and export to a greater extent to compensate for reduced production in rapidly developing and

developed regions, as shown in Figure 2-15-2-16. Therefore, there is an incentive for producers in the least developed regions to increase production.

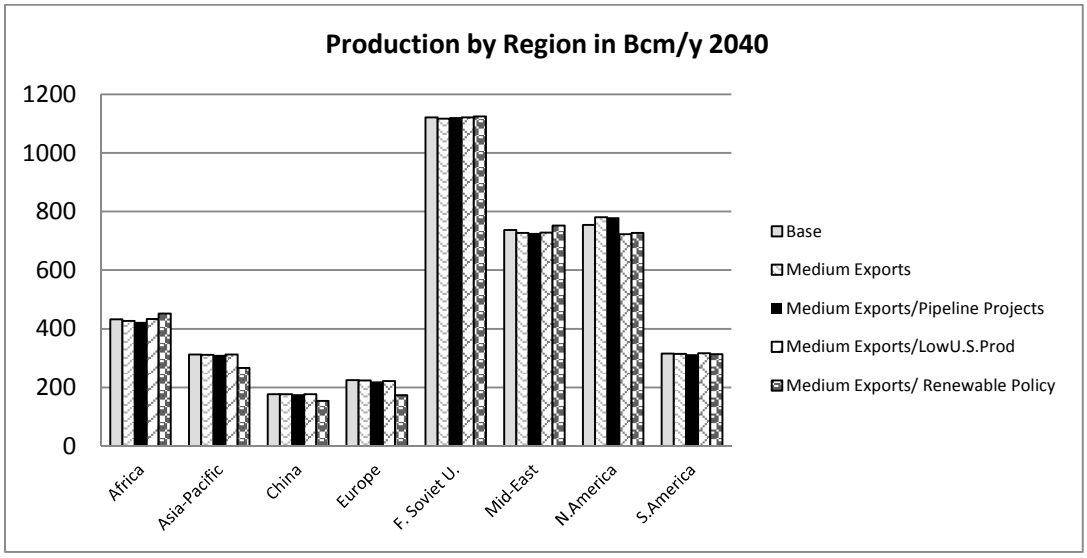

Figure 2-15 Production by region in 2040 Bcm/y

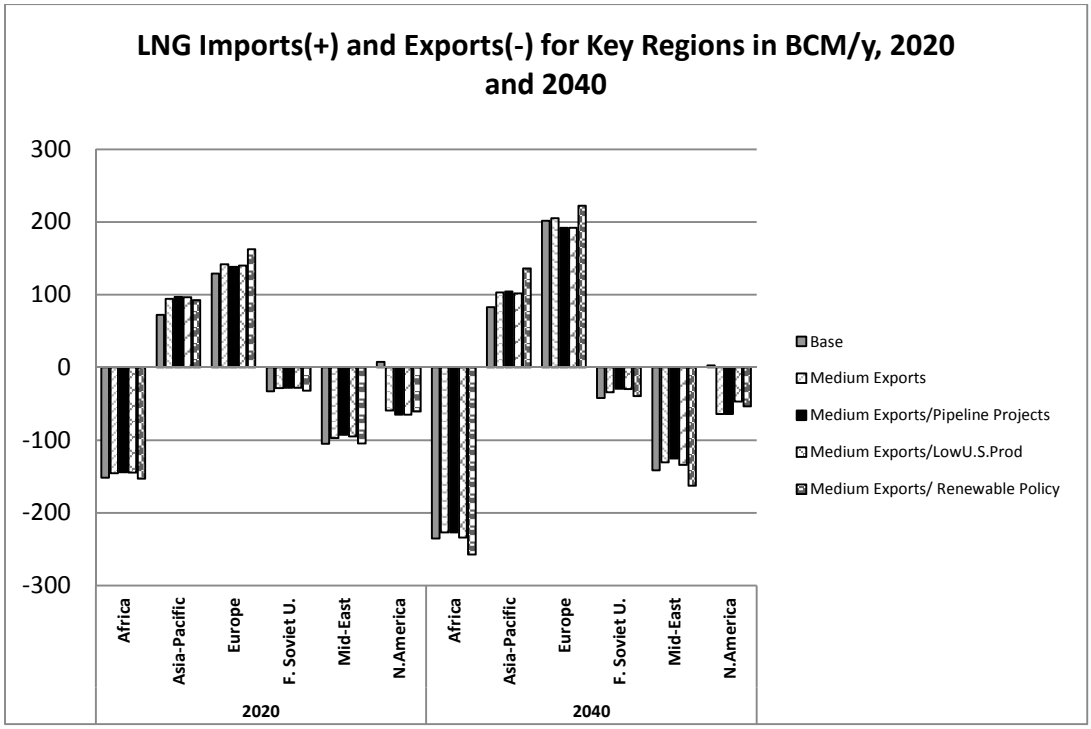

Figure 2-16 LNG imports (+) and exports (-) for key regions in Bcm/y, 2020 and 2040

More interestingly, LNG imports by Europe and Asia increase dramatically, presumably because of reductions in domestic production. Similarly, in 2040, LNG exports from Africa and the Middle East also increase significantly by 22.42 Bcm and 21.22 Bcm, respectively (Figure 2-16). LNG trading plays an important role in balancing demand in the Renewable policy scenario. Production has shifted to regions that have not implemented policies. This type of phenomenon demonstrates that when a policy is not applied equally, some participants will benefit from not being under the policy. Because global trading is allowed, this condition may affect the efficiency of the policy.

Next, we gauge the effects of competition between European pipeline projects and U.S. gas exports under the Medium Exports/Pipeline Projects Scenario. Three pipeline projects are considered. The Nord Stream [11]and South Stream pipelines will transport gas from the Russian reserves directly to European markets, whereas the Southern Corridor will bring gas from the Caspian region to Europe. Comparing this scenario to the Medium Exports, we initially note that U.S. production remains unaffected by the new European pipelines (see Figure 2-15). Likewise, the Medium Exports/Pipeline Projects scenario does not affect the remainder of the world in terms of production, as detailed in Figure 2-12. Figure 2-13 shows that prices remain the same in most regions, except for the Former Soviet Union and Europe. Europe has the most inexpensive

[11]Nord Stream has been fully operating with 55 BCM/y of capacity since October 2012.

prices among all of the scenarios because of the increased supply from U.S. exports and the introduction of new pipelines. In contrast, the Former Soviet Union exhibits a price increase of $0.10 compared with the Medium Exports, perhaps because increased exports via the pipelines may result in less gas available for domestic consumption at low prices. Only a small rise in consumption occurs in Europe (Figure 2-14). The increased pipeline capacity in Europe slightly displaces some of the LNG imports, perhaps from Africa, Russia, and the Middle East, as indicated in Figure 2-16.

Furthermore, we observe the flows from Russia. The Russian flow patterns for the Base Case and Medium Export/Pipeline Projects are summarized in Table 2-10. There are no flows from Russia to Germany or Bulgaria under the Base Case because the Nord Stream and South Stream Pipelines are not considered in the Base Case, which the Russian flows to European markets require to bypass transit countries, namely, Ukraine and Poland.[12] However, flows through the Nord Stream Pipeline will increase greatly, from 0 Bcm/y to 63.7 Bcm/y (see Table 2-10), when the Nord Stream pipeline is available. Overall, the Russian flow patterns will change dramatically because Russian traders who want to maximize profit must consider avoiding transit fees by sending gas directly to Germany. The flows via transits will decrease significantly from the Former Soviet Union to Poland (Ukraine) by 20.54 Bcm (63.01 Bcm) in 2020, and the influence of the new pipelines will become more pronounced in terms of bypassing the Ukraine and Poland in 2040 (Table 2-10). Moreover, Russia will lose 74% of the European LNG markets because of the increased volume of U.S. exports to Spain and the United

[12] In WGM , Belarus is aggregated into the Ukraine node.

Kingdom in 2040, as shown in Table 2-10. Therefore, Russia will increase the flow via the pipelines by approximately 16% in 2040 to compensate for the losses of LNG market share (see the total pipeline export in Table 2-10). In the Medium Exports/Pipeline Projects, three pipeline projects compete with one another and the U.S. exports. Consequently, these situations create a positive effect in Europe as the result in an increase in consumption with lower prices, as shown in Figure 2-14,2-15. However, although the new pipelines offer flexibility in the delivery of gas to Europe, Russian production levels do not significantly increase. The explanation is that Russia can increase profit at the same level of production, as evidenced in Table 2-11. New pipelines reduce transit fees ($1.1 billion in 2020 and $2.75 billion in 2040) and increase the profits of Russian traders ($1.88 billion in 2020 and $2 billion in 2040), as indicated in Table 2-11.

Table 2-10. Russian natural gas flows (exports) in Bcm/y in 2020 and 2040

		2020		2040	
	Destination	Base	Medium Exports/Pipeline Projects	Base	Medium Exports/Pipeline Projects
LNG	Canada	0.00	2.58	0.12	1.95
	France	0.00	0.00	2.96	0.00
	Netherlands	0.00	0.00	2.25	0.00
	Spain	4.97	1.46	5.47	3.12
	U.K.	1.94	0.00	9.25	0.00
	LNG Total	6.91	4.04	20.03	5.07
Pipe	Germany	0.00	63.77	0.00	105.82
	Bulgaria	0.00	21.24	0.00	23.90
	Kazakhstan	2.50	0.00	12.22	10.78
	Turkey	17.49	16.93	27.57	25.17

	Poland	50.24	29.70	63.82	28.91
	Ukraine	165.68	102.67	141.28	79.47
	Pipe Total	235.91	234.32	244.89	274.04
Total Exports		242.82	238.36	264.92	279.11

Table 2-11. Total transit fees[13] and profits for Russian traders in billion $/year, 2020 and 2030

Year	Indicators	Base	Medium Exports	Medium Exports/Pipeline Projects	Medium Exports/ Renewable Policy
2020	Transit Fees	20.392	19.303	19.268	21.719
	Trader Profit	25.686	24.514	27.566	28.043
2040	Transit Fees	27.225	25.748	24.474	28.521
	Trader Profit	39.746	37.701	41.740	41.618

It is interesting to note the investment for each pipeline. Initially, the Nord Stream pipeline will have a capacity of 55 Bcm/y; subsequently, it will be expanded to as high as 109.9 Bcm in 2040 (see Figure 2-17). Nevertheless, the South Stream pipeline capacity will be only 24.83 Bcm/y in 2040. This figure represents only half of the expected capacity as indicated in Table 2-6. There are three reasons for the reduced expansion. First, this pipeline competes with another project, namely, the Southern Corridor, which can also deliver inexpensive gas from the Caspian region to the same consumption node.

[13]Transit fees in WGM are the total of regulated fee plus congestion fees. The regulated fee is an exogenous factor for each pipeline, but the congestion fee is the value of the dual variables associated with the flow conservation constraint in the pipeline operator optimization problem.

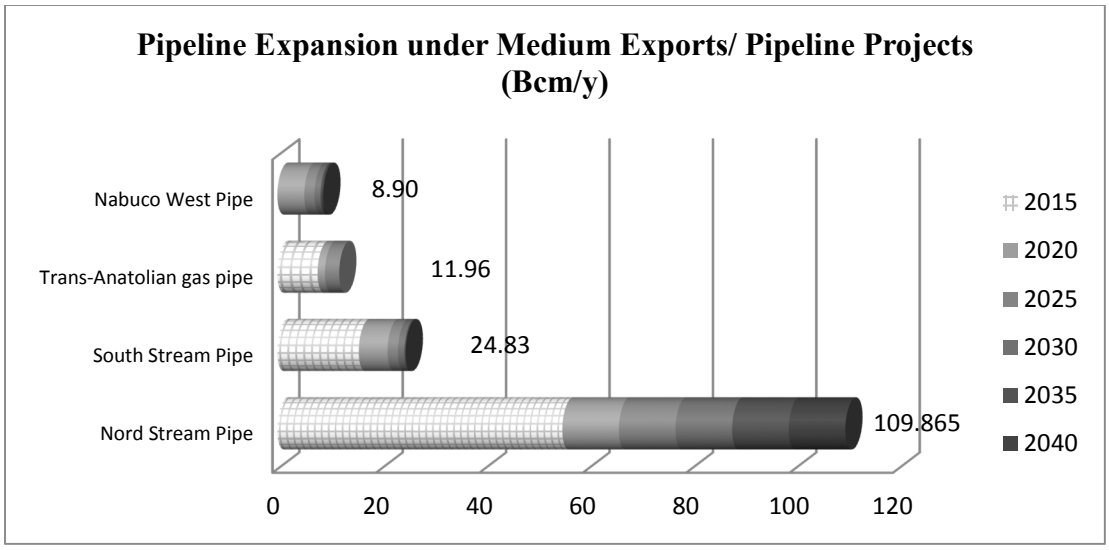

Figure 2-17 Pipeline capacity expansion over time (Bcm)

Second, the South Stream expansion costs more compared with the Southern corridor project because of the off-shore characteristics and longer distances. Finally, the WGM has a low pipeline capacity to connect from Bulgaria to other European countries due to model restriction. Therefore, this consumption node cannot be treated as a transit area, which results in decreased expansion capacity.

2.5. U.S. LNG export study part II:

2.5.1 Asian LNG Focus: scenario description

This section closely examines on the impact of the U.S. LNG exports on Asian markets. Recently, Asia has been considered to be the area with the fastest growing consumption in the next decades driven by the strong population growth as well as other factors (WEO, 2011). In World Energy Outlook (WEO)'s 2011 research data, with the increase of new policy scenario projects, the total demand in Asia will reach above 1,200 Bcm by 2035. Major expansion of gas use in Asia will result from implementing the 12th Five-Year Plan, announced by China in 2011. In particular, the new policy will push

the domestic consumption for China above 500 Bcm by 2035, from 100 Bcm in 2010. Also, the growth of gas demands for the power sector in Japan will increase because of the effects of the nuclear disaster in 2010. Therefore, to capture new demand trends in Asia, we incorporate Asian demand projections from 2015-2035 for this analysis as indicted in (WEO, 2011)

Asian suppliers, namely Australia, have at least ten projects either under construction or under consideration, starting at the end of 2013. The seven LNG export terminals, which are under construction, should allow Australia to bypass Qatar as the world's largest LNG exporter by 2018 (Ross, 2013). However, additional supply expansion may be uncertain and more difficult to accomplish because of project delays, which will increase the cost of investment. In addition, cheap American gas could threaten Australia due to the difference pricing regimes. The LNG pricing in Asia is mostly linked to oil indexation under long-term contract while the LNG trades in North America are based on gas indexation, which offers lower prices depending on Henry Hub prices. The Australian LNG suppliers may need to reduce prices to make it more competitive with the U.S. LNG (Ross, 2013). Therefore, it is interesting to see how the U.S. LNG exports compete with the Australian gas. Therefore, three different scenarios are simulated to analyze the impact of the U.S. LNG exports on Asia and the competitiveness over Asian markets as follows:

- The Reference Scenario, abbreviated "*Reference",* uses the demand projections for Asia based on (WEO, 2011). The Reference Scenario assumes no LNG exports from the U.S.

- The Export Scenario, abbreviated "*U.S. Exports",* is based on the Reference Scenario, but it allows the U.S. to export up to 120 Bcm from the Gulf of Mexico without restricting the destination, representing the LNG contracts with flexibility. It is assumed that the U.S. will start exporting in 2015.
- The Competitive Export Scenario, abbreviated "*Competitive",* is based on the U.S. Export Scenario. However, it also assumes the largest Asian LNG exporters, namely Australia, can ramp up their LNG export capacity by 50% more than the Reference Scenario. The construction for the capacity expansion will be completed by 2020.

2.5.2 Results and analysis of Asian LNG Focus study

2.5.2.1 Reference scenario results

This section presents general results of Asian consumption and production projections for the Reference Scenario and the difference between WGM results and the projections from 2015-2035 in (WEO,2011)According to our simulation, Table 2-12 indicates that as a whole, the percentage difference between the WEO and WGM figures is fairly low. Specifically, it is less than five percent. As shown in Table 2-12, there is a considerable difference between consumption and production. The gap will reach approximately 400 Bcm in 2035, from 161 Bcm in 2015. By 2035, Asia will rely on imports, equating to about one fourth of the total consumption.

Table 2-12 World Gas Model Reference, Asian production and consumption in Billion Cubic Meters.

	2015	2020	2025	2030	2035
Consumption	743.6 (-1.92%)	927.3 (-4.57%)	1,045.70 (-4.97%)	1,169 (-3.47%)	1,280.10 (-0.03%)
Production	582.3	671.4	737.3	811.3	887.4

	(-0.63%)	(-4.77%)	(-4.99%)	(-5.00%)	(-4.79%)

*The numbers in parenthesis are the WEO 2011 values less the World Gas Model values divided by WEO 2011 values.

The next section compares the U.S. Export and Competitive Scenarios to the Reference Scenario. However, the comparison of three scenarios focuses only on the year 2035 as a representative future year. The general results show dynamics in trade changes with broad impacts. U.S. LNG exports are expected to have worldwide impacts, mainly decreasing prices and increasing consumption in importing countries.

2.5.2.2 Market share impact due to the U.S. LNG exports

The U.S.Exports Scenario indicates that the U.S., given a maximum destination-free export capacity of 120 Bcm/y, will actually export approximately half of that (53.75 Bcm/y) to Japan/S. Korea[14] and none elsewhere (Table 2-13). Part of the rationale is that the Japan/S. Korea node has the highest endogenously determined, wholesale prices, which is a motivation for concentrating U.S. exports there. Furthermore the U.S. LNG simultaneously displaces a significant market share of other suppliers. In the Japan/S. Korea market, Algeria and Nigeria lose their market share by approximately 30%, while Australia, Indonesia, Qatar, Trinidad, and Yemen drop their market shares approximately 20%-30% Moreover, it is noted that not just the countries importing the U.S. LNG have market share changed. For example, Australia increased its market share 31.20% in the S.E. Asia/China[15] market, whereas Nigeria and Algeria's market share declined by approximately 10% under the same scenario. Because the Australian LNG is unable to compete with the cheap U.S. LNG, the Australian traders raise sales

[14] Japan/S.Korea is one node in WGM aggregating Japan and South Korea into one country.
[15] S.E. Asia/China is an agrregate node in WGM incluing China, Taiwan, Hong Kong, Thailand, and Myanmar.

in China to make up its profit. The explanation is that once the sales are displaced in one market, the traders try to maintain their profit by increasing their sales in other markets. This is due to the assumption of profit maximization and Cournot behavior. Under the Competitive Scenario, Australia is able to ramp up its export capacity by 50%. Although Australia increases its export capacity, it displaces U.S. LNG by a small amount, 3 Bcm/y, in the Japan/S. Korea market. The U.S. still prevails over the Japan/S. Korea market. Most of the additional Australian LNG flows to S.E. Asia/China, over 200% more in comparison to the Reference Scenario. However, African and Middle East suppliers are displaced significantly. The largest entry with displaced LNG sources is Algerian LNG (-58.28%) and Nigerian LNG (-41.26%) in S.E. Asia/China, Nevertheless, the domestic production does not change for all scenarios.

Table 2-13 Scenario comparison of gas supplied to Asian countries by sources in 2035. Percentage of difference from the WGM Reference Scenario.

Country Nodes	Natural Gas Sources	Reference Scenario (Bcm/y)	U.S.Exports Scenario (Bcm/y)	U.S.Exports Scenario % Change to Reference	Competitive Scenario (Bcm/y)	Competitive Scenario % Change to Reference
S.E.Asia/ China	Domestic Production	379.74	379.74	0.00%	379.74	0.00%
	Algeria	10.06	9.04	-10.12%	4.20	-58.28%
	Australia	13.18	17.29	+31.20%	41.33	+213.68%
	Indonesia	66.75	70.02	+4.90%	68.67	+2.87%
	Kazakhstan	54.00	54.00	0.00%	54.00	0.00%
	Nigeria	7.45	6.45	-13.40%	4.38	-41.26%
	Qatar	20.64	20.09	-2.65%	14.85	-28.06%
	Russia	45.16	45.37	+0.47%	43.73	-3.17%
	Yemen	19.30	19.02	-1.43%	13.12	-32.00%
India/ Pakistan	Domestic Production	190.22	190.19	-0.01%	190.17	-0.02%
	Algeria	6.18	6.28	+1.58%	6.91	+11.81%
	Kazakhstan	48.85	48.39	-0.94%	47.85	-2.04%
	Qatar	34.27	35.31	3.05%	35.97	+4.99%
	Russia	11.49	11.49	+0.00%	11.49	0.00%

	Yemen	10.54	11.05	+4.79%	11.13	+5.52%
Japan/ S. Korea	Domestic Production	1.00	1.00	+0.01%	1.00	+0.27%
	Algeria	22.34	15.41	-31.00%	15.37	-31.20%
	Australia	24.18	18.21	-24.69%	23.56	-2.56%
	Indonesia	24.95	19.34	-22.48%	19.29	-22.69%
	Nigeria	21.86	14.94	-31.66%	15.41	-29.50%
	Qatar	24.56	17.72	-27.84%	17.60	-28.33%
	Russia	25.59	22.60	-11.69%	22.55	-11.91%
	Trinidad	24.43	18.61	-23.84%	18.05	-26.14%
	USA	0.00	53.75	>100%	49.81	>100%
	Yemen	24.05	17.26	-28.22%	17.02	-29.23%

In summary, U.S. LNG exports provide an additional option to transport gas to Asia. However, they increase the competition over Asian Markets. U.S. LNG causes a reduction of flows to Japan/S. Korea for all other (non-domestic) suppliers. Moreover, even though Australia can increase its export capacity, the U.S. LNG exports will still dominate Australian gas in the Japan/S. Korea market.

2.5.2.3 Other impacts on Asian market due to U.S. LNG exports

Besides the market share changes discussed above, the U.S. LNG exports are projected to have other impacts such as changes in consumption and prices worldwide. Table 2-14 shows that the Japan/S.Korea wholesale price goes as high as $16.06/MMbtu in 2035. This represents the highest prices among Asian countries. S.E.Asia/China and India/Pakistan will see 2035 prices of $13.87/MMbtu and $11.24/MMbtu, respectively. All Asian countries exhibit lower gas prices for the U.S. Exports Scenario in comparison to the Reference Scenario but Japan/S. Korea has the highest improvement for prices -7.61% and -8.65% lower than the Reference Scenario for each U.S. exports scenario, respectively. S.E. Asia/China, however, does not import U.S. LNG directly,

but the prices are cheaper in comparison to the Reference due presumably to more supply from Australia shifting to China.

Table 2-14 Comparison of wholesale prices for 2035 in $/MMBtu and percent difference from Reference Scenario

Country Nodes	**Reference Scenario**	**U.S.Exports Scenario**	**U.S.Exports Scenario % Change to Reference**	**Competitive Scenario**	**Competitive Scenario % Change to Reference**
S.E.Asia /China	13.87	13.69	-1.34%	13.57	-2.15%
India/ Pakistan	11.24	11.15	-0.73%	11.09	-1.26%
Japan/ S.Korea	16.06	14.84	-7.61%	14.67	-8.65%

In 2035, there is no significant difference between the Reference and U.S. Exports Scenarios for Asian consumption (Table 2-15). However, Japan/S. Korea will increase its consumption by 3.04% under the U.S. Exports Scenario and 3.48% under the Competitive. It is interesting that S.E. Asia/China consumes more than 600 Bcm/y in 2035, from a previous 120 Bcm/y in 2010. In comparison, India's consumption reaches about 300 Bcm/y in 2035, from a previous approximate 70 Bcm/y in 2010.

Table 2-15 Comparison of consumption for 2035 in Bcm/y and percent difference from Reference Scenario

Country Nodes	**Reference Scenario**	**U.S.Exports Scenario**	**U.S.Exports Scenario % Change to Reference**	**Competitive Scenario**	**Competitive Scenario % Change to Reference**
S.E.Asia/ China	616.27	621.05	+0.78%	624.02	+1.26%
India/Pak istan	301.55	302.71	+0.38%	303.53	+0.66%
Japan/S. Korea	192.95	198.82	+3.04%	199.66	+3.48%

Overall, the impact of U.S. LNG exports on Asia and the presence of U.S. LNG exports leads to higher consumption and lower prices in comparison to the Reference Scenario (for both non-reference scenarios). Since there is an increase of supply flows to the markets, as the supply curve shifts to the right and the new equilibrium price being lower, the consumption will be higher, all things being equal. Also, the U.S. LNG significantly displaces market shares from other prominent exporters.

2.6. Conclusions and future work

This chapter discusses the effect of U.S. LNG exports on the domestic and global markets under various scenarios. The Base Case is specified to simulate the magnitude of the global markets. In addition to two increased export volume scenarios, a global 20/20/20 policy and new European pipeline projects are added to gauge the influence on the global markets. In addition, a decrease in U.S. production is also analyzed as a sensitivity test. Based on the simulation results, the main conclusions can be summarized as follows:

- Increased U.S. LNG exports lead to higher prices, lower consumption, and increasing production in the U.S. domestic market. Prices will be lowered recovered in the long term after supplies are adjusted to meet demands. However, a dramatic effect on price will occur in the event of reduced U.S. production. A 10% shortfall in production with 99.7 Bcm of U.S. LNG exports results in a price increase of approximately $2/MMBtu relative to the Base Case in North America market. It is risky for natural gas exporters to commit to long-term contracts because unconventional production is uncertain, and resources

can decline quickly. However, N. American producers can dominate other producers in terms of profit. Moreover, increased LNG export can create a small increase in the social welfare of the U.S. economy.

- By contrast, increased U.S. exports reduce prices significantly in importing markets. For example, prices in Spain decrease by $2.7/MMBtu in 2020 under the High Exports compared with the Base Case. Increased LNG exportation results in positive effects on Asia and Europe.
- High CO_2 prices under the Renewable policy scenario lead to reductions in production in rapidly developing and developed regions in which the policy is applied. This production would be shifted to the least developed regions and lead to an increase in production and exports to rapidly developing and developing regions. LNG trading plays a key role in the Renewable Policy scenario. Europe and Asia will require 30% more LNG imports than in the Base Case in 2040.
- The influence of new European pipelines does not affect Russian production levels, but the flow patterns change significantly. The flow from Russia to transit countries will be reduced by approximately 50% when the Nord Stream and South Stream pipelines are available. More interestingly, Nord Stream is a preferable target for expansion, and the total capacity could reach 109 Bcm in 2040. The presence of the new pipelines reduces transit fees by approximately 10% each year for Russia. In term of competition between U.S. LNG exports and European pipeline projects, cheap U.S.LNG displaces more expensive

suppliers including Russia in European LNG markets, so Russia increases volume of exports to Europe by new two pipelines.

- Without contract restrictions, the optimal U.S. LNG exports are approximately 50 Bcm/y to Japan/S.Korea in 2035. The U.S. LNG displaces market shares from other suppliers of the Asian Markets.

Future work on U.S. LNG exports should include the improved presentation of long-term contracts and further details regarding LNG transportation. Long-term contracts should be determined endogenously by the model as in (Abada et al, 2012). A natural question arises with regard to the optimal export volume under different given conditions. In addition, more details regarding LNG, including actual cargo routes and transportation limitations, such as canal capacity, can be considered.

Chapter 3: The Influence of Panama Canal Tariffs on LNG Markets

An increasing growth of unconventional gas production in the U.S. has gradually turned it into a potential gas exporter. In near future, increasing LNG exports from the U.S. coupled with the capacity of the Panama Canal will change the LNG market. The Panama Canal expansion is the key to the change because the route via this canal reduces the voyage by 7,000 nautical miles to Japan from the Gulf of Mexico. Applying the World Gas Model from the University of Maryland, this chapter[16] investigates the potential effects of varying Panama Canal toll selection on the LNG markets via six scenarios of possible Panama Canal tariffs. Results are compared and examined with the focus on prices, LNG flows, and supply displacement.

3.1 Introduction

The global natural gas market has undergone a number of changes recently due to new unconventional resources such as shale gas. This has been at roughly the same time as the rise in consumption in liquefied natural gas (LNG) especially in Asian markets. LNG is an attractive alternative to gas transported by pipelines and helps consuming countries to diversify their supply portfolio (Wood, 2012). LNG is also a key option to compensate for domestic resources that are depleting for example in Europe. Over the last decade, LNG market has been dominated by a few exporters. For example, 83%

[16] The analysis and results of this study have been published in S. Moryadee, S.A. Gabriel, F. Rehulka "The influence of the Panama Canal on global gas trade", Journal of Natural Gas Science and Engineering 01/2014; 20:161–174. DOI: 10.1016/j.jngse.2014.06.015

of the global LNG trade in 2012 was supplied by eight countries. Qatar was the largest exporter followed by Malaysia and Indonesia (GIIGNL, 2013). However, in near future the global LNG market will undergo rapid changes as it welcomes the entry of new exporters from the U.S. and increased supplies from Australia (Leather et al., 2012). In the past, LNG trade has been divided into two basins, the Pacific and Atlantic Basins, and most LNG trade is confined within one basin (GIIGNL, 2013). LNG trade between basins is unprofitable due to high shipping costs and a small price gap between these two basins. Recently, the price difference between the basins has increased since mid-2010 due to strong demand in Asia. Therefore, trading LNG between basins became profitable depending on the shipping costs. Thus, while LNG markets previously were separate due to financial disadvantage, the rise of LNG in Asia and elsewhere, coupled with an expanded Panama Canal, are increasing the competitiveness of global LNG markets. For instance, U.S. LNG exports can compete with Australian and Middle Eastern LNG exports in the Japanese and South Korean markets or for other high demand areas in Asia.

The expansion of the Panama Canal is scheduled to be completed in June, 2015. The route via the Panama Canal will shorten voyages by more than 7,500 nautical miles (8,500 miles) from the East Coast of North America to Asia. With shorter distances, the cost of U.S. LNG from the East Coast going to Asia will be very competitive compared to the cost of LNG from the Gulf countries. For example, taking a Henry Hub reference price of $3 /MMbtu, a liquefaction and storage cost of $3 /MMbtu, the MMbtu cost aboard an LNG carrier out of the Gulf of Mexico, Texas or Louisiana, will be $6 /MMbtu. The shipping cost to East Asia without the Panama Canal can be

estimated at between $2.5 /MMbtu and $3/MMbtu. This gives a LNG delivered price of about $9 /MMbtu ($3+$3+$3) to East Asia; a very competitive price for the Asian buyers when compared to the spot price which oscillates around the $15-17 /MMbtu mark (BP, 2013). Although using the Panama Canal can save time (approximately 14 days to Asia from the U.S. East Coast) and transportation costs, the canal fee is still uncertain, and it may be costly. LNG experts expect the canal tariff will around 30 cents per MMBtu based on a $1 million round-trip fee for a medium-sized LNG tanker (Reuters, 2013). After the completion of the Panama Canal, several possible outcomes are possible. First, how will the Panama Canal tariffs affect the decision of LNG exporters and LNG shippers? Second, will more U.S. gas go to Asia given a shorter distance or go to Europe? Therefore, the aim of this study is to address these questions using the University of Maryland's World Gas Model (WGM) (Gabriel at el., 2012); see Section 3.2 for more details. We assume the Panama Canal route is available for LNG shipping with tariffs differing by scenarios. However, we assume that the Panama Canal has unlimited capacity and is never congested which is a best-case scenario but useful in providing guidance.

The rest of this chapter is organized as follows: Section 3.2 provides details for the University of Maryland's World Gas Model. Section 3.3 proposes scenarios involving the Base Case and the Panama Canal toll. Section 3.4 presents the results and the analysis, and Section 3.5 provides conclusions.

3.2 The World Gas Model

The WGM (2012 version) is a large-scale, market equilibrium model based on a mixed complementarity problem (MCP) system (Gabriel et al., 2013). This MCP comprises profit-maximizing optimization problems for the various market agents such as: producers, traders (who controls LNG), an integrated pipeline operator and a storage operator as well as demand functions for describing three consumption sectors (residential/commercial, industrial, and electric power). The WGM then takes the Karush-Kuhn-Tucker (KKT) optimality conditions of these various players along with market-clearing conditions to form the overall MCP (Gabriel et al., 2013). In the modeling framework, the traders are modeled as having market power (depending the country) in order to withhold gas supplies to increase overall prices. For some countries, such as the U.S., such market power is not consistent with market realities and thus traders in the U.S. are modeled via perfect competition. For other countries such as the Former Soviet Union, the traders see a weighted combination of both the perfect competition prices as well as ones derived from inverse demand functions. Such an approach allows for partial market power and has been used successfully for a number of private and public sector projects (e.g., Gabriel et al., 2012). The WGM goes beyond a number of previous and current gas models (Rice, 2005, Holz et al., 2008; Lochner, 2009; Aune et al., 2009; Rosendahl and Sagen, 2009; Abada et al., 2012; Huntington et al., 2010; Huntington et al., 2013) by allowing for nearly global coverage combined with market power, multiple seasons, as well as coverage of conventional and unconventional gas production with separate shale gas production nodes.

3.3 Description of Scenarios

This section describes the scenarios examined as well as hypotheses about how the various case assumptions could impact the model outcomes. First, we define the Base Case as a benchmark for the other scenarios. The Base Case was calibrated to match recent global natural gas market trends and incorporates natural gas market projections from multiple sources. Table 3-1 provides details of the references for the WGM calibration. The Base Case assumed that there was no Panama Canal route. Thus, the Base Case assumes the longer distances from LNG export nodes to regasification.

In terms of the Liquefied Natural Gas (LNG) exports from North America, the Base Case assumes the North America LNG exports begin in 2020 and these LNG export capacities are exogenously realized by the model in 2020. Further, five potential aggregated export terminals across North America are assumed. Three of them are located in the U.S. (West Coast, Gulf of Mexico, and East coast), and the other two are in Canada (East and West Coast). More details about the capacities and long-term contracts and destinations for these LNG contracts are provided in Table 3-2 where both an upper and lower bound on the LNG flows are presented. The upper bound is based on exogenous data from the references and the lower bound is from long-term contracts (LTCs) also referenced. The WGM will pick actual LNG amounts between and possibly equal to these two bounds.

Table 3-1 Base Case References

	Regions	**References**
Consumption	North America	(EIA, 2013)
	Europe	(EDF, 2013), (AIE, 2013)

	China[17]	(EDF, 2013), (OIES, 2011), (OIES, 2012)
	The rest of the world	(EDF, 2013)
Production	North America	(EIA, 2013)
	Europe	(DECC, 2013) (AIE, 2012)(AIE,2013)
	China	(WEO, 2013) and (OIES, 2012)
	The rest of the world	(WEO, 2013)
Price Reference	USA	(EIA, 2013)
	the rest of the world	(IGU, 2013)
	Norway	(AIE, 2013)
Contract Data Base	The rest of the world	(GIGNL, 2013)
	USA	www.freeportlng.com (Macallister,2013)
Liquefaction cost	all regions	(WEO 2013), (AIE, 2013)
Regasification cost	all regions	(WEO, 2013)
LNG shipping cost	all regions	(Petroleum Economist,2011)

Table 3-2 North America LNG Export terminal, capacities, and contracts

Terminals	**Upper bound Capacity (BCM)**	**Lower bound LTC with destination (BCM)**	**destination (BCM)**
U.S. West	8.25	N/A	
U.S. East	8	6.32	USA-Japan/S.Korea (3.16) USA-India (3.16)
U.S. Gulf	72	13.22	USA-Japan/S.Korea (13.22)
Canada West	6.98	1.65	Canada -Japan/S.Korea (1.65)
Canada East	0.96	N/A	

Second, we construct six different Panama Canal toll scenarios as shown in Table 3-3.

The main difference between the Base Case and Panama Canal scenarios is the port-

[17] The China node includes more than one country i.e., Thailand, China, and Taiwan. More details for regional definitions can be found in Appendix 1.

to-port distance for LNG exports. The Base Case assumes the distance between the U.S. Gulf of Mexico to Japan is 15,600 nautical miles (NM) while the Inf_toll scenario assumes 9,500 NM with a significantly large tariff (e.g., numerical infinity). In reality, three other routes are available: the one via the Cape of Good Hope (15,600 NM), the one via the Suez Canal (14,969 NM), and the one via the Cape Horn (17,000 NM). Although besides the Panama Canal route, the route via the Suez Canal is the shortest route, and the Canal fees are applied in order to pass this waterway. Therefore, this study assumes the shortest distance routes with no extra fees applied compared to the route via the Panama Canal. Figure 3-1 shows the difference between the current Panama Canal scenarios and the Base Case in shipping gas from the U.S. Gulf of Mexico The next section presents numerical results for the Base Case and the six canal tariff scenarios.

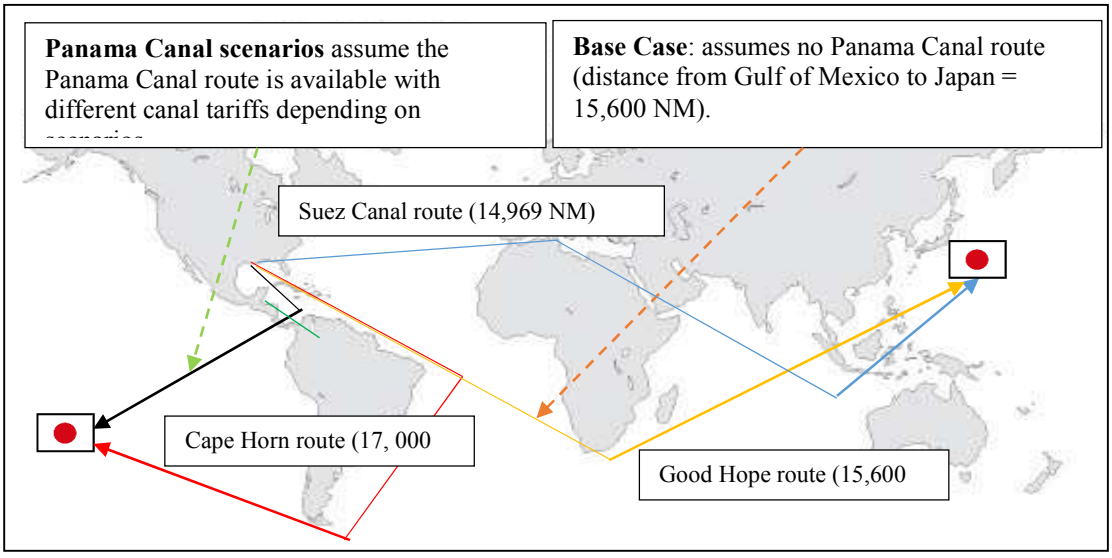

Figure 3-1 the difference between Panama Canal scenarios and the calibration Base Case.

Table 3-3 Panama Canal toll scenarios

Scenarios	Abbreviation	Description
Scenario 1	Zero_toll	“Zero toll" : tariff = $0 /MMBtu
Scenario 2	Regular_toll	“Regular toll" : tariff = $0.35 /MMBtu
Scenario 3	Double_toll	"Double toll" : tariff is regular toll times 2=$0.70/MMBtu
Scenario 4	Threefold_toll	"Threefold toll" : tariff is regular toll times 3=$1.05/MMBtu
Scenario 5	Fivefold_toll	"Fivefold toll" : tariff is regular toll times 5=$1.75/MMBtu
Scenario 6	Inf_toll	"Infinite toll” : tariff is regular toll is high $9,999/MMBtu

3.4 Numerical Results

3.4.1 Base Case: Results

In terms of production, the WGM has 59 aggregated producers covering worldwide production: 39 are conventional gas producers, nine are strictly for shale gas, and 11 are unconventional non-shale producers. It is important to note that the WGM production output differs from the references AEO 2013 and WEO 2013. The Annual Energy Output (AEO, 2013) and The World Energy Outlook (2013) report gross production while the World Gas Model gives net production. The main difference between net and gross production is due to processing losses such as lease and plant fuel. Also, pipeline fuel must be subtracted to account for losses in pipeline transportation. The WGM explicitly accounts for losses in liquefaction, LNG shipment, re-gasification, pipeline and storage losses, but these two references (AEO, 2013) and (WEO, 2013) report aggregate losses only. There are also usage categories, such as own use in the energy sector for enhanced oil recovery but these are not represented in

the World Gas Model. The production capacities and volumes in the World Gas Model are net production volumes, i.e., the volumes delivered to a number of consumption sectors. Figure 3-2 indicates that on the whole, the percentage differences between WGM production values and those from the outside references (AEO, 2013 and WEO, 2013) are fairly small though.

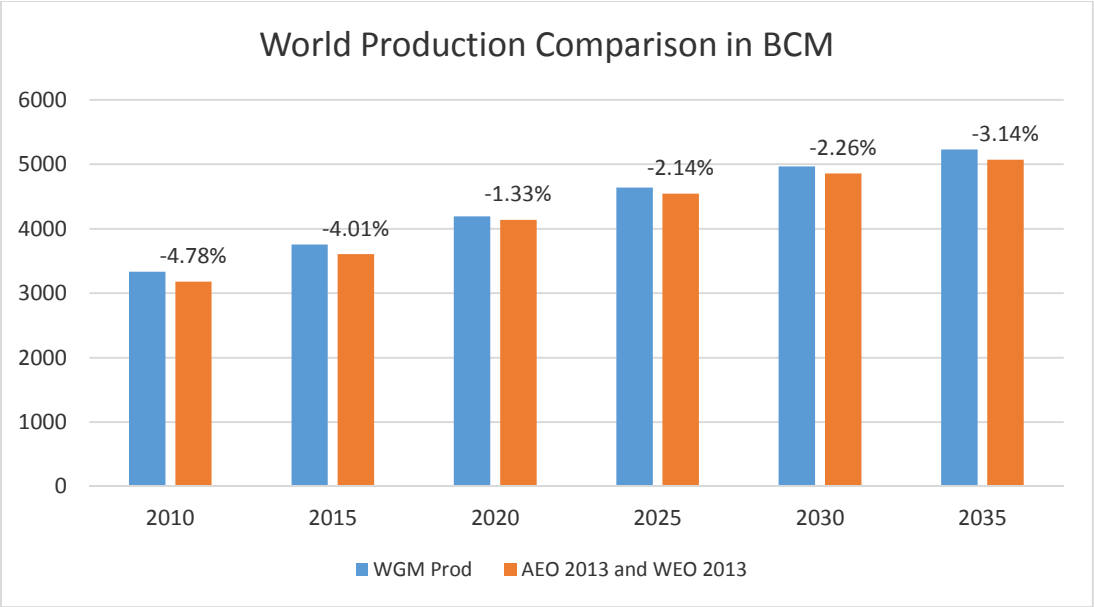

Figure 3-2 World Gas Model Base Case, world production comparison in Bcm and percentage price differences.

Under the Base Case, the gap between what North America consumes and produces narrows over time. In the year 2015, this region needs to import small amounts of gas to meet its consumption. Eventually, after 2020 North America becomes a net exporter as shown in Table 3-4. From this table, we see that there is an average growth rate in North American demand of about 4.37% over the time horizon.

Table 3-4 World Gas Model Base Case, North America Natural Gas Production and Consumption, Bcm.

	2010	**2015**	**2020**	**2025**	**2030**	**2035**
Production	875.1	959.9	1,060.7	1,126.2	1,154.6	1,194.4
Consumption	872.4	964.5	983.6	1,034.0	1,063.0	1,101.5

As shown in Figure 3-3, the Base Case indicates that regionally, wholesale prices will generally rise in the years 2010-2035 throughout the world. This reflects an increase in willingness to pay for natural gas by the consumer. This willingness is captured in WGM by the cost and price inflation factors. From Figure 3-3 it is interesting to note that the natural gas prices in China increase significantly from 2015 to 2020 due to a spike in demand for natural gas rising 114.9 Bcm from 154.8 Bcm to 269.7 Bcm.

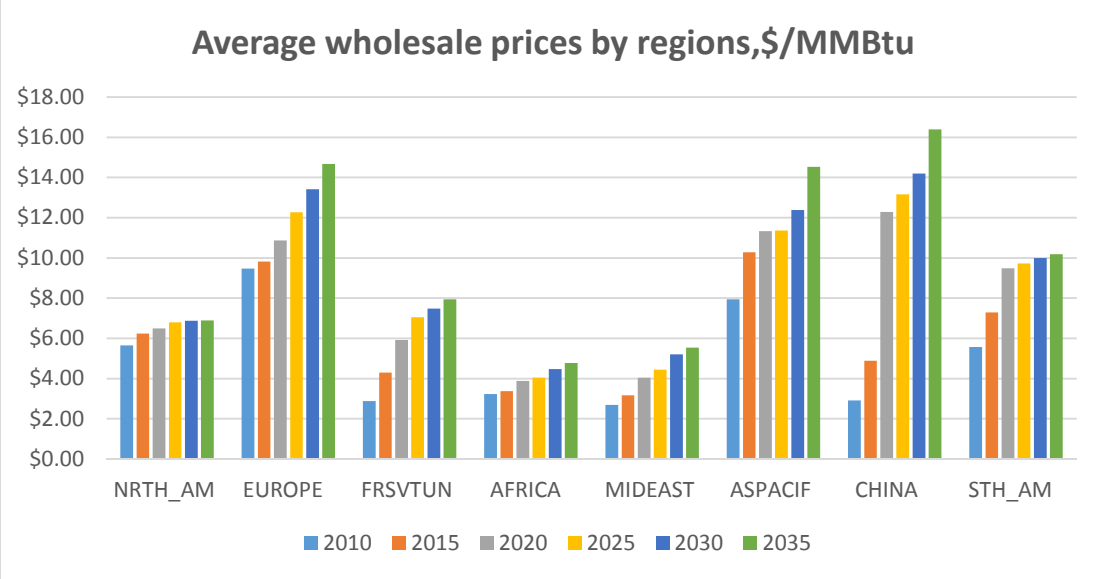

Figure 3-3 World Gas Model Base Case, average wholesale prices by regions, $/MMBtu

Table 3-5 shows that North American [18] wholesale prices only change slightly over the time horizon due to abundant shale gas resources (e.g., $6.89/MMBtu in 2035). China sees the highest 2045 prices of $17.46 because of high demands. It is interesting to note that the Japanese node [19] has the highest country-level prices but this nation is subsumed in the Asia Pacific region. The Former Soviet Union, Africa, and Middle

[18] North America includes Canada, Mexico, and the United States in the World Gas Model.
[19] In the World Gas Model, the Japanese node includes both Japan and South Korea, see Appendix 1 for more details.

East have the least increasing prices due presumably to their vast supplies. For comparison purposes, we compare the WGM prices to the EIA price forecasts in the New Policy Scenario (WEO, 2013) and find that the WGM North American prices are close to the United State prices in the New Policy Scenario ($6.89/MMBtu in WGM vs $6.50/MMBtu in WEO (2013)), but the WGM European prices are slightly higher $14.68/MMBtu vs $12.7/MMBtu, respectively.

Table 3-5. World Gas Model Base Case, Average Wholesale Prices by Regions, $/MMBtu.

	NRTH_AM	EUROPE	FRSVTUN	AFRICA	MIDEAST	ASPACIF	CHINA	STH_AM
2010	$5.66	$9.46	$2.88	$3.23	$2.69	$7.95	$2.92	$5.57
2015	$6.24	$9.82	$4.29	$3.37	$3.17	$10.28	$4.89	$7.29
2020	$6.50	$10.87	$5.91	$3.89	$4.04	$11.34	$12.29	$9.49
2025	$6.80	$12.26	$7.06	$4.04	$4.44	$11.36	$13.16	$9.73
2030	$6.88	$13.42	$7.49	$4.48	$5.20	$12.38	$14.20	$9.99
2035	$6.89	$14.68	$7.95	$4.77	$5.54	$14.53	$16.40	$10.18

In terms of world trade flows of natural gas, from Figure 3-4 the trend is clear. Europe is the largest importer of gas (pipeline and LNG) followed by the Asia Pacific region in general and then the Chinese node. Also, in all these three regions, the natural gas import trend is steadily increasing. By contrast, North America has a steady amount of exports from 2020-2035. Moreover, the Former Soviet Union is seen to have increasing amounts of exports with the Middle East and the Africa following the same trend.

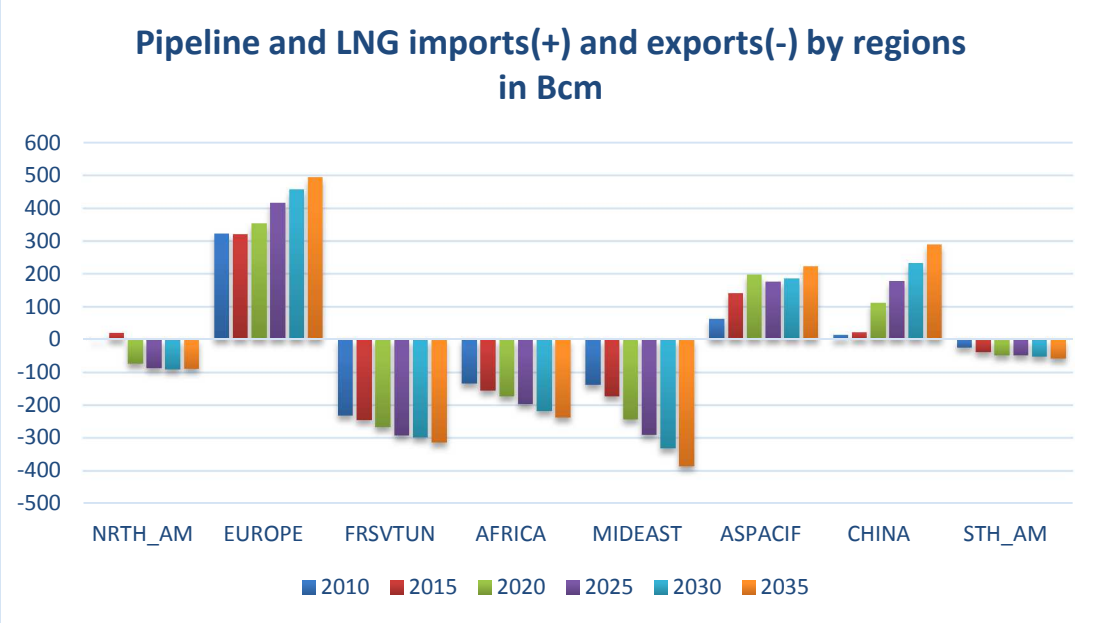

Figure 3-4 World Gas Model Base Case, Pipeline and LNG imports (+) and Exports (-) by Regions in Bcm.

Figure 3-5 displays LNG exports by country node with "L" meaning liquefier, see details for LNG import/export countries in Appendix 2. Qatar (L_QAT) dominates the LNG markets as indicated by its increasing amount of LNG exports over time. Algeria (L_ALG), Yemen (L_YMN), Trinidad & Tobago (L_TRI) also have an upward trend in LNG exports. On the other hand, Indonesia and Nigeria have declining exports. Moreover, Indonesian production decreases over time.

The Gulf of Mexico terminal (L_US7L) has the highest U.S. LNG exports of the three U.S. nodes with the other two being US west coast terminal (L_US9) and US east coast terminal (L_US5W). In 2035, the amounts exported from the Gulf of Mexico to global markets are approximately 59 Bcm, (Table 3-6). 12.39 Bcm of this figure comes from contracts (to Japan/S. Korea) with the remaining 46.82 Bcm supplied to Europe in the spot market; see details in Table 3-6. Also, the U.S. supplies 6.6 Bcm from its East

Coast terminal in 2035, or which 5.92 Bcm is under contract (2.92 Bcm to Japan/S.Korea and 3 Bcm to India), and 0.69 BCM is exported to France without contract. Lastly 6.65 Bcm is delivered to Japan/S.Korea from the U.S. west coast terminal without contract in the same year.

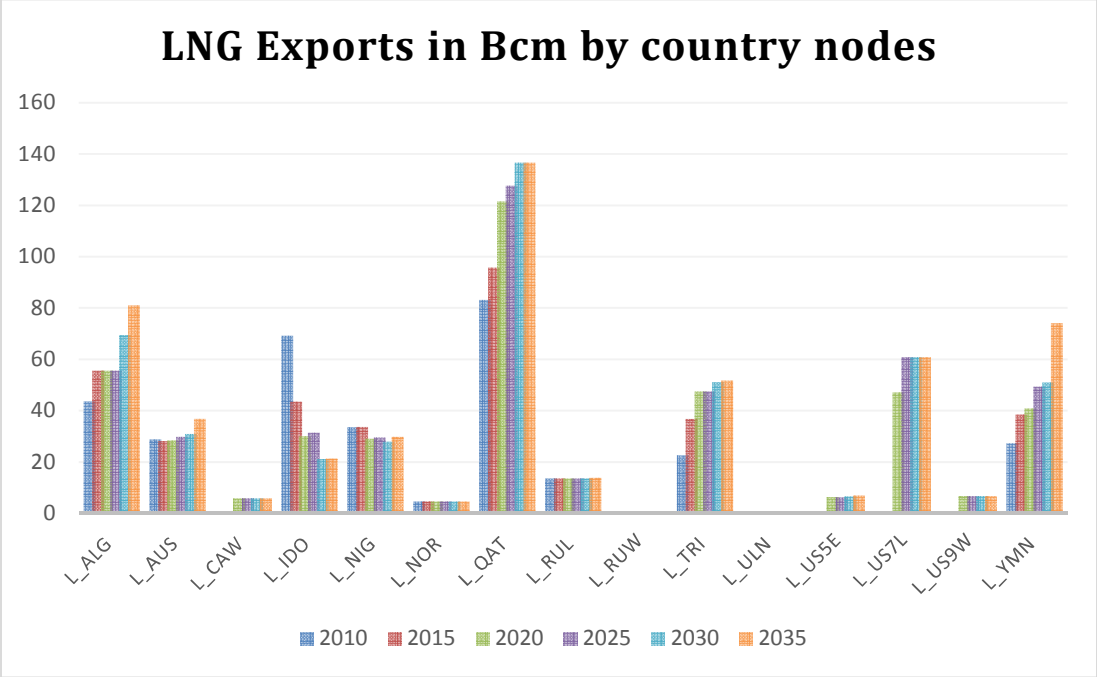

Figure 3-5 World Gas Model Base Case, LNG exports in Bcm by country nodes.

Table 3-6 World Gas Model Base Case, LNG exports from Gulf Coast terminal in Bcm for 2020 and 2035.

From	Year	To regasification terminals								Total
		Brazil	France	Germany	Italy	Japan	Netherlands	Poland	Spain	
U.S. Gulf of Mexico	2020	7.1	7.9	1.8	8	12.3	5.12	3.14	0	45.6
	2035	0	15.2	8.0	12.1	12.3	2.17	3.05	5.87	59.0

Finally, in order to measure the errors of the WGM after calibration, we compare its output versus consumption references (EIA, 2013) (EDF, 2013) (AIE, 2013). For those purposes, we consider the regional consumption between 2010 and 2035 and compare them with the references. It is important to note that the percentage difference is calculated by the reference value less the model output divided by the reference value.

Overall, there is an average model estimation error of 1.66% for consumption with a maximum error of 6.13% which indicates an excellent fit.

3.4.2 Panama Canal toll scenario: results

In this section, the hypothesis that the Panama Canal toll could affect the global gas markets is examined. Each of the tolls considered is compared against each other to gauge the magnitude of potential Panama Canal toll-induced effects. We pay attention to the results up to the year 2035 based on reliable data sources through that year. However, the WGM was run through 2050 with two additional time periods (2055 and 2060) thrown away to avoid the end-of-horizon bias.

First, regional prices are examined under the different scenarios. We look at the average wholesale prices of natural gas around the world by region for the year 2035. The first thing to realize is that most of the world is largely unaffected by the different Panama Canal toll levels as shown by the similar prices across all regions except Europe, Japan/S. Korea, and South America (Figure 3-6). The presence of LNG exports from the Atlantic basin (the U.S. and Trinidad & Tobago[20]), leads to lower prices in Japan/S. Korea as the Panama Canal toll decreases. (The zero and regular toll cases though provide identical Japanese node prices). The differences in Japan are about $1/MMBtu in considering the two extreme scenarios: Inf_Toll and Zero_Toll. However, the prices go in the opposite direction for Europe as a function of the counterfactual Panama Canal toll. As the Panama Canal toll increases, the gas prices in Europe decrease due

[20] We ignore the results from Eastern Canada because of the small size of the exports (0.73 Bcm/y) under contract.

to the shift of U.S. and Trinidad & Tobago LNG flows from Japan to Europe. In general, the U.S. and Trinidad & Tobago become the swing suppliers that can decide to export to either Japan or Europe depending on the transportation costs through the Panama Canal.

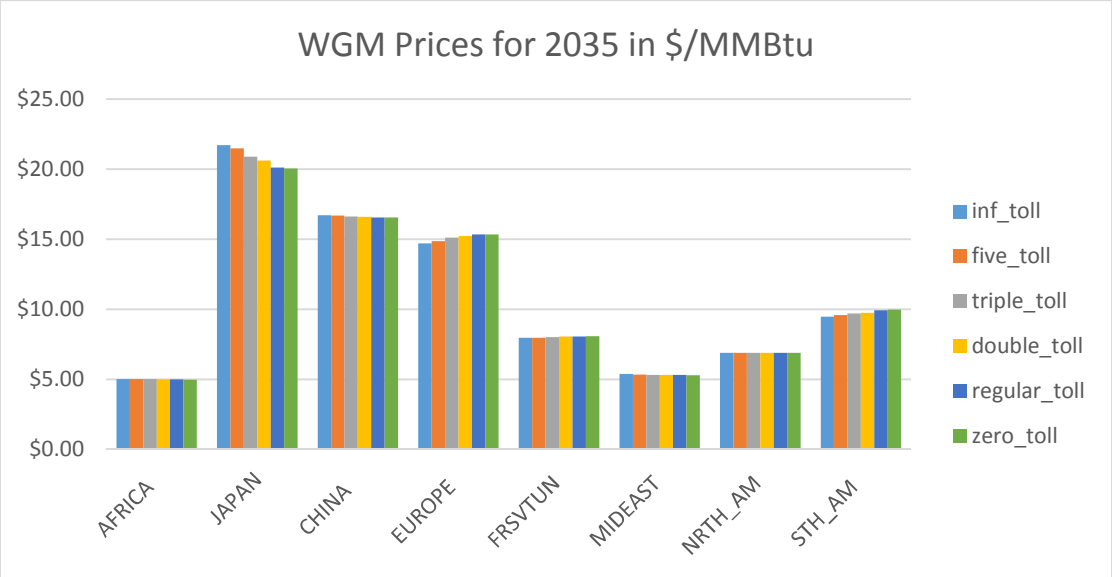

Figure 3-6 WGM prices for 2035 in $/MMBtu.

The production, however, is mostly constant across scenarios. The explanation is that the Panama Canal toll considered as part of the transportation cost only alters the flows among regions. Next, Figure 3-7 depicts regional consumption in Bcm for 2035. Regionally, consumption is barely changed for all scenarios. However, the consumption in the Asia Pacific and European regions (from a regional perspective) changes slightly depending on the Panama Canal toll level. In particular, when the toll increases, more supplies from the Atlantic basin (U.S. and Trinidad & Tobago) flow to Europe. Nonetheless, the flow reroutes to Japan when an inexpensive toll is present (not directly observable in Figure 3-7). The consumption in the Middle East is also affected by the level of the Panama Canal toll. The Middle East supplier exports less

when the Panama Canal toll is small, so more inexpensive gas is available for domestic consumption.

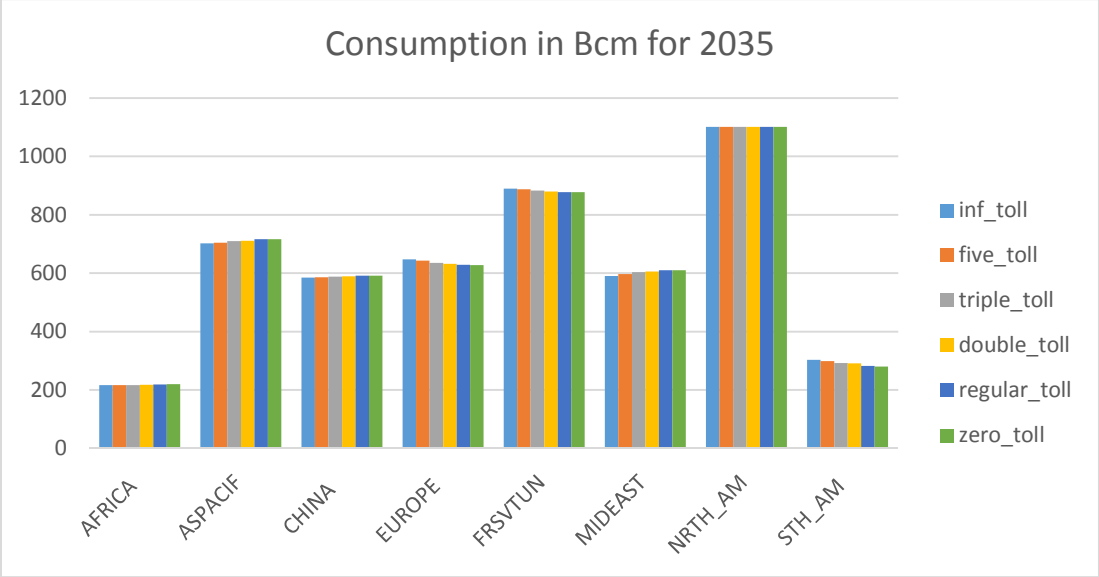

Figure 3-7 Consumption in 2035, in Bcm.

In 2035 for net worldwide imports and exports, the World Gas Model shows a significant reduction in exports, approximately 90 Bcm, from the Former Soviet Union under the Inf_Toll and Five_Toll scenarios (Figure 3-8). Particularly, the flows from Russia-West to Ukraine are reduced significantly when the toll increases. This reflects the side effects of the rerouted U.S. and Trinidad & Tobago gas to Europe in these two scenarios. LNG exports from the U.S. and Trinidad & Tobago are only sent to the following European country nodes: France, Netherlands, Spain, Italy, Germany and Poland. In addition, North American export levels remains unchanged for all scenarios.

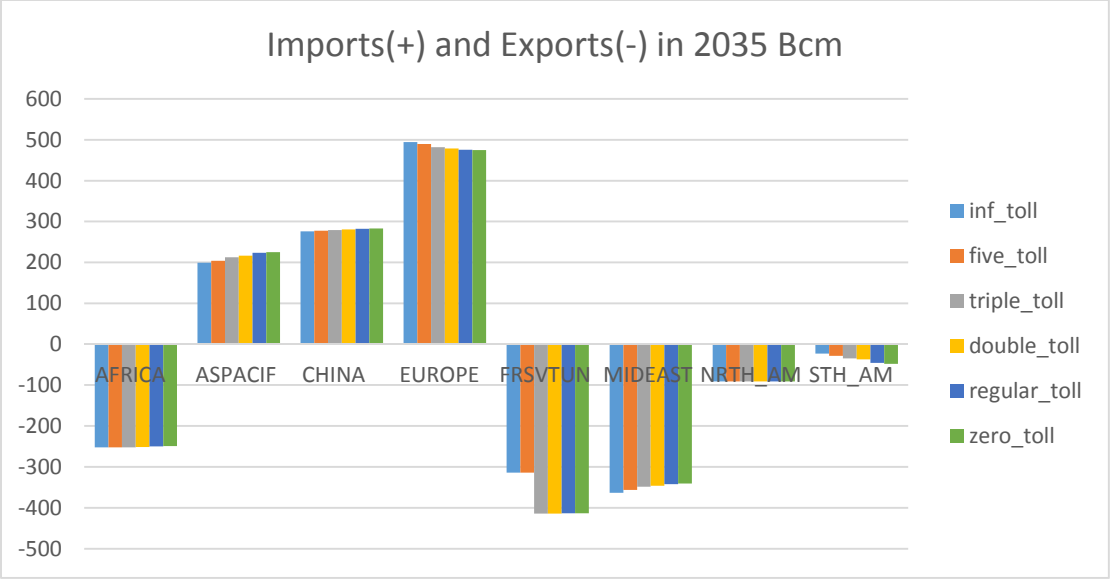

Figure 3-8 Imports (+) and Exports (-) in Bcm for 2035.

3.4.3 Analyses for LNG Markets: Liquefaction

For global LNG markets, Table 3-7 shows values under contract as well as export flows in the different scenarios relative to the total LNG liquefaction capacity arranged by liquefaction node. Additionally, Table 3-7 provides the details of liquefaction capacity utilization. As can be observed from Table 3-7, the worldwide LNG capacity under contract amounts to only about 40% (202.5 Bcm out of about 500 Bcm) in 2035 based on known contracts by the end of 2020, so there is a lot of capacity available for the spot market. Although Australia has the second largest LNG export capacity, the capacity used is only 16%-20% for all scenarios due to high relative liquefaction costs as compared to other LNG exporters (presumably due to cost overruns of construction) (Kelly, 2013). It is important to note that the major LNG exporting countries Qatar and Algeria have only a small share (approximately one third) of contracted exports and are relatively free to supply according to the economic principles laid down in the WGM.

On a global scale, there is a lot of spare liquefaction capacity in the system (approximately 60 % of total capacity).[21]

Table 3-7 LNG export capacity utilization, 2035.

	Capacity	Contracts	inf_toll	five_toll	triple_toll	double_toll	regular_toll	zero_toll
Algeria	148.9	27	61.4%	60.0%	57.2%	56.5%	56.1%	55.9%
Australia	194.2	17.2	22.3%	21.0%	19.0%	18.2%	16.8%	16.5%
E. Canada	0.9	0	85.4%	85.4%	85.4%	85.4%	85.4%	85.4%
W. Canada	7	1.9	84.5%	84.5%	84.5%	84.5%	84.5%	84.5%
Indonesia	163.9	20.5	16.1%	15.0%	13.4%	13.0%	11.9%	11.7%
Nigeria	157	9.6	21.5%	21.5%	21.5%	20.6%	19.7%	19.6%
Norway	31	4	14.8%	14.8%	14.8%	14.8%	14.8%	14.8%
Qatar	381.8	65.7	39.5%	38.4%	37.1%	36.5%	35.3%	35.1%
S. Russia	46	15.5	34.0%	33.9%	33.3%	33.0%	31.9%	31.7%
W. Russia	20.1	0	0.0%	0.0%	0.0%	0.0%	0.0%	0.0%
Trinidad	125.6	10.3	15.1%	19.0%	23.1%	24.7%	30.6%	32.2%
Alaska	0	0	100%	100%	100%	100%	100%	100%
E.U.S.	8.2	7.5	84.5%	84.5%	84.5%	84.5%	84.5%	84.5%
U.S. Gulf	72	15.6	84.5%	84.5%	84.5%	84.5%	84.5%	84.5%
W. U.S.	7.9	0	9.4%	9.4%	9.4%	9.4%	9.4%	9.4%
Yemen	54	7.7	73.3%	70.4%	67.0%	67.0%	67.0%	67.0%
Total	1482.5	202.5	34.1%	33.6%	32.8%	32.4%	32.1%	32.1%

3.4.4 Analyses for LNG Markets: Regasification

The first thing to realize is that there is a lot of spare capacity (about 50% of total regasification capacity) for all scenarios in 2035 (Table 3-8). Interestingly, Table 3-8 suggests that the total usage of regasification goes up slightly when the Panama Canal toll increases due to many factors besides the Panama Canal and varying by country.

[21] This number is calculated by the total capacity less used capacity divided by the total capacity (Table 7).

Also, Inf_Toll and Fivefold_Toll show the highest capacity usages. One explanation is that the high toll forces the U.S. and Trinidad and Tobago to send more LNG to Europe while Middle East exporters can also supply more to Asia with less competition from the Atlantic Basin exporters. This hypothesis is supported by the increase of the utilization rate of LNG import terminals in Europe when the toll is expensive (Table 3-8). The Japan /South Korea node has the highest utilization rate among all countries (nodes) (over 60%). This reflects this region's reliance on LNG to satisfy its demand.

Table 3-8 LNG regasification capacity utilization in percent for 2035.

	Capacity	**Inf_toll**	**Five_ toll**	**Triple_ toll**	**Double_ toll**	**Regular_ toll**	**Zero_ toll**
China	92.9	74.7%	74.0%	74.5%	74.8%	75.7%	75.8%
France	62.1	57.8%	57.8%	55.7%	48.5%	38.6%	37.5%
Germany	9.3	93.4%	74.2%	29.5%	19.2%	8.6%	5.9%
India	59.8	22.5%	22.5%	22.5%	22.5%	22.5%	22.5%
Italy	51.8	45.1%	41.1%	31.8%	26.5%	24.0%	23.6%
Japan	415.3	63.6%	64.0%	64.9%	65.4%	66.2%	66.3%
Mexico	26.1	45.6%	45.6%	45.6%	45.6%	45.6%	45.6%
Netherlands	30.6	22.8%	15.8%	6.2%	11.7%	19.1%	19.6%
Poland	7.4	51.9%	31.4%	1.8%	1.3%	0.0%	0.0%
Spain	99.4	21.8%	20.5%	18.6%	17.6%	16.9%	17.0%
Turkey	23.1	25.1%	22.5%	22.5%	22.5%	22.5%	22.5%
United Kingdom	63.7	27.9%	27.9%	27.9%	27.9%	27.9%	27.9%
East USA	47.5	25.6%	25.6%	25.6%	25.6%	25.6%	25.6%
Total	988.9	50.0%	49.2%	47.9%	47.3%	47.1%	47.0%

3.4.5 Analyses for LNG Markets: LNG Flows

A closer look into the details of the LNG flows reveals that the U.S. LNG exports are stable for all scenarios. The U.S. exports gas regardless of the toll the only difference being the destinations. A further analysis indicated that the limiting factor is the U.S. production capacity. As for other LNG exporting regions, Figure 3-9 shows that LNG exports from Algeria, Australia, Nigeria, Qatar, and Yemen decline as the Panama

Canal toll decreases. These exporters have a significant market share in Asian markets, especially in Japan and South Korea. The displacement of sales from Algeria, Australia, Nigeria, Qatar, and Yemen to Japan is caused by the presence of the U.S. and Trinidad & Tobago gas at the Japanese node. One would expect Qatar, Indonesia, and Australia would shift their sales to China however China consumes gas from domestic production and pipeline imports from Russia and Kazakhstan.

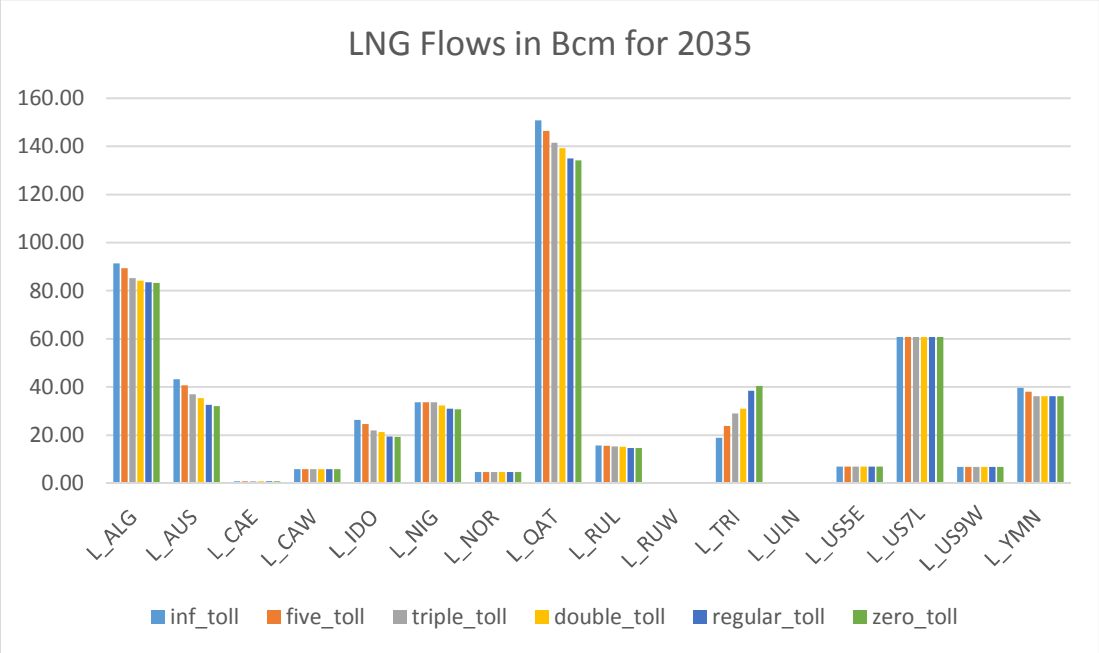

Figure 3-9 LNG Flows in Bcm for 2035.

3.4.6 U.S. LNG Exports from the Gulf of Mexico

Next, we analyze the U.S. LNG flow pattern originating from the Gulf of Mexico. It is important to note that we allow the maximum export capacity of 72 Bcm per year for U.S. Gulf of Mexico (L_US7L) and the numbers presented in Figures 3-10 and 3-11 are net flows taking into account loss along the gas supply chain, e.g., liquefaction and LNG shipping losses with the loss factors.

Surprisingly, the U.S. LNG exports are the same between the Zero_Toll and Regular_Toll scenarios. This observation is supported by similar flows (58.4 Bcm) to Japan/S. Korea for the Zero_Toll and Regular_Toll cases for both 2020 and 2035 (Figures 3-10 and 3-11). However, the amount of U.S. LNG to Japan starts declining when the Panama Canal toll is set more than the regular toll. The same situation is more pronounced when the triple toll is applied. Lastly, even the toll is set to be a very high number, the U.S. still exports approximately 12 Bcm to Japan/S. Korea because of a lower bound contract constraint.

In term of flows to Europe, the U.S. exports from the Gulf of Mexico to Europe are 13.6 Bcm in 2020 under the Inf_Toll scenario but 46.62 Bcm in 2035 under the same scenario. The explanation for increased flows over time is that European prices increase up to $16 /MMBtu in 2035 from $11 /MMBtu in 2020. However, the U.S. gas prices are approximately $6/MMBtu for both years (Figure 3-6). The wider gap between the U.S. and European prices over time means potentially more U.S. profit by sending gas to Europe.

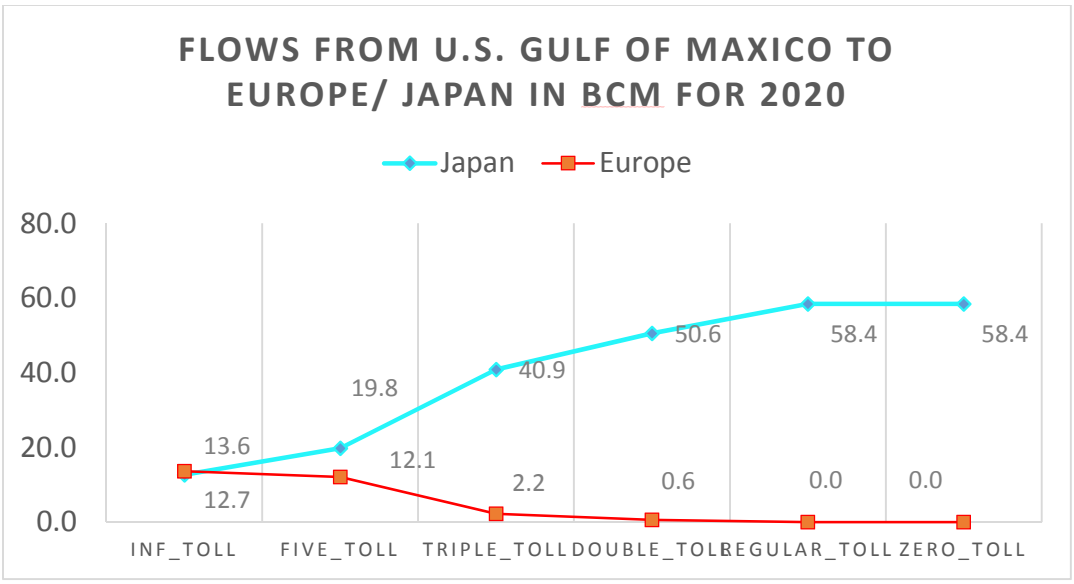

Figure 3-10 LNG exports from U.S. Gulf of Mexico (US7) Bcm, 2020

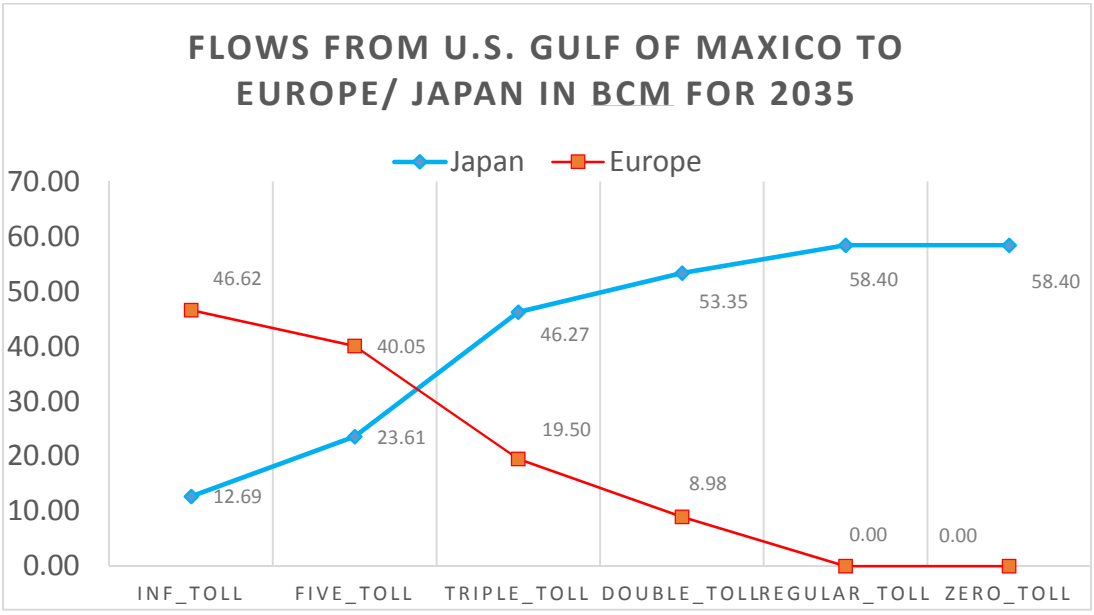

Figure 3-11 LNG export from U.S. Gulf of Mexico Bcm, 2035.

3.4.7 LNG Exports from Trinidad and Tobago

Trinidad & Tobago LNG flows to Japan/S. Korea are more sensitive to the Panama Canal toll as compared to the U.S. flow pattern. This hypothesis is supported by declining flows to the Japanese node starting from the Regular_Toll scenario as compared to the Zero_Toll scenarios; see Figures 3-12 and 3-13. The economic

interpretation is that in 2035, Trinidad & Tobago has higher domestic prices ($ 8.06/MMBtu) as compared to the U.S. domestic prices ($5.66/MMBtu) so that increasing Panama Canal tolls will lower the profit mark-up for Trinidad and Tobago and result in less LNG flows to Japan/S.Korea. On the other hand, increased Panama Canal tolls have less of an effect on the U.S. flows due to larger price differences between U.S. and Japan/S.Korea. The flows to Japan/S. Korea drop significantly, reaching zero, after the Regular Toll is applied for both 2020 and 2035. Trinidad &Tobago is considered as a marginal supplier for Europe because the flows there are based on the spot market; see Table 3-7 for the LNG contracts for Trinidad & Tobago.

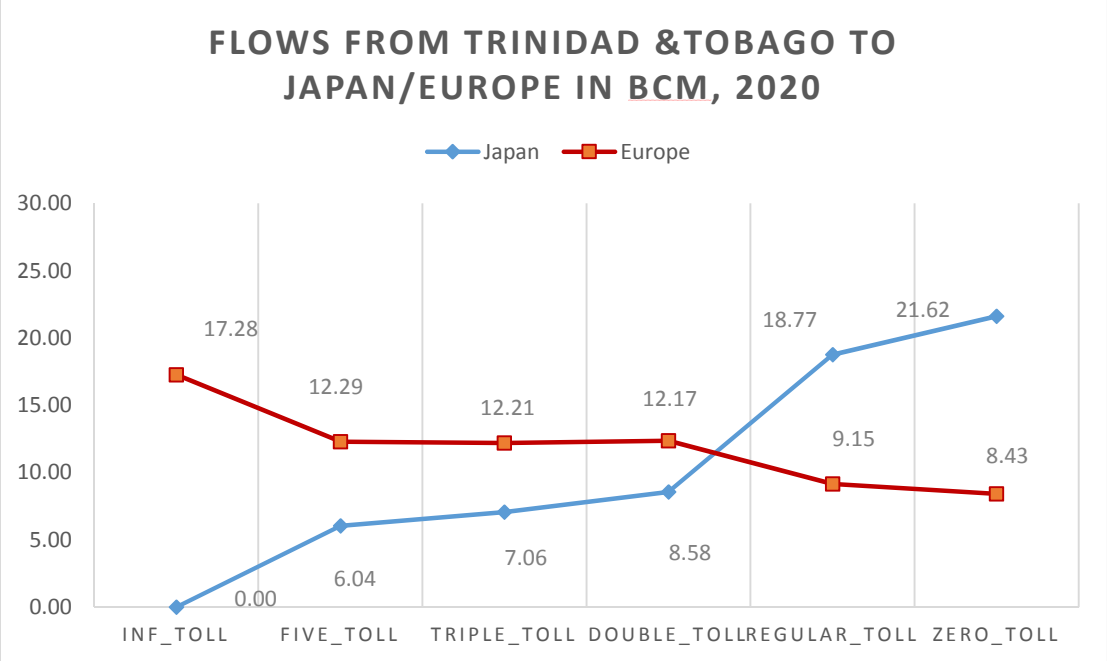

Figure 3-12 LNG flows from Trinidad and Tobago Bcm, 2020.

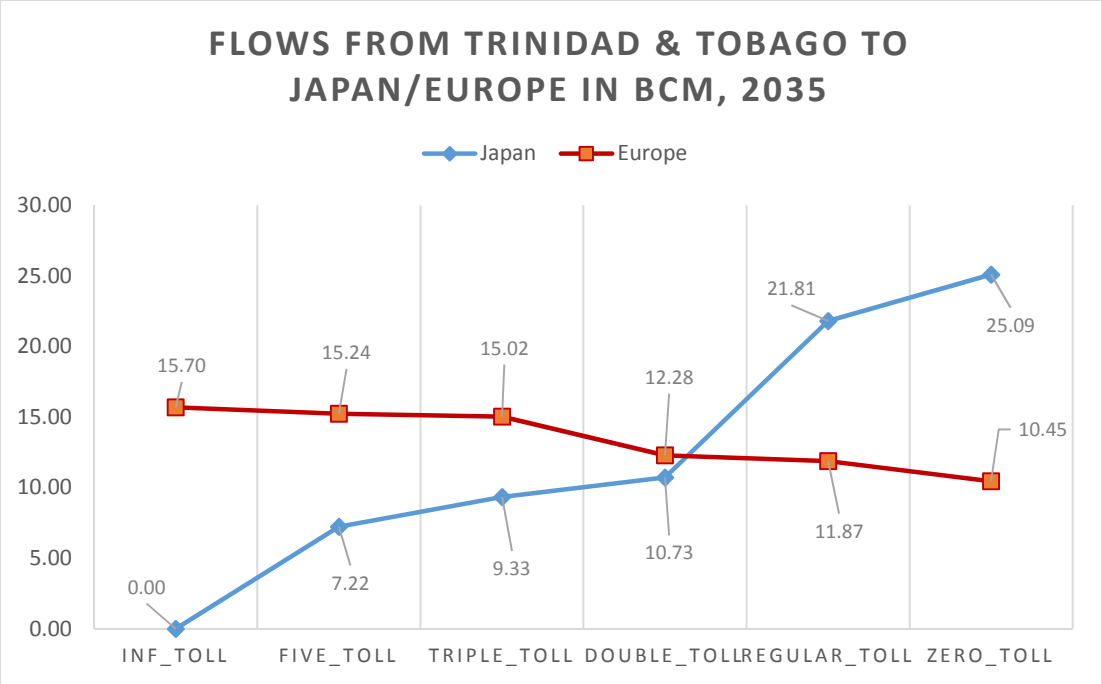

Figure 3-13 LNG flows from Trinidad and Tobago Bcm, 2035.

3.4.8 Market Share by Supplier for the Japanese/South Korean Markets

For 2035, the Japanese node relies on LNG. Table 3-9 gives the details of the supply structure of this node for all Panama Canal scenarios. In the Inf_Toll and Fivefold_Toll scenarios, Qatar is the largest exporter, followed by Australia and Yemen. However, the U.S. (all three U.S. nodes) becomes the largest supplier under the Double_Toll and Regular_Toll scenarios as shown in Table 3-9. One thing to realize is that the U.S. and Qatar supply almost similar quantities to Japan under the Triple_Toll scenario so that this toll represents the "break-even point" in the competition between Qatar and the U.S. to supplying LNG to this market. In terms of an economic interpretation, given the U.S. domestic prices are about $6/MMBtu plus a WGM liquefaction cost of $2.35 /MMBtu and the transportation cost depending on scenarios, the U.S. is competitive to

challenge other suppliers, and eventually will have the largest market share if the toll is inexpensive e.g., less than triple toll of $1.05/MMBtu .

Figure 3-14 compares two scenarios for the Japanese imports by source in 2035. The U.S. becomes the major exporter to the Japanese node with increased sixteen percentage points (Figure 3-14). The imports by Trinidad and Tobago also go up five percentage points. These changes slightly displace other suppliers' shares a bit, but Qatar is the most to suffer due to a six percentage point loss of market share. The results indicate that the U.S. and Trinidad & Tobago LNG displace the spot market sales from Qatar. In fact, 66% of the total Qatari supplies to Japan/S.Korea are the sales from the spot market. The Panama Canal introduces more suppliers to increase the competitiveness in the Japan/S.Korea market so that the spot prices are lower and result in the displacement of existing supplier's sales.

Lastly, Qatar and Yemen are sensitive to LNG exports from the Atlantic basin.

Table 3-9 Natural gas exports to Japan/South Korea by suppliers Bcm, in 2035.

Country	**Inf_ toll**	**Five_ toll**	**Triple_ toll**	**Double_ toll**	**Regular_ toll**	**Zero_ toll**
Algeria	51.04	48.39	43.67	41.04	36.82	36.13
Australia	38.16	35.65	31.94	30.39	27.59	27.05
Canada East	0.76	0.76	0.76	0.76	0.76	0.76
Canada West	5.80	5.80	5.80	5.80	5.80	5.80
Indonesia	15.60	13.75	11.19	10.51	8.74	8.51
Nigeria	24.22	24.22	24.22	22.89	21.23	20.79
Qatar	56.46	53.49	48.70	46.15	41.81	41.09
Russia	10.41	10.35	10.11	9.96	9.46	9.35
Trinidad	0.00	7.22	9.33	10.73	21.81	25.09
US East Coast	3.00	2.93	2.93	2.93	3.00	3.33
US Gulf of Mexico	12.69	18.67	38.35	48.43	58.40	58.40
US West Coast	6.65	6.65	6.65	6.65	6.65	6.65

Yemen	38.55	37.05	35.27	34.50	32.03	31.66
Total Supply	263.34	264.94	268.91	270.74	274.11	274.62

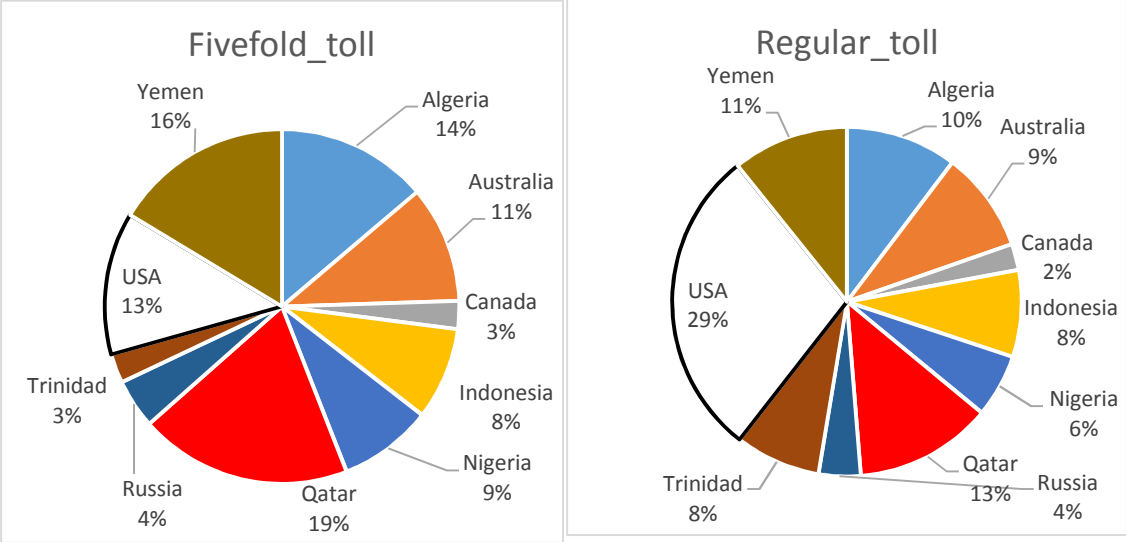

Figure 3-14 Percent of imports to Japan/South Korea in 2035 (a) the Five_Toll scenario (b) Regular Toll scenarios.

3.4.9 Dynamics of Flows across the Regions

This section analyzes and compares the effect of the tolls on the regional flows. We compare three main scenarios, Regular_Toll, Triple_Toll, and Fivefold_Toll. It is important to note that the U.S. LNG flows are the total from three locations, the West Coast (L_US9), the Gulf Coast, (L_US7) and the East Coast (L_US5).

There are interesting dynamics in the competition to supply both the Japanese node (Japan and South Korea) and Europe. One group of suppliers is the Atlantic Basic (the U.S. and Trinidad & Tobago). The other group is composed of: the Middle East, Africa, and Russia. What can be observed from Figures 3-15-3-17 is the following.

An increased Panama toll induces LNG exports from U.S. and Trinidad & Tobago to Europe rather than to Japan, simultaneously increasing the flows from the Middle East

and Africa to Japan to compensate. This hypothesis is seen by flows to Japan from the Middle East and Africa. Under the Regular_Toll scenario in 2035, the U.S. and Trinidad & Tobago export a total of 68.05 Bcm and 21.8 Bcm to Japan (Japan and South Korea), respectively. However, the Middle East and Africa send 73.8 Bcm and 58.0 Bcm to the same destination (Figure 3-15). Under the Triple_Toll, the Middle East and Africa increase their flows up to 83.9 Bcm and 67.8 Bcm to the Japanese node, but the U.S. and Trinidad & Tobago drop their flows to 47.9 Bcm and 9.3 Bcm (Figure 3-16). The situation is even more pronounced under the Fivefold_Toll. The flows from the U.S. and Trinidad & Tobago reroute to Europe as the Panama Canal toll increases, displacing some flows from existing suppliers (i.e., the Middle East, Africa, and Russia). In 2035 the U.S. and Trinidad & Tobago export, respectively, 0.69 Bcm and 11.8 Bcm to Europe under the Regular_Toll while Africa, Russia, and the Middle East export 37.0 Bcm, 346.4 Bcm, 30.8 Bcm, respectively, see Figure 3-15. Under the Threefold_Toll, the U.S. and Trinidad boost their flows up to 20.1 Bcm and 15.2 Bcm to Europe but the flows from Russia, Africa, and Russia are slightly displaced. Lastly, the U.S. still exports even more 40.74 Bcm under Fivefold_Toll, see Figure 3-17.

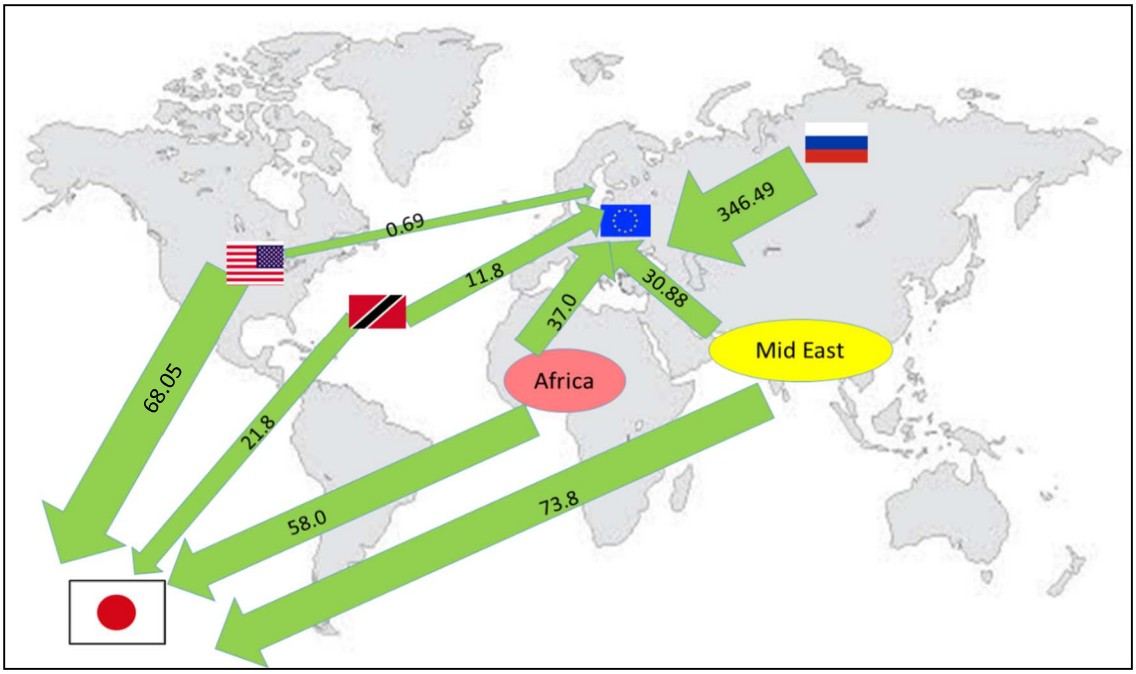

Figure 3-15 Dynamics of flows: Regular Tariff scenario, flows in Bcm for 2035.

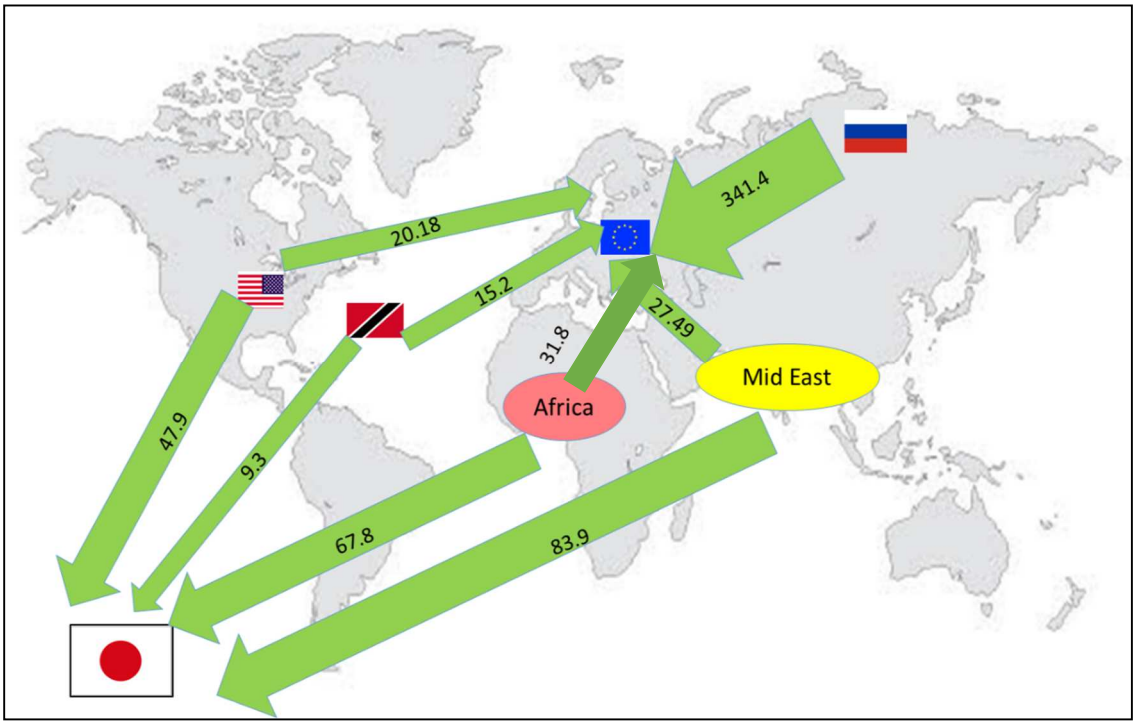

Figure 3-16 Dynamics of flows: Triple Tariff scenario, flows in Bcm for 2035.

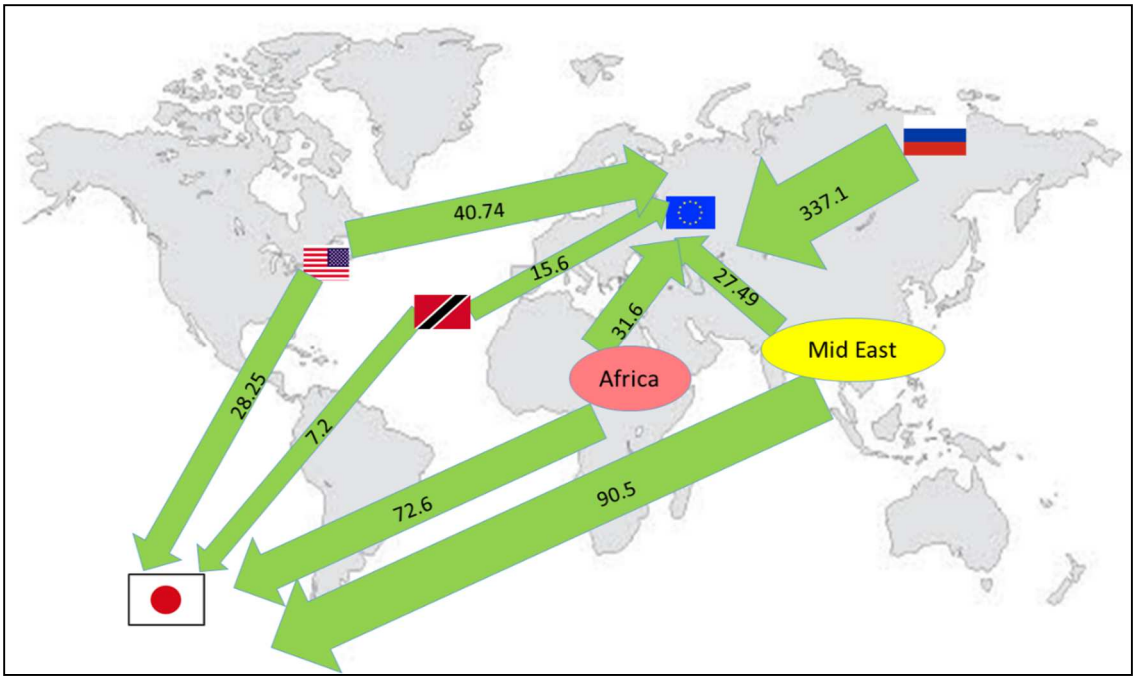

Figure 3-17 Dynamics of flows: Fivefold Tariff Scenario, flows in Bcm for 2035.

3.4.10 European Gas Market Analysis

For 2035, Europe relies to a large extent on imports and only one fourth of the total consumption is supplied from domestic production (about 25 % or 150 Bcm out of 620 Bcm of total supplies). Table 3-10 gives the details of the supply sources for Europe. The European production and storage levels are almost constant for all scenarios. The imports by LNG increases as the Panama Canal toll increases. The LNG imports also displace the imports by pipeline. For example, in the Five_Toll scenario, the imports by pipeline increase from 89.76 Bcm to 106.74 Bcm (as compared to the Triple_Toll scenario), but the imports by pipeline decline from 392.19 to 383.09 Bcm.

Table 3-10 European Gas Market in 2035.

	inf_ toll	**five_ toll**	**triple_ toll**	**double_ toll**	**regular_ toll**	**zero_ toll**
Total consumption in Europe	647.32	642.89	635.06	631.98	628.59	628.19
Total supply to Europe	647.32	642.89	635.06	631.98	628.59	628.19
Domestic Production	153.95	153.97	154	154	154.02	154.02
Pipeline Imports	378.41	383.09	392.19	396.4	399.72	400.29
LNG Imports	115.86	106.74	89.76	82.47	75.7	74.73
Storage	-0.85	-0.93	-0.9	-0.88	-0.91	-0.92

Table 3-11 shows that Russia is the largest exporter to Europe, followed by Norway and Algeria. The U.S. trader has a significant share, 46.21 Bcm and 39.78 Bcm under the Inf_Toll and Five_Toll scenarios, respectively, and displaces a small portion of supplies from Algeria, Kazakhstan, Russia, and Yemen. Norway does not only export via the direct route through the North Sea (26 Bcm), but also via the continent (via France and the Netherlands; see Table 3-12 for more detail). The detailed model structure in WGM allows separation of physical flows from sales flows, with the latter possibly going further than to the next neighboring country. Hence, we can observe Norwegian sales to the UK that are transported from Norway to the continent (France and Netherlands) and then from the continent to the UK. Table 3-12 suggests that the Nord Stream pipeline (N_RUW-N_GER) is utilized at the maximum capacity[22] (95.31 Bcm) whereas the South Stream pipeline (N_RUW-N_ROM) is almost idle. Interestingly, the flows from Ukraine to Poland (N_UKR-N_POL) and Russia to

[22] Nord Stream starts operating in 2015 with capacity of 55 Bcm/y however this pipeline is expanded over time so that the capacity reaches 95.31 Bcm/y in 2035.

Poland (N_RUW-N_POL) considerably decrease when the Panama Canal toll increases. This is likely because Poland imports more supply from LNG using the new terminal (Polski Terminal) so that it has a significant reduction in flows from Ukraine and Russia. This implies that Poland can increase security of gas supply as well as diversify its suppliers as the Panama Canal toll increases. Next, at the end of Table 3-12 we see that the flows from Poland to Germany also decline by about a half when the Panama Canal toll increases. This reflects that not only Poland benefits from U.S. gas but also other countries and Poland has more alternatives besides Russian gas.

Table 3-11 Supplies by traders to Europe in 2035.

	inf_toll	five_toll	triple_toll	double_toll	regular_toll	zero_toll
T_ALG	117.47	119.73	123.69	126.45	129.95	130.26
T_FRA	0.04	0.04	0.04	0.04	0.04	0.04
T_GER	0.04	0.04	0.04	0.04	0.04	0.04
T_ITA	0.04	0.04	0.04	0.04	0.04	0.04
T_KZK	65.57	66.69	68.80	69.87	71.04	71.21
T_NED	16.06	16.08	16.09	16.08	16.07	16.06
T_NIG	12.15	12.42	13.22	13.49	14.27	14.52
T_NOR	114.21	114.22	114.24	114.24	114.26	114.26
T_POL	0.04	0.04	0.04	0.04	0.04	0.04
T_QAT	90.82	90.81	90.75	90.71	90.78	90.73
T_ROM	0.04	0.04	0.04	0.04	0.04	0.04
T_RUS	154.59	155.63	158.17	160.09	161.31	161.60
T_SPA	0.04	0.04	0.04	0.04	0.04	0.04
T_TRI	14.72	12.02	14.93	15.36	11.61	10.23
T_TRK	0.04	0.04	0.04	0.04	0.04	0.04
T_UKD	15.20	15.20	15.20	15.20	15.11	15.10
T_USA	46.21	39.78	19.70	9.43	0.68	0.34
T_YMN	0	0	0	0.76	3.20	3.56
Total	647.28	642.85	635.03	631.95	628.54	628.14

Table 3-12 Selected flows by pipelines in Bcm 2035.

Start	End	inf_ toll	five_ toll	triple_ toll	double_ toll	regular_ toll	zero_ toll
	N_FRA	16.67	16.53	16.71	17.15	17.38	17.38
	N_GER	42.40	42.40	42.40	42.40	42.40	42.40
	N_NED	12.54	12.88	12.88	12.88	12.88	12.88
	N_POL	9.71	9.88	10.02	9.87	9.57	9.55
N_NOR	N_UKD	26.95	26.64	26.40	26.14	26.27	26.29
	N_ITA	61.99	63.83	66.23	66.72	66.97	66.92
N_ALG	N_SPA	40.74	41.54	43.76	44.52	45.29	45.42
	N_GER	95.31	95.31	95.31	95.31	95.31	95.31
	N_POL	36.48	36.91	38.83	39.45	41.15	41.45
	N_ROM	0.00	0.00	0.00	0.00	0.00	0.00
N_RUW	N_TRK	25.73	25.82	26.01	26.12	26.05	26.05
N_KZK	N_TRK	29.33	29.55	29.57	29.58	29.69	29.71
	N_POL	5.17	6.57	9.47	11.98	12.77	12.95
N_UKR	N_ROM	24.61	24.65	24.46	24.44	24.47	24.49
	N_FRA	28.16	28.34	28.31	29.87	31.12	31.26
	N_ITA	22.15	22.82	24.56	25.94	26.36	26.47
	N_NED	11.99	12.19	13.16	13.21	13.74	13.89
N_GER	N_ROM	6.31	6.31	6.06	5.84	5.70	5.68
N_POL	N_GER	8.97	10.10	14.13	17.14	19.39	19.81

3.5 Conclusions

The World Gas Model (WGM) has been used to evaluate the effect of the Panama Canal transit fees on natural gas markets worldwide. WGM is a game theoretic market equilibrium model using forty-two consumption country nodes with multiple market players per country. Multiple sets of scenarios were employed to analyze the resulting prices, quantities, flows, and LNG. The results show that the transit fees affect the flow pattern especially for LNG exports from the U.S. and Trinidad and Tobago. In addition, the wholesale gas prices in Japan/South Korea and Europe are significantly affected by the level of the Panama Canal toll.

Chapter 4: Panama Canal Expansion: Will Panama Canal be a Game Changer for LNG Exports to Asia?

The aim of this chapter is to investigate the effects of the Panama Canal capacity level for LNG shipping and LNG exports from the Gulf of Mexico. The analysis was accomplished by my modifying the WGM 2012 model to include additional market agents such as liquefiers, regasifiers, LNG transportation operators, and a canal operator in addition to gas producers, traders, storage operators, an integrated pipeline operator, and marketers. The mathematical formulation is provided as an Appendix to chapter 4. The expansion of market participants was important because the new model-WGM 2014 can capture the limitation of LNG shipping, capacity of Panama and Suez canals, and the investment for future capacity of LNG shipping (tankers).

4.1 Introduction

The Panama Canal is a major waterway connecting the Atlantic and Pacific Oceans and accommodates more than 14,000 transits per year (Canal de Panama, 2012). However, the Panama Canal is not a significant feature of the liquefied natural gas (LNG) market. Only 21 of the 370 LNG tankers worldwide currently in operation can pass through the Panama Canal, but none of these tankers have done so because LNG tankers have special containment systems that require larger and deeper waterways (Alaskan Natural Gas Transportation Project, 2012). Nonetheless, the canal expansion, which is expected to be completed by 2015, could allow more than 80% of LNG tankers to use the waterway. The newly upgraded canal will provide a shorter distance for LNG trade

between the Atlantic and Pacific basins and thus could change the landscape of the global LNG trade. In particular, the Panama Canal will allow for LNG trade between the two basins at lower transportation costs due to decreased shipping distances. In light of the anticipated upgrades, the impact of the expanded Panama Canal on global LNG trade, especially on U.S. LNG exports, has been asked.

Recently, hydraulic fracturing and horizontal drilling enabled the gas extraction from shale formation economically. In fact, shale gas production in the U.S. increased fivefold from 2006 to 2010. Furthermore, shale gas accounted for 23% of the total U.S. natural gas production in 2010 (EIA, 2011). The increase in domestic natural gas production has depressed domestic natural gas prices and has caused a large disparity between gas prices in the U.S. and those elsewhere in the world. In the near future, the U.S. will not only be gas self-sufficient but may also be an LNG exporter. As a result, several natural gas producers are eager to apply for natural gas export licenses (Ratner, 2011).

The U.S. is more attractive and favorable than other LNG suppliers for several reasons. First, because of the negative effects of Russian-Ukrainian gas disruptions in the past, U.S. LNG would be considered as an alternative for increasing supply security and energy independence in Europe due to the close proximity of the U.S. to Europe. Likewise, Asian LNG buyers, such as Japan, South Korea, and India, aim to diversify their suppliers. U.S. LNG will increase the security of supply in Asia. Second, U.S. LNG sources are more reliable due to the political stability of the country compared to other exporters, such as African producers. For example, supplies have been interrupted by political instability in Egypt (EIA, 2013; ERNST & Young, 2012). Third, several

prominent LNG exporters, such as Indonesia and Malaysia, have decreased their output over time, prompting LNG consumers to search for new LNG sources, especially because many existing long-term contracts will end between 2014 and 2016. Lastly, North American LNG pricing is based on hub prices, which recently are lower than traditional oil index prices. As a result, U.S. LNG exports could affect global LNG prices and could bring more competition to global LNG markets. Moreover, some countries might benefit from U.S. LNG exports, while others might be disadvantaged.

The U.S. Department of Energy (DOE) has granted several NON-FTA licenses allowing natural gas companies to export gas globally (DOE, 2013). As of October 2013, the total U.S. LNG export capacity to NON-FTA countries was 57.8 Bcm/y; of that capacity, 55.6 Bcm/y comes from liquefaction plants in the Gulf of Mexico and 2.2 Bcm/y comes from plants located on the East Coast. Additional export applications with a total capacity of 279 Bcm/y are under consideration by the DOE. Due to these export capacities and lower gas prices, the U.S. will be more competitive in future LNG markets. Moreover, experts believe that the Panama Canal widening will improve the competitive position of LNG exports from the U.S. Gulf Coast and provide buyers in Asia with more opportunities to source supply. However, questions remain regarding how much LNG will flow through the canal, who will use the canal, and who will be positively and negatively impacted by the new route option given unknown capacity and pricing allocated for LNG shipping.

The aim of this chapter is to investigate the effects of the Panama Canal capacity level for LNG shipping and LNG exports from the Gulf of Mexico. The mathematical formulation is provided as an Appendix to chapter 4. The expansion of market

participants was important because the new model-WGM 2014 can capture the limitation of LNG shipping, capacity of Panama and Suez canals, and the investment for future capacity of LNG shipping (tankers). The main issue we analyze here is the capacity of canal allocated to gas shipment. The results can give some insights on how much gas will pass canal to Asian market. In term of congestion prices, it is just the measurement of economic efficiency not a true congestion prices. The Panama Canal booking system is very complicated because they also assign priority for type of ships as well as goods not necessarily related to natural gas.

This chapter also analyzes the impact on LNG shipping economics as well as impacts on global gas prices. In particular, this chapter identifies how much LNG will flow through the Panama Canal given different capacities, who will use the Panama Canal, and what will be the advantages and disadvantages of the expanded capacity of the Panama Canal. Using a mixed complementarity problem (MCP) market equilibrium approach, the 2014 World Gas Model (WGM) provides insightful results for natural gas production levels, consumption, prices, and future expansions of natural gas infrastructure capacity given different market conditions. The results offer policy planning officials and decision makers a better understanding of future LNG markets.

Recently, several equilibrium models have been developed to describe the structure of international gas trade. Some of these models cover specific regional trades (e.g., Europe and North America), including GAMMES (Abada et al., 2011), GASTALE (Lise and Hobbs, 2009), GASMOD (Holz et al., 2008; Holz, 2009), (Gabriel et al., 2005a), (Gabriel et al., 2005b), and (Gabriel et al., 2003). In addition, the FRISBEE model (Aune et al., 2009; Rosendahl and Sagen, 2009), the Rice World Gas Trade

Model (RWGTM) (Rice University, 2004, 2005), the World Gas Model (Gabriel et al., 2012) depict the global gas trade. Some of these models, such as GASTALE, GASMOD WGM-2010, and WGM-2012, include LNG markets, but none account for the limitations of maritime shipment. In fact, transportation is a major component of LNG trade. The COLUMBUS model (Hecking and Panke, 2012) considers the transportation limitations of LNG shipping; however, it assumes only one route between each liquefaction and regasification site pair, and the shipping cost is determined exogenously.

In addition, there is a previous study related to the influence of Panama Canal expansion on the global gas market. The work by (Moryadee et al., 2014) used the WGM-2012 (Gabriel et al., 2012) to investigate the impact of Panama Canal tolls on the global LNG market. However, Moryadee et al. (2014) assumed only one route was available (least distance) for each liquefaction and regasification node. Furthermore, that study distinguished each scenario only by changing distances and shipping costs. Lastly, that study assumed unlimited shipping capacity for LNG tankers as well as unlimited capacity for the Panama Canal. However, in reality LNG tankers need to compete with other ships for the use of the Panama Canal. Moreover, the new lock of the Panama Canal, which is available for large size ships, can accommodate only 15 passages per day. This might be a constraint for LNG shipment between two basins.

To address the limitations of the previous studies, we present WGM-2014, an extension of WGM-2012 (Gabriel et al., 2012). WGM-2014 incorporates more realistic elements to LNG markets. The WGM-2014 takes into account the limitation of canals and restrictions on tanker capacity by modeling the canal operator and LNG shipping

operator as separate market agents. In addition, WGM-2014 endogenously computes the tolls for both the Panama and Suez Canals as opposed to exogenously fixing them in WGM-2012(Gabriel et al., 2012). Also, WGM-2014 includes three types of LNG tankers; small ($\leq$140,000 cm^3), large ($\leq$170,000 cm3), and extra-large ($\geq$170,000 cm^3) while WGM-2012 has no tankers modeled. Lastly, WGM-2014 endogenously determines shipping costs, but WGM-2012 has exogenous shipping costs.

These modeling improvements resulted in more realistic LNG trade flows. For example, the total LNG trade was only about 1.2% off from historical values for 2010; WGM 2012 (Gabriel et al., 2012) is approximately 30% off. More details of WGM 2014 are discussed in Section 4.1 and the mathematical formulation is presented in Appendix 4-A. WGM-2014 was originally based on the works (Gabriel et al., 2005a), (Gabriel et al., 2005b), and (Gabriel et al., 2012). All these versions were developed in mixed complementarity formats, where the Karush-Kuhn Tucker (KKT) conditions of individual gas market players are both necessary and sufficient.

The remaining portion of the chapter is organized as follows: Section 4.2 provides a literature review of issues related to the global LNG trade, LNG shipping, and the Panama Canal expansion. Section 4.3 describes the study method and the input data. Section 4.4 proposes scenarios involving U.S. LNG exports and the Panama Canal. Section 4.5 presents the results and the analysis, and Section 4.6 provides conclusions and describes future work.

4.2 Global LNG trade, LNG shipping cost, and the Panama Canal expansion

4.2.1 Global LNG trade

Unlike oil and coal, due to the gaseous nature of natural gas, before the development of LNG technology, transportation of natural gas was limited by pipeline and was costly due to the low energy density property. Moreover, there was substantial infrastructure investment needed to transport natural gas from supply to demand points. The evolution of LNG has considerably changed all that and enabled the use of maritime transportation so that gas can be shipped and traded internationally. However, LNG has historically been a regional fuel with most LNG trade made within the same basin where it is produced (GIIGNL, 2013). For example, LNG Trade Data for the period 1995-2012 indicates that suppliers in both the Atlantic Basin and Asia/Pacific regions dedicated over 99% of their supply to markets in the same basin. Before the 2010 nuclear disaster in Japan, the difference in the price of gas between Asia and Europe was small, approximately $0.50 (BP, 2013) and this price difference could not cover high shipping costs so that LNG trade between basins was uneconomical. Nonetheless, the price divergence between the basins has increased since mid-2010 due to strong demand in Asia, especially Japan. In 2012, according to BP Statistical Reviews (2013) natural gas price prices were $16.75/MMbtu in Japan[23] but only $9.70/MMBtu in Europe (Heren NBP index) and $2.75/MMBtu in the U.S.

[23] Japan LNG prices include cost +insurance+ freight (average cost).

(Henry Hub). Therefore, exporting LNG between basins became cost effective depending on the shipping costs.

4.2.2 LNG shipping cost

LNG shipping costs involve three main elements: the LNG carrier's capital, the operating cost, and the voyage cost, i.e., marine fuel cost. The capital cost is considered a fixed cost, while the operating and voyage costs are variable. The operating cost includes manning, maintenance, and insurance. LNG projects require large investments. A new standard-size LNG tanker (170,000 m^3) costs more than $200 million USD to build because it requires costly materials and sophisticated cargo-handling equipment (Petroleum Economist, 2011). Because LNG tankers are sophisticated ships, they require specialized crews. As a result, the manning costs are high, accounting for 35% of the operating cost (Petroleum Economist, 2011). The majority of the voyage cost is associated with fuel and port costs. The fuel cost is based on the speed and engine performance, whereas the port costs depend on the destination port; they can be complex and variable depending on the size and volume of the tanker. In addition, the voyage cost also includes transit fees, such as canal tolls. Because the capital cost is fixed, the main variable cost is the voyage cost, which depends on the distance of the trip. Table 4-2 shows the shipping costs in $/MMBtu from various locations to Tokyo, Japan based on data from IHS CERA (Reuters, 2013). The shipping cost from the Atlantic Basin to Japan is three to four times higher than that for the Pacific Basin. However, the Panama Canal route will significantly reduce the time and shipping cost of transportation between the two basins.

Table 4-2 Shipping cost per million Btu in 2012 from various locations to Tokyo, Japan.

Route	Shipping cost
Indonesia-Tokyo	less than $1/MMBtu
Australia-Tokyo	$1.22
Trinidad Tobago-Tokyo	$4.16
Norway-Tokyo	$4.13
North Africa-Tokyo	$3.26
USA (Gulf of Mexico)-Tokyo	$4.40

Because a significant portion of the voyage costs depend on the fuel, which is a function of the distance, the presence of the Panama Canal will reduce the voyage costs from the Atlantic Ocean to the Pacific Ocean. IHS CERA (Reuter, 2013) estimated that the route via the Panama Canal will reduce the shipping cost from the Gulf of Mexico to Japan by approximately $1.50/MMBtu. However, at the time of this research, the Panama Canal Authority has not determined what toll it will charge LNG tankers to pass through the canal, so the final toll could differ. IHS CERA assumed a toll of $0.30/MMBtu based on a $1 million round-trip fee for a medium-sized LNG tanker, which leaves a significant savings of $1.20/MMBtu. Regardless of the toll, the larger canal will improve the economics of LNG shipping between the two basins and will create incentives to exploit pricing differences between the Pacific and Atlantic markets. The price difference between the basins might be narrowed and may benefit Asian consumers.

4.2.3 Panama Canal Expansion

The Panama Canal is currently restricted to vessels with beams[24] of less than 32 meters,294-meters long, with draft[25] of no more than 12 meters (see, Table 4-2) (Panama Canal Authority, 2010). The expansion of the Panama Canal will allow for the first time, large tankers with beams up to a maximum of 49 meters to pass. When the expansion is finished, at least 80 % of the LNG tankers, up to large LNG conventional ones (up to 180,000 $m^{3)}$, operating in 2013 will be able to use the waterway except for Q-Flex (209,000-216,200 m^3) and Q-Max (260,000-266,000 m^3) size tankers. Consequently, the distance to transport U.S. LNG from the Gulf of Mexico will decrease from 16,000 miles to approximately 9,700 miles, reducing the travel time from the U.S. Gulf Coast to Tokyo, Japan from 41 to 25 days. Also, the route can reduce time going from east to west e.g., Peru –Brazil. The comparison of distances in different routes is shown in Table 4-3.

Table 4-2 Maximum allowed containership dimension before and after expansion in meters (m) and dimensions for large conventional LNG carriers.

	Maximum dimension Before expansion	**Maximum dimension After expansion**	**Dimensions for large conventional LNG carriers (150,000-180,000 m^3)**
Length overall	294.30 m	366.00 m	285.00-295.00 m
Draft	32.31 m	49.00 m	43.00-46.00 m
Beam	12.04 m	15.24 m	Up to 12.00 m

(Man Diesel and Turbo, 2011)

Table 4-3 Comparison of distances (nautical miles[26]) between ports

[24] Beam - the greatest width of a nautical vessel.
[25] Draft- the distance between the vessel's waterline and the lowest point of the vessel
[26] The nautical mile equals 1,852 meters exactly (about 6,076 feet).

Origin	Destination	Via Panama Canal	Via Suez Canal	Around Cape Horn	Around Good Hope
Gulf of Mexico	Western Mexico	3,733	21,637	9,783	19,713
	Chile	4,449	19,723	13,476	20,266
	Japan	9,756	14,449	17,060	15,697
	Singapore	12,147	11,910	16,900	13,157
Trinidad & Tobago	Western Mexico	3,331	20,272	7,643	17,573
	Chile	4,048	18,358	11,336	18,126
	Japan	9,355	13,054	14,920	13,557
	Singapore	11,746	10,545	14,761	11,027
Norway	Western Mexico	7,471	19,474	10,801	19,601
	Chile	8,188	17,559	14,493	20,155
	Japan	13,494	12,285	18,078	15,585
	Singapore	15,886	9,746	17,918	13,046

Source: (Popils, 2011)

Currently, the Panama Canal authority operates with two lanes of locks that can handle ships at near its capacity or about 35 ships per day. The expansion of the Panama Canal includes two new sets of locks—one on the Atlantic and one on the Pacific side. Each new lock will have three chambers, and the canal itself will be deepened and widened. Recently, congestion is growing and affecting the total passage time. In the peak demand period, some container ships need to wait one day or longer to enter the canal. After expansion, the new third set of locks will help eliminate some of those backlogs, by adding perhaps 15 passages to the daily total. However, the capacity for LNG transit is still possibly an issue. The priority for the canal booking system is complicated,

including ship characteristics, load type, and daylight restriction. Moreover, LNG tankers need to compete with other ships to use the canal.

4.3 Study methods and input data

This section presents the framework used to determine the impact of the Panama Canal capacity level on LNG exports from Gulf of Mexico in particular and global gas markets in general. The structure of the LNG and shipping markets are identified. Because LNG transportation, including the shipping cost and capacity, is a major component of the market, its impact on the patterns of exports from Gulf of Mexico is analyzed.

4.3.1 The World Gas Model

In the previous version of WGM, WGM-2012 (Gabriel et al., 2012), the market agents include natural gas producers, traders, storage operators, an integrated pipeline and system operator, and marketers. The traders are modeled as strategic players and coordinate both pipeline and LNG flows from the same country. Unlike WGM-2012, WGM-2014 includes additional details on the LNG markets and accounts for the limitations of maritime transportation on these markets (e.g., LNG carrier capacity, LNG shipping routes, and congestion in shipping routes). In this framework, we integrated the shipping markets as part of the LNG markets with endogenously determined prices by tanker category. Therefore, the model includes additional market participants, namely liquefiers, regasifiers, LNG transportation operators, and canal operator. All these new players are modeled by separate optimization problems to account for important constraints, such as capacity as well as future investment

decisions see Appendix 4-A for more details. WGM 2014 has 5-year time periods starting in 2005 and continuing through 2060; each "year" has high and low demand seasons. In terms of LNG contracts, we incorporate an LNG contract data base from GIIGNL (2014) and assume that the contracts will be renewed with the same value after they expire. In WGM-2014, LNG transportation operators have the ability to propose LNG flows for three routes: via the Suez Canal, via the Panama Canal, and via a normal route without canals from the liquefaction node to the regasification node. The actual flows are determined by the equilibrium condition for all players. LNG can be shipped over shorter distances through these canals with an extra charge (toll) or over the normal route with longer distances but no toll. The LNG tankers in this model are considered in terms of their aggregate capacity rather than individually for computational reasons. For simplicity, it is assumed that there are three LNG transportation operators own tankers of different sizes, small ($\leq$140,000 cm^3), large ($\leq$170,000 cm3), and extra-large ($>$170,000 cm^3) e.g., Q-Max and Q-Flex, with different aggregate capacities, future investment costs, and operating speeds. The size the LNG tankers is important because each type of tanker has different operating costs, and extra-large tankers cannot use Panama Canal due to size limitations. In this study, it is assumed that the LNG buyers are responsible for the LNG shipping charges, which come from market-clearing conditions between the regasifiers and the LNG transportation operators for each origin–destination pair. This shipping service charge was exogenous in WGM-2012 but in WGM-2014 is endogenously determined for greater realism. Since the Panama Canal already has other users, the capacity available to LNG is a user defined maximum capacity of the expanded Canal.

Another adjustment that is relevant to LNG markets is that the canal operator is modeled. We assume that the canal operator owns two main canals, the Panama and Suez Canals, for LNG shipping. The canal operator collects transit fees for providing shorter routes, and congestion fees at the canal are imposed when the waterway is busy with traffic. Lastly, all of the market participants except for the canal operator have endogenous future investments. Appendix 4-A provides the complete mathematical formulations and assumptions for each market player, and Appendix 4-B describes the associated KKT and market-clearing conditions. Details of the input data for WGM-2014 are shown in Table 4-4 and Figure 4-1 shows a representation of the LNG market in WGM-2014.

Table 4-4 Market agents and input data in WGM 2014.

Market agents	**Input data and references**
Producers	Production cost function (Golombeck et al., 1995, 1998) Production reference (EIA,2013; IEA,2011)
Storage operator	Storage capacity (EIA, 2007;GSE, 2008) Storage expansion *Oil and Gas Journal*
An integrated pipeline and system operator	Pipeline capacity (GTE, 2005, 2008) Pipeline transportation cost (Oostvoorn , 2003) Pipeline expansion *Oil and Gas Journal*
LNG transportation operators	Shipping capacity (GIIGNL, 2013) Average speed (MAN Diesel & Turbo, 2011) Shipping cost (Petroleum Economist, 2011) LNG shipping distance (PortWorld.com)
Canal operator	Canal toll (Petroleum Economist, 2011)

Liquefiers	Liquefaction capacities (GIIGNL, 2013)
Regasifiers	Regasification capacities (GIIGNL, 2013) LNG contact database (GIIGNL, 2013)
Marketer	Consumption reference (EIA,2013; IEA, 2011) Reference prices (IGU, 2013)

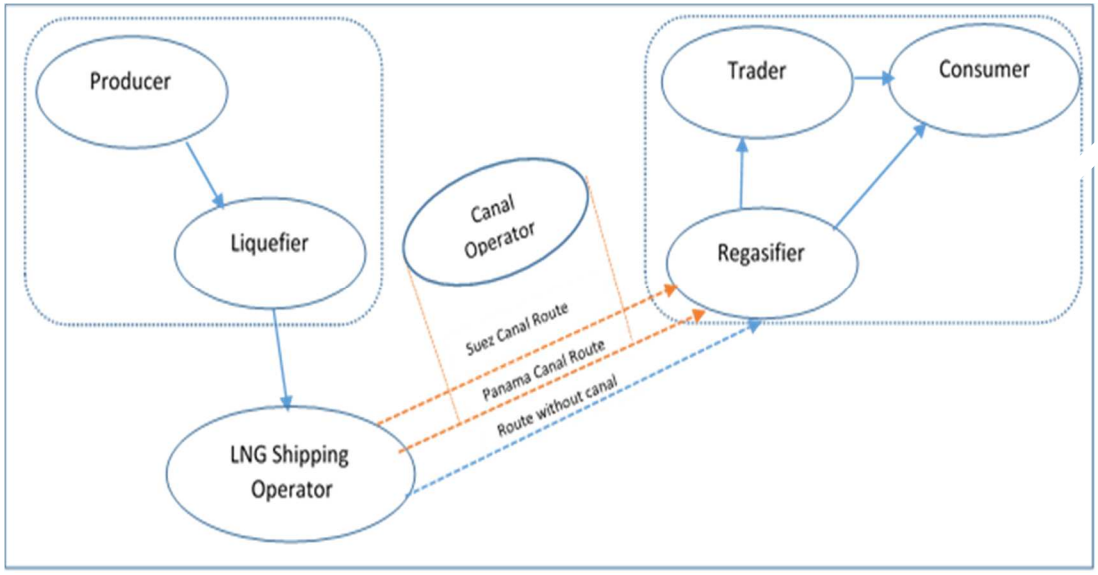

Figure 4-1 Representation of the LNG market in WGM-2014.

It is important to note that for many existing LNG users, particularly in Asia, gas and oil compete for a considerable portion of the market, unlike the U.S. where gas and oil markets are weakly linked. This implies that with greater amounts of inexpensive gas available to those markets, the demand for natural gas could significantly increase, thereby reducing the demand for oil. Since contract prices for LNG to Asia are often linked to the world oil price, more U.S. natural gas exports could also reduce the LNG contract prices to those markets. Since the WGM does not currently capture the oil-

gas interactions, this aspect of the energy market is currently not modeled but may be a topic for future enhancement.

The current version of the model is composed of 42 nodes that represent individual or aggregated countries and covers 98% of the worldwide consumption and production for 2010. On the supply side, the WGM also characterizes three types of producers in each region of the U.S.: conventional gas, shale gas, and non-shale unconventional gas. The model operates in five-year periods from 2005-2050 as well as in high and low demand seasons. The year 2010 is used as a calibration year. On the LNG side, WGM-2014 consists of 15 aggregated liquefaction nodes and 23 regasification nodes and covers more than 85% of the actual long-term contracts that were in place in 2010. In addition, LNG spot markets are used to investigate the state of the global gas market. The model solves for decision variables, including the operating levels (e.g., production, storage injection) and capacity investments (e.g., for pipelines and liquefaction). A total of 103,000 variables make up the WGM complementarity system, which can be solved on a standard personal computer (e.g., 4 GB of RAM and 1.2 GHz clockspeed) in approximately 240 minutes.

4.4 Scenarios

This section describes the scenarios defined in this study. First, we define the Base Case as the baseline for the comparisons with the other scenarios. The Base Case assumes no Panama Canal route and no U.S. LNG exports. Secondly in term of US LNG exports for the rest of scenarios this study assumes the U.S. exports LNG from

the Gulf of Mexico with a capacity of 57.88 Bcm[27]/y, 8.25 Bcm/y from the West Coast, and from the East Coast at 10.33 Bcm/y. Only 4.5 Bcm/y from the Gulf of Mexico is under long-term contract with specific destinations (from the U.S. to India), so the rest of the capacity is endogenously determined by the model and thus corresponds to the LNG spot market.

We assume the U.S. starts exporting LNG with a capacity of 57.88 Bcm/y in 2015.[28] In addition, the U.S. has the ability to expand its export capacity by 50 Bcm[29] during each five-year time period. Lastly, there is an assumption the Panama Canal capacity regarding the competition for canal capacity. The new lock of the Panama Canal will add approximately 15 passages to the daily total (Fountian, 2011). Since no LNG tankers can make it through the Panama Canal due to insufficient lock depth, this means the Panama Canal capacity will vary from 0 to 15 passages for LNG given the other users of the Canal. Since WGM-2014 provides a market equilibrium for global natural gas markets, it only considers LNG tankers for the use of the Panama Canal. Other competition for the Canal, e.g., crude oil, metal ores, agricultural products, and other materials are not directly represented. Therefore, this study estimates the capacity for LNG shipping using the number of LNG vessels transiting through the Panama Canal via four choices of Canal capacity (zero, low-100 ships per year, medium-200 ships per

[27] 1 Bcm =35.3 Bcf.

[28]The U.S. is expected to start LNG exports from Cheniere Energy terminal in 2017, but we assume the U.S. starts earlier in 2015 due to the five-year time steps in the model.

[29] The capacity investment cannot be realized instantaneously by the model. WGM has five-year time steps which are enough for the time lag for construction. In this case, the U.S. can increase its export capacity over the time horizon if it is profitable.

year, high-250 ships per year), assuming the largest sizes of tankers (170,000 m^3) passes through the Canal.[30] The scenarios descriptions are as follows:

1. The Base Case is run without the Panama Canal route and with no U.S. LNG exports. The Base Case consumption outcome uses the data sources presented in Table 4 and is calibrated to multiple sources. Details of this calibration are provided in the next section.
2. The second scenario considers U.S. exports with a capacity of 57.88 Bcm/y as previously discussed without the Panama Canal route and is denoted as "USLNG_Panama0"
3. The third scenario, which is abbreviated "USLNG_Panama100", uses the same assumptions for the U.S. Exports, but the route via the Panama Canal is available starting in 2015 with endogenously determined transit tolls from market-clearing conditions. We estimate the maximum capacity of the Panama Canal by assuming that up to estimated 100 LNG vessels of 70,000 m^3 capacity ships transiting through the Panama Canal each year once the expansion is completed.
4. The fourth scenario, which is abbreviated "USLNG_Panama200", uses the same assumptions as USLNG_Panama100 on the U.S. LNG exports and the availability of the Panama Canal, but assumes that the Canal can accommodate up to 200 LNG tankers of 170,000 m^3 each year.

[30] Although there are 393 LNG vessels in operation (GIIGNL, 2013), only 90% can pass through the Panama Canal. Of these 393 ships more than 80% are already committed under long-term for specific routes that do not use the Panama Canal. We also allow the LNG shipping operator to expand the shipping capacity if the LNG demand increases.

5. The last scenario which is abbreviated "USLNG_Panama250", uses the same assumptions as USLNG_Panama100 but assumes that the Canal can accommodate up to 250 LNG tankers of 170,000 m^3 each year.

The five scenarios were first simulated up to 2035 and allowed for an analysis of the flows of U.S. gas exports in the global market. The global results, including production and consumption, are presented in the next section.

4-5 Results

4.5.1 Model validation and the calibration results

The consumption output of the base case was calibrated to match the global natural gas markets in 2010 provided by the 2013 BP Statistical Review as well as projections from multiple sources. The model outcome for the U.S. considers the rapid growth of shale gas development in the next decades. The U.S.'s natural gas consumption and production are specifically calibrated according to the forecast from the Annual Energy Outlook (EIA, 2013). The production and consumption for the rest of the world is based on the World Energy Outlook (IEA, 2011): New Policy Scenario as a reference, which takes into account rapid growth rates for demands in Asia and the Middle East. For LNG markets, GIIGNL (2011) is a valuable source for natural gas liquefaction and regasification capacities and long-term contracts.

The Base Case is used as the baseline for comparison against other scenarios. To examine the error of the model, we compare its output to historical references. As shown in Table 4-5, the consumption results in 2010 for the Base Case differ slightly

from the reference (BP, 2013). The percentage differences in Table 4-5 are the BP 2013 values minus the WGM values divided by the BP 2013 values. The difference between the WGM consumption and the BP values (2013) is less than 5%. We separate Japan/S. Korea from the Asia Pacific region because this study primarily focuses on the LNG market, of which Japan has the highest consumption in the world. Japan and S. Korea have more than 50% of the total LNG consumption in 2012. Among the remaining regions, North America has the highest consumption while Asia Pacific, Europe, and the Former Soviet Union have intermediate levels of consumption.

Table 4-5 Comparison of natural gas consumption in 2010 from the WGM output and BP (2013) (Bcm).

	WGM	BP (2013)	% difference
AFRICA	102.9	107.8	4.55%
ASPACIF	371.7	387.1	3.98%
EUROPE	537.1	544.6	1.38%
FRSVTUN	580.2	585	0.82%
JAPAN/ S.Korea	144.3	137.5	-4.95%
MIDDLE EAST	339	329	-3.04%
NRTH_AM	774	767	-0.91%
STH_AM	134.5	132.9	-1.20%

Table 4-6 indicates that the total LNG trade in 2010 calculated by WGM-2014 is 272.1 Bcm/y, while the actual trade from GIIGNL was 275.54 Bcm/y. The percentage differences between the GIIGNL (2011) and WGM figures of LNG global trade for 2010 are fairly small. Asia was the dominant LNG importer in 2010, whereas the largest LNG sources are from the Pacific Basin, supplied by Australia, Indonesia, and Malaysia.

Table 4-6 LNG imports by region and source of imports in 2010.

LNG imports by region in 2010 (Bcm)

	WGM	GIIGNL (2011)	Difference
Europe	84.9	81.63	4.0%
Americas	25.6	26.3	2.7%
Asia	161.6	164.87	2.0%
Middle East[31]	-	2.75	-
Total	272.1	275.54	1.2%

Source of imports in 2010 (Bcm)

	WGM	GIIGNL (2011)	Difference
Atlantic Basin	74.7	79.44	5.97%
Middle East	89.8	93.47	3.93%
Pacific Basin	107.6	102.63	4.84%
Total	272.1	275.54	1.25%

In terms of the projected regional consumption, the results of WGM-2014 display the same trend as the Annual Energy Outlook (EIA, 2013) for the U.S. and the World Energy Outlook (IEA, 2011) for the rest of the world, as shown in Figure 4-2. The Asia Pacific region has the highest growth rate from 2010-2035. The consumption of the rest of the world gradually increases after 2015. By the end of 2025, the world's natural gas consumption will reach approximately 4,000 Bcm/y, of which approximately half will come from the Asia Pacific region, the Former Soviet Union, and North America. The results are predicated on the IEA and EIA results for gas demands. However, those gas demands could change substantially depending on the related world oil price assumptions.

[31] The WGM does not combine Kuwait and Dubai as an aggregated node.

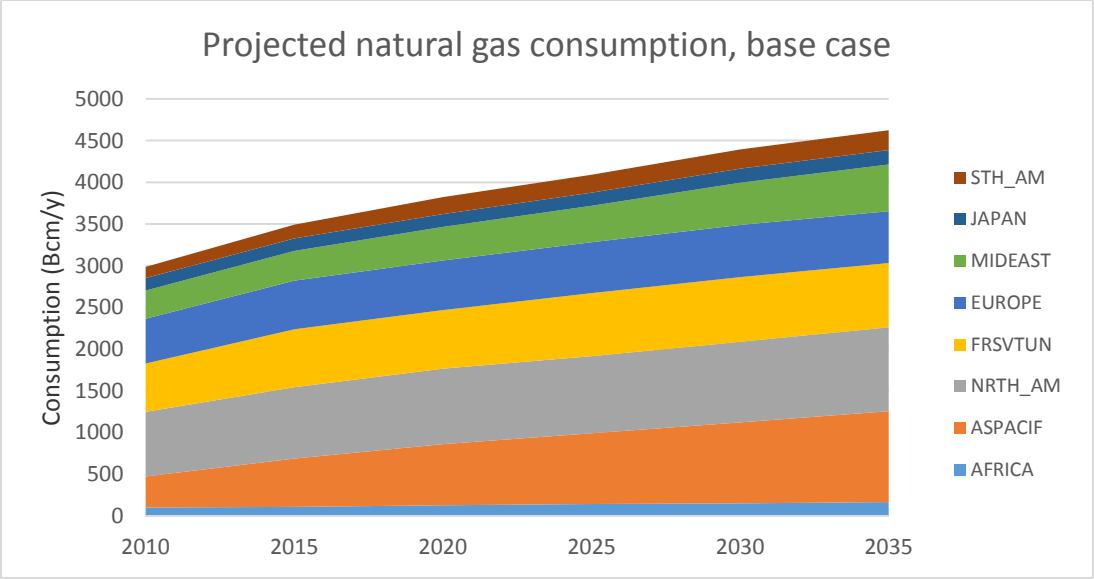

Figure 4-2 projected natural gas consumption for the base case.

4.5.2 Impact of LNG shipping economics

The overall impact of the canal expansion on LNG trade is fairly obvious: shorter distances and voyages lower the shipping costs. What is not so obvious and what was in part the motivation for this study, was the effect on particular shipping patterns (who gets more LNG), resulting regional prices, and other specific results.

In general, shorter distances reduce fuel consumption and LNG boil-off. Shorter voyages reduce the charter period[32] for voyages and increase vessel utilization since the route via the Panama Canal reduces the turnaround times per trip, more shipping capacity turns into availability, and this should improve the total LNG trade. We found that these hypotheses are true if there is enough capacity of the waterway for LNG shipping. The first thing to realize is that the total LNG trade over time under the Base

[32] How long it takes to travel from the origin (export terminal) to the regasification site.

Case is less than the rest of scenarios due to the restriction on U.S. LNG exports, see Figure 4-3.

Next, the difference between USLNG_Panama0 and USLNG_Panama100 scenarios is that there are additional routes via Panama Canal with capacity of 100 ships per year for USLNG_Panama100, but other assumptions for U.S. LNG exports are the same. Figure 4-3 shows that there is almost no difference in total LNG trade between these two scenarios even though the canal route is available. The explanation is that the U.S. LNG exports to Asia are restricted by the capacity of the Panama Canal, see 4.5.3 for more details for U.S. LNG export pattern. The conclusion is that the canal capacity is not enough to improve the total LNG trade. However, under USLNG_Panama200 with a capacity of 200 ships per year, the total LNG trade increases 1-3% from 2015-2030 and becomes more pronounced in 2035 as compared to USLNG_Panama100 scenario; the total LNG trade increases by 5% in 2035. Nonetheless, the total worldwide trade is similar for two scenarios, USLNG_Panama200 and USLNG_Panama250, from 2010 to 2030. The total trade increase a little in 2035 (423.4 Bcm v.s. 417.1 Bcm). This indicates that increasing the Panama Canal capacity from 200 ships per year to 250 does not significantly improve the total trade.

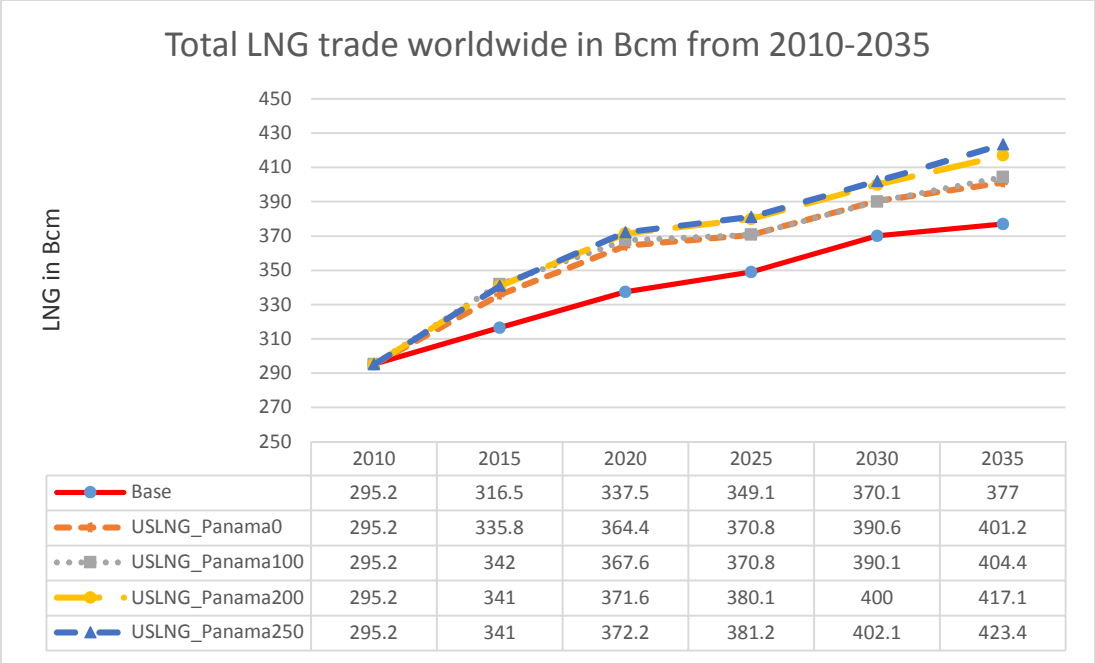

	2010	2015	2020	2025	2030	2035
Base	295.2	316.5	337.5	349.1	370.1	377
USLNG_Panama0	295.2	335.8	364.4	370.8	390.6	401.2
USLNG_Panama100	295.2	342	367.6	370.8	390.1	404.4
USLNG_Panama200	295.2	341	371.6	380.1	400	417.1
USLNG_Panama250	295.2	341	372.2	381.2	402.1	423.4

Figure 4-3 WGM-2014 Total LNG trade in Bcm from 2010-2035[33]

The model results in terms of the Panama Canal utilization show that LNG trade becomes more global; the Panama Canal allows the trade from the Atlantic basin to the Pacific basin, and Asian markets rely more on Gulf of Mexico supply. In the past, LNG was usually traded within the same basin because the shipping cost was too high to ship from one basin to another basin. Figure 4-4 shows the comparison of the Panama Canal utilization for 2015 and 2035. All of the trade flows from the Atlantic basin to Japan/S. Korea; none flows from the Pacific basin going to the Atlantic. For example, Trinidad and Tobago and the U.S. are the major users of the Panama Canal; they transport 20.8 Bcm and 35.9 Bcm in 2015 via the Panama Canal to Japan under USLNG_Panama100 and USLNG_Panama200, respectively. This phenomenon occurs

[33] The reason the total LNG trade drops slightly in 2015 from 342 to 341 Bcm between USLNG_Panama100 and USLNG_Panama200 is presumably due to shifting of supplier market share and non-cooperative, game-theoretic behavior.

because Japan/S .Korea has the highest endogenous wholesale prices in the world while the LNG suppliers have profit maximization as an objective. Therefore, exporting gas to Japan can generate a significant profit depending on the shipping cost. In addition, only the LNG from the Gulf of Mexico will benefit from the Panama Canal although there are other Atlantic basin LNG-exporting plants e.g., Snøhvit terminal in Norway and Nigeria LNG and Angola LNG in West Africa. The distances from Snøhvit terminal, Norway, are closer to Asia via the Suez Canal. Likewise, Japan/S. Korea and China are closer to West Africa traveling around the Cape of Good Hope so that no LNG flows through the Panama Canal to China. Moreover, the model results show that there is a considerable gap for Panama Canal utilization when we assume 100 ships per year (USLNG_Panama100) and 200 ships per year (USLNG_Panama200), see Figure 4-4. The utilization difference is less when compared USLNG_Panama200 and USLNG_Panama250. The utilization rate increases as the given canal capacity increases. However, the results for the Suez Canal utilization stays the same for all scenarios, approximately 36 Bcm in 2035. This means increasing Panama Canal utilization rate does not affect the Suez Canal utilization rate and, the flows from Middle East to Europe through the Suez Canal remain the same. In addition, we did further analysis by sufficiently increasing the capacity for the Panama Canal e.g., 500 ships per year to see what would be the maximum flows through the Panama Canal. We found that the maximum flows reached 68.3 Bcm in 2035 due to the restriction on the gas production and LNG export capacity.

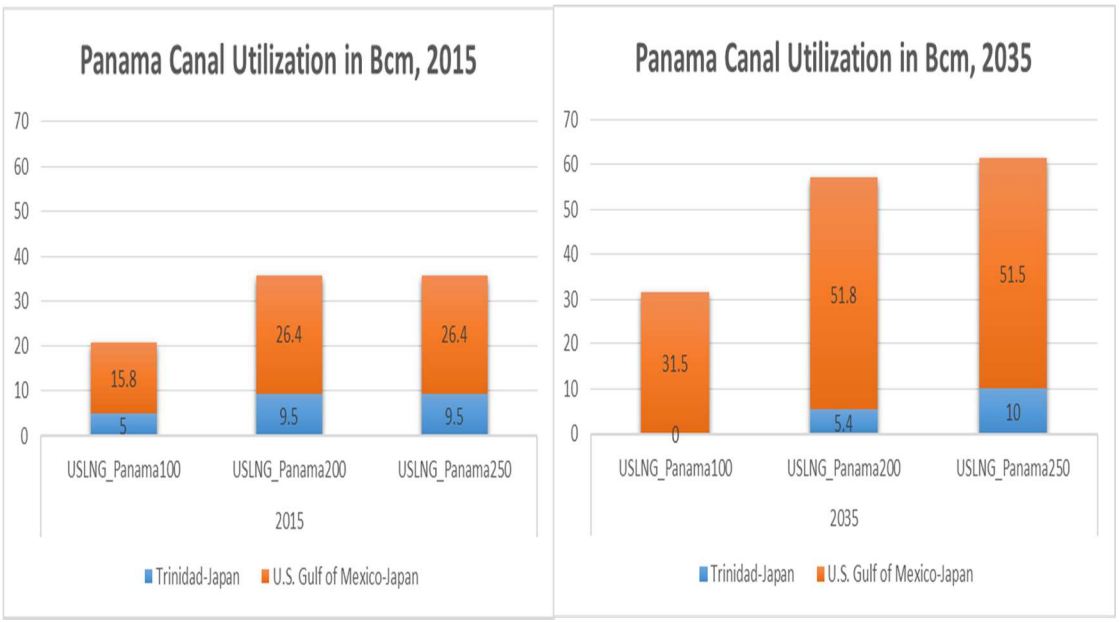

Figure 4-4 WGM-2014 Panama Canal utilization from 2015 and 2035 Bcm.

Figure 4-5 presents the extra-large LNG tanker capacity in 2010 vs. 2035. The model invests in extra-large tankers, even though the investment costs are much higher than that of other tankers. The reason is that extra-large tankers have the lowest unit operating and voyage costs per cm due to the economies of scale of the tankers. It is important to note that the total capacity for extra-large tankers in 2035 decreases when the capacity of the Panama Canal increases, see Figure 4-5. However, the total LNG trade increases, see Figure 4-3. This indicates that the Panama Canal route increases efficiency of LNG shipping; less total shipping capacity generates a higher volume of trade. For example, in 2035 when comparing USLNG_Panama100 with US_LNG Panama200, the total capacity for extra-large tanker are, respectively 15.3 million m^3 and 11.9 million m3, see Figure 4-5. However the total trade for the same year increases from 404.4 Bcm to 417.1 Bcm, respectively, see Figure 4-4. The explanation is as follows. Under the USLNG_Panama100 scenario in 2015, the total LNG flow using small tankers is 15.8 Bcm as compared to 36.6 for the USLNG_Panama200 scenario.

The total LNG flows for the two other sizes of ships (medium and extra-large) stay the same (extra-large) or almost the same (15.7 vs. 15.2 Bcm for the medium size). In sum, larger Panama Canal capacity (200 vs. 100 ships/year) induces substantially more LNG traded on the smaller ships.

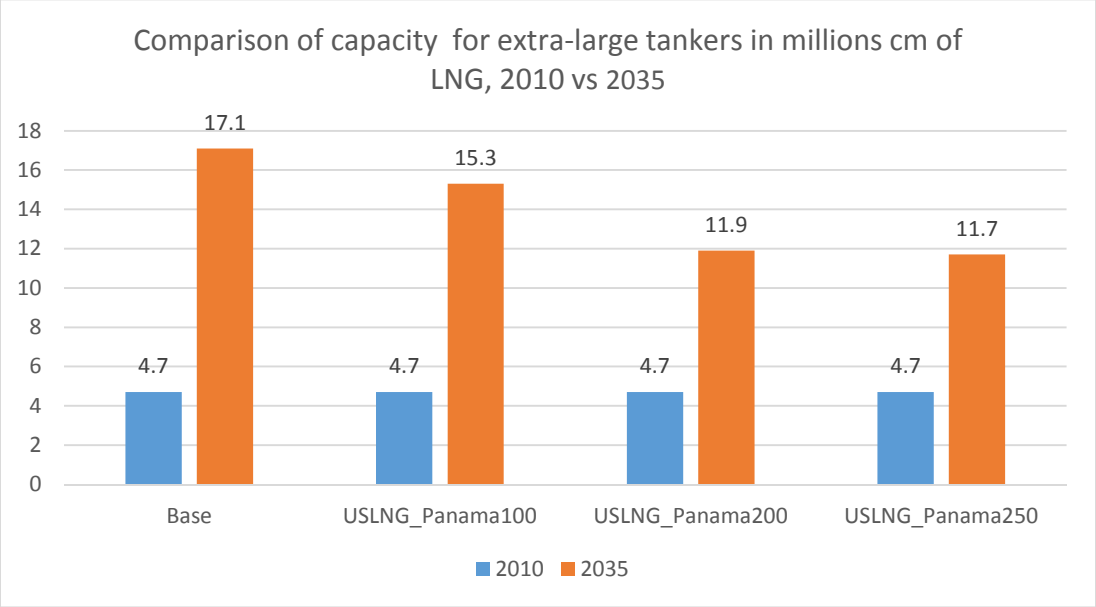

Figure 4-5 WGM-2014 Comparison of capacity for extra-large tanker in millions cubic meters, 2010 vs 2035

4.5.3 Impact on LNG exports from Gulf of Mexico

According to the results of our simulations, LNG from the Gulf of Mexico no longer flows to Japan/S. Korea in the absence of the Panama Canal with expanded capacity, but rather transited to Europe. As shown in Table 4-7, for the year 2015, the U.S. exports scenario without the Panama Canal (USLNG_Panama0), indicates that the U.S. and Trinidad & Tobago will respectively, export 18.4 Bcm and 7.3 Bcm to South America and Europe. Only 4.6 Bcm is transited from the U.S. to India under long-term contract via the Suez Canal. The remainder of the U.S. LNG exports are endogenously determined by the model. Under the USLNG Panama0 scenario the U.S. exports more

to Europe (37.6 Bcm) in 2035, see Table 4-8 as compared to 18.4 Bcm in 2015 in Table 4-7 (. Although the U.S. export capacity is approximately 60 Bcm, the total exports do not reach this maximum. This situation shows that the European gas market has limitations in absorbing U.S.-exported LNG. However, the U.S. will export more when the Panama Canal is utilized. In sum, without the expanded Panama Canal capacity, the U.S. will likely export to Europe rather than to Asia because the endogenously determined shipping cost from the Gulf of Mexico to Asia is much higher than that for Europe.

When compared three Panama Canal scenarios (USLNG_Panama100, USLNG_Panama200, and USLNG_Panama250), the level of the Panama Canal capacity also play a significant role for the direction of U.S. LNG exports. USLNG_Panama100 scenario assumes 100 of LNG ships transited through the Panama Canal each year. Under this scenario, the U.S. increases the total exports up to 29 Bcm from 18.4 Bcm (Table 4-7) in the USLNG_Panama0 scenario and sends 15.8 Bcm to Japan/S.Korea and 8.6 Bcm to Europe (Netherlands, Poland, and Spain) in 2015. With the limited capacity of the Panama Canal in this scenario, the U.S. becomes a swing LNG exporter, sending gas to both east and west. However, when more Panama Canal capacity is available, the U.S. exports almost all of its LNG to Japan/S.Korea. The U.S. exports 26.4 Bcm to Japan/S.Korea in 2015, see Table 4-7 and 51.8 Bcm to the same destination in 2035 (Table 4-8) under this scenario. U.S. LNG exports switch direction from Europe to Asia because Asian prices are a lot higher than European prices. For example in 2035 Japanese's prices are 18$/MMBtu but European prices are 13$/MMBtu, see more details in Section 4.5.4

It is important to note that the total endogenous LNG export volume from the U.S. under USLNG_Panama250 is similar to USLNG_Panama200 although the maximum capacity of the Canal goes up to 250 passages/year. It is conventionally thought that when more capacity is available, the U.S. will export more to that market. However, the reverse occurs for U.S. LNG exports. The U.S. exports only approximately 60 Bcm under USLNG_Panama100 and US_LNGPanama250, see Table 4-8. In the model set-up, we allow additional 50 Bcm per year for the expansion of the U.S. Gulf of Mexico terminal in each time period. The terminal can get expanded if it is profitable. The investment condition is that the terminal will expand if the total future profit is greater than the cost of current investments as part of the liquefier KKT conditions, see Appendix B, equation B16 for more details. However, there is no investment made by the model for capacity expansion for the U.S. Gulf of Mexico terminal

Table 4-7 LNG Exports from Gulf of Mexico in 2015 (Bcm)

Origin	Destination	Scenarios				
		Base	USLNG Panama0	USLNG Panama100	USLNG Panama200	USLNG Panama250
U.S. Gulf of Mexico	Brazil	0	2.2	0	0	0
	India	4.6	4.6	4.6	4.6	4.6
	Japan/S. Korea	0	0	15.8	26.4	26.4
	France	0	2	1.6	0	0
	Netherlands	0	1.5	0.7	0	0
	Poland	0	2.8	2.8	0.8	0.8
	Spain	0	5	3.5	0	0
	Turkey	0	0.3	0	0	0
	Grand Total	**4.6**	**18.4**	**29**	**31.8**	**31.8**
Trinidad &Tobago	Brazil	2.9	2	0	0	0
	Japan/S. Korea	0	0	5	9.5	9.5
	Spain	5.3	5.3	5.3	5.3	5.3

	Grand Total	**8.2**	**7.3**	**10.3**	**14.8**	**14.8**

Table 4-8 LNG Exports from Gulf of Mexico in 2035 (Bcm).

Origin	Destination	Scenarios				
		Base	USLNG Panama0	USLNG Panama100	USLNG Panama200	USLNG Panama250
U.S. Gulf of Mexico	India	4.6	4.6	4.6	4.6	4.6
	Japan/S. Korea	0	0	31.5	51.8	51.5
	France	0	11.5	4.1	0	0
	Netherlands	0	7.5	1.1	0	0
	Poland	0	14.1	5.7	0	0
	The UK	0	4.1	0	0	0
	Spain	0	0.4	0	0	0
	Grand Total	0	42.2	47	56.4	56.1[34]
Trinidad &Tobago	Japan/S. Korea	0	0	0	5.4	10
	Spain	3	3	3	3	3
	Grand Total	3	3	3	8.4	13

4.5.4 Impact on regional prices

In addition to the impacts discussed above, the importance of the Panama Canal expansion from an LNG market perspective is its influence on global gas price convergence. Lower shipping costs improve the relative economics of shipping Gulf of Mexico gas to Asia. Over time this reduces inter-regional price spreads. It is important to note that $2010 is used in this analysis. Figure 4-6 and Figure 4-7 indicate regional price spreads for the USLNG_Panama0 and USLNG_Panama200 scenarios

[34] The U.S. sales decrease because Trinidad & Tobago increases its sales to Japan. Trinidad & Tobago has a higher production cost but is closer distance to the Panama Canal (approximately 500 nautical miles closer).

respectively. The price gaps for Japan-Europe and Japan-North America in 2035 are smaller; the difference between Japanese-European prices is $7.29 for the USLNG_Panama0 scenario (Figure 4-6), and it is narrowed to $6.17 (Figure 4-7) as the Panama Canal route with expanded capacity is employed under the USLNG_Panama200 scenario. Another interesting result is that over time the North American gas prices increase a little under $6 range due to LNG exports.

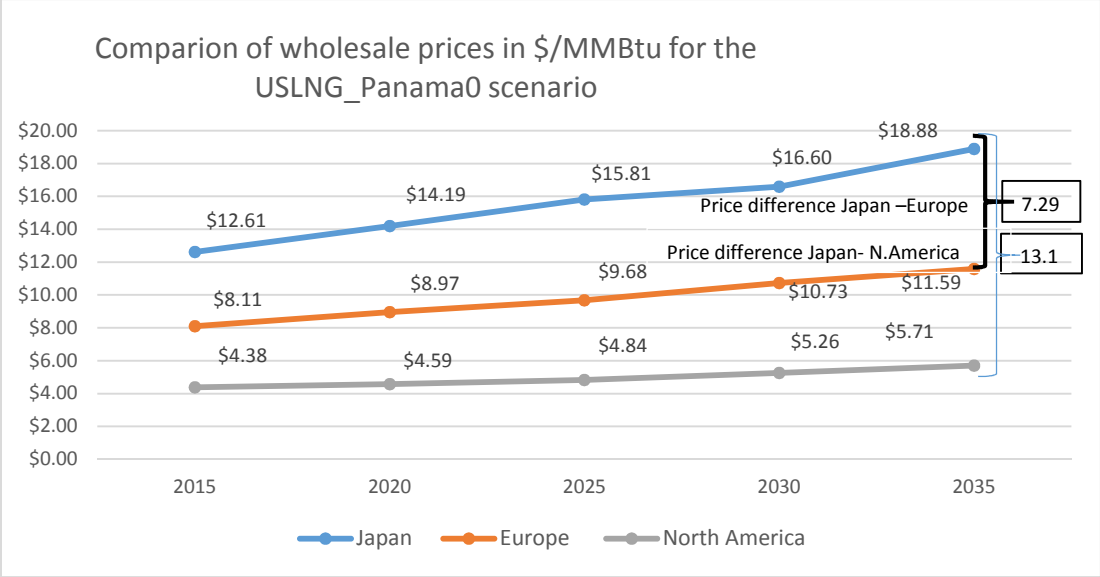

Figure 4-6 Comparison for wholesale prices in $/MMBtu for USLNG_Panama0 scenario.

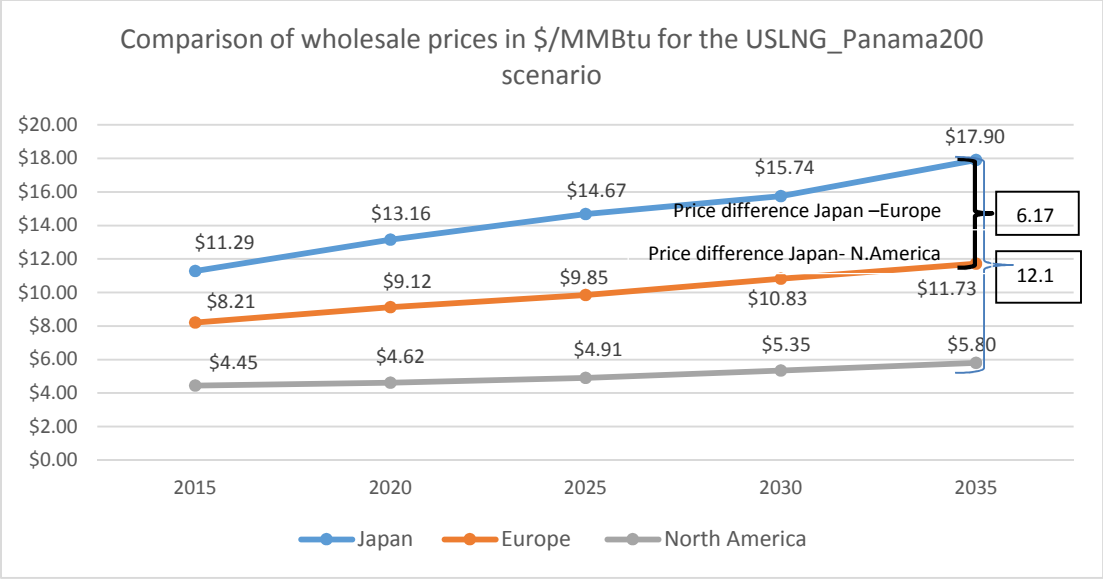

Figure 4-7 Comparison for wholesale prices in $/MMBtu for USLNG_Panama200 scenario.

In terms of country prices, the U.S. LNG exports caused by the Panama Canal expansion are projected to have other impacts, for example on worldwide prices. Table 4-9 shows that under the Base Case, the wholesale price in Japan/S. Korea increases to as high as $18.91/MMbtu in 2035, representing the highest prices among all countries. Southeast Asia/China and India/Pakistan see 2035 prices of $15.69/MMbtu and $11.03/MMbtu, respectively. Under the USLNG_Panama0, due to inexpensive U.S. LNG flowing to Europe, the importing countries experience lower gas prices than in the Base Case. The United Kingdom, the Netherlands, Poland, Turkey, and Spain experience reductions of $0.20-$0.35/MMBtu in wholesale prices. Due to the availability of the Panama Canal, the wholesale prices in China/Southeast Asia and Japan/S. Korea decrease by $0.20-0.30/MMBtu under USLNG_Panama100, USLNG_Panama200, and USLNG_Panama250 scenarios as compared to the Base Case (Table 4-9). Under the same comparison, the prices are also lowered due to more

LNG transported by Qatar and Australia although the U.S. does not export gas to China/Southeast Asia. Lastly, when we compare the USLNG_Panama0 and USLNG_Panama100 scenarios, the results show that the European prices in the USLNG_Panama0 are higher than in USLNG_Panama100 scenario while Asian prices are in the opposite direction. The explanation is that the expanded Panama Canal allows the exports from Gulf of Mexico to Asia. More gas supplies go to Asia and simultaneously decrease flow to Europe.

Table 4-9 Wholesale prices in 2035 ($/MMBtu) for selected country nodes.

Country Nodes	Base	USLNG_ Panama0	USLNG_ Panama100	USLNG_ Panama200	USLNG_ Panama250
Netherlands	$11.61	$11.41	$11.48	$11.54	$11.56
Poland	$11.97	$11.59	$11.82	$11.83	$11.85
Spain	$11.53	$11.20	$11.27	$11.48	$11.51
Turkey	$11.29	$10.95	$11.05	$11.20	$11.21
United Kingdom	$11.44	$11.09	$11.21	$11.28	$11.31
China/S.E. Asia	$15.69	$15.65	$15.36	$14.99	$14.78
India/Pakistan	$11.03	$10.93	$10.91	$10.88	$10.88
Japan/S. Korea	$18.91	$18.88	$18.45	$17.90	$17.60

4.5.5 Other Impacts on the global gas market

Without the Panama Canal expanded capacity, under USLNG_Panama0, the entry of U.S. LNG into Europe displaces the market shares of Algeria and Russia in the European LNG markets (Table 4-10). In 2035, Russia's natural gas flows to Europe decreases significantly from 12.2 Bcm to 0.8 Bcm, and Algeria's flows decreases by approximately 6.1 Bcm under USLNG_Panama0. The WGM results indicate that the greatest effect of the Panama Canal expansion is reflected in the U.S. LNG export pattern, which dynamically changes the market. As shown in Table 4-10, the U.S. exports 31.5 Bcm and 51.8 of LNG to Japan/S. Korea in the USLNG_Panama200 and

USLNG_Panama250 scenarios, respectively compared with zero in USLNG_Panama0. The increased LNG supply from the U.S. displaces that from other exporters to the Japan/S. Korea node (Table 4-10). Under the USLNG_Panama100 scenario as compared to the Base Case, Qatar and Australia experience decreases of approximately 46% (from 47 Bcm to 25 Bcm) and 4% (from 95 Bcm to 80 Bcm), respectively, in their LNG exports to Japan/S. Korea. In contrast, Qatar increases their LNG exports to Chinese markets from 26.9 Bcm to 49.6 Bcm under the USLNG_Panama100 scenario and from 26.9 to 61.8 Bcm under USLNG_200 scenario. Likewise, Australia exports LNG to China a lot more after its market shares are displaced by the Gulf of Mexico LNG from the U.S. The explanation is that as LNG exports are displaced in one market, suppliers will attempt to increase sales in other markets to maintain their profit. Overall, U.S. LNG causes a significant reduction in the total export volume of Asian LNG exporters to the Japanese/S. Korean market.

Table 4-10. Selected LNG flows from major LNG exporters in 2035 (Bcm).

Exporters	To Japan/S.Korea				To other Asia (China/S.E. Asia and India)			
	Base	USLNG Panama0	USLNG Panama100	USLNG Panama 200	Base	USLNG Panama0	USLNG Panama100	USLNG Panama 200
Australia	96.2	95.1	91.4	80	0	0	1.7	10.4
Qatar	47.8	47	25	13	26.9	27.9	49.6	61.8
Russia	8.3	8.3	8.3	8.3	0	0	0	0
USA	0	0	31.5	51.8	4.6	4.6	4.6	4.6
Trinidad	0	0	0	5.4	0	0	0	0
Algeria	0	0	0	0	0	0	0	0
Indonesia	0	0	0	0	3.6	3.6	3.6	3.6
Nigeria	1.8	4	0	0	35.8	35.1	24.6	24.6
Yemen	3	3	3	3	28.5	28.5	26.5	21.1

Exporters	To Europe

	Base	USLNG Panama0	USLNG Panama100	USLNG Panama 200
Australia	0	0	0	0
Qatar	24.9	24.9	24.9	24.9
Russia	12.2	0.8	10.2	12.6
USA	0	37.6	10.9	0
Trinidad	3	3	3	3
Algeria	68.4	62.3	62	66.4
Indonesia	0	0	0	0
Nigeria	5	3.9	12	10.7
Yemen	0	0	0	0

Figure 4-8 shows the changes in import sources for selected Asian countries. Under the USLNG_Panama0 scenario, without the presence of the Panama Canal expanded capacity even the model allows exports from Gulf of Mexico, LNG imports to Asia do not change. However, when the Panama Canal route is open, the total LNG imports to Asia increase for different reasons; Japan/S. Korea receives LNG directly from Gulf of Mexico exporters, the United States, and Trinidad &Tobago while China/Southeast Asia and India import more LNG from Qatar and Australia. Lastly, imports by pipelines for China/Southeast Asia decrease due to the presence of more LNG supplied to the markets, see Figure 4-8.

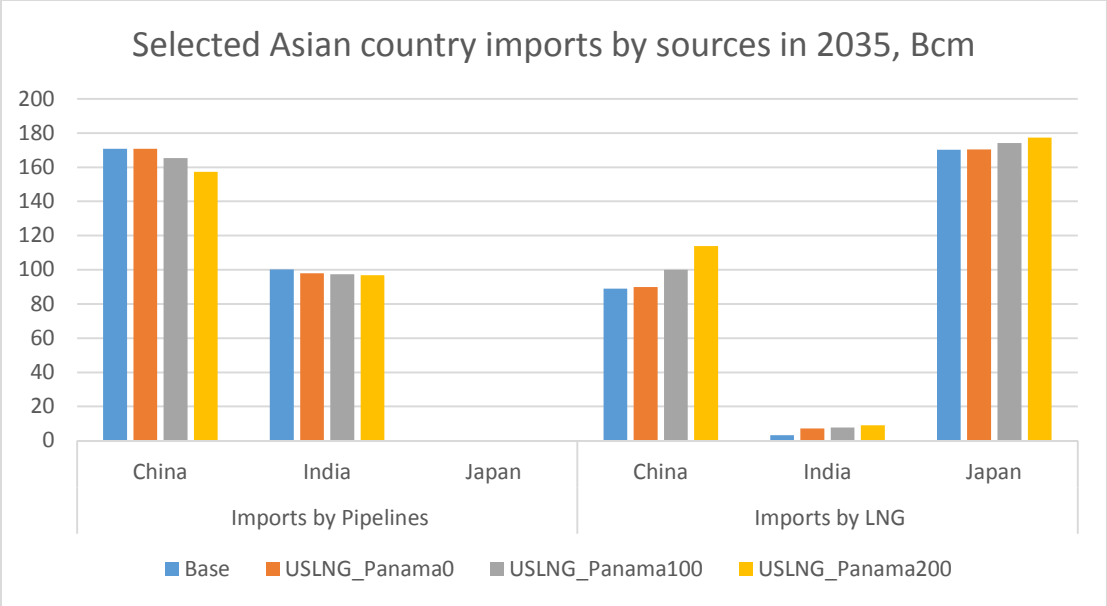

Figure 4-8 Selected Asian country imports by sources in 2035 Bcm

4. 6 Conclusions

The aim of this study is to identify the influence of Panama Canal capacity level on LNG shipping and the LNG exports from the Gulf of Mexico under five different scenarios. The main conclusions can be summarized as follows:

- The model results show that without the Panama Canal expanded capacity, it is unprofitable to ship LNG from the Gulf of Mexico to Japan/S. Korea and U.S. LNG exports are shown to flow to Europe. However, the availability of the expanded Panama Canal allows for trade between the two basins and also reroutes approximately half of the total U.S. LNG exports from Europe to Asia, depending on the Canal capacity level. The main users of the Panama Canal route are the U.S. and Trinidad and Tobago.
- The Panama Canal capacity plays a significant role for the direction of the LNG exports from the Gulf of Mexico. When the capacity is limited, the U.S.

becomes a swing gas exporter supplying both Asian and European gas markets. In addition, although the model allows large capacity for Panama Canal, the maximum gas flows through the Canal is only approximately 60 Bcm per year.

- More Panama Canal capacity (e.g., 100 vs. 200 ships/year) means more LNG trade but translates only to a greater number of small tankers.
- There is no doubt that Asian consumers will benefit from inexpensive gas through Panama Canal. LNG exports from the Gulf of Mexico increase competitiveness in Asian gas markets. The regional price disparity is shown to decrease over time. Japanese prices are improved about $1/MMBtu in 2035 when enough capacity of Panama Canal provided.
- The presence of Gulf of Mexico-based LNG in the Japanese market significantly decreases the market shares of the existing exporters e.g., Qatar and Australia, who dynamically increase their sales to neighboring countries such as China and countries in Southeast Asia to compensate for the losses due to U.S. LNG exports. LNG from other Atlantic producers, such as Nigeria and Trinidad and Tobago, also uses the Panama Canal route.

APPENDIX 4-A. Mathematical Formulation

Table A1. Notation used in the model.

Sets	$a \in A$	Gas transportation arcs
	$d \in D$	Demand seasons e.g., { low, high}
	$p \in P$	Producers
	$m \in M$	Years
	$n \in N$	Model nodes
	$s \in S$	Storage facilities
	$t \in T$	Traders
	$a^{+}(n)$	Inward arcs
	$a^{-}(n)$	Outward arcs
	$l \in L$	Liquefiers
	$r \in R$	Regasifiers
	$j \in J$	LNG shipping route, e.g.,{ route without canal, Panama, Suez}
	$c \in C$	LNG carriers, e.g.,{small, large, extra Large}
Variables	$SALES^{A}_{adm}$	Pipeline capacity assigned to a trader (mcm/d)
	$SALES^{P}_{pdm}$	Quantity sold by a producer to traders and liquefiers (mcm/d)
	$SALES^{SI}_{sdm}$	Storage injection capacity assigned for use by traders (mcm/d)
	$SALES^{SX}_{sdm}$	Storage extraction capacity assigned for use by traders (mcm/d)
	$SALES^{T}_{tndm}$	Quantity sold to end-user markets by traders (mcm/d)
	$SALES^{R\rightarrow T}_{rdm}$	Quantity sold to traders by regasifiers (mcm/d)
	$SALES^{canal\rightarrow B}_{dm}$	Canal capacity assigned for use by LNG transporters (mcm/d)
	$SALES^{L}_{ldm}$	Quantity sold to regasifiers by a liquefier (mcm/d)

	$SALES^{B}_{crljdm}$	LNG transported from liquefier *l* to node *r* via route *j* by LNG shipper c (mcm/d)
	$PURCH^{T}_{tndm}$	Quantity bought from a producer by a trader (mcm/d)
	$PURCH^{L\leftarrow P}_{ldm}$	Quantity bought from a producer by a liquefier (mcm/d)
	$PURCH^{T\leftarrow R}_{tdm}$	Quantity bought from a regasifier by a trader (mcm/d)
	$FLOW^{T}_{tadm}$	Arc flow by a trader (mcm/d)
	$LFLOW^{B}_{rljdm}$	LNG transported from node *l* to node *r* via route *j* (mcm/d)
	INJ^{T}_{tndm}	Quantity injected into storage by a trader (mcm/d)
	XTR^{T}_{tndm}	Quantity extracted from storage by a trader (mcm/d)
	Δ^{A}_{am}	Arc capacity expansion (mcm/d)
	Δ^{SI}_{snm}	Storage injection capacity expansion (mcm/d)
	Δ^{SX}_{snm}	Storage extraction capacity expansion (mcm/d)
	Δ^{SW}_{snm}	Storage working gas capacity expansion (mcm/d)
	Δ^{R}_{rm}	Regasification capacity expansion (mcm/d)
	Δ^{L}_{lm}	Liquefaction capacity expansion (mcm/d)
	Δ^{P}_{pm}	Production capacity expansion (mcm/d)
	Δ^{B}_{cm}	LNG transportation capacity expansion (mcm/d)
Dual variables	$\alpha, \beta \geq 0$	Dual variables of capacity restrictions
	φ *free*	Dual variables of mass balance constraints
	$\rho \geq 0$	Dual variables of capacity expansion limitations
	π *free*	Dual variables of market-clearing conditions for sold and bought quantities

	$\tau\ free$	Dual variables of market-clearing conditions for capacity assignment and usage
	tau^{B}_{rljdm}	Dual variable of LNG transportation cost
Parameters	b^{A}_{am}	Arc capacity expansion costs (k$/mcm)
	b^{SI}_{sm}	Storage injection capacity expansion costs (k$/mcm)
	b^{SX}_{sm}	Storage extraction capacity expansion costs (k$/mcm)
	b^{SW}_{sm}	Storage working gas capacity expansion costs (k$/mcm)
	b^{B}_{cm}	LNG shipping capacity expansion costs (k$/mcm)
	b^{P}_{pm}	Production capacity expansion costs (k$/mcm)
	b^{L}_{lm}	Liquefaction capacity expansion costs (k$/mcm)
	b^{R}_{rm}	Regasification capacity expansion costs (k$/mcm)
	$c^{P}_{pm}(.)$	Production costs (k$/mcm)
	$\overline{CAP}^{A}_{am}$	Arc capacity (mcm/d)
	$\overline{CAP}^{SI}_{sm}$	Storage injection capacity (mcm/d)
	$\overline{CAP}^{SX}_{sm}$	Storage extraction capacity (mcm/d)
	$\overline{CAP}^{B}_{cm}$	LNG shipping capacity (mcm/d)
	$\overline{CAP}^{L}_{lm}$	Liquefaction capacity (mcm/d)
	$\overline{CAP}^{R}_{lm}$	Regasification capacity (mcm/d)
	$\overline{CAP}^{CJ}_{jm}$	Canal capacity (mcm/d)
	δ^{C}_{tn}	Level of market power exerted by a trader in a market $\delta^{C}_{tn} \in [0,1]$
	$days_{d}$	Number of days in a season
	γ_{m}	Discount rate for a year, $\gamma_{m} \in (0,1]$

	INT^{W}_{ndm}	Intercept of inverse demand curve (mcm/d)
	$loss_a$	Loss rate of gas in the transport arc, $l_a \in [0,1)$
	$loss_s$	Loss rate of gas storage injection, $l_s \in [0,1)$
	$\overline{PR}^{P}_{pm}$	Initial daily production capacity (mcm/d)
	$\overline{PH}^{P}_{p}$	Total producible reserves in the time horizon (mcm)
	SLP^{W}_{ndm}	Slope of the inverse demand curve (mcm/d/k$)
	$\tau^{A,reg}_{adm}$	Regulated fee for arc usage (k$/mcm)
	$\tau^{SI,reg}_{sdm}$	Regulated fee for storage injection (k$/mcm)
	$\overline{WG}^{S}_{sm}$	Storage working gas capacity (mcm/d)
	$\bar{\Delta}^{A}_{am}$	Upper bound of arc capacity expansion (mcm/d)
	$\bar{\Delta}^{SI}_{sm}$	Upper bound of injection capacity expansion (mcm/d)
	$\bar{\Delta}^{SX}_{sm}$	Upper bound of extraction capacity expansion (mcm/d)
	$\bar{\Delta}^{SW}_{sm}$	Upper bound of working gas capacity expansion (mcm)
	$\bar{\Delta}^{B}_{cm}$	Upper bound of LNG shipping capacity expansion (mcm)
	$\bar{\Delta}^{P}_{pm}$	Upper bound of production capacity expansion (mcm)
	$\bar{\Delta}^{L}_{lm}$	Upper bound of liquefaction capacity expansion costs (mcm)
	$\bar{\Delta}^{R}_{rm}$	Upper bound of regasification capacity expansion costs(mcm)
	CC_m	CO_2 cost ($/ton of CO2e)
	CE_{player}	CO_2 emissions factor (0.1]
	$Dist_{rlj}$	Distance from *r* to *l* via route *j* in units of 1,000 nautical miles
	$MaxDist$	maximum distance for tanker *c* that can travel in 1 day
	α^{cost}_{pm}	Linear term in production cost function

	β_{pm}^{cost}	Quadratic cost term in production cost function
	γ_{pm}^{cost}	logarithmic production cost function
	$CanalDist$	Distance from start to end of Panama Canal
	$AllowSpeed$	Maximum speed permitted on Panama Canal route
	Dayhr	Number of day-light hours
	CAP^{P_canal}	Panama Canal Capacity after converted to mcm/d
	CAP^{S_canal}	Suez Canal Capacity after converted to mcm/d

Producer problem

A natural gas producer $p \in P$ is modeled as profit maximization. The daily profit is determined by the difference between the revenue,$\pi_{n(p)dm}^{P} SALES_{pdm}^{P}$, and the total costs, which are composed of the production cost $C_{pm}^{P}\left(SALES_{pdm}^{P}\right)$, the emission cost[35] $CC_{pm}^{ton} SALES_{pdm}^{P} CE_{p}^{P}$, and the capacity expansion cost, $b_{pm}^{p}\Delta_{pm}^{p}$ which are new features for producers in WGM 2014 The production cost function $C_{pm}^{P}\left(SALES_{pdm}^{P}\right)$ is a logarithmic function (see equation A7) of the involved capacity of capacity utilization. The annual profit is calculated by the sales rate multiplied by the number of day $days_d$ for each season with the discount rate γ_m for that particular year. The producer supplies gas to traders and liquefiers.

$$\underset{\substack{SALES_{pdm}^{P} \\ \Delta_{pm}^{p}}}{\mathbf{max}} \quad \sum_{m \epsilon M} \gamma_m \left\{ \sum_{d \epsilon days} days_d \begin{bmatrix} \pi_{n(p)dm}^{P} SALES_{pdm}^{P} \\ -C_{pm}^{P}\left(SALES_{pdm}^{P}\right) \\ -CC_{pm}^{ton} SALES_{pdm}^{P} CE_{p}^{P} \end{bmatrix} - b_{pm}^{p}\Delta_{pm}^{p} \right\} \text{(A1)}$$

[35] In this study the emissions cost is zero.

The daily sales rates are restricted by the maximum initial capacity PR_p^P and the expansion in the previous years $\sum_{m'<m} \Delta_{pm}^p$.

$$\textbf{s.t.} \quad SALES_{pdm}^P \leq \overline{PR_{pm}^P} + \sum_{m'<m} \Delta_{pm'}^p \quad \forall d, m \quad (\alpha_{pdm}^P) \tag{A2}$$

The total sales over the time horizon are limited by the reserves.

$$\sum_{m \in M} \sum_{d \in D} days_d \, SALES_{pdm}^P \leq \overline{PH_p^P} \quad \forall m \ (\beta_p^{PH}) \tag{A3}$$

The production capacity expansion is less than the budgetary constraints.

$$\Delta_{pm}^p \leq \overline{\Delta_{pm}^p} \quad \forall m \ (\rho_{pm}^P) \tag{A4}$$

The sales rate and the capacity expansion must not be negative.

$$SALES_{pdm}^P \geq 0 \quad \forall d, m \tag{A5}$$

$$\Delta_{pm}^p \geq 0 \quad \forall m \tag{A6}$$

The production cost function follows the fossil fuel supply cost proposed by Golombek et al. (1995), but we consider the expansion from the previous year. Details of the expansion of a logarithmic production cost function can be found in Huppmann (2013).

$$C_{pm}^P\left(SALES_{pdm}^P\right) =$$

$$\left(\alpha_{pm}^{cost} + \gamma_{pm}^{cost}\right) SALES_{pdm}^P + \beta_{pm}^{cost} SALES_{pdm}^2$$

$$+\gamma_{pm}^{cost}\left(\overline{PR_{pm}^P} + \sum_{m'<m} \Delta_{pm}^p - SALES_{pdm}^P\right) \ln\left(1 - \left(\frac{SALES_{pdm}^P}{\overline{PR_{pm}^P} + \sum_{m,<m} \Delta_{pm}^p}\right)\right) \tag{A7}$$

Trader problem

Equation (A8) is the objective function for the trader and optimizes gas sales levels $SALES^{T}_{tndm}$, purchases of gas $PURCH^{T\leftarrow P}_{tndm}$ from producers and regasifiers. In addition, we assume the trader decides how much to inject INJ^{T}_{tndm} and XTR^{T}_{tndm} from storage. The trader maximizes the discounted profits, which come from the revenue $(\delta^{C}_{tn}\Pi^{W}_{ndm}(.) + (1-\delta^{C}_{tn})\pi^{W}_{ndm})SALES^{T}_{tndm}$ and the purchasing costs $\pi^{P}_{ndm}PURCH^{T\leftarrow P}_{tndm}$ and $\pi^{R}_{ndm}PURCH^{T\leftarrow R}_{tndm}$, the cost of using storage, $(\tau^{SI,reg}_{sndm} + \tau^{SI}_{sndm})INJ^{T}_{tndm} + \tau^{SX}_{sndm}XTR^{T}_{tndm}$, and the emission cost[36] $(CC^{ton}_{tm}SALES^{T}_{tndm}.CE^{T}_{T})$. The traders are modeled as a weighted combination of strategic/competitive players depending on the market power parameter $\delta^{C}_{tn} \in [0,1]$, where 0 represents competitive behavior and 1 indicates oligopolistic behavior with a knowledge of demand in the market. In addition, the trader is responsible for the transportation costs, $(\tau^{A,reg}_{adm} + \tau^{A}_{adm})FLOW^{T}_{tadm}$, for the gas.

$$\max_{\substack{SALES^{T}_{tndm}\\ PURCH^{T\leftarrow P}_{tndm}\\ PURCH^{T\leftarrow R}_{tndm}\\ FLOW^{T}_{tadm}\\ INJ^{T}_{tndm}\\ XTR^{T}_{tndm}}} \sum_{m\epsilon M}\gamma_m \sum_{d\epsilon D} days_d \left\{ \sum_{n\epsilon N(t)} \left[\begin{array}{c} (\delta^{C}_{tn}\Pi^{W}_{ndm}(.) + (1-\delta^{C}_{tn})\pi^{W}_{ndm})SALES^{T}_{tndm} \\ -\pi^{P}_{ndm}PURCH^{T\leftarrow P}_{tndm} \\ -\pi^{R}_{ndm}PURCH^{T\leftarrow R}_{tndm} \\ -(CC^{ton}_{tm}SALES^{T}_{tndm}CE^{T}_{T}) \\ -\sum_{s\epsilon S(t)} \left(\begin{array}{c} (\tau^{SI,reg}_{sndm} + \tau^{SI}_{sndm})INJ^{T}_{tndm} \\ +\tau^{SX}_{sndm}XTR^{T}_{tndm} \end{array} \right) \end{array} \right] - \left(\sum_{a\epsilon A(t)} (\tau^{A,reg}_{adm} + \tau^{A}_{adm})FLOW^{T}_{tadm} \right) \right\} \quad (A8)$$

This constraint ensures the mass balance of sales, purchases, flows, and storage.

$$PURCH^{T\leftarrow R}_{tndm} + PURCH^{T}_{tndm} + \sum_{a\epsilon a^{+}(n)} (1-loss_a)\, FLOW^{T}_{tadm} + XTR^{T}_{tndm} =$$

[36] In this study the emissions cost is zero.

$$SALES^{T}_{tndm} + \sum_{a\epsilon a^-} FLOW^{T}_{tadm} + INJ^{T}_{tndm} \quad \forall n, d, m \; (\varphi^{T}_{tndm}) \tag{A9}$$

In each yearly storage cycle, the total extracted volumes must equal the loss-corrected injection volumes.

$$(1 - loss_s) \sum_{d\epsilon D} days_d \, INJ^{T}_{tndm} = \sum_{d\epsilon D} days_d \, XTR^{T}_{tndm} \quad \forall n, s\epsilon S\big(N(t)\big), d, m \quad \left(\varphi^{S}_{tndm}\right) \tag{A10}$$

All of the variables must be nonnegative.

$$SALES^{T}_{tndm} \geq 0 \quad \forall n, d, m \tag{A11}$$

$$PURCH^{T}_{tndm} \geq 0 \quad \forall n, d, m \tag{A12}$$

$$FLOW^{T}_{tadm} \geq 0 \quad \forall a, d, m \tag{A13}$$

$$INJ^{T}_{tndm} \geq 0 \quad \forall n, d, m \tag{A14}$$

$$XTR^{T}_{tndm} \geq 0 \quad \forall n, d, m \tag{A15}$$

Liquefier problem

Liquefiers buy gas from the producers and sell it to regasifiers globally. The liquefier maximizes the discounted profit $\pi^{L}_{n(l)dm} SALES^{L}_{ldm}$ minus the purchasing costs, $\pi^{P}_{n(l)dm} PURCH^{L\leftarrow P}_{ldm}$, liquefaction costs $C^{L}_{lm}(SALES^{L}_{ldm})$, and capacity investment costs $b^{L}_{lm}\Delta^{\mathrm{L}}_{lm}$.

$$\underset{\substack{SALES^{L}_{ldm} \\ PURCH^{L\leftarrow P}_{ldm} \\ \Delta^{\mathrm{L}}_{lm}}}{Max} \sum_{m\epsilon M} \gamma_m \left\{ \sum_{d\epsilon D} day_d \begin{bmatrix} \pi^{L}_{n(l)dm} SALES^{L}_{ldm} \\ -\pi^{P}_{n(l)dm} PURCH^{L\leftarrow P}_{ldm} \\ -C^{L}_{lm}(SALES^{L}_{ldm}) \end{bmatrix} - b^{L}_{lm} \, \Delta^{\mathrm{L}}_{\mathrm{lm}} \right\} \tag{A16}$$

The sales are restricted by the initial capacity CAP_l^L plus the total expansion $\sum_{m'<m} \Delta_{lm'}^L$ from the previous period.

$$SALES_{ldm}^L \leq CAP_l^L + \sum_{m'<m} \Delta_{lm'}^L \quad \forall d, m \; (\alpha_{ldm}^L) \tag{A17}$$

The sales rates are also restricted by losses from the liquefaction process.

$$(1 - loss_l) PURCH_{ldm}^{L \leftarrow P} - SALES_{ldm}^L \geq 0 \quad \forall d, m \; (\phi_{ldm}^L) \tag{A18}$$

The expansion in each time period is limited by budget restrictions.

$$\Delta_{lm}^L \leq \bar{\Delta}_{lm}^L \quad \forall m \; (\rho_{lm}^L) \tag{A19}$$

All of the variables must be nonnegative.

$$SALES_{ldm}^L \geq 0 \tag{A20}$$

$$PURCH_{ldm}^{L \leftarrow P} \geq 0 \tag{A21}$$

$$\Delta_{lm}^L \geq 0 \tag{A22}$$

LNG shipping operators

LNG transporters provide maritime transportation capacity to ship gas from a liquefier *l* to a regasifier *r*. Each transporter $c \in C$ owns ships of different sizes and operates at different shipping costs depending on the distances and tanker types. The capacity of each transporter is the aggregated capacity of all of the LNG carriers of a particular size that are available in the shipping market. The LNG transporter maximizes the discounted profit $\sum_{r,l,j} tau_{rljdm}^B SALES_{crljdm}^B$ minus the shipping cost $C_{cm}^B\left(SALES_{crljdm}^B\right)$ and the costs of using the canal $\tau_{dm}^{P\_toll}$ for Panama Canal and

$\tau_{dm}^{S\_toll}$ Suez Canal plus congestion fees $\tau_{dm}^{P_con}$and $\tau_{dm}^{S\_con}$ for LNG flows on route $j \in \{Panama, Suez\}$. The endogenous investment for LNG tanker $b_{cm}^{B}\Delta_{\mathrm{cm}}^{\mathrm{B}}$ is also considered if it is profitable in the future time period.

$$Max_{\substack{SALES_{crljdm}^{B} \\ \Delta_{cm}^{B}}} \sum_{m\epsilon M} \gamma_m \left\{ \sum_{d\epsilon D} day_d \left\{ \begin{array}{c} \sum_{r,l,j} tau_{rljdm}^{B} SALES_{crljdm}^{B} \\ -C_{cm}^{B}\left(SALES_{crljdm}^{B}\right) \\ -\sum_{r,l,j\in\{p_{canal}\}}(\tau_{dm}^{P\_toll} + \tau_{dm}^{P\_con})SALES_{crljdm}^{B} \\ -\sum_{r,l,j\in\{S_{canal}\}}(\tau_{dm}^{S\_toll} + \tau_{dm}^{s\_con})SALES_{crljdm}^{B} \end{array} \right\} - b_{cm}^{B}\Delta_{\mathrm{cm}}^{\mathrm{B}} \right\} \quad \text{(A23)}$$

The sales rates on maritime shipping are constrained by the capacity of the LNG carrier, the average ship speed, and the maximum distance traveled in one day. This constraint has units of mcm/1,000 nautical miles. The total capacity is the initial capacity plus the expansion from the previous time periods $\sum_{m'<m} \Delta_{cm'}^{B}$. We also assume LNG tankers take the same route back and forth from origin to destination.

$$\sum_{r,l} 2 * (SALES_{crljdm}^{B} * Dist_{rlj}) \leq max\_dis_c * (CAP_c^B + \sum_{m'<m} \Delta_{cm'}^{B}) \quad \forall d, m \ (\alpha_{cdm}^{B}) \quad \text{(A24)}$$

The expansion for each time period is constrained by budget restrictions.

$$\Delta_{cm}^{B} \leq \bar{\Delta}_{cm}^{B} \quad \forall m \ (\rho_{cm}^{B}) \quad \text{(A25)}$$

The sales of extra-large ships are restricted on the Panama and Suez Canal routes.

$$SALES_{c\in\{Exlarge\}rlj\epsilon\{S_{Canal}\}dm}^{B} = 0 \quad \forall r, l, d, m \ (\beta_{c\in\{Exlarge\}rldm}^{B}) \quad \text{(A26)}$$

$$SALES_{c\in\{Exlarge\}rlj\epsilon\{P_{Canal}\}dm}^{B} = 0 \quad \forall r, l, d, m \ (\beta_{c\in\{Exlarge\}rldm}^{B}) \quad \text{(A27)}$$

All of the variables must be nonnegative.

$$SALES^{B}_{crldm} \geq 0 \quad \text{(A28)}$$

$$\Delta^{B}_{cm} \geq 0 \quad \text{(A29)}$$

Regasifier problem

The regasifier maximizes the discounted profit from the sellers to the traders $SALES^{R\rightarrow T}_{rdm}$ minus the costs of purchases,$\sum_{rlj} \pi^{L}_{n(l)dm} LFLOW^{B}_{rljdm}$ the cost of shipping from the LNG transporter$\sum_{(r,l,j)}\{LFLOW^{B}_{rljdm}\,(tau^{B}_{rljdm})\}$, the cost of the regasification process $C^{R}_{rm}\left(SALES^{R\rightarrow T}_{rdm}\right)$, and the capacity expansion cost $b^{R}_{rm}\Delta^{\mathrm{R}}_{\mathrm{rm}}$.

$$Max \underset{\substack{SALES^{R\rightarrow T}_{rdm} \\ SALES^{R\rightarrow M}_{rdm} \\ LFLOW^{B}_{rljdm}, \Delta^{R}_{rm}}}{} \sum_{m\epsilon M} \gamma_m \left\{ \sum_{d\epsilon D} day_d \left[\begin{array}{c} \pi^{R}_{n(r)\mathrm{dm}} SALES^{R\rightarrow T}_{rdm} \\ -\sum_{rlj} \pi^{L}_{n(l)dm} LFLOW^{B}_{rljdm} \\ -\sum_{rlj}\{LFLOW^{B}_{rljdm}\,(tau^{B}_{rljdm})\} \\ -C^{R}_{rm}\left(SALES^{R\rightarrow T}_{rdm}\right) \end{array} \right] - b^{R}_{rm}\,\Delta^{\mathrm{R}}_{\mathrm{rm}} \right\} \quad \text{(A30)}$$

The sales rates are constrained by the initial capacity plus the expansion from the previous time periods.

$$SALES^{R\rightarrow T}_{rdm} \leq CAP^{R}_{r} + \sum_{m'<m} \Delta^{R}_{rm'} \quad \forall d, m\ (\alpha^{R}_{rdm}) \quad \text{(A31)}$$

This constraint considers losses incurred in maritime transport and the regasification process.

$$\sum_{lrj}\left(1 - loss_{lrj}\right) * (1 - loss_{r}) * LFLOW^{B}_{rljdm} \geq SALES^{R\rightarrow T}_{rdm} \quad \forall d, m\ (\phi^{R}_{rdm}) \quad \text{(A32)}$$

The expansion for each time period is constrained by budget restrictions.

$$\Delta^{R}_{rm} \leq \bar{\Delta}^{R}_{rm} \quad \forall m\ (\rho^{R}_{rm}) \quad \text{(A33)}$$

The minimum purchases for long-term LNG contracts are enforced. Future contracts are assumed to have the same volume before their term expires.

$$\sum_j LFLOW^B_{rljdm} \geq Contract^R_{rldm} \; \forall r,l,d,m \;\; (\varepsilon^R_{rldm}) \qquad \text{(A34)}$$

All of the variables must be non-negative.

$$SALES^{R\to M}_{rdm} \geq 0 \qquad \text{(A35)}$$

$$SALES^{R\to T}_{rdm} \geq 0 \qquad \text{(A36)}$$

$$LFLOW^B_{rljdm} \geq 0 \qquad \text{(A37)}$$

$$\Delta^R_{rm} \geq 0 \qquad \text{(A38)}$$

Canal operator problem

The canal operator provides shorter distances to the LNG transporter compared to the regular route from the liquefier *l* to the regasifier *r* for an additional charge. The canal operator maximizes his discounted profit from the canal toll $\tau^{P\_toll}_{dm}, \tau^{S\_toll}_{dm}$ and congestion fees $\tau^{P\_con}_{dm}, \tau^{S\_con}_{dm}$ minus the operating costs $C^{P_{Canal}}_{dm}(SALES^{P_{canal}\to B}_{dm})$ and $C^{S_{Canal}}_{dm}(SALES^{S_{canal}\to B}_{dm})$.

$$Max_{\substack{SALES^{P\_canal\to B}_{dm} \\ SALES^{S\_canal\to B}_{dm}}} \sum_{m\epsilon M} \gamma_m \left\{ \sum_{d\epsilon D} day_d \begin{bmatrix} (\tau^{P\_toll}_{dm} + \tau^{P\_con}_{dm}) SALES^{P\_canal\to B}_{dm} \\ (\tau^{S\_toll}_{dm} + \tau^{S\_con}_{dm}) SALES^{S\_canal\to B}_{dm} \\ -C^{P_{Canal}}_{dm}(SALES^{P_{canal}\to B}_{dm}) \\ -C^{S_{Canal}}_{dm}(SALES^{S_{canal}\to B}_{dm}) \end{bmatrix} \right\} \text{(A39)}$$

The sales rates for the Panama Canal is restricted by speed allowance and daylight hours, see A40. [37] The left-hand side of this constraint shows how much gas flows in mcm per day through the Canal multiplied by the distance from the start of the canal to the end of Canal (50 nautical miles), so the units of the left-hand side are mcm.nautical miles per day. For the right-hand side, the allowed average speed (8 nautical miles per hour) is multiplied by the number of operating hours per day (12 hours from sunrise to sunset) and the capacity in mcm per day, so we get the same units (mcm*nautical miles per day) as the left- hand side.

$$SALES_{dm}^{P\_canal\to B} CanalDist \leq AllowSpeed * Dayhr * CAP^{P\_canal} \quad \forall d,m\left(\alpha_{dm}^{P\_Canal}\right) \quad \text{(A40)}$$

The sales rates for the Suez canals are limited by its capacity. [38]

$$SALES_{dm}^{S\_canal\to B} \leq CAP^{S\_canal} \quad \forall d,m\left(\alpha_{dm}^{S\_Canal}\right) \quad \text{(A41)}$$

All of the variables must be non-negative.

$$SALES_{dm}^{P\_canal\to B} \geq 0 \quad \text{(A42)}$$

$$SALES_{dm}^{S\_canal\to B} \geq 0 \quad \text{(A43)}$$

Transmission system operators

The transmission system operator (TSO) provides an economic mechanism to efficiently allocate international transport capacity to traders. The TSO maximizes the discounted profit that results from selling arc capacity to traders from $SALES_{adm}^{A}$ minus

[37] The Panama Canal Authority requires the fleets to maintain a speed of 5 knots. However, the average speed is 8 knots.

[38] The Suez Canal can accommodate up to 106 vessels in one north-bound and two south-bound convoys. In addition Suez Canal operate at night so that the constraint is simpler than Panama Canal.

the investment costs for capacity expansions Δ_{am}^{A} and CO_2 costs $CC_{tsom}^{ton} SALES_{adm}^{A} CE_{tso}^{TSO}$.

$$Max_{\substack{SALES_{adm}^{A} \\ \Delta_{am}^{A}}} \quad \sum_{m\epsilon M} \gamma_m \left\{ \sum_{d\epsilon D} days_d \begin{bmatrix} \sum_a \tau_{adm}^{A} SALES_{adm}^{A} \\ -CC_{tsom}^{ton} SALES_{adm}^{A}. CE_{tso}^{TSO} \end{bmatrix} - \sum_a b_{am}^{A} \Delta_{am}^{A} \right\} \text{(A44)}$$

The assigned capacity is restricted by the available capacity. The available arc capacity at arc *a* is the sum of the initial arc capacity $\overline{CAP}_{am}^{A}$ and the capacity expansions in the previous year $\sum_{m'<m} \Delta_{am'}^{A}$. The sales are limited by capacity and the expansion from the previous year.

$$SALES_{adm}^{A} \leq \overline{CAP}_{am}^{A} + \sum_{m<m'} \Delta_{am'}^{A} \qquad \forall a, d, m \ (\alpha_{adm}^{A}) \qquad \text{(A45)}$$

There may be budgetary or other limits on the yearly capacity expansions.

$$\Delta_{am}^{A} \leq \overline{\Delta}_{am}^{A} \quad \forall a, m \quad (\rho_{am}^{A}) \qquad \text{(A46)}$$

All of the variables must be non-negative.

$$SALES_{adm}^{A} \geq 0 \quad \forall m, d \qquad \text{(A47)}$$

$$\Delta_{am}^{A} \geq 0 \quad \forall m \qquad \text{(A48)}$$

Storage operator

The storage operator provides storage capacity to the traders. The revenue term is calculated by $\tau_{sdm}^{SI} SALES_{sdm}^{SI} + \tau_{sdm}^{SX} SALES_{sdm}^{SX}$ minus the expansion cost $b_{sm}^{SX} \Delta_{sm}^{SX} + b_{sm}^{SI} \Delta_{sm}^{SI} + b_{sm}^{SW} \Delta_{sm}^{SW}$ and the emission cost$CC_{sm}^{ton} (SALES_{pdm}^{SI} + SALES_{pdm}^{SX}) CE_{s}^{S}$.

$$max_{\substack{SALES_{sdm}^{SX} \\ SALES_{sdm}^{SI} \\ \Delta_{sm}^{SX}, \Delta_{sm}^{SI}, \Delta_{sm}^{SW}}} \quad \sum_{m\epsilon M} \gamma_m \sum_{d\epsilon D} days_d \begin{bmatrix} \tau_{sdm}^{SI} SALES_{sdm}^{SI} + \tau_{sdm}^{SX} SALES_{sdm}^{SX} \\ -(b_{sm}^{SX} \Delta_{sm}^{SX} + b_{sm}^{SI} \Delta_{sm}^{SI} + b_{sm}^{SW} \Delta_{sm}^{SW}) \\ -(CC_{sm}^{ton} (SALES_{pdm}^{SI} + SALES_{pdm}^{SX}) CE_{s}^{S}) \end{bmatrix}$$

(A49)

The aggregate injection rate in any season is restricted by the injection capacity (A50). Injection capacities can be expanded; therefore, the aggregate previous yearly expansions $\sum_{m'<m} \Delta_{sm'}^{SI}$ must be added to the initial capacity $\overline{INJ}_s^S$ to determine the total capacity. Equation (A51) provides the limits on the extraction from storage, and condition (A52) represents the working gas limitations.

$$SALES_{sdm}^{SI} \leq \overline{CAP}_{sm}^{SI} + \sum_{m<m'} \Delta_{sm'}^{SI}, \quad \forall m, d \ (\alpha_{sdm}^{SI}) \tag{A50}$$

$$SALES_{Sdm}^{SX} \leq \overline{CAP}_{sm}^{SX} + \sum_{m<m'} \Delta_{sm'}^{SX}, \quad \forall m, d \ (\alpha_{sdm}^{SX}) \tag{A51}$$

$$\sum_{d \epsilon D} days \ SALES_{sdm}^{SX} \leq \overline{WG}_{sm}^{S} + \sum_{m<m'} \Delta_{sm'}^{SX}, \quad \forall m \ (\alpha_{sm}^{SW}) \tag{A52}$$

The limitations on the allowable capacity expansions are modeled as follows:

$$\Delta_{sm}^{SW} \leq \bar{\Delta}_{sm}^{SW} \quad , \forall m \quad (\rho_m^{SW}) \tag{A53}$$

$$\Delta_{sm}^{SI} \leq \bar{\Delta}_{sm}^{SI} \quad , \forall m \quad (\rho_m^{SI}) \tag{A54}$$

$$\Delta_{sm}^{SX} \leq \bar{\Delta}_{sm}^{SX} \quad , \forall m \quad (\rho_m^{SX}) \tag{A55}$$

All of the variables must be non-negative.

$$SALES_{Sdm}^{SI} \geq 0 \quad , \forall m, d \tag{A56}$$

$$SALES_{Sdm}^{SX} \geq 0 \quad , \forall m, d \tag{A57}$$

$$\Delta_{sm}^{SW} \geq 0 \quad , \forall m \tag{A58}$$

$$\Delta_{sm}^{SX} \geq 0 \quad , \forall m \tag{A59}$$

$$\Delta_{sm}^{SI} \geq 0 \quad , \forall m \tag{A60}$$

Market-clearing conditions

Market clearing conditions tie the producers to traders and liquefiers. The total sales from producers equals the purchases from traders and liquefiers.

$$SALES_{pdm}^{P} = \sum_{l \in L(p)} PURCH_{ldm}^{L \leftarrow P} + \sum_{t(p)} PURCH_{tn(p)dm}^{T}, \quad \forall p, d, m \ (\pi_{n(p)dm}^{P}) \tag{A61}$$

The injection capacity offered by a storage operator equals the total of injection from all traders. The market clearing condition injection capacity is

$$SALES_{sdm}^{SI} = \sum_{t \epsilon T(N(s))} INJ_{tsdm}^{T} \quad \forall s, d, m \ (\tau_{sdm}^{SI}) \tag{A62}$$

The extraction capacity offered by a storage operator equals the total of extraction from all traders. The market clearing condition extraction capacity is

$$SALES_{sdm}^{SX} = \sum_{t\epsilon T(N(s))} XTR_{tsdm}^{T} \quad \forall s,d,m \quad (\tau_{sdm}^{SX}) \tag{A63}$$

The pipeline capacity offered by a pipeline operator equals the total of flows from all traders. The market clearing condition for arc capacity flow is

$$SALES_{adm}^{A} = \sum_{t} FLOW_{tadm}^{T} \quad \forall a,d,m \quad (\tau_{adm}^{A}) \tag{A64}$$

The total sales from liquefiers equals the total flows from different routes to regasifier. The market clearing condition between the liquefiers and the regasifiers is

$$\sum_{\boldsymbol{l\epsilon L(n(l))}} SALES_{ldm}^{L} = \sum_{j\in J} \sum_{r\in R} LFLOW_{rljdm}^{R\leftarrow L} \quad \forall d,m \quad \left(\pi_{n(l)dm}^{L}\right) \tag{A65}$$

The flow on the route j from liquefier l to regasifier j equals the total shipping capacity offered by different shipping operators. The market clearing condition between the regasifiers and the LNG transporters is

$$\sum_{c} SALES_{crljdm}^{B} = LFLOW_{rljdm}^{B} \; \forall r,l,\mathrm{j},d,m \quad (tau_{rljdm}^{B}) \tag{A66}$$

The canal capacity offered by canal operator equals the total flows from all LNG shipping operators on the canal routes. The market-clearing conditions between the canal operators and the LNG transporters are:

$$SALES_{dm}^{P\_canal\rightarrow B} = \sum_{c,r,l} SALES_{crljdm}^{B} \; \forall j \in \{P\_Cannal\},d,m \quad (\tau_{dm}^{P\_canal\ toll}) \tag{A67}$$

$$SALES_{dm}^{S\_canal\rightarrow B} = \sum_{c,r,l} SALES_{crljdm}^{B} \; \forall j \in \{S\_Cannal\},d,m \quad (\tau_{dm}^{S\_canal\ toll}) \tag{A68}$$

Market-clearing conditions for final demand

$$\pi_{ndm}^{W} = INT_{ndm}^{W} - SLP_{ndm}^{W}\left(\sum_{t} SALES_{tndm}^{T}\right) \quad \forall n,d,m \quad (\pi_{ndm}^{W}) \tag{A69}$$

APPENDIX 4-B: KKT conditions

KKT conditions for the producer problem

$$0 \leq days_d \left[\gamma_m \left(-\pi^P_{n(p)dm} + \frac{\partial c^P_{pm}\left(SALES^P_{pdm}\right)}{\partial SALES^P_{pdm}} + CC^{ton}_{pm} CE^p_p\right)\right] + \alpha^P_{pdm} + days_d \beta^P_p \perp$$

$$SALES^P_{pdm} \geq 0 \quad \forall d, m \tag{B1}$$

$$0 \leq \overline{PR^P_{pm}} + \sum_{m'<m} \Delta^p_{pm} - SALES^P_{pdm} \perp \ \alpha^P_{pdm} \geq 0 \quad \forall d, m \tag{B2}$$

$$0 \leq \overline{PH^P_p} - \sum_{m\in M} \sum_{d\in D} days_d \, SALES^P_{pdm} \perp \beta^P_p \ \geq 0 \tag{B3}$$

$$0 \leq \gamma_m b^p_{pm} + \sum_{m'>m} \frac{\partial c^P_{pm'}(.)}{\partial \Delta^p_{pm}} - \sum_{m'>m} \sum_d \alpha^P_{pdm} + \rho^P_{pm} \perp \ \Delta^p_{pm} \geq 0 \quad \forall m \tag{B4}$$

$$0 \leq \bar{\Delta}^P_{pm} - \Delta^P_{pm} \perp \ \rho^P_{pm} \geq 0 \ \ \forall m \tag{B5}$$

KKT conditions for the trader problem

$$0 \leq days_d \left[\gamma_m \begin{pmatrix} \delta^C_{tn} SLP^M_{ndm} SALES^T_{tndm} \\ -\left(\delta^C_{tn} \Pi^{W(T)}_{ndm} + (1-\delta^C_{tn})\pi^W_{ndm}\right) \\ +(CC^{ton}_{tm} . CE^T_T) \end{pmatrix}\right] + \phi^T_{tndm} \perp SALES^T_{tndm} \geq$$

$$0, \quad \forall n, d, m \tag{B6}$$

$$0 \leq days_d [\gamma_m \pi^P_{ndm}] - \phi^T_{tndm} \perp \ PURCH^{T\leftarrow P}_{tndm} \geq 0 \quad \forall n \epsilon N\left(p(t)\right), d, m \tag{B7}$$

$$0 \leq days_d \left[\gamma_m \pi^R_{n(r)\mathrm{dm}}\right] - \phi^T_{tndm} \perp \ PURCH^{T\leftarrow R}_{tndm} \geq 0 \quad \forall n \epsilon N\left(r(t)\right), d, m \tag{B8}$$

$$0 \leq days_d \gamma_m \left(\tau^{SI,reg}_{ndm} + \tau^{SI}_{ndm}\right) + \phi^T_{tndm} - (1 - loss_n) days_d \phi^S_{tnm} \perp \ INJ^T_{tdnm} \geq$$

$$0 \ \forall n, m \tag{B9}$$

$$0 \leq days_d \gamma_m (\tau^{SX}_{ndm}) - \phi^T_{tndm} + days_d \phi^S_{tndm} \perp \ XTR^T_{tndm} \geq 0 \quad \forall n, m \tag{B10}$$

$$0 \le days_d \gamma_m \left(\tau^{A,reg}_{sndm} + \tau^{A}_{sndm}\right) + \phi^{T}_{tna^- dm} - (1 - loss_a)\phi^{T}_{tna^+ dm} \perp \quad FLOW^{T}_{tndm} \ge 0$$

$$\forall a = \left(n_{a^-}, n_{a^+}\right), \forall d, m \tag{B11}$$

$$0 = \begin{bmatrix} PURCH^{T}_{tndm} + PURCH^{T \leftarrow R}_{tndm} + \sum_{a \epsilon a^+(n)} (1 - loss_a)\, FLOW^{T}_{tadm} + XTR^{T}_{tndm} \\ -SALES^{T}_{tndm} - \sum_{a \epsilon a^-} FLOW^{T}_{tadm} - INJ^{T}_{tndm} \end{bmatrix}, \varphi^{T}_{tndm}, free, \forall n, d, m$$

(B12)

$$0 = (1 - loss_s) \sum_{d \epsilon D} days_d\, INJ^{T}_{tsdm} - \sum_{d \epsilon D} days_d\, XTR^{T}_{tsdm}\,, \varphi^{S}_{tsm}, free \;\; \forall n, s \epsilon S\left(N(t)\right), d, m$$

(B13)

KKT conditions for the liquefier problem

$$0 \le day_d \left[\gamma_m \left(-\pi^{L}_{n(l)dm} + \frac{\partial C^{L}_{lm}\left(SALES^{L}_{ldm}\right)}{\partial SALES^{L}_{ldm}}\right)\right] + \alpha^{L}_{ldm} + \phi^{L}_{ldm} \perp SALES^{L}_{ldm} \ge$$

$$0 \;\; \forall d, m \tag{B14}$$

$$0 \le day_d \left[\gamma_m \left(\pi^{P}_{n(l)dm}\right)\right] - (1 - loss_l)\phi^{L}_{ldm} \perp PURCH^{L \leftarrow P}_{ldm} \ge 0 \;\; \forall d, m \tag{B15}$$

$$0 \le \gamma_m b^{L}_{lm} - \sum_d \sum_{m' > m} \alpha^{L}_{ldm} + \rho^{L}_{lm} \perp \Delta^{L}_{lm} \ge 0 \;\; \forall m \tag{B16}$$

$$0 \le CAP^{L}_{l} + \sum_{m' < m} \Delta^{L}_{lm'} - SALES^{L}_{ldm} \perp \alpha^{L}_{ldm} \ge 0 \;\; \forall d, m \tag{B17}$$

$$0 \le (1 - loss_l) PURCH^{L \leftarrow P}_{ldm} - SALES^{L}_{ldm} \perp \phi^{L}_{ldm} \ge 0 \quad \forall d, m \tag{B18}$$

$$0 \le \bar{\Delta}^{L}_{lm} - \Delta^{L}_{lm} \perp \quad \rho^{L}_{lm} \ge 0 \quad \forall m \tag{B19}$$

KKT conditions for the LNG shipper problem

$$0 \le day_d \gamma_m \left(-tau^{B}_{rljdm} + \frac{\partial C^{B}_{cm}\left(SALES^{B}_{crljdm}\right)}{\partial SALES^{B}_{crljdm}} + \begin{Bmatrix} \tau^{Ptoll}_{jdm} & j \in \{P_{Canal}\} \\ \tau^{Stoll}_{jdm} & j \in \{S_{Canal}\} \end{Bmatrix}\right) + 2 * Dist_{rlj} *$$

$$\alpha^{B}_{cdm} \perp SALES^{B}_{crljdm} \ge 0 \;\; \forall d, m \tag{B20}$$

$$0 \le \gamma_m b^{B}_{m} - \sum_d \sum_{m' > m} MaxDist_c * \alpha^{B}_{cdm} + \rho^{B}_{cbm} \perp \Delta^{R}_{crm} \ge 0 \;\; \forall m \tag{B21}$$

$$0 \le -\sum_{r,l,j} 2 * (SALES^{B}_{crljdm} * Dist_{rlj}) + MaxDist_c * (CAP^{B}_{c} + \sum_{m' < m} \Delta^{B}_{cm'}) \tag{B22}$$

$\perp\ \alpha^{B}_{cdm} \geq 0\ \ \forall d, m$ (B23)

$0 \leq \bar{\Delta}^{B}_{cm} - \Delta^{B}_{cm} \perp \rho^{B}_{m} \geq 0 \qquad \forall m$ (B24)

KKT conditions for the regasifier problem

$$0 \leq day_d \gamma_m \left[\begin{pmatrix} -\pi^{r}_{n(r)dm} \\ + \frac{\partial C^{R}_{rm}(SALES^{R\to T}_{rdm})}{\partial SALES^{R\to T}_{rdm}} \end{pmatrix} \right] + \alpha^{R}_{rdm} + \phi^{R}_{rdm} \perp SALES^{R\to T}_{rdm} \geq 0\ \ \forall d, m \quad \text{(B25)}$$

$$0 \leq day_d \gamma_m \left(\pi^{L}_{n(l)dm} + tau^{B}_{rljdm}\right) - \left(\left(1 - loss_{lrj}\right) * \left(1 - loss_{r}\right)\right) \phi^{R}_{rdm} - \varepsilon^{R}_{rldm} \perp$$

$$LFLOW^{B}_{rljdm} \geq 0\ \forall r, l, j, d, m \quad \text{(B26)}$$

$0 \leq \gamma_m b^{R}_{rm} - \sum_{m'>m} \sum_{d\epsilon D} \alpha^{R}_{rdm} + \rho^{R}_{rm} \perp \Delta^{R}_{rm} \geq 0\ \ \forall m$ (B27)

$0 \leq CAP^{R}_{r} + \sum_{m'<m} \Delta^{R}_{rm'} - \left(SALES^{R\to T}_{rdm}\right) \perp \alpha^{R}_{rdm} \geq 0\ \forall d, m$ (B28)

$0 \leq \bar{\Delta}^{R}_{rm} - \Delta^{R}_{rm} \perp\ \ \rho^{R}_{rm} \geq 0\ \ \forall m$ (B29)

$$0 \leq \sum_{r,l,j} \left(\left(1 - loss_{lrj}\right) * \left(1 - loss_{r}\right) * LFLOW^{B}_{rljdm}\right) - SALES^{R\to T}_{rdm} \perp \phi^{R}_{rdm} \geq 0 \quad \forall d, m \quad \text{(B30)}$$

$0 \leq \sum_{j} LFLOW^{B}_{rljdm} - Contract^{R}_{rldm} \perp \varepsilon^{R}_{rldm} \geq 0 \qquad \forall r, l, d, m$ (B31)

KKT conditions for the storage operator problem

$0 \leq -days_d \gamma_m (\tau^{SI}_{sdm} + CC^{ton}_{sm} . CE^{S}_{s}) + \alpha^{SI}_{sdm} \perp\ SALES^{SI}_{sdm} \geq 0 \quad \forall d, m$ (B32)

$$0 \leq -days_d \gamma_m (\tau^{SX}_{sdm} + CC^{ton}_{sm} . CE^{S}_{s}) + \alpha^{SX}_{sdm} + days_d \alpha^{SW}_{sdm} + \perp\ SALES^{SX}_{sdm} \geq 0 \quad \forall d, m \quad \text{(B33)}$$

$0 \leq \gamma_m b^{SI}_{sm} - \sum_{d\epsilon D} \sum_{m\prime>m} \alpha^{SI}_{sdm'} + \rho^{SI}_{m} \perp\ \Delta^{SI}_{sm'} \geq 0 \quad \forall m$ (B34)

$0 \leq \gamma_m b^{SX}_{sm} - \sum_{d\epsilon D} \sum_{m\prime>m} \alpha^{SX}_{sdm'} + \rho^{SX}_{m} \perp\ \Delta^{SX}_{sm'} \geq 0 \quad \forall m$ (B35)

$0 \leq \gamma_m b^{SW}_{sm} - \sum_{d\epsilon D} \sum_{m\prime>m} \alpha^{SW}_{sdm'} + \rho^{SW}_{m} \perp\ \Delta^{SW}_{sm'} \geq 0 \quad \forall m$ (B36)

$$0 \leq \overline{CAP}_{sm}^{SI} + \sum_{m<m'} \quad \Delta_{sm'}^{SI} - SALES_{sdm}^{SI} \perp \alpha_{sdm}^{SI} \geq 0 \quad \forall m, d \tag{B37}$$

$$0 \leq \overline{CAP}_{sm}^{SX} + \sum_{m<m'} \quad \Delta_{sm'}^{SX} - SALES_{sdm}^{SX} \perp \alpha_{sdm}^{SX} \geq 0 \quad \forall m, d \tag{B38}$$

$$0 \leq \overline{WG}_{sm}^{S} + \sum_{m<m'} \quad \Delta_{sm'}^{SW} - days_d SALES_{sdm}^{SX} \perp \alpha_{sm}^{SW} \geq 0 \quad \forall m \tag{B39}$$

$$0 \leq \overline{\Delta}_{sm}^{SW} \quad - \Delta_{sm}^{SW} \perp \rho_m^{SW} \geq 0 \ \ \forall m \tag{B40}$$

$$0 \leq \overline{\Delta}_{sm}^{SI} \quad - \Delta_{sm}^{SI} \perp \rho_m^{SI} \geq 0 \ \ \forall m \tag{B41}$$

$$0 \leq \overline{\Delta}_{sm}^{SX} \quad - \Delta_{sm}^{SX} \perp \rho_m^{SX} \geq 0 \ \ \forall m \tag{B42}$$

KKT conditions for Canal Operator

$$0 \leq day_d \gamma_m \left(-\tau_{dm}^{P\_toll} - \tau_{dm}^{P\_con} + \frac{\partial C_{jdm}^{P\_canal}\left(SALES_{jdm}^{P\_canal \to B}\right)}{\partial SALES_{jdm}^{P\_canal \to B}} \right) + Dist^{Pcanal} \alpha_{jdm}^{P\_canal} \perp$$

$$SALES_{jdm}^{P\_canal \to B} \geq 0 \ \ \forall d, m, j \epsilon \{P\_canal\} \tag{B43}$$

$$0 \leq day_d \gamma_m \left(-\tau_{dm}^{S\_toll} - \tau_{dm}^{S\_con} + \frac{\partial C_{jdm}^{S\_canal}\left(SALES_{jdm}^{S\_canal \to B}\right)}{\partial SALES_{jdm}^{S\_canal \to B}} \right) + \ \alpha_{jdm}^{S\_canal} \perp$$

$$SALES_{jdm}^{S\_canal \to B} \geq 0 \ \ \forall d, m, j \epsilon \{S\_canal\} \tag{B43}$$

$$0 \leq \ AllowSpeed * Dayhr * \ CAP^{P_{canal}} - SALES_{dm}^{P\_canal \to B} CanalDist \perp \alpha_{jdm}^{P_{Canal}} \geq$$

$$0 \ \ \forall d, m, j \epsilon \{P\_canal\} \tag{B44}$$

$$0 \leq SALES_{jdm}^{S_{canal} \to B} - \ \ CAP^{S_{canal}} \perp \alpha_{jdm}^{S_{Canal}} \geq 0 \ \ \forall d, m, j \epsilon \{S\_canal\} \tag{B45}$$

KKT conditions for the system operator problem

$$0 \leq \gamma_m days_d (-\tau_{adm}^{A} + CC_{tsom}^{ton} CE_{tso}^{TSO}) + \alpha_{adm}^{A} \perp SALES_{adm}^{A} \geq 0 \ \ \forall a, d, m \tag{B46}$$

$$0 \leq \gamma_m b_{am}^{A} - \sum_{d \epsilon D} \sum_{m'>m} \alpha_{adm'}^{A} + \rho_m^{A} \perp \Delta_{adm}^{A} \geq 0 \ \ \forall a, m \tag{B47}$$

$$0 \leq \overline{CAP}_{am}^{A} + \sum_{m<m'} \quad \Delta_{am'}^{A} - SALES_{adm}^{A} \ \ \perp \ \ \alpha_{adm}^{A} \geq 0 \ \ \forall a, d, m \tag{B48}$$

APPENDIX 4-C A sensitivity Analysis on LNG Shipping Costs

In this Appendix, a sensitivity analysis on LNG shipping costs is documented. The following section presents the sensitivity of the model results to changes in LNG shipping costs. Three sensitivity scenarios were run to check the robustness of results against LNG shipping costs;

- *Base* baseline scenario displays the LNG shipping costs from the references
- *Low* LNG shipping costs are 20% lower than the Base Case
- *High* LNG shipping costs are 20% higher than the Base Case

The results in term of prices, consumption, and production for the year 2035 respectively, are shown in Tables C-1, C-2, and C-3. As can be seen, across three sensitivity scenarios the LNG shipping costs only slightly modify the model results. For example, the prices in most regions are unchanged, but the wholesale prices in Japan change about $0.20/MMBtu because Japan imports a large volume of LNG to meet domestic demand. Changes in LNG shipping costs have a small effect on results for consumption and production. Production and consumption remain the same as the Base Case, see Tables C-2 and C-3. In general, the model results are fairly unchanging to changes in LNG shipping costs.

Table C-1 Price in $/MMBtu for 2035

	Prices		
	Low	Base	High
AFRICA	$3.32	$3.27	$3.22
ASPACIF	$13.36	$13.40	$13.49

EUROPE	$11.78	$11.85	$11.86
FRSVTUN	$4.92	$4.93	$4.93
JAPAN	$18.78	$18.91	$19.11
MIDEAST	$5.17	$5.17	$5.17
NRTH_AM	$5.49	$5.49	$5.49
STH_AM	$6.68	$6.68	$6.68
WORLD	$8.31	$8.33	$8.35

Table C-2 Consumption in Bcm/y for 2035

	Consumption		
	Low	Base	High
AFRICA	168.9	169.8	170.9
ASPACIF	1091.7	1090.3	1086.9
EUROPE	626.2	624.3	623.9
FRSVTUN	772.1	771.2	770.6
JAPAN	174.2	173.9	173.5
MIDEAST	558.9	558.9	558.8
NRTH_AM	1004.2	1004.2	1004.2
STH_AM	246.7	246.8	246.8
WORLD	4642.8	4639.4	4635.5

Table C-3 Production in Bcm/y for 2035

	Production		
	Low	Base	High
AFRICA	404.5	400.9	395.9
ASPACIF	942.2	940.4	940.3
EUROPE	211.3	211.9	212
FRSVTUN	1180.8	1180.9	1180.8
JAPAN	0	0	0
MIDEAST	777.2	777.2	777.3
NRTH_AM	1004.6	1004.6	1004.6
STH_AM	250.4	250.4	250.4
WORLD	4772	4767.3	4762.2

Chapter 5: A New Benders-SOS1 Method to Solve MPECs with an Application to Natural Gas Markets

This chapter presents a methodology to solve mathematical programs with equilibrium constraints (MPECs). MPECs are very challenging problems to solve as noted in Chapter 1 due to the non-convexities associated with putting the solution set of the lower-level problem as constraints. The method we develop uses an SOS1 approach based on (Siddiqui and Gabriel, 2012) to replace complementarity in the lower-level problem's optimality conditions. Then, Benders algorithm decomposes the MPECs into a master and a subproblem (Conejo et. al., 2006) and solves the overall problem iteratively. This methodology is then applied to a large-scale natural gas model as well as other small, illustrative examples. One advantage of Benders decomposition is when the complicating variables are fixed the problem separates into a number of independent optimization problems for which parallel computations can be applied.

While no formal mathematical convergence proof of the resulting Benders-SOS1 approach is shown, the positive, numerical results indicate that this new method has promise for solving MPECs more efficiently than some existing approaches. The connection of this chapter with the previous natural gas-based ones is that one of the MPECs considered and solved with this approach is an MPEC version of the World Gas Model. In this MPEC, the Panama Canal operator is a Stackelberg leader with a reduced version of the rest of the global gas markets considered as followers.

5.1 Mathematical Programs with Equilibrium Constraints (MPECs)

5.1.1 MPEC Formulation

We are concerned with solving the following two-level mathematical program which we refer to as MPEC:

$$\begin{aligned} &\min f(x,y) \\ &s.t.\,(x,y) \in \Omega \\ &y \in S(x) \end{aligned} \tag{5.1}$$

where the continuous variables $x \in R^{n_x}, y \in R^{n_y}$ are respectively, the vector of upper-level and lower-level variables and $f(x,y)$ is the objective function to the problem. Here, Ω is the joint feasible region between this set of the variables and $S(x)$ is the solution set of the lower-level problem which can be one or more optimization problems and/or mixed complementarity problems (MCP). Problem (5.1) is also called a mathematical program with complementarity constraints (MPCC). The term MPCC is often used if $S(x)$ consists of just complementarity conditions (e.g., from the KKT optimality conditions to an optimization problem) (Gabriel et al., 2013). However, more generally, (5.1) is called an MPEC. The main focus of our approach is when $S(x)$ corresponds to the solution set of a complementarity problem which includes the KKT conditions of nonlinear programs and other constraints. In general, the lower-level problem then is to find a vector *y* such that:

$$\begin{aligned} &y \geq 0 \\ &g(x,y) \geq 0 \\ &y^T g(x,y) = 0 \end{aligned} \tag{5.2}$$

where *g(x, y)* is a vector of constraint functions and the function $g(x,y)\colon R^{n_x} \times R^{n_y} \to R^{n_y}$. If *S(x)* is the solution set for an MCP[39], (5.1) can be rewritten as:

$$\begin{aligned} &\min f(x,y) \\ &s.t.\,(x,y) \in \Omega \\ &y \geq 0 \\ &g(x,y) \geq 0 \\ &y^T g(x,y) = 0 \end{aligned} \tag{5.3}$$

5.1.2 Solving MPECs

In general, $y^T g(x,y) = 0$ is non-convex function of y (when x is fixed) which complicates finding a solution to the overall MPEC. One approach that is often used is to transform the problem via disjunctive constraints introduced by Fortuny-Amat and McCarl (1981) and used in (Gabriel and Leuthold, 2010). In this case, a large constant K is introduced along with a vector of binary variables $r \in \{0,1\}^{n_y}$ to represent complementarity. Consequently, we can rewrite (5.3) as:

$$\begin{aligned} &\min f(x,y) \\ &s.t.\,(x,y) \in \Omega \\ &0 \leq y \leq K(1-r) \\ &0 \leq g(x,y) \leq Kr \\ &r \in \{0,1\}^{n_y}, \end{aligned} \tag{5.4}$$

where $K \in R_{++}$ is a fixed parameter suitably chosen, the continuous variables $x \in R^{n_x}, y \in R^{n_y}$ are the vector of upper-level and lower-level variables, respectively and the given function $g\colon R^{n_x} \times R^{n_y} \to R^{n_y}$. If the vector constraint function *g(x,y)* is linear, we can solve (5.4) as a mixed-integer linear, (binary) program (MIP) for each

[39] Here for ease of presentation and without loss of generality, we assume no equations and associated free variables in the MCP.

fixed value of K . However, the computation time will increase exponentially with the number of binary variables. Additionally, in some applications it is not immediately obvious how to find a correct value of K and some sort of numerical procedure is needed to find a best value (or values). Alternatively, the approach by Siddiqui and Gabriel (2012) used special ordered sets of type 1 (SOS1) variables to solve (5.3). SOS1 variables are used to transform the complementarity conditions from above into mixed-integer nonlinear constraints. The key idea is to use a transformation of variables to re-express the complementarity of the vector y and $g(x,y)$. More specifically, for each index i, let

$$u_i = \frac{y_i+g_i(x,y)}{2} \tag{5.5}$$

$$v_i = \frac{y_i-g_i(x,y)}{2} \tag{5.6}$$

and note that

$$y^T g(x,y) = 0 = (\frac{y+g(x,y)}{2} - \frac{y-g(x,y)}{2})(\frac{y+g(x,y)}{2} + \frac{y-g(x,y)}{2}) = [u_i - v_i][u_i + v_i]$$

$$= u_i^2 - v_i^2$$

so $u_i = |v_i|$ noting that $u_i = \frac{y_i+g_i(x,y)}{2}$ is nonnegative. This allows both u_i and v_i to be rewritten as, respectively, the sum and the difference of two nonnegative variables v_i^+, v_i^-. More specifically,

$$u_i = \frac{y_i+g_i(x,y)}{2} = v_i^+ + v_i^- \tag{5.7}$$

$$v_i = \frac{y_i-g_i(x,y)}{2} = v_i^+ - v_i^- \tag{5.8}$$

with the restriction that at most one of the variables v_i^+, v_i^- is nonzero, i.e., that these are SOS1 variables. Considering the vector versions u, v and other related vector versions of the other variables mentioned above, this leads to the following equivalent formulation of (5.3).

$$min\, f(x,y)$$

$$s.t.\, (x,y) \in \Omega$$

$$
\begin{aligned}
& y \geq 0 \\
& g(x,y) \geq 0 \\
& u - (v^{+} + v^{-}) = 0 \\
& u = \tfrac{y+g(x,y)}{2} \\
& (v^{+} - v^{-}) = \tfrac{y-g(x,y)}{2} \\
& u \geq 0
\end{aligned}
\tag{5.9}
$$

where v^{+} and v^{-} are SOS1 (nonnegative) variables .

When comparing the disjunctive-constraints technique (Fortuny-Amat and McCarl, 1981) and SOS1 transformation technique (Siddiqui and Gabriel, 2012), the disjunctive-constraints technique has two main disadvantages. First, it is computationally expensive for large models and second, it requires good selections for a large constant *K*. The SOS1 technique overcomes those two problems. However as discussed in (Siddiqui, 2011), the SOS1 approach initially failed to find a solution for a large-scale North America Gas model (based on the World Gas Model) (Gabriel et. al, 2012) as it requires a good starting point. In order to obtain good starting points, Siddiqui and Gabriel (2012) needed to solve a penalty method version of the SOS 1 formulation before applying (5.9) and then iterating heuristically between these two approaches with the solver failed to maintain the SOS1 property. Sometimes finding a right penalty is troublesome since the penalty is not known beforehand. The Benders-SOS1 method we present in this dissertation has an advantage when compared with other these two methods because it does not require either a large constant value or solving another problem beforehand, but it just needs to start with a feasible value of the complicating variables to the subproblem. Details will be discussed later in this chapter.

Besides these two mentioned approaches, MPECs can be solved in a variety of ways examples of which include: NLPEC (a commercial solver), nonlinear programming, integer programming, and other methods. As for the nonlinear programming approach for solving MPECs, there are three main directions in the literature. First, the regularization and complementarity-penalty approaches (Scholtes, 2001; Hu and Ralph, 2004; Ralph and Wright, 2004). In their framework, the MPEC is approximated by nonlinear programming (NLPs) and a sequence of NLPs is solved to identify stationary points of the MPEC. Second is are Penalty Interior Point Algorithms (Luo et al, 1996; Benson et al., 2002; de Miguel et al., 2005; Raghunathan and Biegler, 2005, Leyffer et al., 2007). These methods are based on complementarity-penalty version of sequential of NLP and solve one linear system of KKT conditions with a log barrier penalty function for each iteration. However, a drawback in this method is finding a right initial penalty. A third MPEC solution method is Sequential Quadratic Programming (SQP) (Kojima and Shindo, 1986; Fletcher et al., 2002; Fletcher and Leyffer, 2002, Fletcher and Leyffer, 2004; Anitescu, 2005). The SQP method approximates the Lagrangian function via a quadratic function using linearized versions of the constraints at each iteration. SQP provides positive results on small and medium-scale problems (Anitescu, 2005). However, Chen et al. (2006) found that no single NLP solver could solve their large-scale electricity model, but they applied SNOPT and FILTER solvers in sequence and eventually find a solution.

Integer programming approaches have also been widely used for solving MPECs. The branch- and-bound algorithm (Bard and J. Falk, 1982; Bard and Moore, 1990; Al-Khayyal, Horst and Pardalos, 1992; Bard, 1988; Edmunds and Bard, 1992) was

developed to satisfying linear/nonlinear complementary constraints. This algorithm reformulates the KKT conditions of the lower-level problem and applies branch-and-bound techniques. Convergence to a global optimum can only be guaranteed when certain convexity and separability properties hold.

By contrast, the current work employs a somewhat related idea to the branch-and-bound algorithm in that the KKT conditions are reformulated, but in different way using SOS1 variables. Instead of using branch-and-bound, our approach employs Benders decomposition solving the problem iteratively. Apart from branch-and-bound, Wen and Yang (1990) proposed an exact algorithm, but it only worked for relatively small problems. Later, Wen and Hung (1996) presented a Simple Tabu Search heuristic algorithm to solve mixed-integer, linear bilevel programs. Two strategies need to be done for the Tabu Search method. First, an upper bound-screening approach generates neighborhood points, then an advanced start method selects the points to initiate the search. The Tabu Search works well with small mixed-integer linear bilevel programs where the upper-level problem needs to decide on values for zero-one variables.

In addition, other methods, for example, a relaxation scheme (Steffensen and Ulbrich 2010) and exact penalty functions with nonlinear perturbations (Uderzo 2010) also exist but have not been shown to work for large-scale models. However, larger problems of MPEC are more difficult to solve (Siddiqui and Gabriel, 2012) due to non-convexity of MPECs. The motivation behind developing an algorithm for MPECs was to find an alternative to previous techniques to solve large-scale problems but based on a decomposition approach which could potentially alleviate the computational issues with big test problems. In the next section, we provide a brief overview of Benders

decomposition method as a prelude to the new Benders-SOS1 method developed later in this chapter.

5.2 Benders Decomposition

Benders (1962) developed partitioning procedures for solving linear programming problems. Geoffrion (1972) extended Benders algorithm and proposed a Generalized Benders decomposition (GBD) for a broader class of problems using nonlinear convex duality theory to drive optimality cut generation. Later, Geoffrion and Graves (1974) applied GBD solve a mixed-integer linear program for the design industrial distribution systems. The work done by Polito et al. (1980) used GBD to find a solution to the spatial equilibrium problem. Beptistella and Geromel (1980) proposed a method to solve the unit commitment problem where the master problem is an integer, nonlinear program representing the unit commitment and the subproblem is the economic dispatch (stochastic nonlinear program). Rouhani et al. (1985) used GBD to solve an MINLP model for reactive power planning in power systems. In addition, the work done by Floudas and Ciric (1989) also applied GBD to a MINLP formulation for a heat exchanger network. Benders decomposition has also been applied to a wide range of energy applications e.g., generation capacity expansion (Kazempour and Conejo, 2012; Jae Hyung Roh et. al, 2007), voltage security (Rabiee and Parniani, 2013), and hydrothermal scheduling (Sifuentes and Vargus, 2007).

There is also a strong connection between Benders method and stochastic programming, in particular recourse problems. When Benders decomposition is applied to these problems, it is called the L-shaped method (Birge and Louveaux, 1997)

and specialized results are available. In addition, GBD was also applied to nonconvex programming, see (Geoffrion, 1972; Floudas et al., 1989). Besides optimization problems, Benders method has been also applied to complementarity problems. The work done by Cabero et al., (2010) applied Benders algorithm to linear complementarity problems. Gabriel and Fuller (2010) developed a Benders approach to solve stochastic variational inequality/MCPs problems. Egging (2013) implemented Benders algorithm to large-scale, stochastic mixed complementarity problems. This work applied the variational inequality method developed in Gabriel and Fuller (2010). In addition, Gabriel et al. (2010) developed a Benders algorithm combined with a heuristic procedure to solve discretely-constrained mathematical programs with equilibrium constraints (DC-MPECs) and applied it to a variety of test problems including some in electric power.

5.2.1 Benders decomposition procedure

This section gives a brief introduction to Benders decomposition using a simple example taken from (Conejo et. al., 2006). It is important to note that the standard Benders algorithm is more for linear programs but we present it here as a way to introduce GBD later which has more relevant to MPECs analyzed in this chapter.

Consider a linear program of the following form:

$$\begin{aligned} & min_{x,y} \;\; c^T x + d^T y \\ & s.t. \quad Ax + By = b \\ & y \geq 0, x \in X \subseteq R^n \end{aligned} \tag{5.10}$$

where $x \in R^n, y \in R^m$, and X is a polyhedron, A, B are matrices, and b, c, d are vectors having appropriate dimensions. The complicating variables x make the problem hard

to solve. When the vector x is fixed, the problem is decomposable or easier to solve. First, it is important to note that problem (5.10) can be written in terms only of the complicating variables x as follows:

$$\begin{aligned} &min\ \ c^T x+\alpha(x) \\ &s.t. \quad x \in X, \end{aligned} \tag{5.11}$$

where $\alpha(x)$ is defined as:

$$\begin{aligned} &\alpha(x) = min_y\ \ d^T y \\ &s.t.\ By = b - Ax \\ &y \geq 0 \end{aligned} \tag{5.12}$$

Based on this reformulation, Benders decomposition defines and a master (MP) and subproblem (SP) and solves them iteratively. The master problem (MP) is as follows:

$$\begin{aligned} &min_{x,\alpha}\ \ c^T x + \alpha \\ &s.t. \quad \alpha \geq \alpha^{down} \\ &d^T y^{(k)} + \lambda^{(k)}\left(x - x^{(k)}\right) \leq \alpha;\ k = 1, \dots, it-1 \end{aligned} \tag{5.13}$$

where α is the optimal objective function value of the subproblem for a given, fixed value of the complicating variables x, it is the iteration counter, and α^{down} is a user-specified parameter. The values $y^{(it)}$ and $\lambda^{(it)}$ are respectively, a primal and a (part of a) dual solution vector from the subproblem with $\lambda^{(it)}$ related to fixing constraints specified below. Note that the last set of constraints in (5.13) are called Benders cuts are used to approximate from below, the optimal value function $\alpha(x)$. For this reason Benders method is sometimes called an "outer approximation" as opposed to an inner one for example, the Dantzig-Wolfe decomposition (Conejo et al., 2006). Problem (5.13) is updated each iteration by new constraints (Benders cuts) added based on the information from the subproblem. The MP is a relaxed version of the original problem since it only approximates the function $\alpha(x)$. Thus, the objective function value, $z_{down}^{(it)}$

, from the MP is a lower bound on the optimal objective function to the original problem and defined as:

$$z_{down}^{(it)} = \ c^T x^{(it)} + \alpha^{(it)} \tag{5.14}$$

For a fixed value of the complicating variables *x*, Benders subproblem (SP) is defined as:

$$\begin{aligned} & min_y \ d^T y \\ & s.t. \ \ By = b - Ax \\ & y \geq 0 \\ & x = x^{(it)} : \lambda^{(it)} \end{aligned} \tag{5.15}$$

A solution for the subproblem provides $y^{(it)}$ (primal values) and the dual variable vector $\lambda^{(it)}$ associated with the constraints that fix the complicating variables. The subproblem solves a more restricted version of the original problem (since the vector *x* has been fixed) so that the objective function value for the subproblem, $z_{up}^{(it)}$, is an upper bound of the original problem. This value is defined as follows:

$$z_{up}^{(it)} = d^T y^{(it)} \tag{5.16}$$

Benders method iterates between the MP and the SP until the difference between the upper and lower bounds is small enough. Lastly in terms of convergence of the algorithm, we cite the theorem 3.2 from Conejo et. al (2006):

Problem (5.13) and (5.15) are equivalent to the original problem (5.10). However, the original problem (5.10) is harder to solve because it requires to get an exact $\alpha(x)$. Benders decomposition approximates $\alpha(x)$ using hyperplanes and improves the approximation using additional hyperplanes from the subproblem at each iteration. The same theorem also shows that the $\alpha(x)$ is convex and easily obtained using hyperplanes

5.2.2 Benders Algorithm Stpes Conejo et. al., (2006)

Step 0: **Initialization.** Find feasible values x_0 for the complicating variables x so that $x \in X$, set $it = 1, x^{fix(it)} = x_0, z_{down}^{(it)} = -\infty$.

Step 1: **Subproblem solution**. Solve the subproblem

$$\begin{aligned} & min_y \ d^T y \\ & s.t. \ \ By = b - Ax \\ & y \geq 0 \\ & x = x^{(it)} : \lambda^{(it)} \end{aligned} \tag{5.17}$$

This problem provides $d^T y^{(it)}, \lambda^{(it)}$. Update the objective function upper bound $z_{up}^{(it)} = d^T y^{(it)}$.

Step 2: Convergence check. If $z_{up}^{(it)} - z_{down}^{(it)} \leq \varepsilon$, STOP. Otherwise, go to the next step.

Step 3: Master solution. Update the iteration counter, $it \longleftarrow it + 1$

$$\begin{aligned} & min_{x,\alpha} \ c^T x + \alpha \\ & s.t. \ \ \alpha \geq \alpha^{down} \\ & d^T y^{(k)} + \lambda^{(k)^T} \left(x - x^{(k)}\right) \leq \alpha; \ k = 1, \dots, it - 1 \end{aligned} \tag{5.18}$$

Note: a new constraint (Benders cut) is added $d^T y^{(k)} + \lambda^{(k)^T} \left(x - x^{(k)}\right) \leq \alpha$ at each iteration. The objective function lower bound, $z_{down}^{(it)} = \ c^T x^{(it)} + \alpha^{(it)}$ is updated. The algorithm returns to Step 1.

5.3 Generalized Benders Decomposition

The Generalized Benders Decomposition (GBD) was proposed by Geoffion (1972), for exploiting the structure of broader class of programs beyond linear programs. GBD was derived for a problem of the form:

$$
\begin{aligned}
&min \;\; f(x,y) \\
&s.t \;\; g(x,y) \leq 0 \\
&\; y \in Y \subseteq R^n, x \in X \subseteq R^m,
\end{aligned}
\tag{5.19}
$$

where g is a vector of coupling constraint functions. The vector x is represents complicating variables in the sense that:

- For fixed x, the problem separates into a number of independent optimization problems in which parallel computation can be applied.
- For fixed x, the original problem becomes easier to solve. Examples include mixed- integer linear/mixed-integer nonlinear programming problems in which a fixed x gives rise to linear and nonlinear programming problems, respectively.
- Lastly, (5.19) can represent nonconvex programs having x and y jointly to be determined e.g., a NLP involving bilinear terms of the form xy, but fixing x removes the nonlinearity.

In GBD, the subproblem results from fixing the x variables, which we denote as $x^{(it)}$ where it is the iteration counter. The subproblem (SP) is as follows:

$$
\begin{aligned}
&min_y \;\; f(\, x^{(it)}, y) \\
&s.t \;\; g(\, x^{(it)}, y) \leq 0 \\
&x = x^{(it)} : \lambda^{(it)} \\
&y \in Y
\end{aligned}
\tag{5.20}
$$

whose optimal objective value is $\alpha(x)$ and the relaxed master problem,

$$
\begin{aligned}
&min_{\alpha,x} \;\; \alpha \\
&s.t \;\; \alpha \geq f\big(\, x^{(k)}, y^{(k)}\big) + \lambda^{(k)^T}\big(x - x^{(k)}\big), \forall k = 1, \dots, it-1 \\
&\qquad x \in X
\end{aligned}
\tag{5.21}
$$

whose solution is $x^{(it)}$ and $\lambda^{(k)^T}$ is optimal multiplier vector for the subproblem. The feasibility of the subproblem in GBD is guaranteed by relaxing constraints to introduce slack/surplus variables when necessary to avoid initial feasibilities.

Next, function $\alpha(x)$ (Conejo et. al, 2006) expresses the objective function of the original problem as a function solely of the complicating variables. The optimal objective function value given *x* fixed is defined as:

$$\begin{aligned} &\alpha(x) = minimum_y\, f(x,y) \\ &s.t.\ g(x,y) \leq 0 \\ &y \in Y \end{aligned} \tag{5.22}$$

The steps of GBD are;

1. Initialize; $it = 1$, find $x_0 \in X, z_{down}^{(it)}$(lower bound)$= -\infty, z_{up}^{(it)}$(upper bound)$= \infty, \varepsilon =$ convergence tolerance
2. Solve SB, obtaining an optimal value $y^{(it)}$ and optimal vector $\lambda^{(it)}$. Update $z_{down}^{(it)} = \alpha(x^{(it)})$.
3. Generate a Benders cut (constraint to the master problem) $\alpha \geq f\left(x^{(k)}, y^{(k)}\right) + \lambda^{(k)^T}\left(x - x^{(k)}\right)$.
4. Solve the master problem with optimal value $\alpha^{(it)}$. Set $z_{up}^{(it)}$(upper bound)$= \alpha^{(it)}$.
5. If $(z_{up}^{(it)} - z_{down}^{(it)})/abs(z_{down}^{(it)}) < \varepsilon$, stop. $(x^{(it)}, y^{(it)})$ is an optimal solution to the original problem (5.19).
6. Replace it by $it + 1$ and go to Step 2.

Assumptions which guarantee finite convergence of the procedure are:

1. f and g are convex on y for each fixed $x \in X$.
2. Y is nonempty and convex.
3. It must be possible to solve the master problem globally
4. It must be possible to obtain a closed-form expression for a Benders cut for each fixed $\lambda^{(it)}$

5.4 Benders-SOS1 Algorithm (Solving MPECs Using a Combination of SOS1 Method and Benders Decomposition)

The main idea to be explored in this chapter is to make use of Generalized Benders decomposition but applied to MPECs using an SOS1 transformation (Siddiqui and Gabriel, 2012). Recall the function $g(x,y) \geq 0$ and the bilinear term $y^T g(x,y) = 0$. We introduce the SOS1 variables, v^+ and v^- noting that z is a nonnegative vector that equals the function *g(x,y)* for notational simplicity. Furthermore, it is assumed that SOS1 variables are nonnegative. Noting that

$$u = v^+ + v^- = \frac{(z+y)}{2}$$

$$v = v^+ - v^- = \frac{(z-y)}{2}$$

we can rewrite the original MPEC in (5.3) using SOS1 variables as:

$$\begin{aligned} &\min f(x,y) \\ &s.t.\ (x,y) \in \Omega \\ &z = g(x,y) \\ &z \geq 0 \\ &2v^+ + 2v^- = z + y \\ &2v^+ - 2v^- = z - y \\ &y \geq 0 \end{aligned} \tag{5.23}$$

where v^+ and v^- are SOS1 variables

The vector x is considered as the complicating set of variables (or at least a subset of them) and whose values are determined in the master problem. In (5.23), if the vector x is fixed, the resulting problem will become a simpler or decomposable one. By applying Benders decomposition, we propose the following Benders subproblem (SP) as follows where the vector x has been fixed as shown in the last constraint:

$$\begin{aligned} &\min f(x,y) \\ &s.t.\,(x,y) \in \Omega \\ &z = g(x,y) \\ &z \geq 0 \\ &2v^+ + 2v^- = z + y \\ &2v^+ - 2v^- = z - y \\ &y \geq 0 \\ &x = x^{fix(it)} \ (\lambda) \end{aligned} \tag{5.24}$$

where v^+ and v^- are SOS1 variables

The master problem (MP) becomes:

$$\begin{aligned} &\min_{\alpha,x} \alpha \\ &s.t. \\ &\alpha \geq \alpha^{down} \\ &\alpha \geq f\left(x^{(k)}, y^{(k)}\right) + \lambda^{(k)^T}(x - x^{(k)}) \ \ \forall k = 1,..,it-1 \end{aligned} \tag{5.25}$$

The Benders-SOS1 Algorithm works with problem (5.3) is thus as follows:

5.4.1 Benders-SOS1 Algorithm:

Step 0: Set $it = 1$. Select a tolerance value ε, α^{down}, and $x^{fix(it)}$ being a feasible solution for the complicating variable x for the first iteration.

Step 1: Transform the complementarity conditions in problem (5.3) into SOS1 format. We rewrite the problem as:

$$\begin{aligned} &\min f(x,y) \\ &s.t.\,(x,y) \in \Omega \\ &z = g(x,y) \\ &z \geq 0 \\ &2v^{+} + 2v^{-} = z + y \\ &2v^{+} - 2v^{-} = z - y \\ &y \geq 0 \end{aligned} \tag{5.26}$$

where v^{+} and v^{-} are SOS1 variables

Step 2: Subproblem solution. Solve the subproblem

$$\begin{aligned} &\min f(x,y) \\ &s.t.\,(x,y) \in \Omega \\ &z = g(x,y) \\ &z \geq 0 \\ &2v^{+} + 2v^{-} = z + y \\ &2v^{+} - 2v^{-} = z - y \\ &y \geq 0 \\ &x = x^{fix(it)} \ (\lambda) \end{aligned} \tag{5.27}$$

where v^{+} and v^{-} are SOS1 variables

A solution for this problem gives $x^{(it)}, y^{(it)}, z^{(it)}, f(x^{(it)}, y^{(it)})$ and $\lambda^{(it)}$, the dual variable of the fixing constraint. Update the objective function upper bound, $z_{up}^{(it)} =$

$f(\,x^{(it)}, y^{(it)})$. However in some cases, the subproblem may infeasible. The alternative always-feasible subproblem from Conejo et. al., (2006) is as follows:

$$\begin{aligned} &\min f(x,y) + L(e^+ + e^-) \\ &s.t.\,(x,y) \in \Omega \\ &z = g(x,y) + e^+ - e^- \\ &z \geq 0 \\ &2v^+ + 2v^- = z + y \\ &2v^+ - 2v^- = z - y \\ &e^+, e^-, y \geq 0 \\ &x = x^{fix} : \ (\lambda^{(it)}) \end{aligned} \tag{5.28}$$

where v^+ and v^- are SOS1 variables - and $L \in R_+$ is the penalty for violating constraints.

<u>Step 3</u>: Check for convergence. Compute upper and lower bounds of the optimal value of the objective function of the original problem:

$$z_{up}^{(it)} = f(\,x^{(it)}, y^{(it)}). \tag{5.29}$$

$$z_{down}^{(it)} = \alpha^{(it)} \tag{5.30}$$

If $z_{up}^{(it)} - z_{down}^{(it)} \leq \varepsilon$, then a solution to the original MPEC is $x^* = x^{(it)}, y^* = y^{(it)}$. STOP.

<u>Step 4</u>: Master problem solution. Update the iteration counter, $it \leftarrow it + 1$ and solve the master problem:

$$\begin{aligned} &\min_{\alpha,x} \alpha \\ &s.t. \\ &\alpha \geq \alpha^{down} \\ &x \geq 0 \\ &\alpha \geq f\big(x^{(k)}, y^{(k)}\big) + \lambda^{(k)^T}\big(x - x^{(k)}\big); \forall k = 1,..,it-1 \end{aligned} \tag{5.31}$$

Note: a new constraint is added at every iteration. A solution for the master problem provides $x^{(it)}, \alpha^{(it)}$. Update the objective function lower bound, $z_{down}^{(it)} = \alpha^{(it)}$. The algorithm continues to Step 2.

5.4.2 Numerical Example (Example 1) to Show Methodology Step-by-Step

A simple numerical example is presented to show how Benders algorithm is used to obtain solutions to the MPEC. First, a simple linear program with complementarity constraints (LPCC) is presented to show the proposed methodology step-by-step. A linear program with complementarity constraints is expressed as:

$$\begin{aligned} & min\, c^T x + d^y y \\ & s.t. \quad Ax + By \geq f \\ & 0 \leq y \perp q + Nx + My \geq 0 \end{aligned} \tag{5.32}$$

The following LPCC from (Hu and Pang, 2008) is considered.

$$\begin{aligned} & min\, 3x - 5y \\ & s.t. \quad 0 \leq y \leq 1 \\ & 2x + 3y \geq 6 \\ & 0 \leq y \perp 2x + 3y - 6 \geq 0 \end{aligned} \tag{5.33}$$

A solution for this problem is x=1.5, y=1 (Hu and Pang, 2008) with an objective function value of -0.5. Next we proceed to the Benders-SOS1 method for MPECs.

Step 0: Pick the tolerance value $\varepsilon = 10^{-6}$ to control the convergence and $\alpha_{down} = -25$, $z_{down}^{(it)} = -\infty$ and $x^{fix(it)} = 1$. α_{down} is the bound that can be determined from economic or physical consideration (Conejo, 2006). Set the iteration counter $it = 1$.

Step 1: Transform the complementarity condition in problem (5.33) into the SOS1 format as shown in (5.26):

$$
\begin{aligned}
&min\ 3x - 5y \\
&s.t. \quad 0 \le y \le 1 \\
&-6 + 2x + 3y = z \\
&z \ge 0 \\
&2v^{+} + 2v^{-} = z + y \\
&2v^{+} - 2v^{-} = z - y
\end{aligned} \tag{5.34}
$$

where v^{+} and v^{-} are SOS1 variables

Step 2: Subproblem Solution. Solve the subproblem with a fixed value $x^{fix(1)} = 1$ for the complicating variables .We arbitrarily pick x =1 as a starting point however, the subproblem is infeasible. We introduce the nonnegative variable e^{+}, e^{-} to prevent infeasibility with a penalty of 10 in the subproblem and penalize the violating constraint as shown in (5.28) [40]:

$$
\begin{aligned}
&min\ 3x - 5y + 10(e^{+} + e^{-}) \\
&s.t. \quad 0 \le y \le 1 \\
&-6 + 2x + 3y + e^{+} - e^{-} = z \\
&2v^{+} + 2v^{-} = z + y \\
&2v^{+} - 2v^{-} = z - y \\
&e^{+}, e^{-}, z \ge 0 \\
&x = 1
\end{aligned} \tag{5.35}
$$

where v^{+} and v^{-} are SOS1 variables

This gives: $y^{(1)} = 1, x = 1, z^{(1)} = 0, e^{+(1)} = 1, e^{-(1)} = 0$. Its optimal objective function value is 8. An optimal dual variable associated with the fixing constraint is given as: $\lambda^{(1)} = -17$.

[40] The penalty needs to be a positive value. It is important to note that not all positive values will work. The appropriate value of the penalty should make e^{+}, e^{-} become zero in the last iteration of Benders algorithm otherwise a new value needs to be tried.

Step 3: Check for convergence. Calculate the upper and lower bounds for this problem:

$$z_{up}^{(1)} = f(x^{(1)}, y^{(1)}) = 3 * (1) - 5 * (1) + 10 * (1) = 8$$
$$z_{down}^{(1)} = -\infty$$

Check for convergence with $z_{up}^{(1)} - z_{down}^{(1)} = 8 - (-\infty) = \infty \geq \varepsilon$. This value is not small enough when compared with the tolerance, so a Benders cut is added. Go to Step 4.

Step 4: Master problem solution. The iteration counter is updated, $it = 1 + 1 = 2$. Based on the solution of the subproblem, $f(x^{(1)}, y^{(1)}) = 8$ and $\lambda^{(1)} = -17$ in Step 3, the algorithm constructs a new Benders cut: $\alpha \geq f(x^{(1)}, y^{(1)}) + \lambda^{(1)}(x - x^{(1)})$ and adds $\alpha \geq 8 + (-17)(x - 1)$ to the master problem and solves the master problem (MP) with the Benders cut added:

$$\begin{aligned} &\min \ \alpha \\ &s.t. \ \alpha \geq -25 \\ &\alpha \geq 25 - 17x \end{aligned} \tag{5.36}$$

Solving this problem gives $\alpha^{(2)} = -25, x^{(2)} = 2.941$. Go to Step 2.

Step 2 Subproblem solution. Set $x^{fix(2)} = x^{(2)} = 2.941$ and then solve the following subproblem:

$$\begin{aligned} &min \ 3x - 5y + 10(e^+ + e^-) \\ &s.t. \ \ 0 \leq y \leq 1 \\ &-6 + 2x + 3y + e^+ - e^- = z \\ &2v^+ + 2v^- = z + y \\ &2v^+ - 2v^- = z - y \end{aligned} \tag{5.37}$$

$$e^+, e^-, z \geq 0$$
$$x = 2.94$$
where v^+ and v^- are SOS1 variables

Solving this problem gives $y^{(2)} = 0.039, z^{(2)} = 0, e^{+(2)}, e^{-(2)} = 0$. with an optimal objective function value of 8.627. An optimal dual variable associated with the constraint $x = 2.941$ is $\lambda^{(2)} = 6.333$.

Step 3: Check for convergence.

$$z_{up}^{(2)} = f(x^{(2)}, y^{(2)}) = 3 * (2.941) - 5 * (0.039) + 10 * (0) = 8.627$$

$$z_{down}^{(2)} = \alpha^{(2)} = -25$$

Check for convergence with $z_{up}^{(2)} - z_{down}^{(2)} = 8.627 - (-25) \geq \varepsilon$. This value is not small enough when compared with the tolerance, so a Benders cut is added: Go to Step 4.

Step 4: Master problem solution. The iteration counter is updated, $it = 2 + 1 = 3$. Based on the solution of the subproblem, $f(x^{(2)}, y^{(2)}) = 8.627$ and $\lambda^{(2)} = 6.33$, the algorithm constructs a new Benders cut: $\alpha \geq f\left(x^{(2)}, y^{(2)}\right) + \lambda^{(2)}(x - x^{(2)})$ and adds $\alpha \geq 8.627 + (6.33)(x - 2.941)$ to the master problem and solves the master problem (MP) with the Benders cut added:

$$\begin{aligned} &\min \ \alpha \\ &s.t. \ \alpha \geq -25 \\ &\alpha \geq 25 - 17x \\ &\alpha \geq -9.989 + 6.33x \end{aligned} \qquad (5.38)$$

Solving this problem gives $\alpha^{(3)} = -0.5, \ x^{(3)} = 1.5$.

Step 2 Subproblem solution. Set $x^{fix(3)} = x^{(3)} = 1.5$ and then solve the following subproblem:

$$\begin{aligned} & min\ 3x - 5y + 10(e^+ + e^-) \\ & s.t.\ \ 0 \le y \le 1 \\ & -6 + 2x + 3y + e^+ - e^- = z \\ & 2v^+ + 2v^- = z + y \\ & 2v^+ - 2v^- = z - y \\ & e^+, e^-, z \ge 0 \\ & x = 1.5 \end{aligned} \qquad (5.39)$$

where v^+ and v^- are SOS1 variables

Solving this problem gives $y^{(3)} = 1, e^{+(3)} = 0, e^{-(3)} = 0\ , z^{(3)} = 0$ with an optimal objective function value of -0.5.

Step 3: Check for convergence. Check for convergence with $z_{up}^{(3)} - z_{down}^{(3)} = -0.5 - (-0.5) = 0 \le \varepsilon$ and the algorithm is terminated. A summary of the iterations is provided below.

Table 5-1 Iterative Values for Benders Decomposition Approach for Sample MPEC:

Iteration (it)	x^{it}	y^{it}	z_{down}^{it}	z_{up}^{it}
1	1	1	-25	8
2	2.95	1	-25	8.627
3	1.5	1	-0.5	-0.5

5.4.3 Validating a solution from Benders SOS1 approach

The question whether Benders can find a global optimum of example 1 from any starting point is considered in Table 5-2 below where the results of the application of the algorithm are shown for four different starting points. Starting with x=0, x=1, x=2, and x=2.8 leads to the same global optimum x=1.5. It is important to note that the algorithm still works for starting points larger than 2.8, but it requires a new penalty

value in the objective function. It is important to note that this form of this penalty is exact. Hence, if the problem is feasible, there is a positive threshold value for the penalty such that any value above that threshold yields optimal solutions with all slack variables equal to zero and the remaining variables optimal for the original problem (5.33).

Table 5-2 Solutions from different starting points[41] for Benders Decomposition Approach for the Example 1:

Starting Points: x=0

Iterations (it)	Primal Variables		SOS1 Variables		Penalty Variables	Dual of fixing variable con	Objective function	
	$x^{(it)}$	$y^{(it)}$	$v^{+(it)}$	$v^{-(it)}$	$e^{+(it)}$	$\lambda^{(it)}$	$z_{down}^{(it)}$	$z_{up}^{(it)}$
1	0.00	1.00	0	0.50	3.00	-27.32304	-25.00	25.00
2	1.83	0.78	0	0.39	0.00	6.33333	-25.00	1.62
3	1.04	1.00	0	0.50	0.92	-17.00000	-3.41	7.32
4	1.50	1.00	0	0.50	0.00	-16.79178	-0.50	-0.50

Starting Points: x=1

Iterations (it)	Primal Variables		SOS1 Variables		Penalty Variables	Dual of fixing variable con	Objective function	
	$x^{(it)}$	$y^{(it)}$	$v^{+(it)}$	$v^{-(it)}$	$e^{+(it)}$	$\lambda^{(it)}$	$z_{down}^{(it)}$	$z_{up}^{(it)}$
1	1.00	1.00	0	0.50	1.00	-17.00	-25.00	8.00
2	2.95	0.03	0	0.02	0.00	6.33333	-25.00	8.71
3	1.50	1.00	0	0.50	0.00	-17.00	-0.50	-0.5

Starting Points: x=2

Iterations (it)	Primal Variables		SOS1 Variables		Penalty Variables	Dual of fixing variable con	Objective function	
	$x^{(it)}$	$y^{(it)}$	$v^{+(it)}$	$v^{-(it)}$	$e^{+(it)}$	$\lambda^{(it)}$	$z_{down}^{(it)}$	$z_{up}^{(it)}$
1	2.00	0.67	0	0.33	0.00	6.33333	-25.00	2.67
2	0.00	1.00	0	0.50	3.00	-28.92319	-10.00	25.00
3	0.99	1.00	0	0.50	1.01	-17.00000	-3.71	8.12

[41] Note that we use a nonnegative starting point becasue nonnegativity of x is implied from the constraint 2x-3y ≥6 and y≤1. In particular, x needs to be ≥3/2.

4	1.50	1.00	0	0.50	0.00	-16.84348	-0.50	-0.50

Starting Points: x=2.8

Iterations (it)	Primal Variables		SOS1 Variables		Penalty Variables	Dual of fixing variable con	Objective function	
	$x^{(it)}$	$y^{(it)}$	$v^{+(it)}$	$v^{-(it)}$	$e^{+(it)}$	$\lambda^{(it)}$	$z_{down}^{(it)}$	$z_{up}^{(it)}$
1	2.80	0.13	0	0.07	0.00	6.33333	-25.00	7.73
2	0.00	1.00	0	0.50	3.00	-17.31788	-10.00	25.00
3	1.48	1.00	0	0.50	0.04	-17.00000	-0.63	-0.16
4	1.50	1.00	0	0.50	0.00	-16.52307	-0.50	-0.50

In order to understand why a global optimum is found or why the algorithm works, we look at the optimal value function $\alpha(x)$ for the lower-level problem at given fixed values of the complicating variable x from the master problem. Function $\alpha(x)$ expresses the objective function of the original problem as a function solely of the complicating variables. For this problem $\alpha(x)$ is defined as:

$$
\begin{aligned}
&\alpha(x) = minimum_y\ 3x - 5y + 10(e^+ + e^-) \\
&s.t. \\
&0 \le y \le 1 \\
&-6 + 2x + 3y + e^+ - e^- = z \\
&2v^+ + 2v^- = z + y \\
&2v^+ - 2v^- = z - y \\
&e^+, e^-, z \ge 0
\end{aligned}
\tag{5.40}
$$

In general, the function $\alpha(x)$ is not known in closed form. The requirement for the standard Benders approach (for linear programs) is that the optimal objective value function $\alpha(x)$ needs to be convex for the method to converge, see Theorem 3.2 in (Conejo et.al, 2006). In our case, the lower-level problem (related to (x)) is a mixed

integer program due to the SOS1 property, [42] which is not directly applicable for the above-mentioned convergence theorem. For illustration of this point, Figure 5-1 presents the α-function for different x. It is clear for this example that the α-function is piecewise linear, but not convex. We see that α has one line with a negative slope (furthest left), then a positively sloped line, and finally another positively sloped line (furthest right). Since the SOS1 property only allows at most one variable in the set to be nonzero, there are three possible cases: case 1 ($v^+ > 0, v^- = 0$), case 2 ($v^+ = 0, v^- = 0$), and case 3 ($v^+ = 0, v^- > 0$). The correspondence with these cases and the three slopes are indicated in the figure below. Lastly, the reason that each part is a straight line (more generally convex function) is because the problem is a linear program as shown in (5.40) when the SOS1 variable are fixed.

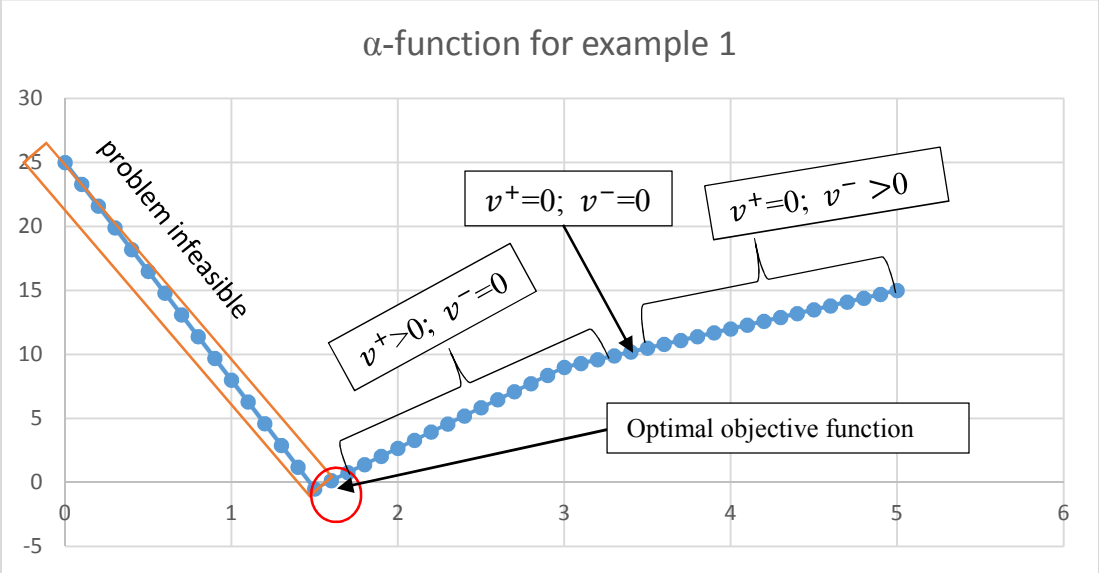

Figure 5-1 The optimal value function for example 1

[42] The property is that at most one of the pair variables can be non-zero.

It is important to note that each portion of the α-function is determined by the SOS1 variables which define the slopes for the α-function. The first downward slope x= [0, 1.4] is due to infeasibility of the subproblem having $e^+ > 0$. The second portion has two upward slopes due to the SOS1 variables. The first slope of α-function starts in the range x = [1.5, 2.9] where v^+ is nonezero while v^- is zero, the second slope has v^- is nonzero and $v^+ = 0$ from x=3.1 to x=5, and the last slope is just a point at (3, $\alpha(3)$) where $v^- = 0$ and $v^+ = 0$. Table 5-3 also shows the values for all related variables. In addition, Figure 5-1 also shows that α-function is a piecewise linear function of x and therefore is convex for specific ranges of x. As stated in (Conejo et al, 2006 page 257), the convergence of Benders decomposition for MINLP problems is guaranteed as long as the envelope of α-function is convex.

Table 5-3 Solutions from different starting point for Benders Decomposition Approach for α-function

Iteration	x	Objective function	y	e^+	v^+	v^-
1	0.0	25.0	1.0	3.0	0.0	0.5
2	0.1	23.3	1.0	2.8	0.0	0.5
3	0.2	21.6	1.0	2.6	0.0	0.5
4	0.3	19.9	1.0	2.4	0.0	0.5
5	0.4	18.2	1.0	2.2	0.0	0.5
6	0.5	16.5	1.0	2.0	0.0	0.5
7	0.6	14.8	1.0	1.8	0.0	0.5
8	0.7	13.1	1.0	1.6	0.0	0.5
9	0.8	11.4	1.0	1.4	0.0	0.5
10	0.9	9.7	1.0	1.2	0.0	0.5
11	1.0	8.0	1.0	1.0	0.0	0.5
12	1.1	6.3	1.0	0.8	0.0	0.5
13	1.2	4.6	1.0	0.6	0.0	0.5
14	1.3	2.9	1.0	0.4	0.0	0.5
15	1.4	1.2	1.0	0.2	0.0	0.5
16	1.5	-0.5	1.0	0.0	0.0	0.5

17	1.6	0.1	0.9	0.0	0.0	0.5
18	1.7	0.8	0.9	0.0	0.0	0.4
19	1.8	1.4	0.8	0.0	0.0	0.4
20	1.9	2.0	0.7	0.0	0.0	0.4
21	2.0	2.7	0.7	0.0	0.0	0.3
22	2.1	3.3	0.6	0.0	0.0	0.3
23	2.2	3.9	0.5	0.0	0.0	0.3
24	2.3	4.6	0.5	0.0	0.0	0.2
25	2.4	5.2	0.4	0.0	0.0	0.2
26	2.5	5.8	0.3	0.0	0.0	0.2
27	2.6	6.5	0.3	0.0	0.0	0.1
28	2.7	7.1	0.2	0.0	0.0	0.1
29	2.8	7.7	0.1	0.0	0.0	0.1
30	2.9	8.4	0.1	0.0	0.0	0.0
31	3.0	9.0	0.0	0.0	0.0	0.0
32	3.1	9.3	0.0	0.0	0.1	0.0
33	3.2	9.6	0.0	0.0	0.2	0.0
34	3.3	9.9	0.0	0.0	0.3	0.0
35	3.4	10.2	0.0	0.0	0.4	0.0
36	3.5	10.5	0.0	0.0	0.5	0.0
37	3.6	10.8	0.0	0.0	0.6	0.0
38	3.7	11.1	0.0	0.0	0.7	0.0
39	3.8	11.4	0.0	0.0	0.8	0.0
40	3.9	11.7	0.0	0.0	0.9	0.0
41	4.0	12.0	0.0	0.0	1.0	0.0
42	4.1	12.3	0.0	0.0	1.1	0.0
43	4.2	12.6	0.0	0.0	1.2	0.0
44	4.3	12.9	0.0	0.0	1.3	0.0
45	4.4	13.2	0.0	0.0	1.4	0.0
46	4.5	13.5	0.0	0.0	1.5	0.0
47	4.6	13.8	0.0	0.0	1.6	0.0
48	4.7	14.1	0.0	0.0	1.7	0.0
49	4.8	14.4	0.0	0.0	1.8	0.0
50	4.9	14.7	0.0	0.0	1.9	0.0
51	5.0	15.0	0.0	0.0	2.0	0.0

5.5 Numerical Examples

The following numerical examples serve to demonstrate applicability of the proposed algorithm. In particular, the proposed algorithm is compared to other known procedures to solve MPECs to show the different types of problems that can be solved and the superiority of the new method (at least numerically on these examples). Example 2 from (Siddiqui and Gabriel, 2012) is solved by Benders-SOS1 and compared with the disjunctive-constraints and SOS1 methods. Examples 3 and 4 applied Benders decomposition to stochastic MPEC problems. Example 5 presents a nonlinear program constrained by a nonlinear complementarity problem (Dirkse and Ferris, 1998) solved by the Benders-SOS1 approach. Lastly, we apply this algorithm to an MPEC derived from the World Gas Model MPEC version which serves as the natural gas link to the other chapters in this dissertation.

Example 2: Shale Gas MPEC-Linear Complementarity-Constrained Nonlinear Program

This MPEC is a Stackelberg game as reported in (Siddiqui and Gabriel, 2012). This small example has three shale natural gas producers where one producer is the leader in the market and the other two are the followers. The leader makes its decisions first, and then the two followers decide their own production with the leader's production fixed. The objective function for the leader is to maximize profit taking into account the anticipated sales from other two producers. The formulation is shown as follows

$$\begin{aligned} & min\, f(q_1, q_2, Q) \coloneqq -\{(a - b(q_1 + q_2 + Q))Q - CQ\} \\ & 0 \le -a + c_1 + 2bq_1 + bq_2 + bQ \perp q_1 \ge 0 \end{aligned} \tag{5.41}$$

$$0 \le -a + c_2 + bq_1 + 2bq_2 + bQ \perp q_2 \ge 0$$
$$0 \le Q$$

where a is the intercept and b is the slope of the inverse demand curve, and *C,c1,c2* are the marginal production costs for the leader and the two followers, respectively. The value for these parameters are presented in Table 5-4 with three datasets considered as in (Siddiqui and Gabriel, 2012). Also, *Q, q1, q2* are the production levels for the leader and the two followers, respectively. We applied Benders-SOS1 to this problem by considering Q as a complicating variable. In this problem we define the master problem as:

$$\begin{aligned} & min_{\alpha,Q}\ \alpha \\ & s.t.\ \ \alpha \ge \alpha^{down} \\ & 0 \le Q \\ & \alpha \ge f\left(Q^{(k)}, q_i^{(k)}\right) + \lambda^{(k)^T}\left(Q - Q^{(k)}\right); \forall k = 1, .., it-1 \end{aligned} \tag{5.42}$$

The subproblem is as follows:

$$\begin{aligned} & min\ _{q_1,q_2 s_1^+,s_1^-,s_2^+,s_2^-,z_1,z_2} -\{(a - b(q_1 + q_2 + Q))Q - CQ\} \\ & z_1 = -a + c_1 + 2bq_1 + bq_2 + bQ \\ & z_2 = -a + c_2 + bq_1 + 2bq_2 + bQ \\ & 2s_1^+ + 2s_1^- = z_1 + q_1 \\ & 2s_1^+ - 2s_1^- = z_1 - q_1 \\ & 2s_2^+ + 2s_2^- = z_2 + q_2 \\ & 2s_2^+ - 2s_2^- = z_2 - q_2 \\ & Q = Q^{(k)} : \lambda^{(k)} \\ & Q, q_1, q_2, z_1, z_2 \ge 0 \\ & s_1^+, s_1^-, s_2^+, s_2^- \text{ are SOS1 variables} \end{aligned} \tag{5.43}$$

As defined in (5.22), the α-function is defined as:

$$\begin{aligned} & \alpha(Q) = minimum_{q_1,q_2 s_1^+,s_1^-,s_2^+,s_2^-,z_1,z_2} -\{(a - b(q_1 + q_2 + Q))Q - CQ\} \\ & z_1 = -a + c_1 + 2bq_1 + bq_2 + bQ \\ & z_2 = -a + c_2 + bq_1 + 2bq_2 + bQ \\ & 2s_1^+ + 2s_1^- = z_1 + q_1 \\ & 2s_1^+ - 2s_1^- = z_1 - q_1 \end{aligned} \tag{5.44}$$

$$2s_2^+ + 2s_2^- = z_2 + q_2$$
$$2s_2^+ - 2s_2^- = z_2 - q_2$$
$$0 \leq z_1, z_2, q_1, q_2$$
$s_1^+, s_1^-, s_2^+, s_2^-$ are SOS1 variables

Figure 5-2 shows the optimal lower-level objective value function (α) for fixed Q from the master problem for test 1 data. The α-function is convex, but the first part $Q = [0,12]$ is not linear due to nonlinearity (quadratic term) in the objective function of the original problem (5.41). It is interesting to note however, that this α-function is piecewise convex.

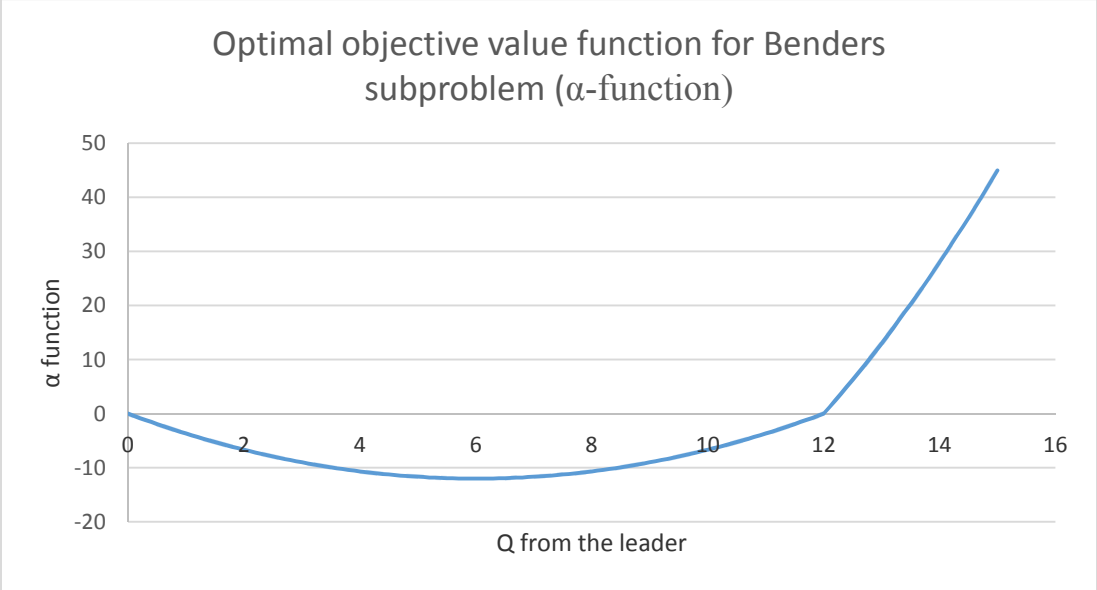

Figure 5-2 Lower-level optimal objective value function for example 2

The computational objective was to compare the results for the methods of disjunctive constraints, SOS1 variables (Siddiqui and Gabriel, 2012), and Benders-SOS1 algorithm. Later, the number of followers is increased to compare the efficacy of the algorithm. The solutions for three data sets from the literature are shown in Table 5-4.

Table 5-4 Comparison of the solutions for three approaches

Method	Problem	Optimal Objective function	Production	Computation time
Benders-SOS1	**Test 1** dataset1 (a=13 b=1 C,c1,c2=1)	12	Q=6, q1=q2=2	2.37 s
SOS1		12	Q=6, q1=q2=2	0.459 s
Disjunctive constraints		12	Q=6, q1=q2=2	0.209 s
Benders-SOS1	**Test 2** dataset2 (a=13 b=0.1 C,c1,c2=1)	120	Q=60, q1=q2=20	2.415 s
SOS2		120	Q=60, q1=q2=20	0.131 s
Disjunctive constraints		120	Q=60, q1=q2=20	0.428 s
Benders-SOS1	**Test 3** dataset3 (a=13 b=0.1 C,c1,c2=2)	100.83	Q=55, q1=q2=18.33	2.754 s
SOS1		100.83	Q=55, q1=q2=18.33	0.117 s
Disjunctive constraints		100.83	Q=55, q1=q2=18.33	0.149 s

These results indicate that the computational time is longer for the Benders-SOS1 method but the same solution is obtained compared with the other two approaches. Next, the test problem was changed so that instead of just two players at the lower level, there were *N* followers with similar costs and parameters. The decision variable q_i represents the quantity supplied by producer *i*. The number of players was increased to test the computational time taken for the disjunctive-constraints, SOS1, and Benders-SOS1 approaches. The results are shown in the Table 5-5 and Figure 5-3. All methods were able to obtain the correct solutions presented in (Siddiqui and Gabriel, 2012).

Table 5-5 Comparison of the solution with increased number of followers for the three approaches

Number of followers *N*	**Solution[43]**	**Time**		
		Disjunctive-constraints	**SOS1**	**Benders-SOS1**
5	Q=6 q1,..,q5=1	0.349 s	0.339 s	3.877 s
10	Q=6 q1,..,q10=0.545	0.482 s	0.264 s	4.54 s
50	Q=6 q1,..,q50=0.118	1.663 s	0.329 s	6.706 s
100	Q=6 q1,..,q100=0.059	3.518 s	0.414 s	6.977 s
300	Q=6 q1,…,q300=0.020	57.8 s	1.534 s	9.635 s
500	Q=6 q1,…,q500=0.012	376.8 s	4.232 s	15.48 s
750	Q=6 q1,…,q750= 0.008	1,281.6 s	14.084 s	32.11 s
1500	Q=6 q1,…,q1500= 0.004	3,209.4 s	81.0 s	62.3 s
2000	Q=6 q1,…,q1500= 0.003	No solution returned	138.85 s	123.6 s
2500	Q=6 q1,…,q1500= 0.002	No solution returned	257.4 s	148.2 s

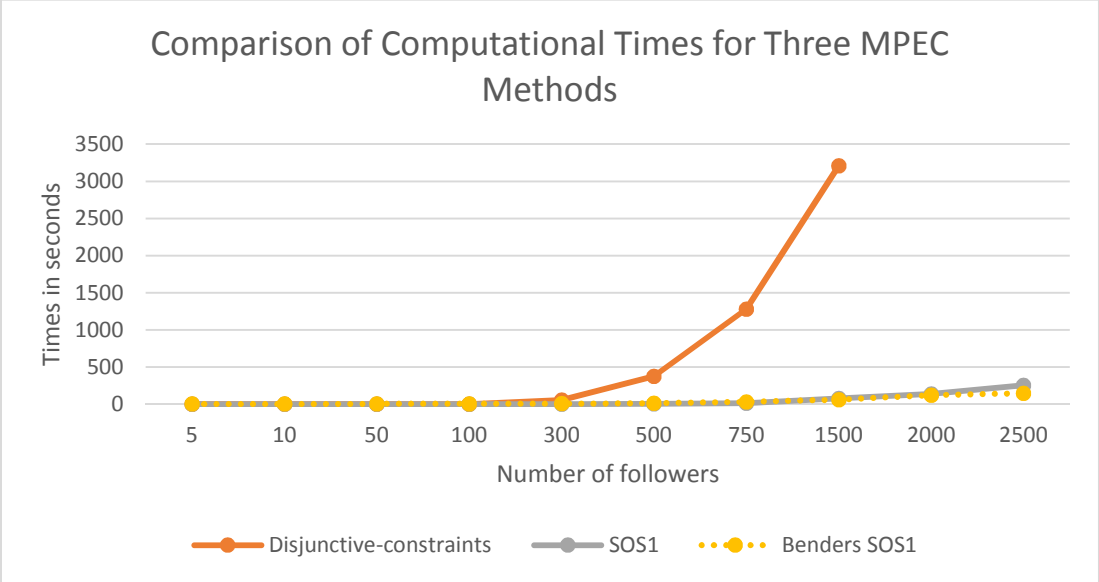

Figure 5-3 Comparison of Computational Time for the Three MPEC Methods

[43] The solution for this problem is unique, see (Siddiqui and Gabriel, 2012).

Clearly, the disjunctive-constraints method becomes extremely computationally expensive when the number of players is increased. When comparing the SOS1 and Benders-SOS1 approaches, Benders-SOS1 is slower for N< 1500, but faster when for N greater than or equal to 1500. So on this example, it seems that the computational advantage of the new Benders-SOS1 method shows up for larger problems. This is an indication that the overhead associated with the Benders approach is worth the computational effort for large enough problems. Lastly, we increase the number of followers up to 5,000, but the problem becomes infeasible and is terminated by GAMS for all three approaches.

Example 3: Two-Stage Stochastic Shale Gas MPEC

This problem is a modified example from the literature (Siddiqui and Gabriel, 2012) resulting in a two-stage, stochastic MPEC. In this example, the producers face uncertain demand. This problem has one leader and two followers ($i = 1,2$). The uncertainty is represented by equal probabilities *Pr(s)=0.5* for two scenarios $s\epsilon\{1,2\}$ representing low and high demand cases. The values $a_s = \{15,30\}$ are the intercepts of the demand curves for scenarios s=1,2 and $b_{s=1,2} = \{1,1\}$ are the slopes of the demand curves. The values C, c_{is} are the production costs for the leader and followers, respectively, and Q, q_{is} are the production level decision variables for the leader and followers, respectively, see Figure 5-4. The leader has an initial capacity of 3 units at time period 0 and needs to make an investment decision Inv with an investment cost (inv_c)of \$2 per unit in the first stage. The associated scenario tree is as follows:

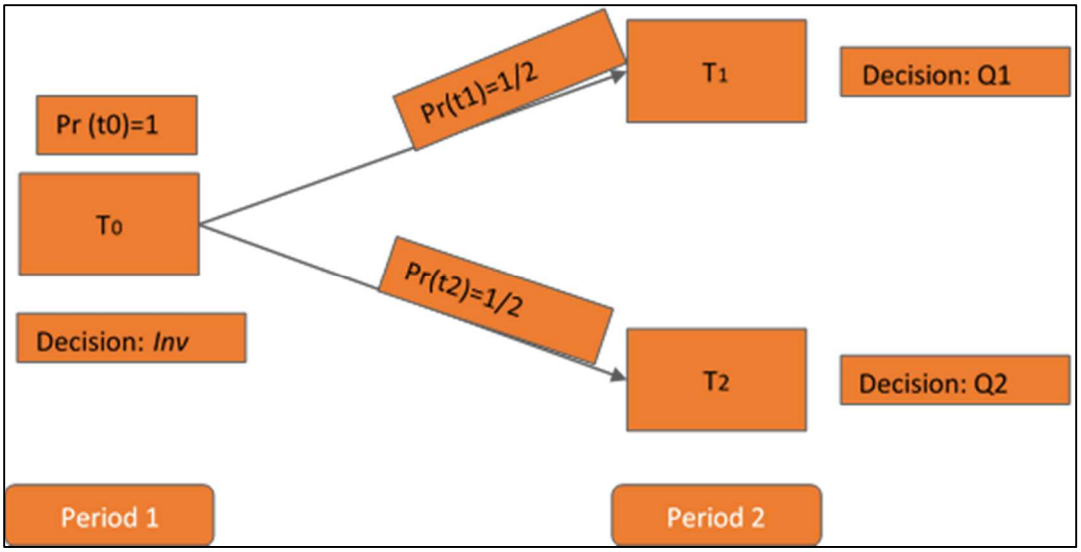

Figure 5-4 Scenario tree for small two-stage MPEC problem.

The complete formulation for the problem is as follows:

$$Min\left(\sum_s Pr_s\{(a_s - b_s(\sum_i q_{is} + Q_s))Q_s - CQ_s\}\right) - inv\_c * Inv$$

$$s.t.\ 0 \le -a_s + c_i + 2b_s q_{is} + b_s \sum_{j\neq i} q_{js} + b_s Q_s \perp q_{is} \ge 0\ \forall s, i \qquad (5.45)$$

$$Q_s \le 3 + inv\ \forall s$$

$$Q_s, inv, q_{is}\ \ge 0$$

Note that the complementarity constraints $0 \le -a_s + c_i + 2b_s q_{is} + b_s \sum_{j\neq i} q_{js} + b_s Q_s \perp q_{is} \ge 0$ represent the KKT conditions from the followers' problems. In this problem we consider the leader variables for each scenario, Q_s, as complicating variables, and the master problem is as follows:

$$min_{\alpha, Q_s}\ \alpha$$

$$s.t.\ \alpha \ge \alpha^{down} \qquad (5.46)$$

$$\alpha \ge f\left(inv^{(k)}, Q_s^{(k)}, q_{is}^{(k)}\right) + \lambda^{(k)^T}\left(Q_s - Q_s^{(k)}\right); \forall k = 1, .., it-1$$

The subproblem is as follows:

$$Min_{q_{is,Inv,s_{is}^{+},s_{is}^{-},z_{is},}} \left(\sum_{s} \Pr_s\{(a_s - b_s(\sum_i q_{is} + Q_s))Q_s - \mathrm{CQ}_s\}\right) - inv\_c * Inv$$

$$s.t.\ Q_s \leq 3 + inv$$

$$z_{is} = -a + c_i + 2bq_{is} + bq_{j\neq i,s} + bQ_s \qquad (5.47)$$

$$2s_{is}^{+} + 2s_{is}^{-} = z_{is} + q_{is}$$

$$2s_{is}^{+} - 2s_{is}^{-} = z_{is} - q_{is}$$

$$Q_s = Q_s^{(k)} : \lambda^{(k)}$$

$$q_i, z_i, inv \geq 0$$

s_i^{+}, s_i^{-} are SOS1 variables

In addition, as discussed in (5.22), the α-function in this problem is defined as:

$$Minimum_{q_{is,Inv,s_{is}^{+},s_{is}^{-},z_{is},}} \left(\sum_{s} \Pr_s\{(a_s - b_s(\sum_i q_{is} + Q_s))Q_s - \mathrm{CQ}_s\}\right) - inv\_c * Inv$$

$$s.t.\ Q_s \leq 3 + inv$$

$$z_{is} = -a + c_i + 2bq_{is} + bq_{j\neq i,s} + bQ_s \qquad (5.47)$$

$$2s_{is}^{+} + 2s_{is}^{-} = z_{is} + q_{is}$$

$$2s_{is}^{+} - 2s_{is}^{-} = z_{is} - q_{is}$$

$$Q_s = Q_s^{(k)} : \lambda^{(k)}$$

$$q_i, z_i, inv \geq 0$$

s_i^{+}, s_i^{-} are SOS1 variables

Figure 5-5 shows the lower-level optimal objective value function (α function) in three dimensions. Table 5-6 reports and compares the results for the disjunctive-constraints method and the Benders-SOS1 algorithm. We have three starting points with the same parameter values as follows; $\alpha_{down} = -30, \varepsilon = 10^{-5}$. Table 5-7 shows the comparison of three starting points $(i.e., Q_{(s)}^{(1)} = 0,5,10)$. Three different starting

points lead to the same optimal objective function value, but each uses a different number of iterations.

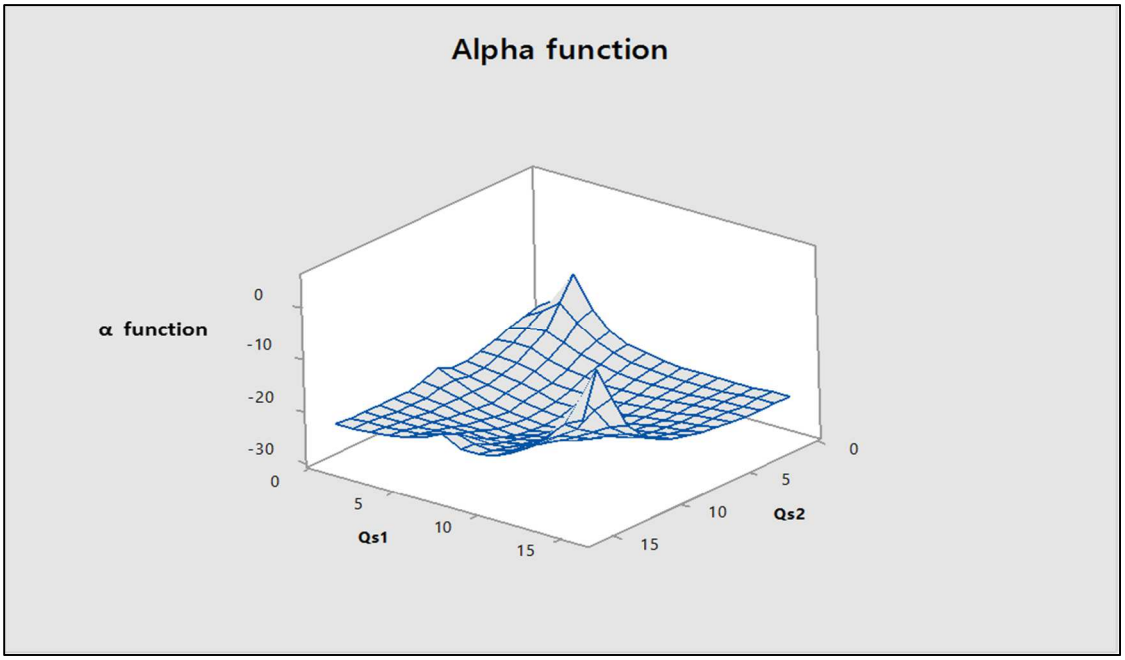

Figure 5-5 α function (α (Q_{s1}, Q_{s1})) for example 3

Table 5-6 Comparison of the solution for Benders Decomposition and disjunctive-constraints approaches.

Results	**Disjunctive-constraints method**	**Benders-SOS1 method**
Inv	5.5	5.5
S=1: *q11=q21*	2.33	2.33
S=1: *Q1*	7	7
S=1:Price	3.33	3.33
S=2: *q12=q22*	6.83	6.83
S=2: *Q2*	8.5	8.5
Price	7.83	7.83

Table 5-7 Convergence for small stochastic MPEC problem for three starting points.

Starting Point: $Q_s^{(1)} = 0$

Iterations (it)	**Primal Variables**			**Objective function**	
	$Q_{s=1}^{(it)}$	$Q_{s=2}^{(it)}$	inv	$z_{down}^{(it)}$	$z_{up}^{(it)}$
1	0	0	0	-30	0

2	12.86	0	9.86	-30	17.26531
3	0	6.21	3.21	-30	-17.16528
4	0	23	20	-30	16.99123
5	2.75	14.6	11.6	-30	-16.9915
6	5.87	10.3	7.3	-30	-25.41
7	5.93	3.96	2.93	-29.27605	-18.65371
8	14.44	10.81	11.44	-28.72596	-6.75323
9	11.98	9.57	8.98	-28.43799	-17.08443
10	8.13	7.65	5.13	-27.98784	-24.90819
11	5.87	6.51	3.51	-27.72095	-25.32879
12	7.87	8.46	5.46	-27.39181	-26.08311
13	5.97	8.41	5.41	-26.63095	-26.02845
14	6.89	9.47	6.47	-26.37924	-26.04963
15	6.91	8.52	5.52	-26.35879	-26.20704
16	7.33	7.39	4.39	-26.22475	-25.98365
17	7.36	8.04	5.04	-26.22249	-26.15097
18	7.39	8.52	5.52	-26.22085	-26.18277
19	7.15	8.29	5.29	-26.21512	-26.19717
20	7.15	8.53	5.53	-26.21387	-26.20431
21	7.04	8.41	5.41	-26.21124	-26.20673
22	7.03	8.53	5.53	-26.21040	-26.20801
23	6.98	8.47	5.47	-26.20921	-26.20808
24	6.97	8.53	5.53	-26.20869	-26.20809
25	7	8.5	5.5	-26.20861	-26.20833
26	6.97	8.5	5.5	-26.20837	-26.20822
27	6.99	8.51	5.51	-26.20835	-26.20828
28	6.99	8.5	5.5	-26.20835	-26.20831
29	7	8.51	5.51	-26.20834	-26.20833
30	7	8.5	5.5	-26.2083356	-26.20833
31	7	8.5	5.5	-26.2083354	-26.20833
32	7	8.5	5.5	-26.2083353	-26.20833

Starting Point: $Q_s^{(1)} = 5$

	Primal Variables			**Objective function**	
Iterations (it)	$Q_{s=1}^{(it)}$	$Q_{s=2}^{(it)}$	inv	$z_{down}^{(it)}$	$z_{up}^{(it)}$
1	5	5	2	-30.00000	-23.50000
2	23.5	0	20.5	-30.00000	152.62500
3	0	13.43	10.43	-30.00000	-13.99320

4	4.89	10.63	7.63	-30.00000	-24.70922
5	9.68	7.9	6.68	-30.00000	-21.38216
6	7.25	7.86	4.86	-28.33738	-26.12985
7	13.46	15.53	12.53	-27.24756	-11.00248
8	9.64	12.28	9.28	-26.87270	-22.66860
9	7.58	10.53	7.53	-26.67160	-25.46176
10	6.19	9.35	6.35	-26.53526	-25.97910
11	7.53	9.18	6.18	-26.38780	-26.08299
12	6.79	8.65	5.65	-26.33701	-26.19689
13	7.45	8.51	5.51	-26.25131	-26.17452
14	7.05	8.28	5.28	-26.23487	-26.19957
15	7.12	8.61	5.61	-26.22307	-26.20372
16	6.94	8.48	5.48	-26.21646	-26.20757
17	7.1	8.44	5.44	-26.21082	-26.20595
18	7.04	8.53	5.53	-26.21015	-26.20791
19	7.02	8.45	5.45	-26.20910	-26.20788
20	6.99	8.5	5.5	-26.20888	-26.20831
21	7.03	8.49	5.49	-26.20847	-26.20816
22	7.01	8.52	5.52	-26.20840	-26.20826
23	7.01	8.49	5.49	-26.20839	-26.20831
24	7	8.51	5.51	-26.20836	-26.20832
25	7	8.5	5.5	-26.20835	-26.20833
26	7	8.5	5.5	-26.2083430	-26.20833
27	7	8.5	5.5	-26.2083413	-26.20833
28	7	8.5	5.5	-26.20833	-26.20833

Starting Point: $Q_s^{(1)} = 10$

	Primal Variables			**Objective function**	
Iterations (it)	$Q_{s=1}^{(it)}$	$Q_{s=2}^{(it)}$	inv	$z_{down}^{(it)}$	$z_{up}^{(it)}$
1	10	10	7	-30	-24.33333
2	0	0	0	-30	0
3	2.43	5.03	2.03	-30	-20.72517
4	3.52	11.62	8.62	-30	-22.57294
5	6.01	7.82	4.82	-29.40744	-25.96997
6	6.83	11.07	8.07	-26.971	-25.10218
7	7.92	9.07	6.07	-26.87787	-26.01292
8	6.29	9.48	6.48	-26.43491	-25.96467
9	6.92	8.52	5.52	-26.42473	-26.20709
10	10.82	2.57	7.82	-26.36138	-1.43512
11	8.47	6.88	5.47	-26.26271	-22.24697

12	7.91	7.91	4.91	-26.23926	-26.01238
13	7.87	7.97	4.97	-26.23776	-26.03547
14	7.56	8.54	5.54	-26.22481	-26.15563
15	7.25	8	5	-26.22038	-26.15608
16	7.24	8.36	5.36	-26.21735	-26.19536
17	7.23	8.75	5.87	-26.21408	-26.18833
18	7.14	8.56	5.56	-26.2129	-26.20471
19	7.05	8.38	5.38	-26.21187	-26.20564
20	7.03	8.5	5.5	-26.21048	-26.20816
21	6.96	8.43	5.43	-26.20896	-26.2072
22	6.97	8.49	5.49	-26.20883	-26.20817
23	6.99	8.58	5.58	-26.20864	-26.20724
24	7	8.53	5.53	-26.20856	-26.20816
25	7	8.5	5.5	-26.2085	-26.20833
26	7	8.45	5.45	-26.20834	-26.20796
27	6.99	8.48	5.48	-26.20834	-26.20823
28	6.99	8.49	5.49	-26.20834	-26.20829
29	7	8.49	5.49	-26.208340	-26.208310
30	6.99	8.49	5.49	-26.208340	-26.208320
31	6.99	8.51	5.51	-26.208340	-26.208280
32	6.99	8.5	5.5	-26.208333	-26.208320
33	7	8.5	5.5	-26.208332	-26.208330
34	7	8.5	5.5	-26.208331	-26.208330
35	7	8.5	5.5	-26.208330	-26.208330

Example 4: Two-Stage Stochastic Shale Gas MPEC with binary variables in the first-stage, upper level problem

This is a modification of Example 3 so that the problem becomes a two-stage stochastic MPEC with binary variables in the first stage. In particular, this problem is an instance of a planning problem including build/don't build decisions. The decision variable *'inv'* for capacity expansion for the leader's problem in the first stage becomes a binary variable. If the leader decides to expand the production capacity from 3 to 3+6=9 units,

a fixed investment cost of \$10 is needed for the capacity expansion. The production capacity constraint for the leader becomes $Q_s \leq 3 + 6 * inv$.

The complete formulation for this problem is as follows:

$$Min_{q_{is},Q_s,inv} \left(\sum_s \Pr_s\{(a_s - b_s(\sum_i q_{is} + Q_s))Q_s - \mathrm{CQ}_s\} \right) - 10 * Inv$$

$$s.t.\ 0 \leq -a_s + c_i + 2b_s q_{is} + b_s \textstyle\sum_{j \neq i} q_{js} + b_s Q_s \perp q_{is} \geq 0 \qquad (5.49)$$

$$Q_s \leq 3 + 6 * inv$$

$$Q_s, inv, q_{is} \geq 0$$

$$Inv \in \{0,1\}$$

In this problem, we consider the binary variable Inv as a complicating variable because if it is fixed, the subproblem becomes a nonlinear program instead of a mixed-integer nonlinear program. Therefore Q_s is not in the master problem unlike the previous problem. For this problem, the master problem is as follows:

$$min_{\alpha,inv}\ \alpha$$

$$s.t.\ \alpha \geq \alpha^{down} \qquad (5.50)$$

$$0 \leq inv \leq 1$$

$$\alpha \geq f\left(inv^{(k)}, Q_s^{(k)}, q_{is}^{(k)}\right) + \lambda^{(k)^T}\left(inv - inv^{(k)}\right); \forall k = 1, .., it - 1$$

The subproblem is as follows:

$$Min_{Q_s,q_{is},s_{is}^+,s_{is}^-,z_{is}} \left(\sum_s \Pr_s\{(a_s - b_s(\sum_i q_{is} + Q_s))Q_s - \mathrm{CQ}_s\} \right) - 10 * Inv$$

$$s.t. \qquad z_{is} = -a + c_i + 2bq_{is} + bq_{j \neq i,s} + bQ_s \qquad (5.51)$$

$$2s_{is}^+ + 2s_{is}^- = z_{is} + q_{is}$$

$$2s_{is}^+ - 2s_{is}^- = z_{is} - q_{is}$$

$$Q_s \leq 3 + 6 * inv$$

$Q_s, inv, q_{is}, z_{is} \geq 0$

$Inv = inv^{(k)} : \lambda^{(k)}$

s_i^+, s_i^- are SOS1 variables

We initialize the parameters to be: $\alpha_{down} = -30, \varepsilon = 10^{-5}$. The binary investment variable is relaxed in the master problem to be in the range between zero to one. Four different starting points $Inv = 0,0.4,0.8,1$ lead to the same optimal solution. Three starting points $Inv = 0,0.4,0.8$ converge within three iterations. When $Inv = 1$ is used as a starting point, the algorithm converges to an optimal solution within two iterations as shown in Table 5-8. Table 5-9 compares the results to the disjunctive-constraints approach for Example 4. Benders-SOS1 has quicker a computational time (0.588 vs 1.045 seconds) and achieves the same optimal solution as the disjunctive-constraints approach.

Table 5-8 Comparison of three starting points for Example 4
Benders-SOS1

Starting Points: $Inv = 0$

	Primal Variables[44]			**Objective function**	
Iterations (it)	$Q_{s=1}^{(it)}$	$Q_{s=2}^{(it)}$	Inv	$z_{down}^{(it)}$	$z_{up}^{(it)}$
1	3	3	0	-30	-18.5
2	7	9	1	2	-30
3	7	9	1	-28.1667	-28.1667

Starting Points: $Inv = 0.4$

	Primal Variables			**Objective function**	
Iterations (it)	$Q_{s=1}^{(it)}$	$Q_{s=2}^{(it)}$	Inv	$z_{down}^{(it)}$	$z_{up}^{(it)}$
1	5.4	5.4	0.4	-30	-24.98
2	7	9	1	-30	-28.1667

[44] We show only a solution for the leader problem because there are too many variables in the lower-level problem.

3	7	9	1	-28.1667	-28.1667

Starting Points: $Inv = 0.8$

	Primal Variables			Objective function	
Iterations (it)	$Q_{s=1}^{(it)}$	$Q_{s=2}^{(it)}$	Inv	$z_{down}^{(it)}$	$z_{up}^{(it)}$
1	7	7.8	0.8	-30	-27.7267
2	7	9	1	-28.4067	-28.1667
3	7	9	1	-28.1667	-28.1667

Starting Points: $Inv = 1$

	Primal Variables			Objective function	
Iterations (it)	$Q_{s=1}^{(it)}$	$Q_{s=2}^{(it)}$	Inv	$z_{down}^{(it)}$	$z_{up}^{(it)}$
1	7	9	7	-30	-28.1667
2	7	9	7	-28.1667	-28.1667

Table 5-9 A comparison of solutions for the two-Stage Stochastic Shale Gas MPEC

Results	**Disjunctive-constraints method**	**Benders-SOS1 method**
Inv	1	1
S=1: *q11=q21*	2.33	2.33
S=1: *Q1*	7	7
S=1:Price	3.33	3.33
S=2: *q12=q22*	6.67	6.67
S=2: *Q2*	9	9
Price	7.67	7.67
Computational time	1.045 seconds	0.588 seconds

Example 5: Nonlinear Complementarity-Constrained Nonlinear Program

This two-variable example is from (Dirkse and Ferris, 1998) and is a nonlinear complementarity problem (NCP)-constrained mathematical program[45] with the variables being x and y. An optimal solution for this problem is $(x = 1, y = 0)$ (Dirkse and Ferris, 1998). The problem is as follows:

[45] This problem has nonlinear complementarity constraints while other problems showed earlier have linear complementarity constraints.

$$
\begin{aligned}
& min\, f(x,y) \coloneqq (x-1-y)^2 \\
& s.t. \qquad x^2 \le 2 \\
& -1 \le x \le 2 \\
& (x-1)^2 + (y-1)^2 \le 3 \\
& 0 \le y - x^2 + 1 \perp y \ge 0
\end{aligned} \tag{5.52}
$$

In this problem, x is defined as the complicating variable. Thus, the master problem is as follows:

$$
\begin{aligned}
& min_{\alpha,x}\, \alpha \\
& s.t.\ \alpha \ge \alpha^{down} \\
& x^2 \le 2 \\
& -1 \le x \le 2 \\
& \alpha \ge f\left(x^{(k)}, y^{(k)}\right) + \lambda^{(k)^T}\left(x - x^{(k)}\right); \forall k = 1, .., it-1
\end{aligned} \tag{5.53}
$$

The subproblem is:

$$
\begin{aligned}
& Min_{\,y}(x-1-y)^2 \\
& s.t. \quad (x-1)^2 + (y-1)^2 \le 3 \\
& z = y - x^2 + 1 \\
& 2s^+ + 2s^- = z + y \\
& 2s^+ - 2s^- = z - y \\
& z, y \ge 0 \\
& x = x^{(k)} : \lambda^{(k)} \\
& s^+, s^- \text{are SOS1 variables}
\end{aligned} \tag{5.54}
$$

This example is solved with a lower bound $\alpha \ge -25$ and $\varepsilon = 10^{-5}$. The Benders-SOS1 algorithm was tried with three starting points considering x as the complicating variable. The question whether Benders-SOS1 can find an optimal solution from any starting points is shown in Table 5-10 where the results are displayed for three different

initial values $\left(x^{(1)} = 0,0.5,0.9\right)$. The algorithm provides a solution which is close to an optimal solution from these three starting points, see Table 5-10. In addition, as discussed in (5.22), the optimal objective function value given fixed x in this problem is defined as:

$$\begin{aligned} &\alpha(x) = Minimum_{\ y}(x-1-y)^2 \\ &s.t.\ \ (x-1)^2 + (y-1)^2 \le 3 \\ &z = y - x^2 + 1 \\ &2s^+ + 2s^- = z + y \\ &2s^+ - 2s^- = z - y \\ &z, y\ \ge 0 \\ &s^+, s^- \text{are SOS1 variables} \end{aligned} \tag{5.55}$$

We notice that the α-function (the optimal value of the objective function of subproblem given x is fixed) in this problem is convex, see Figure 5-6. The Benders-SOS1 converges to a point that is very close to an optimal solution.

Table 5-10 Convergence for Example 5 Using the Benders-SOS1 Approach

$x^{(1)} = 0$					
Iteration (it)	$x^{(it)}$	$y^{(it)}$	$\lambda^{(it)}$	$z_{down}^{(it)}$	$z_{up}^{(it)}$
1	0	0	-2	-20	1
2	1.41421	1.6224	1000	-3	5.393055011
3	1.40701	0.97967	2.07763	-1.814	0.32794037
4	0.88171	0	-0.23657	-0.76342512	0.013991919
5	1.21765	0.48266	0.76075	-0.06548138	0.070232982
6	1.08157	0.16979	0.20522	-0.03328857	0.007782751
7	0.9886	0	-0.02279	-0.01129561	0.000129898
8	1.03871	0.07892	0.08664	-0.00101229	0.001616794
9	1.01469	0.02959	0.03068	-0.00046469	0.000222106
10	1.00184	0.00369	0.00371	-0.000171940	0.000003419
11	0.99523	0	-0.00954	-0.000021120	0.000022777
12	0.99854	0	-0.00292	-0.000008830	0.000002138

13	1.0002	0.0004	0.00039	-0.000002690	0.000000042
14	0.99937	0	-0.00126	-0.000000280	0.000000402
15	0.99979	0.00001	-0.00043	-0.000000120	0.000000048
16	1	0	0	-0.000000030	0.000000000

$x^{(1)} = 0.5$					
Iteration (it)	$x^{(it)}$	$y^{(it)}$	$\lambda^{(it)}$	$z_{down}^{(it)}$	$z_{up}^{(it)}$
1	0.5	0	-1	-20.000000000	0.250000000
2	1.41421	0.87274	1000	-1.250000000	15.570800000
3	1.39799	0.95439	1.99856	-0.647994770	0.309574959
4	1.07865	0.16349	0.19637	-0.328651340	0.007197380
5	0.79793	0	-0.40415	-0.047927060	0.040833474
6	0.94574	0	-0.10853	-0.018902660	0.002944647
7	1.01739	0.03508	0.03662	-0.004832050	0.000313050
8	0.98194	0	-0.03611	-0.000984950	0.000326051
9	0.99997	0	-0.00005	-0.000324910	0.000000001
10	1.00883	0.01774	0.01813	-0.000000410	0.000079358
11	1.00444	0.0089	0.009	-0.000000200	0.000019914
12	1.00222	0.00444	0.00447	-0.000000100	0.000004945
13	1.0011	0.0022	0.00221	-0.000000050	0.000001213
14	1.00053	0.00107	0.00107	-0.000000020	0.000000291
15	1.00025	0.0005	0.0005	-0.000000010	0.000000063
16	1.00007	0.00014	0.00011	0.0000000000	0.0000000050
17	1.00001	0.00003	0.00003	0.0000000000	0.0000000002
18	0.99983	0.00001	-0.00034	0.0000000100	0.0000000340
19	0.99999	0	0	0.0000000005	0.0000000001
20	0.99999	0	0.00002	0.0000000002	0.0000000000

$x^{(1)} = 0.9$					
Iteration (it)	$x^{(it)}$	$y^{(it)}$	$\lambda^{(it)}$	$z_{down}^{(it)}$	$z_{up}^{(it)}$
1	0.9	0	-0.2	-20	0.01
2	1.41421	0.37358	1000	-0.21	32.0372
3	1.38209	0.91017	1.86327	-0.08641799	0.278871308
4	1.20505	0.45214	0.69684	-0.05100914	0.061053196
5	1.08009	0.1666	0.20073	-0.02601858	0.007483598
6	0.99649	0	-0.00702	-0.00929802	0.000012319
7	1.04131	0.08432	0.09313	-0.00030227	0.001849961
8	1.01981	0.04002	0.04202	-0.00015141	0.000408349

9	1.0084	0.01687	0.01722	-0.00007128	0.000071734
10	1.0025	0.00501	0.00504	-0.00002986	0.000006279
11	0.9995	0.00001	-0.001	-0.00000882	0.000000258
12	1.00101	0.00201	0.00202	-0.00000125	0.00000101
13	1.00026	0.00052	0.00051	-0.00000050	0.00000007
14	0.99988	0	-0.00023	-0.00000012	0.00000001
15	1.00007	0.00014	0.00011	-0.00000003	0.00000001
16	0.99997	0	-0.00004	0.00000000	0.00000000
17	1.00003	0.00006	0.00006	0.00000001	0.00000000
18	0.99998	0	-0.00002	0.000000003	0.000000000
19	0.99999	0	-0.00001	0.000000010	0.000000000

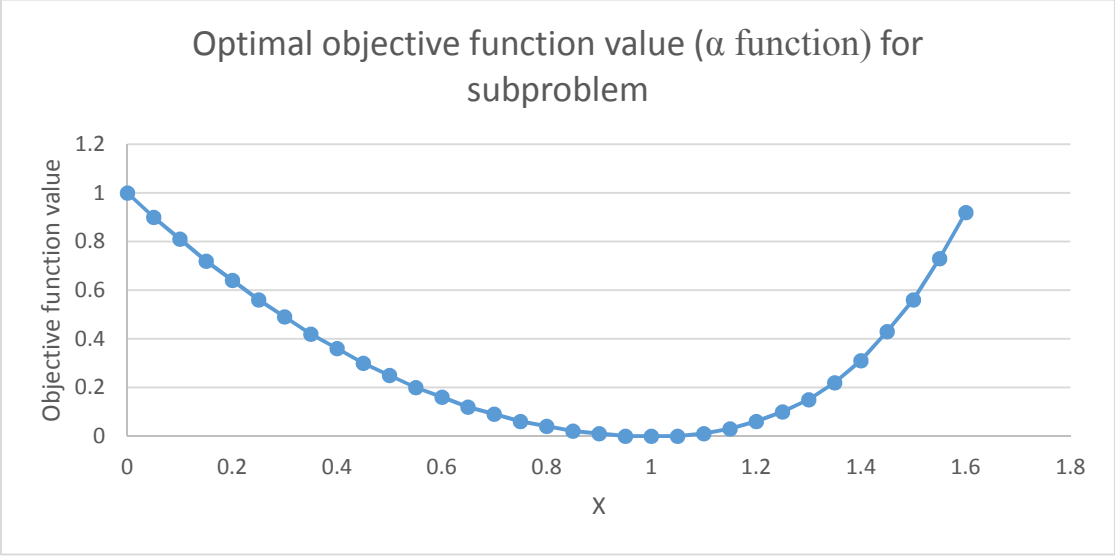

Figure 5-6 optimal objective function value for example 5

5.6 A large-scale MPEC version of the World Gas Model

In order to test the efficiency of the algorithm on larger problems than those already described, this section introduces a Stackelberg version (Gibbons 1996) of the World Gas Model (Gabriel et al., 2012) in which the Panama Canal operator is the leader and the rest of the gas market are the followers. The canal operator anticipates the reactions of other market participants in its own decisions, and endogenously determines canal

tariffs. The leader's objective function is profit maximization and includes the constraints from the WGM in addition to the KKT conditions of the followers (i.e., other market players). The lower level of this problem includes natural gas producers, traders, pipeline operator, and marketers represented by the inverse demand curve. The lower level is the reduced version of the WGM model because we take out the storage operator to reduce the size of the problem. Also, only six time periods (2005-2030) are considered here. Section 5.6.1 presents the mathematical notation used.

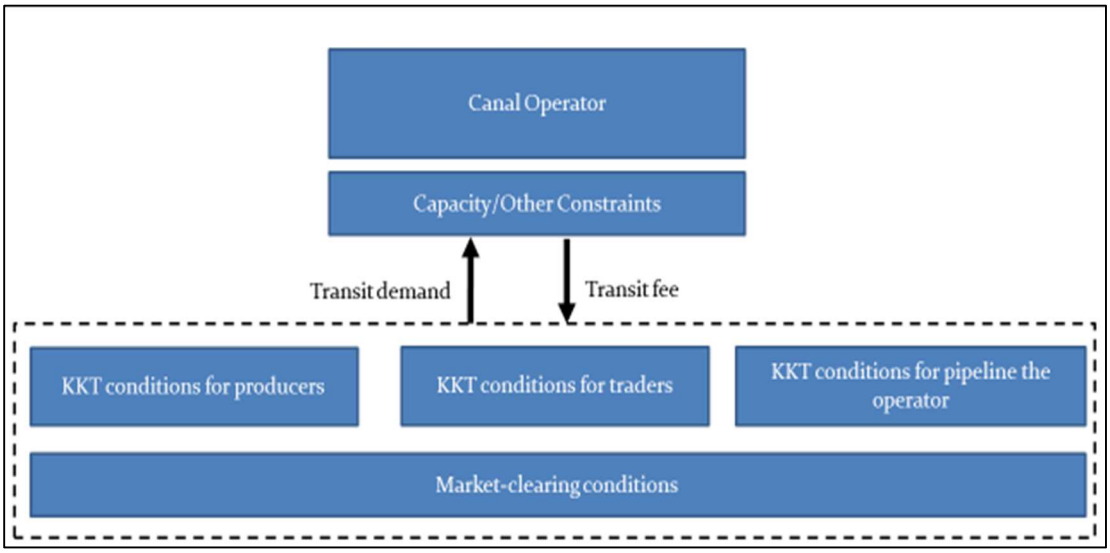

Figure 5-7 WGM MPEC version

5.6.1 Mathematical Notation

Indices:

$a \in A$	Gas transportation arcs
$d \in D$	Seasons, i.e., {low, high}
$p \in P$	Producers
$m \in M$	Years
$n \in N$	Model nodes
$t \in T$	Traders

$a^+(n)$ Inward arcs at node n

$a^-(n)$ Outward arcs at node n

Variables:

$\tau_{dm}^{P\_toll}$ Canal transit fee in $ per kcm (thousand cubic meters)

$SALES_{dm}^{P_{canal}}$ Capacity of the canal in terms of kcm offered to traders

$SALES_{adm}^{A}$ Pipeline capacity assigned to a trader (mcm/d)

$SALES_{Pdm}^{P}$ Quantity sold by a producer to traders and liquefiers (mcm/d)

$SALES_{tndm}^{T}$ Quantity sold to end-user markets by traders (mcm/d)

$PURCH_{tndm}^{T}$ Quantity bought from a producer by a trader (mcm/d)

$FLOW_{tadm}^{T}$ Arc flow by a trader (mcm/d)

$\alpha \geq 0$ Dual variables of capacity restrictions

$\varphi, free$ Dual variables of mass balance constraints

$\rho \geq 0$ Dual variables of capacity expansion limitations

$\pi, free$ Dual variables of market-clearing conditions for sold and bought quantities

$\tau\ free$ Dual variables of market-clearing conditions for capacity assignment and usage

Parameters:

$C_{pm}^{P}(.)$ Production costs (k$/mcm)

$\overline{CAP}_{am}^{A}$ Arc capacity (mcm/d)

δ_{tn}^{C} Cournot coefficient; Level of market power exerted by a trader in a market $\delta_{tn}^{C} \in [0,1]$

day_d	Number of days in a season
γ_m	Discount rate for a year, $\gamma_m \in (0,1]$
INT_{ndm}^{W}	Intercept of inverse demand curve (mcm/d)
$loss_a$	Loss rate of gas in the transport arc, $loss_a \in [0,1)$
SLP_{ndm}^{W}	Slope of the inverse demand curve (mcm/d/k$)
CC_m	CO_2 cost ($/ton of CO2e)
CE_{player}	CO_2 emissions factor [46] with values in (0.1]
M	Conjectural variation slope, *M*<0, see more explanation on this parameter in the next section

5.6.2 Canal operator problem (Upper Level Problem)

The main assumption of this model is that the Panama Canal is a local leader since traders that use the Suez Canal would not be directly affected. The first term $(\tau_{dm}^{P\_toll})SALES_{dm}^{P_{canal}}$ is the revenue gained from collecting transit fees. The second term $C_{dm}^{P_{Canal}}(SALES_{dm}^{P_{canal}})$ is the operating cost for using the canal. The canal operator can decide the canal toll $\tau_{dm}^{P\_toll}$ on the total flows from traders through the canal route. However, this model assumes that the canal operator faces a decreasing demand curve [47] for its transit service because without this assumption, the transit fees $\tau_{dm}^{P\_toll}$ could be unbounded which would complicate things computationally. Therefore, a transit demand curve approach is implemented. It is important to note that this represents a bilinear term in the sales and tariff variables, but this computational challenge is

[46] The gas industry assumes that 27% of the carbon dioxide is emitted from the production process,12% in the processing process, 28% in transmission, 24% from the distributing process, and 9% from storage. In this model, we assume 1 mcm of natural gas produced emits 2.76 metric tons of CO2 and CO2 emission is allocated to each market player as follows; producers 0.105 MT/MCM, traders 1.194 MT/MCM, storage operator 0.017 MT/MCM,TSO 0.294 MT/MCM, marketers 1.194 MT/MCM.

[47] This also gives an implicit bound on the canal transit fees otherwise the transit fees will go to positive infinity and make the overall problem unbounded.

overcome by the Benders-SOS1 algorithm. The variable $SALES_{dm}^{P_{canal}}$ is considered as complicating variables for Benders-SOS1. The master problem has the variable $SALES_{dm}^{P_{canal}}$ and α. The subproblem is solved with fixed $SALES_{dm}^{P_{canal}}$ from the master problem. Fixing $SALES_{dm}^{P_{canal}}$ removes the nonlinearity in the subproblem. There is no $\tau_{dm}^{P\_toll}$ in the master problem.

$$Max_{\substack{SALES_{dm}^{P\_canal} \\ \tau_{dm}^{P\_toll}}} \sum_{m\epsilon M} \gamma_m \left\{ \sum_{d\epsilon D} day_d \begin{bmatrix} (\tau_{dm}^{P\_toll}) SALES_{dm}^{P_{canal}} \\ -C_{dm}^{P_{Canal}}(SALES_{dm}^{P_{canal}}) \end{bmatrix} \right\} \quad (5.56)$$

s.t.

The sales rates for the Panama canals are limited by its capacity.

$$SALES_{dm}^{P_{canal}} \leq \ CAP^{P\_canal} \quad \forall d, m \quad (5.57)$$

The total flows from traders in the lower level problem through the canal route equal the capacity of the Canal offered by the upper-level player:

$$\sum_{t,a\epsilon Pcanal} FLOW_{tadm}^{T} = SALES_{dm}^{P_{canal}} \quad \forall d, m \quad (5.58)$$

The canal transit demand is represented by a conjectured transit demand curve approach.

$$SALES_{dm}^{P_{canal}} + M(\tau_{dm}^{P\_toll}) \leq 0 \quad \forall d, m \quad (5.59)$$

All of the variables must be nonnegative.

$$SALES_{dm}^{P_{canal}} \geq 0 \quad (5.60)$$

$$\tau_{dm}^{P\_toll} \geq 0 \quad (5.61)$$

In this model, canal transit interaction is represented by a transit demand curve approach, which assumes that the Panama Canal operator will face a decreasing demand for increased transit fees. To be clear, this does not necessarily mean that the canal operator exerts market power over the traders. One reason is that the transit

demand curve is not in the objective function of the canal operator unlike for the trader optimization problem (5.66) which has market demand taken into account along with the decisions of other traders. The canal operator has no ability to withhold transit capacity to obtain higher transit fees. The transit demand curve condition just represents the interaction between these two sets of players and shows a canal operator's belief about the reaction (or variation) of traders to potential adjustments in the canal operator's actions. The same approach is used in the work by Chyong and Hobbs (2014) that considers transit market power between Ukraine and Russian gas exports. The conjectural variations approach is also widely used in the electricity market modelling literature, for example in the form of the conjectured supply function and the conjectured transmission price function (Day et al., 2002; Hobbs and Rijkers, 2004; Hobbs et al., 2004). In our context, this approach suggests that the transit quantity $SALES_{dm}^{P_{canal}}$ will diverge from the equilibrium point $SALES_{dm}^{P_{canal*}}$ in proportion to the change of transit fee ($\tau_{dm}^{P\_toll*}$) with assumed exogenous slope. Therefore, in our case the conjectured transit demand equation is

$$\left(SALES_{dm}^{P_{canal}} - SALES_{dm}^{P_{canal*}}\right) - M * \left(\tau_{dm}^{P\_toll} - \tau_{dm}^{P\_toll*}\right) = 0, M < 0 \; \forall d, m \quad (5.62)$$

where $\left(SALES_{dm}^{P_{canal}} - SALES_{dm}^{P_{canal*}}\right)$ is the difference in demand for canal transit that cause by the change of transit fee $\left(\tau_{dm}^{P\_toll} - \tau_{dm}^{P\_toll*}\right)$, and slope is a conjectured slope for canal transit demand curve, which is measured in mcm per day. WGM assumes a maximum of 200 mcm per day for capacity of Panama Canal transit daily. [48] Figure 5-8 shows the demand curve for Panama Canal under three slopes. Also, Figure 5-8

[48] 200 mcm equals to two largest size LNG carriers (170,000 cm) that can pass the Canal.

shows that for a large slope, *M*= -200, a small change in transit fees cause significant changes in flows through the Panama Canal. This makes sense in the way that if the traders see the high canal fee so that they decide to use alternative routes or ship gas to elsewhere.

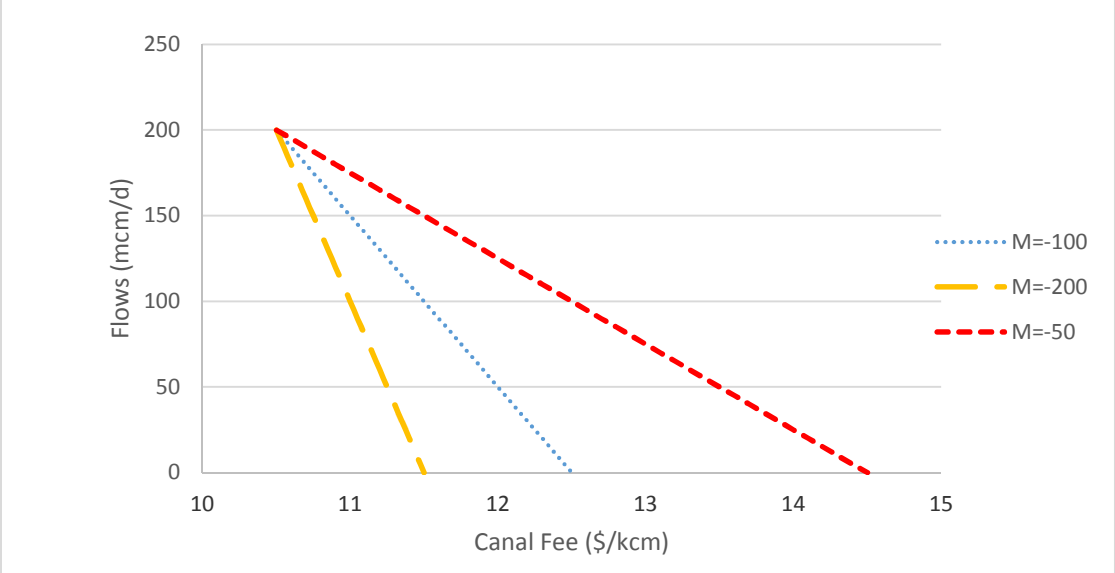

Figure 5-8 Panama Canal's transit demand curve.

5.6.3 Lower-Level Problems

5.6.3.1 Producer problem

A natural gas producer $p \in P$ is modeled as a profit maximizer. The daily profit for the producer is determined by the difference between the revenue, $\pi^{P}_{n(p)dm} SALES^{P}_{pdm}$, and the total costs, which are the production cost $C^{P}_{pm}\left(SALES^{P}_{pdm}\right)$ and the emissions cost[49] $CC^{ton}_{pm} SALES^{P}_{pdm} CE^{P}_{p}$. The production cost function $C^{P}_{pm}\left(SALES^{P}_{pdm}\right)$ is linear[50]. The

[49] In this study the emissions cost is zero.
[50] The production cost function differs from the previuos WGM because we would like to simplify the problem without logarithmic cost fuction in the objective function of the lower-level problem.

annual profit is calculated by the sales rate multiplied by the number of days $days_d$ for each season with a discount rate γ_m for year m. The producer supplies gas to traders.

$$\mathbf{max}_{SALES^P_{pdm}} \quad \sum_{m\epsilon M} \gamma_m \left\{ \sum_{d\epsilon days} days_d \begin{bmatrix} \pi^P_{n(p)dm} SALES^P_{pdm} \\ -C^P_{pm}\left(SALES^P_{pdm}\right) \\ -CC^{ton}_{pm} SALES^P_{pdm} CE^P_p \end{bmatrix} \right\} \tag{5.63}$$

The daily sales rates are restricted by the maximum capacity $\overline{PR^P_{pm}}$.

$$\textbf{s.t.} \qquad SALES^P_{pdm} \leq \overline{PR^P_{pm}} \quad \forall d, m \quad (\alpha^P_{pdm}) \tag{5.64}$$

The sales rate and the capacity expansion must be nonnegative.

$$SALES^P_{pdm} \geq 0 \quad \forall d, m \tag{5.65}$$

5.6.3.2 Trader Problem

The trader maximizes discounted profits, which come from the revenues $(\delta^C_{tn} \Pi^W_{ndm}(.) + (1 - \delta^C_{tn})\pi^W_{ndm}) SALES^T_{tndm}$ and the purchasing costs $\pi^P_{ndm} PURCH^{T\leftarrow P}_{tndm}$ and the emissions cost $(CC^{ton}_{tm} SALES^T_{tndm} CE^T_T)$. The expression $(\delta^C_{tn} \Pi^W_{ndm}(.) + (1 - \delta^C_{tn})\pi^W_{ndm})$ can be viewed as a weighted average of market prices resulting from the inverse demand function $\Pi^W_{ndm}(.)$ and a perfectly competitive market-clearing wholesale price π^W_{ndm}. In addition, the trader is responsible for the transportation costs, $(\tau^{A,reg}_{adm} + \tau^A_{adm}) FLOW^T_{tadm}$, for the gas. Also, the term $\left(\sum_{a\epsilon Pcanal}\left(\tau^{A,reg}_{adm} + \tau^{P\_toll}_{dm}\right) FLOW^T_{tadm}\right)$ corresponds to if the traders flow gas through the Panama Canal. The traders are modeled as a weighted combination of strategic/competitive players depending on the market power parameter $\delta^C_{tn} \in [0,1]$, where 0 represents competitive behavior and 1 indicates oligopolistic behavior with a knowledge of demand in the market.

$$\boldsymbol{max}_{\substack{SALES^{T}_{tndm} \\ PURCH^{T\leftarrow P}_{tndm} \\ FLOW^{T}_{tadm}}} \sum_{m\epsilon M}\gamma_m \sum_{d\epsilon D} days_d \left\{ \begin{array}{c} \sum_{n\epsilon N(t)} \left[\begin{array}{c} (\delta^{C}_{tn}\Pi^{W}_{ndm}(.) + (1-\delta^{C}_{tn})\pi^{W}_{ndm})SALES^{T}_{tndm} \\ -\pi^{P}_{ndm}PURCH^{T\leftarrow P}_{tndm} \end{array} \right] \\ -\left(\sum_{a\epsilon A(t)}\left(\tau^{A,reg}_{adm}+\tau^{A}_{adm}\right)FLOW^{T}_{tadm}\right) \\ -\left(\sum_{a\epsilon Pcanal}\left(\tau^{A,reg}_{adm}+\tau^{P\_toll}_{dm}\right)FLOW^{T}_{tadm}\right) \\ -(CC^{ton}_{tm}SALES^{T}_{tndm}CE^{T}_{T}) \end{array} \right\} \quad (5.66)$$

The next constraint ensures the mass balance of sales, purchases, and flows.

$$PURCH^{T}_{tndm} + \sum_{a\epsilon a^{+}(n)}(1-loss_a)\,FLOW^{T}_{tadm} = SALES^{T}_{tndm} + \sum_{a\epsilon a^{-}} FLOW^{T}_{tadm} \quad \forall n,d,m\ (\varphi^{T}_{tndm}) \quad (5.67)$$

Some traders have contractual obligations, that can be modeled as follows:

$$FLOW^{T}_{tadm} \geq CON^{T}_{tadm} \quad \forall a,d,m \ \left(\varepsilon^{T}_{tadm}\right) \quad (5.68)$$

All of the variables must be nonnegative.

$$SALES^{T}_{tndm} \geq 0 \quad \forall n,d,m \quad (5.69)$$

$$PURCH^{T}_{tndm} \geq 0 \quad \forall n,d,m \quad (5.70)$$

$$FLOW^{T}_{tadm} \geq 0 \quad \forall a,d,m \quad (5.71)$$

5.6.3.3 Transmission system operator

The transmission system operator (TSO) provides an economic mechanism to efficiently allocate international transport capacity to traders. It is assumed that there is one central TSO for the model. The TSO maximizes discounted profits that result from selling arc capacity to traders via the$SALES^{A}_{adm}$ variables.

$$Max_{SALES^{A}_{adm}} \quad \sum_{m\epsilon M}\gamma_m \left\{ \sum_{d\epsilon D} days_d \left[\begin{array}{c} \sum_{a\notin Pcanal} \tau^{A}_{adm}\,SALES^{A}_{adm} \\ -CC^{ton}_{tsom}SALES^{A}_{adm}CE^{TSO}_{tso} \end{array} \right] \right\} \quad (5.72)$$

The assigned capacity is restricted by the available capacity

$$SALES^{A}_{adm} \leq \overline{CAP}^{A}_{am} \quad \forall a \notin Pcanal,d,m \ (\alpha^{A}_{adm}) \quad (5.73)$$

All of the variables must be nonnegative.

$$SALES^{A}_{adm} \geq 0 \quad \forall a \notin Pcanal,d,m \quad (5.74)$$

5.6.3.4 Market-clearing conditions

Market-clearing conditions tie the producers to traders. The total sales from producers equals the purchases from traders.

$$SALES^{P}_{pdm} = \sum_{t(p)} PURCH^{T}_{tn(p)dm} \quad , \forall p, d, m \quad (\pi^{P}_{n(p)dm}) \tag{5.75}$$

The pipeline capacity offered by a pipeline operator equals the total of flows from all traders. The market-clearing conditions for arc capacity flow are:

$$SALES^{A}_{adm} = \sum_{t} FLOW^{T}_{tadm} \quad \forall a, d, m \quad (\tau^{A}_{adm}) \tag{5.76}$$

Market-clearing conditions for final demand represented by inverse demand curve are:

$$\pi^{W}_{ndm} = INT^{W}_{ndm} - SLP^{W}_{ndm}\left(\sum_{t} SALES^{T}_{tndm}\right) \quad \forall n, d, m \quad (\pi^{W}_{ndm}) \tag{5.77}$$

In order to write the problem in the way we can apply the decomposition method, we first write out the KKT conditions for the lower-level problems.

5.6.4 The Karush–Kuhn–Tucker (KKT) conditions of the lower-level problems

5.6.4.1 KKT conditions for the producer problem

$$0 \leq days_{d}\left[\gamma_{m}\left(-\pi^{P}_{n(p)dm} + \frac{\partial c^{P}_{pm}\left(SALES^{P}_{pdm}\right)}{\partial SALES^{P}_{pdm}} + CC^{ton}_{pm} CE^{p}_{p}\right)\right] + \alpha^{P}_{pdm} \perp$$

$$SALES^{P}_{pdm} \geq 0 \quad \forall d, m \tag{5.78}$$

$$0 \leq \overline{PR^{P}_{pm}} - SALES^{P}_{pdm} \perp \quad \alpha^{P}_{pdm} \geq 0 \quad \forall d, m \tag{5.79}$$

5.6.4.2 KKT conditions for the trader problem

$$0 \leq days_{d}\left[\gamma_{m}\begin{pmatrix} \delta^{C}_{tn} SLP^{M}_{ndm} SALES^{T}_{tndm} \\ -\left(\delta^{C}_{tn}\Pi^{W(T)}_{ndm} + (1-\delta^{C}_{tn})\pi^{W}_{ndm}\right) \\ +(CC^{ton}_{tm} CE^{T}_{T}) \end{pmatrix}\right] + \phi^{T}_{tndm} \perp SALES^{T}_{tndm} \geq$$

$$0, \quad \forall n, d, m \tag{5.80}$$

$$0 \leq days_{d}[\gamma_{m}\pi^{P}_{ndm}] - \phi^{T}_{tndm} \perp \quad PURCH^{T\leftarrow P}_{tndm} \geq 0 \quad \forall n \epsilon N\left(p(t)\right), d, m \tag{5.81}$$

$$0 \leq days_d \gamma_m \left(\tau_{adm}^{A,reg} + \tau_{adm}^{A}\right) + \phi_{tna^- dm}^{T} - (1 - loss_a)\phi_{tna^+ dm}^{T} \perp \; FLOW_{tadm}^{T} \geq 0$$
$$\forall a \notin Pcanal = \left(n_{a^-}, n_{a^+}\right), d, m \quad (5.82)$$

$$0 \leq days_d \gamma_m \left(\tau_{adm}^{A,reg} + \tau_{dm}^{P\_toll}\right) + \phi_{tna^- dm}^{T} - (1 - loss_a)\phi_{tna^+ dm}^{T} \perp \; FLOW_{tadm}^{T} \geq 0$$
$$\forall a \in Pcanal = \left(n_{a^-}, n_{a^+}\right), d, m \quad (5.83)$$

$$0 = \begin{bmatrix} PURCH_{tndm}^{T} + \sum_{a \epsilon a^+(n)} (1 - loss_a)\, FLOW_{tadm}^{T} \\ -SALES_{tndm}^{T} - \sum_{a \epsilon a^-} FLOW_{tadm}^{T} \end{bmatrix}, \varphi_{tndm}^{T}, free, \forall n, d, m \quad (5.84)$$

5.6.4.3 KKT conditions for the system operator problem

$$0 \leq \gamma_m days_d (-\tau_{adm}^{A} + CC_{tsom}^{ton} CE_{tso}^{TSO}) + \alpha_{adm}^{A} \perp SALES_{adm}^{A} \geq 0 \quad \forall a, d, m \quad (5.85)$$

$$0 \leq \overline{CAP}_{am}^{A} - SALES_{adm}^{A} \perp \alpha_{adm}^{A} \geq 0 \quad \forall a, d, m \quad (5.86)$$

Then the complementarity conditions in the lower level are replaced by SOS1 variables. The purpose of this form is to have mixed-integer linear constraint at hand. We get the following mixed-integer problem for the WGM MPEC as follows:

$$Max_{\substack{SALES_{dm}^{P\_canal} \\ \tau_{dm}^{P\_toll}}} \sum_{m \epsilon M} \gamma_m \left\{ \sum_{d \epsilon D} day_d \begin{bmatrix} (\tau_{dm}^{P\_toll}) SALES_{dm}^{P_{canal}} \\ -C_{dm}^{P_{Canal}} (SALES_{dm}^{P_{canal}}) \end{bmatrix} \right\} \quad (5.87A1)$$

s.t.

$$SALES_{dm}^{P_{canal}} \leq \; CAP^{P\_canal} \quad \forall d, m \quad (5.87A2)$$

$$\sum_{t, a \epsilon Pcanal} FLOW_{tadm}^{T} = SALES_{dm}^{P_{canal}} \quad \forall d, m \quad (5.87A3)$$

$$SALES_{dm}^{P_{canal}} + M(\tau_{dm}^{P\_toll}) \leq 0 \quad \forall d, m \quad (5.87A4)$$

$$SALES_{pdm}^{P} - \sum_{t(p)} PURCH_{tn(p)dm}^{T} = 0 \; \forall p, d, m \quad (5.87A5)$$

$$SALES_{adm}^{A} - \sum_{t} FLOW_{tadm}^{T} = 0 \quad \forall a \notin Pcanal, d, m \quad (5.87A6)$$

$$\pi_{ndm}^{W} = INT_{ndm}^{W} - SLP_{ndm}^{W} \left(\sum_{t} SALES_{tndm}^{T}\right) \quad \forall n, d, m \quad (5.87A7)$$

$$days_d\left[\gamma_m\left(-\pi^P_{n(p)dm}+\frac{\partial c^P_{pm}(SALES^P_{pdm})}{\partial SALES^P_{pdm}}+CC^{ton}_{pm}CE^p_p\right)\right]+\alpha^P_{pdm}=zp^1_{pdm}\quad \forall p,d,m \tag{5.87A8}$$

$$0\le zp^1_{pdm}\quad \forall d,m \tag{5.87A9}$$

$$2sp1^+_{pdm}+2sp1^-_{pdm}=zp^1_{pdm}+SALES^P_{pdm}\ \forall p,d,m \tag{5.87A10}$$

$$2sp1^+_{pdm}-2sp1^-_{pdm}=zp^1_{pdm}-SALES^P_{pdm}\ \forall p,d,m \tag{5.87A11}$$

$$\overline{PR^P_{pm}}-SALES^P_{pdm}=zp^2_{pdm}\quad \forall p,d,m \tag{5.87A12}$$

$$0\le zp^2_{pdm}\quad \forall p,d,m \tag{5.87A13}$$

$$2sp2^+_{pdm}+2sp2^-_{pdm}=zp^2_{pdm}+\alpha^P_{pdm}\ \forall p,d,m \tag{5.87A14}$$

$$2sp2^+_{pdm}-2sp2^-_{pdm}=zp^2_{pdm}-\alpha^P_{pdm}\ \forall p,d,m \tag{5.87A15}$$

$$days_d\left[\gamma_m\left(\begin{array}{c}\delta^C_{tn}SLP^M_{ndm}SALES^T_{tndm}\\-\left(\delta^C_{tn}\Pi^{W(T)}_{ndm}+(1-\delta^C_{tn})\pi^W_{ndm}\right)\\+(CC^{ton}_{tm}CE^T_T)\end{array}\right)\right]+\phi^T_{tndm}=zt^1_{tndm}\quad \forall t,n,d,m \tag{5.87A16}$$

$$0\le zt^1_{tndm}\quad \forall t,n,d,m \tag{5.87A17}$$

$$2st1^+_{tndm}+2st1^-_{tndm}=zt^1_{tndm}+SALES^T_{tndm}\forall t,n,d,m \tag{5.87A18}$$

$$2st1^+_{tndm}-2st1^-_{tndm}=zt^1_{tndm}-SALES^T_{tndm}\forall t,n,d,m \tag{5.87A19}$$

$$days_d[\gamma_m\pi^P_{ndm}]-\phi^T_{tndm}=\ zt^2_{tndm}\ \forall t,n\epsilon N\big(p(t)\big),d,m \tag{5.87A20}$$

$$0\le\ zt^2_{tndm}\ \forall t,n\epsilon N\big(p(t)\big),d,m \tag{5.87A21}$$

$$2st2^+_{tndm}+2st2^-_{tndm}=zt^2_{tndm}+\ PURCH^{T\leftarrow P}_{tndm}\ \forall t,n\epsilon N\big(p(t)\big),d,m \tag{5.87A22}$$

$$2st2^+_{tndm}-2st2^-_{tndm}=zt^2_{tndm}-PURCH^{T\leftarrow P}_{tndm}\ \forall t,n\epsilon N\big(p(t)\big),d,m \tag{5.87A23}$$

$$days_d\gamma_m\left(\tau_{adm}^{A,reg}+\tau_{adm}^{A}\right)+\phi_{tna^-dm}^{T}-(1-loss_a)\phi_{ta^+dm}^{T}= \ zt_{tadm}^{3}\forall t,a\notin Pcanal\ ,d,m \quad (5.87A24)$$

$$0\leq \ zt_{tadm}^{3}\forall t,a\notin Pcanal\ ,d,m \quad (5.87A25)$$

$$2st3_{tndm}^{+}+2st3_{tndm}^{-}=zt_{tndm}^{3}+\ FLOW_{tndm}^{T}\ \forall t,a\notin Pcanal\ ,d,m \quad (5.87A26)$$

$$2st3_{tadm}^{+}-2st3_{tadm}^{-}=zt_{tadm}^{3}-FLOW_{tadm}^{T}\ \forall t,a\notin Pcanal\ ,d,m \quad (5.87A27)$$

$$days_d\gamma_m\left(\tau_{adm}^{A,reg}+\tau_{dm}^{ptoll}\right)+\phi_{ta^-dm}^{T}-(1-loss_a)\phi_{ta^+dm}^{T}= \ zt_{tadm}^{4}$$

$$\forall t,a\in Pcanal\ ,d,m \quad (5.87A28)$$

$$0\leq \ zt_{tadm}^{4}\forall a\in Pcanal\ ,d,m \quad (5.87A29)$$

$$2st4_{tadm}^{+}+2st4_{tadm}^{-}=zt_{tadm}^{4}+\ FLOW_{tadm}^{T}\ \forall t,a\in Pcanal\ ,d,m \quad (5.87A30)$$

$$2st4_{tadm}^{+}-2st4_{tadm}^{-}=zt_{tadm}^{4}-FLOW_{tadm}^{T}\ \forall t,a\in Pcanal\ ,d,m \quad (5.87A31)$$

$$0=\begin{bmatrix}PURCH_{tndm}^{T}+\sum_{a\epsilon a^+(n)}(1-loss_a)\ FLOW_{tadm}^{T}\\ -SALES_{tndm}^{T}-\sum_{a\epsilon a^-}FLOW_{tadm}^{T}\end{bmatrix},\varphi_{tndm}^{T},free,\forall t,n,d,m \quad (5.87A32)$$

$$\gamma_m days_d(-\tau_{adm}^{A}+CC_{tsom}^{ton}CE_{tso}^{TSO})+\alpha_{adm}^{A}=zi_{adm}^{1}\forall a,d,m \quad (5.87A31)$$

$$0\leq zi_{adm}^{1}\forall a,d,m \quad (5.87A32)$$

$$2si1_{adm}^{+}+2si1_{adm}^{-}=zi_{adm}^{1}+SALES_{adm}^{A}\ \forall a,d,m \quad (5.87A33)$$

$$2si1_{adm}^{+}-2si1_{adm}^{-}=zi_{adm}^{1}-SALES_{adm}^{A}\ \forall a,d,m \quad (5.87A34)$$

$$0 \leq \overline{CAP}_{am}^{A} - SALES_{adm}^{A} = zi_{adm}^{2} \; \forall a, d, m \quad (5.87A35)$$

$$0 \leq zi_{adm}^{2} \forall a, d, m \quad (5.87A36)$$

$$2si2_{adm}^{+} + 2si2_{adm}^{-} = zi_{adm}^{2} + \alpha_{adm}^{A} \; \forall a, d, m \quad (5.87A37)$$

$$2si2_{adm}^{+} - 2si2_{adm}^{-} = zi_{adm}^{2} - \alpha_{adm}^{A} \; \forall a, d, m \quad (5.87A38)$$

$sp1_{pdm}^{+}, sp1_{pdm,}^{-} sp2_{pdm}^{+}, sp2_{pdm}^{-}, st1_{tndm}^{+}, st1_{tndm'}^{-} st2_{tndm}^{+}, st2_{tndm,}^{-} st3_{tadm}^{+}$
$, st3_{tadm}^{-} st4_{tadm}^{+}, st4_{tadm}^{-} si1_{adm}^{+}, si1_{adm}^{-}, si2_{adm}^{+}, si2_{idm}^{-}$ are SOS1 variables

Now when the KKT conditions are transformed into an SOS1 formulation, the problem (5.87A) is decomposed using the Benders-SOS1 approach. The variables $SALES_{dm}^{P_{canal}}$ are considered as the complicating variables for Benders-SOS1. It is important to note that the bilinear term $(\tau_{dm}^{P_{-}toll}) \sum_{t,a \epsilon Pcanal} SALES_{dm}^{P_{canal}}$ is in the subproblem so that the master problem has the variable α , the complicating variable $SALES_{dm}^{P_{canal}}$, and the capacity constraint. Benders cuts are obtained at each iteration based on information of the dual variables λ_{dm}^{k} from the subproblem. Benders decomposition approximates α using hyperplanes and improves the approximation using additional hyperplanes from the subproblem at each iteration which yield the following master and subproblem.

$$min_{SALES_{dm}^{P_{canal}}, \alpha} \; \alpha$$

$$s.t.$$

$$\alpha^{down} - \alpha \leq 0 \quad (5.8787B)$$

$$f\left(SALES_{dm}^{pcanal,k}\right) + \lambda_{dm}^{k^T}\left(SALES_{dm}^{P_{canal}} - SALES_{dm}^{P_{canal},k}\right) - \alpha \leq 0\,; \quad \forall k, .., it-1$$

$$SALES_{dm}^{P_{canal}} \leq CAP^{P_{canal}} \; , \forall d, m$$

$$0 \leq SALES_{dm}^{P_{canal}} \; \forall d, m$$

The Benders-SOS1algorithm proceeds by solving the master problem then provides the vector of fixed master variables $SALES_{dm}^{P_{canal}}$ to the subproblem. The subproblem with fixed $SALES_{dm}^{P_{canal}}$ is as follows:

$$Max_{\substack{SALES_{dm}^{P\_canal} \\ \tau_{dm}^{P\_toll}}} \sum_{m\epsilon M} \gamma_m \left\{ \sum_{d\epsilon D} day_d \begin{bmatrix} (\tau_{dm}^{P\_toll}) SALES_{dm}^{P_{canal}} \\ -C_{dm}^{P_{Canal}} (SALES_{dm}^{P_{canal}}) \end{bmatrix} \right\} \quad (5.87C1)$$

s.t.

$$SALES_{dm}^{P_{canal}} = SALES_{dm}^{P_{canal}(it)}, \lambda_{dm}\ free\ \forall d, m \quad (5.87C2)$$

$$SALES_{dm}^{P_{canal}} \leq \ CAP^{P\_canal} \ \ \forall d, m \quad (5.87C3)$$

$$\sum_{t,a\epsilon Pcanal} FLOW_{tadm}^{T} \ = SALES_{dm}^{P_{canal}} \quad \forall d, m \quad (5.87C4)$$

$$SALES_{dm}^{P_{canal}} + M(\tau_{dm}^{P\_toll}) \leq 0 \quad \forall d, m \quad (5.87C5)$$

$$SALES_{pdm}^{P} - \sum_{t(p)} PURCH_{tn(p)dm}^{T} \ = 0 \ \forall p, d, m \quad (5.87C6)$$

$$SALES_{adm}^{A} - \sum_{t} FLOW_{tadm}^{T} = 0 \quad \forall a \notin Pcanal, d, m \quad (5.87C7)$$

$$\pi_{ndm}^{W} = INT_{ndm}^{W} - SLP_{ndm}^{W}\left(\sum_{t} SALES_{tndm}^{T}\right) \quad \forall n, d, m \quad (5.87C8)$$

$$days_d \left[\gamma_m \left(-\pi_{n(p)dm}^{P} + \frac{\partial c_{pm}^{P}(SALES_{pdm}^{P})}{\partial SALES_{pdm}^{P}} + CC_{pm}^{ton} CE_{p}^{p} \right) \right] + \alpha_{pdm}^{P} = zp_{pdm}^{1} \quad \forall p, d, m \quad (5.87C9)$$

$$0 \leq zp_{pdm}^{1} \quad \forall p, d, m \quad (5.87C10)$$

$$2sp1_{pdm}^{+} + 2sp1_{pdm}^{-} = zp_{pdm}^{1} + SALES_{pdm}^{P} \ \forall p, d, m \quad (5.87C11)$$

$$2sp1_{pdm}^{+} - 2sp1_{pdm}^{-} = zp_{pdm}^{1} - SALES_{pdm}^{P} \ \forall p, d, m \quad (5.87C12)$$

$$\overline{PR_{pm}^{P}} - SALES_{pdm}^{P} \ = zp_{pdm}^{2} \quad \forall p, d, m \quad (5.87C13)$$

$$0 \leq zp_{pdm}^{2} \quad \forall p, d, m \quad (5.87C14)$$

$$2sp2_{pdm}^{+} + 2sp2_{pdm}^{-} = zp_{pdm}^{2} + \alpha_{pdm}^{P} \ \forall p, d, m \quad (5.87C15)$$

$$2sp2_{pdm}^{+} - 2sp2_{pdm}^{-} = zp_{pdm}^{2} - \alpha_{pdm}^{P} \ \forall p, d, m \quad (5.87C16)$$

$$days_d \left[\gamma_m \left(\begin{array}{c} \delta_{tn}^{C} SLP_{ndm}^{M} SALES_{tndm}^{T} \\ -\left(\delta_{tn}^{C} \Pi_{ndm}^{W(T)} + (1 - \delta_{tn}^{C}) \pi_{ndm}^{W} \right) \\ +(CC_{tm}^{ton} CE_{T}^{T}) \end{array} \right) \right] + \phi_{tndm}^{T} = zt_{tndm}^{1} \quad \forall t, n, d, m \quad (5.87C17)$$

$$0 \leq zt_{tndm}^{1} \quad \forall t, n, d, m \quad (5.87C18)$$

$$2st1^{+}_{tndm} + 2st1^{-}_{tndm} = zt^{1}_{tndm} + SALES^{T}_{tndm} \forall t, n, d, m \quad (5.87C19)$$

$$2st1^{+}_{tndm} - 2st1^{-}_{tndm} = zt^{1}_{tndm} - SALES^{T}_{tndm} \forall t, n, d, m \quad (5.87C20)$$

$$days_d[\gamma_m \pi^{P}_{ndm}] - \phi^{T}_{tndm} = \ zt^{2}_{tndm} \ \forall t, n \epsilon N\big(p(t)\big), d, m \quad (5.87C21)$$

$$0 \leq \ zt^{2}_{tndm} \ \forall t, n \epsilon N\big(p(t)\big), d, m \quad (5.87C22)$$

$$2st2^{+}_{tndm} + 2st2^{-}_{tndm} = zt^{2}_{tndm} + \ PURCH^{T \leftarrow P}_{tndm} \ \forall t, n \epsilon N\big(p(t)\big), d, m \quad (5.87C23)$$

$$2st2^{+}_{tndm} - 2st2^{-}_{tndm} = zt^{2}_{tndm} - PURCH^{T \leftarrow P}_{tndm} \ \forall t, n \epsilon N\big(p(t)\big), d, m \quad (5.87C24)$$

$$days_d \gamma_m \big(\tau^{A,reg}_{adm} + \tau^{A}_{adm}\big) + \phi^{T}_{tna^{-}dm} - (1 - loss_a)\phi^{T}_{ta^{+}dm} = \ zt^{3}_{tadm} \forall t, a \notin Pcanal\ , d, m \quad (5.87C25)$$

$$0 \leq \ zt^{3}_{tadm} \forall a \notin Pcanal\ , d, m \quad (5.87C26)$$

$$2st3^{+}_{tadm} + 2st3^{-}_{tadm} = zt^{3}_{tadm} + \ FLOW^{T}_{tadm} \ \forall t, a \notin Pcanal\ , d, m \quad (5.87C27)$$

$$2st3^{+}_{tadm} - 2st3^{-}_{tadm} = zt^{3}_{tadm} - FLOW^{T}_{tadm} \ \forall t, a \notin Pcanal\ , d, m \quad (5.87C28)$$

$$days_d \gamma_m \big(\tau^{A,reg}_{adm} + \tau^{ptoll}_{dm}\big) + \phi^{T}_{ta^{-}dm} - (1 - loss_a)\phi^{T}_{ta^{+}dm} = \ zt^{4}_{tadm}$$

$$\forall t, a \in Pcanal\ , d, m \quad (5.87C29)$$

$$0 \leq \ zt^{4}_{tadm} \forall t, a \in Pcanal\ , d, m \quad (5.87C30)$$

$$2st4^{+}_{tadm} + 2st4^{-}_{tadm} = zt^{4}_{tadm} + \ FLOW^{T}_{tadm} \ \forall t, a \in Pcanal\ , d, m \quad (5.87C31)$$

$$2st4^{+}_{tadm} \text{-}2st4^{-}_{tadm} = zt^{4}_{tadm} - FLOW^{T}_{tadm}\ \forall t, a \in Pcanal\ , d, m \quad (5.87C32)$$

$$0 = \begin{bmatrix} PURCH^{T}_{tndm} + \sum_{a\epsilon a^{+}(n)}(1 - loss_a)\ FLOW^{T}_{tadm} \\ -SALES^{T}_{tndm} - \sum_{a\epsilon a^{-}} FLOW^{T}_{tadm} \end{bmatrix}, \varphi^{T}_{tndm}, free, \forall t, n, d, m \quad (5.87C33)$$

$$\gamma_m days_d(-\tau^{A}_{adm} + CC^{ton}_{tsom} CE^{TSO}_{tso}) + \alpha^{A}_{adm} = zi^{1}_{adm} \forall a, d, m \quad (5.87C34)$$

$$0 \leq zi^{1}_{adm} \forall a, d, m \quad (5.87C35)$$

$$2si1^{+}_{adm} \text{+}2si1^{-}_{adm} = zi^{1}_{adm} + SALES^{A}_{adm}\ \forall a, d, m \quad (5.87C36)$$

$$2si1^{+}_{adm} \text{-}2si1^{-}_{adm} = zi^{1}_{adm} - SALES^{A}_{adm}\ \forall a, d, m \quad (5.87C37)$$

$$0 \leq \overline{CAP}^{A}_{am} - SALES^{A}_{adm} = zi^{2}_{adm}\ \forall a, d, m \quad (5.87C38)$$

$$0 \leq zi^{2}_{adm} \forall a, d, m \quad (5.87C39)$$

$$2si2^{+}_{adm} \text{+}2si2^{-}_{adm} = zi^{2}_{adm} + \alpha^{A}_{adm}\ \forall a, d, m \quad (5.87C40)$$

$$2si2^{+}_{adm} \text{-}2si2^{-}_{adm} = zi^{2}_{adm} - \alpha^{A}_{adm}\ \forall a, d, m \quad (5.87C41)$$

$sp1^{+}_{pdm}, sp1^{-}_{pdm} sp2^{+}_{pdm}, sp2^{-}_{pdm}, st1^{+}_{tndm}, st1^{-}_{tndm}, st2^{+}_{tndm}, st2^{-}_{tndm}, st3^{+}_{tadm}$, $st3^{-}_{tadm}, st4^{+}_{tadm}, st4^{-}_{tadm} si1^{+}_{adm}, si1^{-}_{adm}, si2^{+}_{adm}, si2^{-}_{adm}$ are SOS1 variables

5.7 Model Validation

In order to validate the results from Benders Algorithm, a check of the solution from the model has been performed as follows:

- We solve the model with many different starting points. Eight different starting points are employed for one time period (2005), see Table 5-11

where the results for the upper-level problem are shown for different initial points. We apply Benders-SOS1 with $SALES_{dm}^{P_{canal}}$ as the complicating variables. A tolerance of 10^{-5} and a value of α^{down} of -10^{-9} are selected. Overall, the model has 13,303 variables: 3,640 are discrete (SOS1 variables to replace the complementarity condition in the lower problem) and the remaining 10,663 are continuous. Although we use different starting points, Benders-SOS1 obtains the same solution for each of the starting points. However, the computational time and number of Benders iterations were different depending on the starting points. The number of iterations vary from 6-8.

- We compare the results for the Benders-SOS1 with SOS1 approaches, both give the same solution, see Table 5-12.
- Lastly, we validate a solution for this problem by fixing and varying the upper-level variables $SALES_{dm}^{P_{canal}}$ and solving the problem. Then a solution from each fixed $SALES_{dm}^{P_{canal}}$ is compared. Each fixed $SALES_{dm}^{P_{canal}}$ results in different values for $\tau_{dm}^{P\_toll}$ and the corresponding objective function values are displayed in Figure 5-9. The comparison in Figure 5-9 shows that the transit fees $\tau_{dm}^{P\_toll}$ decrease as the variables $SALES_{dm}^{P_{canal}}$ increase. In addition, the comparison in Figure 5-9 shows that an objective function value is -335,703.1.

Table 5-11 Comparison of the solution of different starting points $SALES_{dm}^{P_{canal}}$ for one time period (2005).

Starting Point: $\text{SALES}_{\text{low,2005}}^{\text{P}_{\text{canal}}}, \text{SALES}_{\text{high,2005}}^{\text{P}_{\text{canal}}} = 0$				
Iterations (it)	**Average sales (mcm/d)**[51]	**Average transit fee ($/MMBtu)**[52]	$z_{\text{down}}^{(it)}$	$z_{\text{up}}^{(it)}$
1	0	0.66	-100,000,000.0	0.0
2	200	0.64	-1,679,270.0	3,191,960,800.0
3	0	0.64	-340,416.1	402,846,580.0
4	40.32	0.64	-338,528.6	-335,702.3
5	80.64	0.64	-336,390.1	402,850,610.0
6	40.32	0.64	-335,703.1	-335,702.8

Starting Point: $\text{SALES}_{\text{low,2005}}^{\text{P}_{\text{canal}}}, \text{SALES}_{\text{high,2005}}^{\text{P}_{\text{canal}}} = 1$				
Iterations (it)	**Average sales (mcm/d)**	**Average transit fee ($/MMBtu)**	$z_{\text{down}}^{(it)}$	$z_{\text{up}}^{(it)}$
1	1.0	0.72	-100,000,000.0	-9,323.1
2	200.0	0.64	-1,864,629.0	3,191,960,800.0
3	80.6	0.64	-376,908.0	402,810,090.0
4	40.3	0.64	-375,878.2	-335,690.6
5	40.3	0.64	-335,703.1	-335,703.1

Starting Point: $\text{SALES}_{\text{low,2005}}^{\text{P}_{\text{canal}}}, \text{SALES}_{\text{high,2005}}^{\text{P}_{\text{canal}}}$ **= 5**				
Iterations (it)	**Average sales (mcm/d)**	**Average transit fee ($/MMBtu)**	$z_{\text{down}}^{(it)}$	$z_{\text{up}}^{(it)}$

[51] Average sales are the total sales of canal capacity in the year 2005 for high and low demand seasons devided by 2.
[52] Average transit fees are the sum of high and low demand season transit fees in the year 2005 devided by 2.

1	5.0	0.64	-100,000,000.0	-46,615.7
2	200.0	0.64	-1,864,629.0	3,191,960,800.0
3	80.6	0.64	-376,908.0	402,810,090.0
4	40.3	0.64	-375,878.2	-335,690.6
5	40.3	0.64	-335,703.1	-335,703.1

Starting Point $SALES_{low,2005}^{P_{canal}}, SALES_{high,2005}^{P_{canal}} = 10$				
Iterations (it)	**Average sales (mcm/d)**	**Average transit fee ($/MMBtu)**	$z_{down}^{(it)}$	$z_{up}^{(it)}$
1	10.0	0.72	-100,000,000.0	-93,231.4
2	200.0	0.64	-1,864,629.0	3,191,960,800.0
3	80.6	0.64	-376,908.0	402,810,090.0
4	40.3	0.64	-375,878.2	-335,690.6
5	40.3	0.64	-335,703.1	-335,703.1

Starting Point: $SALES_{low,2005}^{P_{canal}}, SALES_{high,2005}^{P_{canal}} = 20$				
Iterations (it)	**Average sales (mcm/d)**	**Average transit fee ($/MMBtu)**	$z_{down}^{(it)}$	$z_{up}^{(it)}$
1	20.0	0.72	-100,000,000.0	-186,462.9
2	200.0	0.64	-1,864,629.0	3,191,960,800.0
3	80.6	0.64	-376,908.0	402,810,090.0
4	40.3	0.64	-375,878.2	-335,690.6
5	40.3	0.64	-335,703.1	-335,703.1

Starting Point $SALES_{low,2005}^{P_{canal}}, SALES_{high,2005}^{P_{canal}} = 50$				
Iterations (it)	**Average sales (mcm/d)**	**Average transit fee ($/MMBtu)**	$z_{down}^{(it)}$	$z_{up}^{(it)}$

1	50.0	0.64	-100,000,000.0	193,209,690.0
2	20.7	0.68	-100,000,000.0	96,508,811.0
3	40.3	0.68	-100,000,000.0	-302,176.5
4	40.3	0.64	-338,286.9	-318,138.0
5	40.3	0.64	-338,285.9	-335,702.3
6	45.3	0.64	-335,788.1	49,513,830.0
7	40.3	0.64	-335,703.1	-335,056.9
8	40.3	0.64	-335,703.1	-335,703.1

Starting Point: $SALES_{low,2005}^{P_{canal}}, SALES_{high,2005}^{P_{canal}} = 150$				
Iterations (it)	**Average sales (mcm/d)**	**Average transit fee ($/MMBtu)**	$z_{down}^{(it)}$	$z_{up}^{(it)}$
1	150.0	0.64	-100,000,000.0	2,192,377,100.0
2	0.0	0.64	-100,000,000.0	303,187,000.0
3	0.0	0.68	-100,000,000.0	-133,803.1
4	80.6	0.68	-360,532.6	402,826,470.0
5	40.3	0.64	-338,296.1	-327,827.8
6	40.3	0.64	-338,294.6	-335,701.5
7	40.3	0.64	-335,703.1	-335,703.1

Starting Point: $SALES_{low,2005}^{P_{canal}}, SALES_{high,2005}^{P_{canal}} = 200$				
Iterations (it)	**Average sales (mcm/d)**	**Average transit fee ($/MMBtu)**	$z_{down}^{(it)}$	$z_{up}^{(it)}$
1	200.0	0.64	-100,000,000.0	3,191,960,800.0
2	70.7	0.64	-100,000,000.0	303,187,000.0
3	30.3	0.64	-100,000,000.0	-134,538.5
4	0.0	0.64	-358,824.6	402,828,180.0
5	40.3	0.64	-338,310.3	-327,784.5

6	40.3	0.64	-338,308.8	-335,701.5
7	40.3	0.64	-335,703.1	-335,703.1

Table 5-12 Comparison of two methods for the WGM MPECs for one time period (2005)

Methods	**Number of Discrete variables**	**Upper –Level Objective function value**	**Average Canal transit fees**	**Average Sales mcm/d**
SOS1 (Siddiqui and Gabriel, 2012)	3,640	-335,703.141009	$22.812/Kcm ($0.646/MMBtu)	40.319
Benders-SOS1 Decomposition	3,640	-335,703.14150	$22.812/Kcm ($0.646MMBtu)	40.319

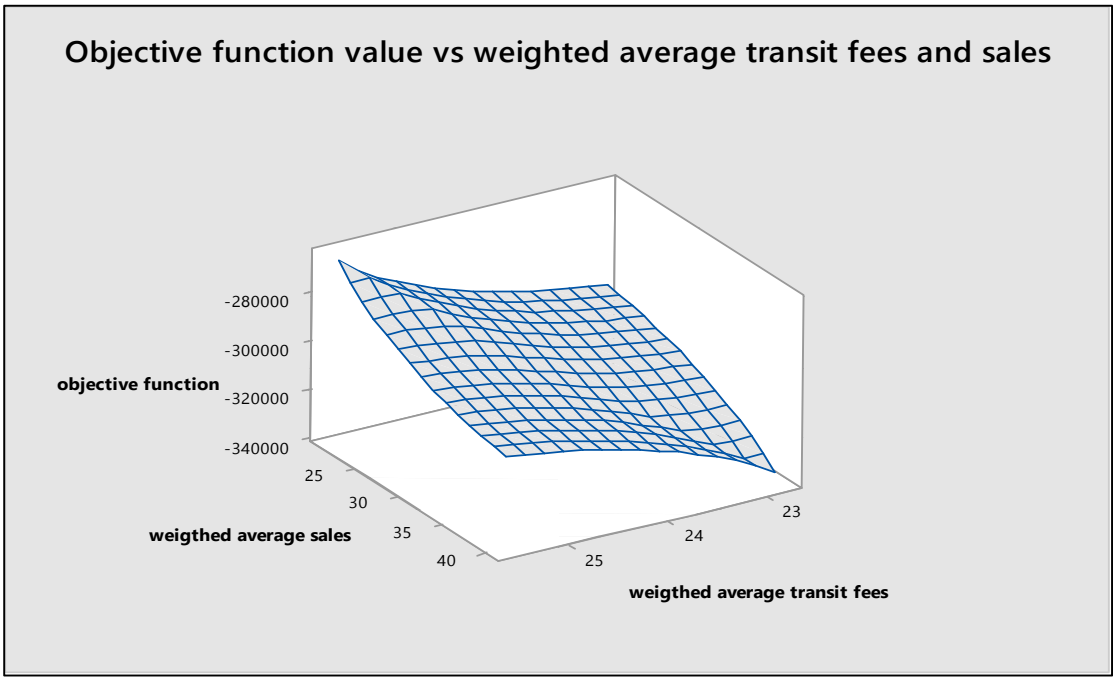

Figure 5-9 Grid search for optimal solutions, weighted average sales (mcm/d) and transit fees ($/Kcm) solved by the Benders-SOS1 method

5.8 Computational Results for the World Gas Model MPEC Version

5.8.1 Base Case Results

The purpose of this section is to demonstrate that the Benders-SOS1 method can be applied to large-scale MPECs. This WGM MPEC version includes 42 nodes covering 98 percent of the total world consumption in 2010 (WEO, 2013). This version of the World Gas Model operates with six time periods: 2005, 2010, 2015, 2020, 2025, and two seasons (high and low demand) in each time period. In this section, we run the model up to 2025. Consequently, the model has over 80,025 variables; 21,946 of these are discrete variables (SOS1 variables to replace complementarity conditions in the lower level) and the rest are continuous.

A complementarity version of this problem, where the problem has the Panama Canal operator as a player at the same level with other market players in the market, was solved thus showing that a solution exists, which means that a feasible solution exists for this MPEC as well. Before we applied Benders-SOS1. The MPEC version of the problem was tried with the disjunctive-constraints method using the solver SBB in GAMS, but it did not provide a feasible solution. In addition, we solved the MPEC version of the problem using the SOS1 method proposed in (Siddiqui and Gabriel, 2012), and obtained an optimal solution. Later, we applied the Benders-SOS1 decomposition approach to this problem. In that case, we consider the $SALES_{dm}^{P_{canal}}$ variables as complicating. A tolerance of 10^{-4} and a value of α^{down} of -1.2×10^{-7} were selected. Additionally, the value of *M* (transit demand slope) =-7 was used.

At first, the Benders-SOS1 algorithm did not proceed due to infeasibility of the subproblem. Therefore, we followed the approach in (Conejo et al., 2006) (see problem

(5.28) for more details) to make the subproblem always feasible using penalties for violating constraints, then the problem was solved.

The Benders-SOS1 algorithm is slow in the first subproblem solution stage however it goes quicker in later iterations. The first iteration takes 20.32 minutes to solve while other iterations take less than an average of 20 seconds each. This implies that GAMS uses a "warm start" from previous iterations as a starting point for the second iterations and later iterations. Table 5-13 shows the comparison of three methods for this particular MPEC. As displayed in Figure5-10, Benders-SOS1 used 31 iterations before the difference between the subproblem and master problem was less than the tolerance. A validation of the model has been performed as follows;

- The algorithmic results for the Benders-SOS1 method were verified to confirm that all the constraints, such as, production, pipeline and LNG capacities as well as energy balances at each node were satisfied by the solutions.
- We compared the results for Benders-SOS1 with the SOS1 approach and note that both methods gave similar solution with differences in the decimal places. Initially the SOS1 approach was terminated by the SBB solver in GAMS. However, this problem was overcome by adjusting the node limits (the maximum number of nodes to process in the branch and bound tree for a MIP problem) in GAMS, see Table 5-13.

Table 5-13 Comparison of three methods for the WGM MPECs (up to the year 2025)[53]

[53] We report the results only for 2015 becuase the results for last two time periods (2020 and 2025) are ignored to aviod the end-of-horizon effect.

	Disjunctive Constraints	SOS1 (Siddiqui and Gabriel, 2012)	Benders-SOS1 Decomposition
Computation time (CPU)	No solution returned	34.46 minutes	27.28 minutes
Number of continuous variables	53,369	58,079	58,079
Number of discrete variables	18,836	21,946	21,946
Upper –level objective function value	NA	-899,670.92491	-899,670.6532
Average Canal transit fees in 2015	NA	$0.63/MMBtu	$0.63/MMBtu
Sales in 2015 Bcm/y	NA	16.1432	16.1418

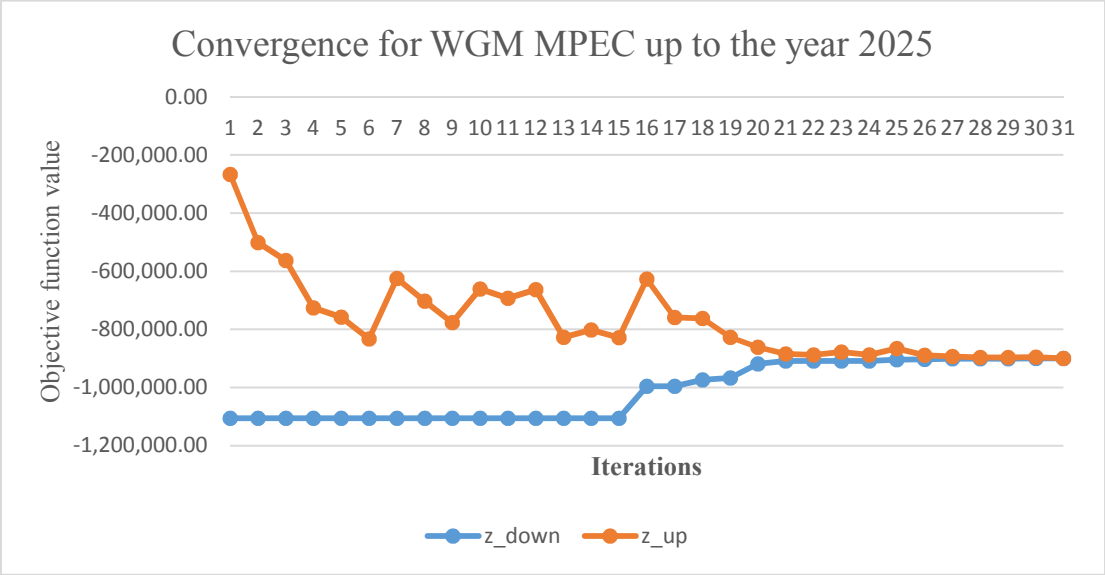

Figure 5-10 Convergence for WGM MPEC (Year 2005-2025)

5.8.2 Analysis on impact of the leader on U.S. LNG exports

This section describes the scenarios of U.S. LNG exports analyzed as well as presents the results and compares the MPEC version of the problem with the MCP one. To clarify, the MCP version has one level where the Panama Canal operator is assumed as a profit maximizer who collects the congestion rent from the traders.

For this comparison, we ran the model up to the year 2025. The Base Case is formulated as an MPEC and assumes that the U.S. starts exporting LNG in 2015 from three locations with different capacities as follows: the Gulf of Mexico with a capacity of 57.88 Bcm/y, 8.25 Bcm/y from the West Coast, and from the East Coast at 10.33 Bcm/y. In order to analyze the impacts of the leader on U.S. LNG exports, we define an additional U.S. LNG exports scenario (Exports2) which allows more export capacity for the U.S. The scenarios descriptions are presented in Table 5-14.

Table 5-14 Cases and description of cases

Scenario	**Description**
MCP	Mixed complementarity version of WGM and U.S. Gulf Mexico export capacity equals 57.88 Bcm/y
Base	The Base Case (Slope of transit demand curve equals -7) [54] and U.S. Gulf Mexico export capacity equals 57.88 Bcm/y
Exports2	The assumptions are the same as the Base Case , but the U.S. LNG export capacity from Gulf of Mexico increases up to 115 Bcm/y

As can be seen from Table 5-15 below, the first thing to realize is that the canal operator's profit for the two MPECs scenarios is substantially higher than for the MCP case. In comparing the Exports2 Case to the Base Case , the canal operator's profit increases 6.95% given increased U.S. LNG exports. An important conclusion is that level of U.S. LNG exports substantially affects the profits of the leader. Under the Exports2 scenario, the flows through the Panama Canal increase 126.15% compared to the Base Case, however the weighted average transit fee decreases about $0.20. As the LNG flows increase, the new equilibrium prices for transit fees are formed as described

[54] We used -7 for the Base Case because the results (canal transit fee) are close to the real world ones of 0.30$/MMBtu for the Suez Canal since actual Panama Canala transit fees were not available at the time of this dissertation..

in the transit demand approach. Table 5-15 also shows that the transit fees calculated in the MCP version are 0. It is important to note that the transit fee for the MCP comes from the market-clearing conditions between traders and the canal operator. In the MCP form of the problem, total flows in 2015 (17.2 Bcm) by all traders through the Panama Canal do not reach the maximum capacity level of the Canal[55], so congestion fees are zero in this case.

In terms of lower-level problem results, when two MPECs scenarios (Base and Exports2) are compared with the MCP version, the production and consumption both decrease due to higher prices for all regions, see Table 5-15. This can represent the influence of the leader on the global gas market. However, when compared Exports with the Base Case, only North American production increases. The rest of the world remains the same. This is because we allow North America to export more LNG so that it ramps up the production given the increased capacity. Increased U.S. LNG exports reduce prices in Asian and Chinese markets. Under the Exports2 scenario as compared to the Base Case, the prices in Asian and Chinese markets decrease -4.12% and -1.55% respectively. This makes sense since as more supplies come to the market, they will reduce prices and increase consumption in the particular market.

Table 5-15 Results for upper level and lower problems in 2015

	MCP	**Base**	**Exports2**
Canal operator profit (2005-2025) in $	341,951.08 [56]	899,670.92	962,173.84

[55] The maximum canal capacity is 73 Bcm/y.

[56] It is important to note that the profit displayed in this table is the overall profit from 2005-2025. Although congestion fees for 2015 equal zero, which makes revenue for this year equal to zero, the congestion fess for the last two time periods are positive with full capacity of the canal utilization (73 Bcm/y). That's why the Canal operator has a positive profit.

Flows through the Panama for 2015 in Bcm	17.2	16.14	36.5
Average Transit fee for 2015 in $/MMBtu	$0	$0.63	$0.40
Selected Lower-Level results			
	Wholesale Prices in $/MMBtu		
AFRICA	$3.57	$4.52	$4.49
ASPACIF	$18.04	$20.24	$19.40
CHINA	$10.04	$10.80	$10.63
EUROPE	$14.04	$14.21	$15.45
FRSVTUN	$4.92	$6.15	$6.52
MIDEAST	$3.73	$4.31	$4.08
NRTH_AM	$6.92	$8.35	$8.15
STH_AM	$11.27	$14.94	$13.34
	Consumption in Bcm		
AFRICA	120.5	81.6	86.7
ASPACIF	437.6	355.4	378.6
CHINA	298.2	278.7	284.6
EUROPE	515.2	519	495.7
FRSVTUN	757.6	594	509.9
MIDEAST	472	447.9	376.1
NRTH_AM	951.4	798.9	727.5
STH_AM	195.6	109.2	141.5
	Production in Bcm		
AFRICA	294.9	275.9	275.9
ASPACIF	272.6	262.9	262.9
CHINA	266.1	254.2	254.2
EUROPE	254.3	238.3	238.3
FRSVTUN	1010.7	1012.3	1012.3
MIDEAST	654.3	614.9	614.9
NRTH_AM	992.3	973.3	1165.9
STH_AM	237.8	217.8	217.8

5.8 Conclusions

This chapter presents a promising methodology to decompose large-scale MPECs using Benders decomposition and SOS1 techniques. The method was first applied to numerical examples for MPECs. This method is able to solve large-scale MPECs where

the lower level is a complementarity problem. The method solves a large-scale natural gas model in which the Panama Canal is the dominant player who can influence the market and decide the transit fees. We found that increasing U.S. LNG exports will improve the leader's profit and reduce prices in China and other non-Chinese Asian markets such as Japan and South Korea.

APPENDIX 5-A. A Machine-Independent Measure: Function Calls

In Chapter 5 of this dissertation, we measure computational effort of different algorithms using a comparison of CPU time. The CPU time represents how quickly the algorithm can find a solution. However, CPU times depend on various factors i.e., computer platforms.

A machine-independent measure is required in order to measure and compare efficiency of algorithms. Using the number of function calls is a measure of computational effort that is machine independent. In general, the number of function calls to a nonlinear objective and constraints is a measure of the computational effort required to reach the optimum. The definition of function calls by GAMS (GAMS, 2010) is the number of times that subroutines FUNOBJ and FUNCON have been called to evaluate the nonlinear objective function and nonlinear constraints.

GAMS (SBB solver) can display the number of function calls using the "option sysout=on;" command. The following section shows a comparison of function calls for selected test problems (Shale Gas Producer problem and WGM MPECs). It is important to note that the number of function calls for the Benders-SOS1 approach is per iteration since Benders algorithm needs multiple iterations before it finds an optimal solution.

From Table 5 A1, it is clear that the new Benders-SOS1 approach is superior to the SOS1 method. GAMS shows only two function calls for tests solved by Benders-SOS1 approach. However, function calls for the SOS1 approach increase significantly when the number of followers goes up.

Table 5A-1 Function calls for shale gas problem (Example 2)

Number of followers N	Solution	Function Calls	
		SOS1	Benders-SOS1
5	Q=6 q1,..,q5=1	15	2
10	Q=6 q1,..,q10=0.545	25	2
50	Q=6 q1,..,q50=0.118	108	2
100	Q=6 q1,..,q100=0.059	210	2
300	Q=6 q1,…,q300=0.020	618	2
500	Q=6 q1,…,q500=0.012	1026	2
750	Q=6 q1,…,q750= 0.008	1536	2
1500	Q=6 q1,…,q1500= 0.004	3066	2
2000	Q=6 q1,…,q1500= 0.003	4086	2
2500	Q=6 q1,…,q1500= 0.002	5106	2

Next, we compare the number of function calls for WGM MPECs version. The model was solved with two approaches and the number of function calls was compared.

	SOS1 (Siddiqui and Gabriel, 2012)	**Benders-SOS1 Decomposition**
Number of continuous variables	58,079	58,079
Number of discrete variables	21,946	21,946
Number of function calls	47	6

The SOS1 approach required 47 function calls while Benders-SOS1 Decomposition needed only 6 function calls. Clearly, Benders-SOS1 approach requires less computational effort before it finds a solution. One reason is because the complicating variables are fixed, the nonlinearity (bilinear term) in the objective function is removed. The overall problem becomes easier to solve. That is why it probably needs less number of function evaluations.

Chapter 6: Summary and Future Research

6.1 Summary

In this dissertation, two applied studies were conducted using The World Gas Model (WGM, 2012) in Chapters 2 and 3. In Chapter 2, the WGM 2012 (Gabriel et al., 2012) has been used to investigate the effects of U.S. LNG exports on international gas prices and consumption as well as the impact on changes in the distribution of supply and demand. A number of scenarios were employed to analyze the resulting prices, quantities, flows, and LNG trade patterns. The main results from Chapter 2 shows that U.S. LNG will influence global gas markets, especially Asian and European ones. Increased U.S. exports reduce prices significantly in importing markets. For example, prices in Spain decrease by $2.7/MMBtu in 2020 compared with the Base Case. when the U.S. exports 100 Bcm of LNG to the global gas market. Increased LNG exportation results in positive effects on Asia and Europe.

Chapter 3 uses WGM 2012 (Gabriel et al., 2012) to find the influence of Panama Canal tolls on the global gas market. We found that the Panama Canal transit fees affect the flow pattern especially for LNG exports from the U.S. and Trinidad and Tobago. In addition, the wholesale gas prices in Japan/South Korea and Europe are significantly affected by the level of the Panama Canal toll. The presence of LNG exports from the Atlantic basin (the U.S. and Trinidad & Tobago), leads to lower prices in Japan/S. Korea as the Panama Canal toll decreases. (The zero and regular toll cases though provide identical Japanese node prices). The differences in Japan are about $1/MMBtu in considering the two extreme scenarios: Inf_Toll and Zero_Toll. However, the prices

go in the opposite direction for Europe as a function of the counterfactual Panama Canal toll. As the Panama Canal toll increases, the gas prices in Europe decrease due to the shift of U.S. and Trinidad & Tobago LNG flows from Japan to Europe.

In Chapter 4, a new version of the World Gas Model (WGM-2014) was presented. A significant extension of the World Gas Model 2012 was developed. This new version called WGM 2014, distinguishes itself from the previous one by adding more detail for LNG markets including more market participants e.g., liquefiers, regasifiers, LNG shipping operators, and a canal operator as new players with separate optimization problems and market-clearing conditions. Moreover, the LNG shipping costs and congestion tariffs for the canal transit fees are endogenously determined inside the model as opposed to being exogenously determined before. Also, WGM 2014 has flexible LNG routes. In particular, there are three route options for each LNG shipping operator: 1. Sending LNG via the Panama Canal, 2. the Suez Canal, or using a regular route without a canal. Moreover, WGM 2014 takes into account the limitations of maritime transportation by limiting the size of the LNG tankers that can pass through the Panama and Suez canals. The results derived from the WGM-2014 could assist decision makers e.g., gas producers, gas traders, and gas transmission operator, to have better understand of the gas market, especially the LNG market. WGM-2014 is able to identify the possibility of natural gas flow through Panama and Suez Canals and their direction. In addition, the model also suggests the future requirements for LNG tankers.

Chapter 5 presents a methodology to solve mathematical programs with equilibrium constraints (MPECs). The method we develop uses an SOS1 approach to replace

complementarity in the lower-level problem's optimality conditions. Then, Benders algorithm decomposes the MPECs into a master and a subproblem and solves the overall problem iteratively. Thus, the name for this new approach is Benders-SOS1. In addition, the MPEC version of WGM, a Stackelberg leader-follower game version of WGM, was formulated with the Panama Canal Operator as the leader having a Stackelberg leader influence on the other market players and solved with the new Benders-SOS1 method. The canal operator anticipates the reactions of these other market participants in making its own decisions, especially the canal tariff. This problem and other small MPECs were solved in this chapter.

6.2 Future Research

6.2.1 Natural Gas Modeling

- Future work on natural gas modeling could include the improved presentation of long-term contracts (LTC). The complex structure of long-term contracts and the flexibility of new current contracts need to be taken into account. In the current WGM, the model assumes natural gas prices coming from market-clearing conditions. In fact, approximately 85 % of traditional LNG trades are based on long-term contracts tied to the price of crude oil. The long-term contracts in gas represent risk sharing between sellers and buyers. Therefore, the contract prices need consider better risk sharing. Future work could improve the structure of LTC prices. For example, long-term contracts could be determined endogenously by the model.
- In addition, it is interesting to see the original WGM incorporated with some with some integer/binary constraints. That would be more appropriate for LNG and

canal decisions because their decision on shipping are related to integer/binary variables. For example, how many LNG tankers will use the Panama Canal route?

- Future work on U.S. LNG exports could include optimal U.S. export volume under different given conditions, given very limited analysis on how much LNG exports from the U.S. and from Canada can be absorbed by the global market. Most studies focus on the price impacts rather than volumes. So examining how much could be exported from the U.S. would be a good future research direction. Also, how much U.S. LNG will be on the spot market?

6.2.2 Extension for Benders Decomposition

Besides the numerical evidence in Chapter 5 for the Benders-SOS1 decomposition method working, the convergence theory still needs to be considered in future research. Moreover, the future research on Benders-SOS1 could include:

- The methods presented in this dissertation were only applicable to MPECs where the decision variables for the upper-level problem is continuous. This approach should be tried on more complex MPEC, for example, discretely-constrained MPECs (Gabriel et. al., 2010) where the upper-level problem has binary variables.
- Chapter 5 presents deterministic MPECs version of WGM. However future research could include a stochastic Stackelberg model where future transit demand is still uncertain. This makes sense because LNG tankers need to compete with other ships in order to use the canal.
- Lastly, future research could involve parallel computing because independent subproblems of Benders-SOS1 decomposition are separable into a number of

independent optimization problems for which parallel computations could be applied.

Bibliography

Abada, I., Briat, V., Gabriel, S.A., Massol, O. (2012) "A Generalized Nash-Cournot Model for the Northwestern European Natural Gas Markets with a Fuel Substitution Demand Function:the GaMMES Model," *Networks and Spatial Economics*, 13(1), 1-42.

Alaskan Natural Gas Transportation Project, 2012, "Expanded Panama Canal Could Reroute LNG Industry", November 2012. http://www.arcticgas.gov/expanded-panama-canal-could-reroute-lng industry

Al-Khayal FA, Horst R, Pardalos PM (1992) Global optimization of concave functions subject to quadratic constraints: an application in nonlinear bilevel programming. Annals of Operations Research 34: 125–147

Anitescu, M. (2005). Global convergence of an elastic mode approach for a class of mathematical programs with complementarity constraints. SIAM J. Optimization, 16(1):120–145.

Aune, F.R., Rosendahl, K.E., Sagen, E.L. (2009). "Globalisation of natural gas markets —effects on prices and trade patterns" , Special Issue of the *Energy Journal*, 30, 39–54.

Avetisyan, H. (2013).Sustainable Infrastructure Modeling and policy Analysis: Construction, Energy,and On Road Transportation Industries. PhD. Dissertation University of Maryland.

AIE, 2013, Natural Gas Information 2013.

AIE, 2013, MT Gas Report, 2013.

Bard, J., Falk, J., An explicit solution to the multi-level programming problem, Computer and Operations Research 9 (1982) 77–100.

Bard, J. (1988). Convex Two-Level Optimization. Mathematical Programming , 40 (1), 15-27.

Bard, J., & Moore, J. (1990). A Branch and Bound Algorithm for the Bilevel Programming Problem. SIAM Journal on Scientific and Statistical Computation , 11 (2), 281-292.

Benders, J. (1962). Partitioning Procedures for Solving Mixed-Variables Programming Problems. *Numerische Mathematik , 4*, 238-252.

Benson, H., Sen, A., Shanno, D. F., and Vanderbei, R. V. D. (2006). Interior-point algorithms, penalty methods and equilibrium problems. Computational Optimization and Applications, 34(2):155–182.

Beptistella, L. F. B., Geromel, J.C. (1980). Decomposition approach to problem of unit commitment schedule for hydrothermal systems, *Control Theory and Applications*, IEE Proceedings(Volume:127 , Issue: 6).

Berdikeeva,S.(2012). Taking a Second Look at the Southern Gas Corridor. OILPRICE.com Assessed May 2012. Available from http://oilprice.com/Energy/Natural-Gas/Taking-a Second-Look- the Southern-Gas-Corridor.html

Birge, J., Louveaux, F., 1997. Introduction to stochastic programming. Springer, New York.

BP Statistical Review of World Energy (2013). Available from: www.bp.com

Cabero, J., Baillo, A., Cerisola, S., & Ventosa, M. (2005a). Electricity market equilibrium model with risk constraints via Benders decomposition. In *INFORMS annual conference*, San Francisco, November.

Cabero, J., Baillo, A., Ventosa, M., & Cerisola, S. (2005b). Application of Benders decomposition to an equilibrium problem. In *15th PSCC*, Liege, August.

Cabero, J., Ventosa, M.J., Cerisola, S., Baillo, Á., 2010. Modeling Risk Management in Oligopolistic Electricity Markets: A Benders Decomposition Approach. IEEE Trans. Power Syst. 25, 263-271.

Calvin, K., Edmonds, J., Bond-Lamberty, B., Clarke, L., Kim, S.H., Kyle, P. ,Smith, S.J., Thomson, A.Wise,M. (2009). 2.6: Limiting climate change to 450 ppm CO_2 equivalent in the21st century. *Energy Economics* , 31, S107-S120.

Calvin, K., and Edmonds, J. (2014) The EU20-20-20 energy policy as a model for global climate mitigation. Submitted to J Climate Policy, Forthcoming.

Cheniere Energy (2012), Investor Analyst Day Conference.Available from: http://phx.corporate-ir.net/phoenix.zhtml?c=101667&p=irol-presentations

Chen Y, Hobbs BF, Leyffer S, and Munson TS (2004). Leader-follower equilibria for electricpower and NOx allowances markets, Preprint ANL/MCS-P1 191-0804, Mathematics and Computer Science Division, Argonne National Laboratory, Argonne, IL, USA 60439

Cohen, D (2009).A shale gas boom? Energy Bulletin.. Available online at: http://www.energybulletin.netnode/49342 (Accessed 22 April 2011).

Cote, G., Laughton, M A. (1979). Decomposition techniques in power system planning: the Benders partitioning method, *International Journal of Electrical Power & Energy Systems* vol.1 issue 1,1979).

Cottle, R., Pang, J. S., Stone, R. (2009). The linear complementarity problem. SIAM, Philadelphia, PA

Considine, T. Watson,R., Blumsack, S.(2011).The Pennsylvania Marcellus natural gas industry: Status, economic impacts and future potential (2011). Available from: http://marcelluscoalition.org/wp-content/uploads/2011/07/Final-2011 PA-Marcellus-Economic-Impacts.pdfAvailable

Conejo, A.J., Castillo, E., Minguez, R., Garcia-Bertrand, R. (2006). " Decomposition Techniques in Mathematical Programming, Spring, New York.

Dirkse, S. P. and Ferris , M.C. (1998). Modeling and Solution Environments for MPEC: GAMS& MATLAB.

Bai,J., Aizhu,C. (2012) China CNPC to expand LNG sales, spur cleaner fuel use. Reuters. Available from: http://www.reuters.com/article/2012/06/12/cnpc-lng sales idUSL3E8HC22320120612

DECC,2013,https://www.gov.uk/government/uploads/system/uploads/attachment_daa/file/24923/production_projections.pdf

De Miguel, V., Friedlander,M.P., Nogales, F.J., Scholtes, S., 2005. A two-sided relaxation scheme for mathematical programs with equilibrium constraints. SIAM J. Optim.16 (2), 587–609.

Deloitte Center for Energy Solutions, 2011,Made in America: The economic impact of LNG exports from the United States. (Accessed October 2011). Available from http://www.deloitte.com/assets/DcomUnitedStates/Local%20Assets/Documents/Energyus_er/us_er_MadeinAmerica_LNGPaper_122011.pdf

Dirkse, S.P., Ferris, M.C., Meerhaus, A., 2002. Mathematical programs with equilibrium constraints: automatic reformulation and solution via constraint optimization. Technical Report NA-02/11. Oxford University Computing laboratory. July.

DOE, 2013. Summary of Export Application August 2013 Available online at: http://energy.gov/sites/prod/files/2013/08/f2/Summary_of_Export_Applications.pdf

Dlouhy, A., J. (2013). "Obama Administration Authorizes More Natural Gas Exports" FuelFlix September.

EDF R&D, Private Communications, 2013.

Egging, R., Gabriel, S.A., Holz, F., and Zhuang, J., 2008a, "A Complementarity Model for the European Natural Gas Market," *Energy Policy*, January, Volume 36, Issue 7, Pages 2385 2414.

Egging, R., Holz, F., and Gabriel, S.A., 2010, "The World Gas Model," Energy, 2010, doi:10.1016/j.energy.2010.03.053

Egging E. (2013). Benders Decomposition for multi-stage stochastic mixed complementarity problems – Applied to a global natural gas market model. European Journal of Operational Research. Volume 226, Issue 2, 16 April 2013, Pages 341–353

EIA, 1999,Natural gas 1998: Issues and trends . Available from: http://www.eia.gov/pub/oil_gas/natural_gas/analysis_publications/natural_ga_1998_issues_trends/pdf/chapter2.pdf

EIA, 2009, Annual Energy Outlook 2009 with projection to 2030. Available from:.www.eia.doe.gov/oiaf/aeo

EIA, 2010, International Energy Outlook. Available from: http://large.stanford.edu/courses/2010/ph240/riley2/docs/EIA-0484-2010.pdf

EIA, 2011, Review of emerging resources: U.S. shale gas and shale oil plays. Available from:ftp://ftp.eia.doe.gov/natgas/usshaleplays.pdf

EIA, 2011, Annual energy outlook 2011 with projection to 2035. Available from: http://www.electricdrive.org/index.php?ht=a/GetDocumentAction/id/27843

EIA, 2011, International energy outlook (2011). Available from: http://www.eia.gov/forecasts/ieo/pdf/0484(2011).pdf

EIA, 2012, U.S. Natural gas imports. Available from: http://www.eia.gov/dnav/ng/hist/n9100us2a.htm

EIA, 2012, U.S. Natural gas imports by State . Available from:http://www.eia.gov/dnav/ng/NG_MOVE_STATE_A_EPG0_IM0_MMF_A.htm, [Accessed 19 June 2012].

EIA, 2012, U.S. Natural gas exports. Available from http://www.eia.gov/dnav/ng/hist/n9130us2a.htm

EIA, 2012, Voluntary Reporting of Greenhouse Gases Program. Available from: http://www.eia.gov/oiaf/1605/coefficients.htmlt:

EIA, 2012, Country analysis brief. Available from:
http://www.eia.gov/countries/cab.cfm?fips=JA

EIA, 2012,Effect of increased natural gas exports on domestic markets. Available from: http://www.eia.gov/analysis/requests/fe/pdf/fe_lng.pdf

EIA, 2013a, Annual Energy Outlook 2013.

EIA,2013b,Internattional Energy Statistics 2013.
http://www.eia.gov/cfapps/ipdbproject/IEDIndex3.cfm?tid=3&pid=26&aid=2

EIA,2014, U.S. Shale Gas Production
http://www.eia.gov/dnav/ng/ng_prod_shalegas_s1_a.htm

ERNST&YOUNG, 2012. "Natural gas in Africa the frontiers of the Golden Age", 2012. Available online at
http://www.ey.com/Publication/vwLUAssets/Natural_gas_in_Africa_frontier_of_the_Golden_Age/$FILE/Natural_Gas%20in_Africa.pdf

European Commission, 2008, European energy and transport: Trends to 2030. Update 2007. Office for Official Publications of the European Communities,

Luxembourg Federal Energy Commission, 2012, World LNG estimated prices 2012 landed prices. Available from http://www.ferc.gov/market-oversight/othr mkts/lng/2012/04-2012-othr-lng-archive.pdf

Fletcher, R., Leyffer, S., Ralph, D., Scholtes, S. (2002). Local convergence of SQP methods for Mathematical Programs with Equilibrium Constraints. SIAM J Optimization, 17: 259 286, 2006.

Fletcher, R., Leyffer, S., 2002. Numerical experience with solving MPECs as NLPs, numerical analysis report NA/210, Department of Mathematics, University of Dundee. Dundee, UK.

Fletcher, R. and Leyffer, S. (2004). Solving mathematical program with complementarity constraints as nonlinear programs. Optimization Methods and Software, 19(1):15–40.

Fletcher,R., Leyffer, S. (2004) Solving mathematical programs with complementary constraints as nonlinear programs. Optim Meth Software 19(1):15–40

Floudas, C.A., and A.R, Ciric, "Strategies for overcoming uncertainties in heat exchanger network synthesis11, Computers and Chemical Engineering, 13(10), 1133-1152(1989).

Floudas, C.A., A. Aggarwal, and A.R. Ciric, "Global Optimum Search for Nonconvex NLP and MINLP problems", Computers and Chemical Engineering, 13(10), 1117-1132 (1989).

Folks, J. (2012). Export gas to create jobs. American Thinker. Available from: http://www.americanthinker.com/2012/06/export_natural_gas_to_create_jo

Fortuny-Amat, J.and McCarl, B. (1981). A representation and economic interpretation of a two level programming problem. *The Journal of Operational Research Societies* 39(2).

Friedlander, A. D. M., Nogales, F., and Scholtes, S. (2005). A two-sided relaxation scheme for mathematical programs with equilibrium constraints. SIAM

Journal on Optimization,16(1):587–609

Gabriel, S.A., Manik, J., Vikas S., 2003, “Computational Experience with a Large Scale, Multi Period, Spatial Equilibrium Model of the North American Natural Gas System”, Networks and Spatial Economics June 2003, Volume 3, Issue 2, pp 97-122.

Gabriel, S., & Leuthold, F. (2010). Solving Discretely-Constrained MPEC Problems with Applications in Electric Power Markets. *Energy Economics , 32*, 3-14.

Gabriel, S., Shim, Y., Conejo, A., de la Torre, S., & Garcia-Bertrand, R. (2010). A Benders Decomposition Method for Discretely-Constrained Mathematical Programs with Equilibrium Constraints. *Journal of the Operational Research Society ,61*, 1-16.

Gabriel, S.A., Rosendahl, K.E. Egging, R., Avetisyan, H.G. Siddiqui, S. (2012). Cartelization in gas market: Study the potential for a “Gas OPEC”. Energy Economics 34,134-152.

Gabriel, S.A., Kiet,S., Zhuang,J. (2005)."A Mixed Complementarity-Based Equilibrium Model of Natural Gas Markets ", Operations Research (2005), 53(5), 799-818.

Gabriel, S.A. ,Zhuang, J., Kiet,S.(2005) "A Large-Scale Complementarity Model of the North American natural gas market *Energy Economics*, vol. 27, issue 4, pages 639-665.

Gabriel,S.A.,Conejo,A.J., Hobbs, B.F. ,Fuller., C. Ruiz*, C*.(2013)*Complementarity Modeling In Energy Markets*, Springer, 2013.

Gabriel & J. Fuller, 2010. "A Benders Decomposition Method for Solving Stochastic Complementarity Problems with an Application in Energy," Computational Economics, Society for Computational Economics, vol. 35(4), pages 301 329, April.

GIIGNL 2011. LNG Industry in 2010. 2011.

GIIGNL, 2013, the LNG Industry 2012.

Gabriel, S.A., Fuller, J., 2010. A Benders Decomposition Method for Solving Stochastic Complementarity Problems with an Application in Energy. Computational Economics 35. 301-329

Geoffrion, A. M. (1972). Generalized Benders Decomposition. *Journal of Optimization Theory and Application Vol.10 No.4*.

Geoffrion, A.M., and G.W. Graves, "Multicommodity Distribution System Design by Benders Decomposition", Management Srience, 20(9), 822-844 (1974).

Geoffrion, A. M. and Graves, G.W. (1976). Multicommodity Distribution System Design by Bender Decomposition.

Gibbons, R. (1996). Game Theory for Applied Economists. Princeton, NJ: Princeton University Press.

Golombeck,R. Gjelsvik, E., K.E. Rosendahl, K.E. (1999). Effects of liberalizing the natural gas markets in Western Europe. Energy Journal,16(1), 85,111.

Golombeck,R. Gjelsvik, E., K.E. Rosendahl, K.E.(1998) Increased competition on the

supply side of the Western European natural gas market. Energy Journal, 19(3), 1-18.

GTE, 2005. Capacities of cross-border points on the primary market. Gas Transmission Europe, Brussels (December 2005)

GTE, 2008. Capacities of cross-border points on the primary market. Gas Transmission Europe, Brussels (June, 2008)

Gumus Z, Floudas C (2001) Global optimization of nonlinear bilevel programming problems. J Global Optim 20:1–31

Hansen P., Jaumard,B., Savard G., " New branch-and-bound rules for linear bilevel programing," *SIAM* 13, 1194-1217

Hayes, H. M. (2007). Flexible LNG supply and gas market integration: A simulation approach for Available from: http://iisdb.stanford.edu/pubs/21224/Hayes_Ch_4_LNG_Arb1.pdf.

Hecking H. and Panke T., 2012, "COLUMBUS - A global gas market model, 2012.IEA, 2007. Natural gas information",OECD/International Energy Agency, Paris 2007.

Henderson, J. (2011). The pricing debate over Russian gas exports to China. Oxford Institute for Energy Study. (Accessed September 2011). Available from: http://www.oxfordenergy.org/wpcms/wp-content/uploads/2011/10/NG561.pdf

Henderson, J. (2012). The potential impact of North America LNG exports. Oxford Institute for Energy Study. (Accessed November 2012). Available from: http://www.oxfordenergy.org/wpcms/wp content/uploads/2012/10/NG 68.pdf

Holz, F. Von Hirschhausen, C. Kemfert, C.(2008). "A strategic model of European gas supply (GASMOD), " *Energy Economics* 30, 766–788, 2008.

Hu.,J. and Pang J. S. (2008). On Linear Programs with Linear complementarity constraints, PhD Thesis.

Huntington, H.(2010)"The Energy Journal 2009 Special Issue: World Natural Gas Markets and Trade: A multimodeling Perspective, ", the Energy Journal, 2010.

Huntington, H. (2013)."EMF 26: Changing the Game? Emissions and Market Implications of New Natural Gas Supplies, report, ", Energy Modeling Foru 2013,http://emf.stanford.edu/publications/emf_26_changing_the_game_emis ions_and market implications_of_new_natural_gas_supplies/, 2013.

IAE, 2011. World Energy Outlook 2011, Nov 2011.

IEA, 2007, Natural Gas Information. Paris: OECD/International Energy Agency.

IEA,2011, Are we entering a golden age of gas? Available from: http://www.worldenergyoutlook.org/media/weowebsite/2011/WEO2011_Go denAgeofasReport.pdf

IGU, 2013. World LNG Report - 2013 Edition. International Gas Union, 2013.

IGU, 2013. Wholesale Gas Price Survey - 2013 Edition, 2013.INGAA Foundation, 2000, Activities to reduce greenhouse gas emissions from natural gas operations.

Jae Hyung Roh, Shahidehpour M., and Fu Yong. Market-based coorination of transmission and generation capacity planning. IEEE Transactions on Power Systems, 22(4):1406 1419,Nov. 2007.

Jensen S. T. (2004). The Development of a Global LNG Market Is it Likely? If so, When? Oxford institute for Energy Studies

Kazempour S. J. and Conejo A. J., 2012 Strategic generation investment under uncertainty viaBenders decomposition. IEEE Transactions on Power Systems, 27(1):424-432, Feb. 2012

Kelly, R. (2013). U.S. Shale Boom Threatens Australian Gas Projects The Wall Street JournalJuly 2013.

Kojima M. and Shindo, S. (1986).Extensions of Newton and quasi Newton Methods to system of PC equations. Journal of Operations Research Society Japan,29:352-374.

Macalister ,E.(2013). Dominion signs deals to export U.S. natural gas from Cove Point. http://www.reuters.com/article/2013/04/01/us-lng-dominion-export idUSBRE9300CH20130401

MAN Diesel & Turbo, 2011. Propulsion Trends in LNG Carriers, 2011. Available online at http://www.mandieselturbo.com/files/news/filesof8074/5510-003502ppr_low.pdf

Medlock, K.B.,(2012)U.S. LNG exports: Truth and consequence. Institute For public Policy Research ,Rice University. Available from:http//bakerinstitute.org/publications/US%20LNG%20Exports%20%20ruth%20ad%20Consequence%20Final_Aug12-1.pdf

Moore JT and Bard JF (1990). A branch and bound algorithm for the bilevel programming problem. SIAM J Sei Stat Comput 11: 281-292.

Moore JT and Bard JF (1990). The mixed integer linear bilevel programming problem. Oper Res38: 911-921.

Moryadee S., Gabriel S.A., Rehulka F., 2014, "The influence of the Panama Canal on global gas trade," Journal of Natural Gas Science and Engineering 20 (2014) 161e174

Noonan, F. and Giglio, R. J. (1997).Planning Electricity Generation: A Nonlinear Mixed Integer Model Employing Benders decomposition, *Management Science* Vol.23 No.9,946-956.

Navigant Consulting Inc., 2012,Jordan Cove LNG export project market analysis study (2012). Available from: http://www.jordancoveenergy.com/pdf /Navigant_Jordan_Cove_LNG_Export_Study_012012.pdf

Nord Stream, 2012, the Pipeline. (Accessed May 2012) Available from: http://www.nord-stream.com/pipeline

Leather, D. T.B. , Bahadori, A. , Nwaoha, C. and A. Wood, D. (2013). A review of Australia's natural gas resources and their exploitation. *Journal of Natural Gas Science andEngineering* 10 , 66-88, 2013

Leyffer, S., 2003. Mathematical programs with complementarity constraints. SIAG/OPT Views-and-News 14 (1), 15–18 April.

Leyffer, S., Lopez-Calva, G., Nocedal, J., 2006. Interior methods for mathematical programs with complementarity constraints. SIAM Journal on Optimization 17 (1).

Leyffer, S., Lo´pez-Calva, G. & Nocedal, J. 2007 Interior methods for mathematical programs with complementarity constraints. SIAM J. Optim. 17, 52–77. (doi:10.1137/040621065)

Lise W. and Hobbs, B.F. , 2009, "A Dynamic Simulation of Market Power in the Liberalised European Natural Gas Market," Energy Journal (30).119 – 136.

Liu, X., Perakis, G., and Sun, J. (2005). A robust SQP method for mathematical programs with linear complementarity constraints. Computational Optimization and Applications, 34(1):5–33.

Lochner, S. (2011)"Modeling the European natural gas market during the 2009 Russian Ukrainian gasconflict: Ex-post simulation and analysis, " *Journal of Natural Gas Science and Engineering*, 3(1), 341-348.

Luo, Z. Pang, J.S., Ralph,D. (1996) Mathematical programs with equilibrium constraints. Cambridge University Press, Cambridge, U.K

OIES, 2011, the pricing debate over Russian gas exports to china.

OIES, 2012, Will there be a shale gas revolution in China by 2020?

Petroleum Economist, 2011, LNG shipping economics on the rebound, 2011,

Ostvoorn F.V., 2003, "Long-term gas supply security in an enlarged Europe",Final Report ENGAGED Project ECN, Petten (2003)

Outrata, J.,Kocvara, M., and Zowe, J.(1998).Nonsmooth approach to optimization problem with equilibrium constraints. Kluwer Academic Publisher.

Olson, R. (2012).How to Boost U.S. Exports: Legalize Them. The Foundry. Available from:http://blog.heritage.org/2012/09/26/how-to-boost-u-s-exports legalize-them/

Panama Canal Authority, 2010. "OP NOTICE TO SHIPPING No. N-1-2010, Rev. 1" http://www.pancanal.com/eng/maritime/notices/2010/N01-2010-r1.pdf

Petroleum Economist, 2011, "LNG Shipping Economics on the Rebound ", Mar 2011.

Pirani,S., Stern,J.,Yafimava,K.(2009). The Russo-Ukrainian gas dispute of January 2009: A comprehensive assessment. Oxford Institute for Energy Study. (Accessed 15 October 2012). Available from: http://www.globalcitizen.net/data/topic/knowledge/uploads/2011063022313033.pdf

Polito, J., McCarl , A.B. , Molin, T.L. (1980). Solution of Spatial Equilibrium

Popils, J., 2011, "Panama Canal Expansion's Impact on LNG Shipping and Trade," 2011.

PortWorld.com

Problem with Benders Decomposition, *Management Science* Vol.26 No.6 (June, 1980).

Rabiee A. and Parniani M. Voltage security constraints multi-period optimal reactive power flow using Benders and optimality condition decomposition. IEEE Transactions on Power Systems, 28(2):696-708 May 2013.

Raghunathan, A. and Biegler, L. T. (2005). An interior point method for mathematical programs with complementarity constraints (MPCCs). SIAM Journal on Optimization, 15(3):720 750.

Ralph, D., Wright, S.J., 2004. Some properties of regularization and penalization schemes for MPECs. Optimizations Methods and Software 19 (5), 527–556.

Ratner, M.(2011). U.S. natural gas exports: New opportunities, uncertain outcomes. Congressional Research Service (2011). R42074. Available from http://www.arcticgas.gov/sites/default/files/articles/772/11-11-4-crs-us-lng exports.pdf

Ratner, M., Belkin, P.,Nichol, J., Woehrel, S.(2012).Europe's energy security: Options and challenges to Natural gas supply diversification. Congressional Research Service .R42405.Available from: http://www.fas.org/sgp/crs/row/R42405.pdf

Reuters, 2013. "U.S. gas via Panama frightens LNG exporters worldwide" September, 2013.http://www.reuters.com/article/2013/09/05/energy-lng world idUSL6N0GV37820130905

Rice, 2005. http://www.rice.edu/energy/publications/docs/GAS_BIWGTM_March 2005. pdf.

Rouhani, R., L. Lasdon, W. Lebow, and A.D. Waren, "A Generalized Benders Decomposition Approach to Reactive Source Planning in Power Systems", Mathematical Programming Study, 25,62-75 (1985).

SINTEF, 2012, LinkS – Linking global and regional energy Strategies. Available from http://www.sintef.no/home/SINTEF-Energy-Research/Project work/LinkS--Linking global-and-regional-energy-Strategies/

Scott, M. (2013). Europe struggle in Shale Gas Race. New York Times , April 2013 http://www.nytimes.com/2013/04/25/business/energy-environment/europe faces challenges-in-effort-to-embrace-shale-gas.html

Scholtes, S., 2001. Convergence properties of regularization schemes for mathematical programs with complementarity constraints. SIAM Journal on Optimization 11 (4), 918–936.

Siddiqui S., 2011, Solving Two-Level Optimization Problems with Applications to Robust Design and Energy Markets. PhD.Dissertation University of Maryland.

Siddiqui, S., Gabriel, S.A. (2012). "An SOS1-Based Approach for Solving MPECs with a Natural Gas Market Application," *Networks and Spatial Economics*, DOI: 10.1007/s11067-012 9178-y.

Sifuentes W.S. and Vargas A. Hydrothermal scheduling using Benders decomposition: Accelerating techniques. IEEE Transactions on Power Systems, 22(3):1351 1359,Aug.20087.

South Stream, 2012, Gas Pipeline. Accessed October 2012. Available from http://www.south- stream.info/en/pipeline/

Steffensen S, Ulbrich M (2010) A new relaxation scheme for mathematical programs with equilibrium constraints. SIAM J Optim 20(5):2504‑2539

The Economist, 2012, A liquid market Thanks to LNG, spare gas can now be sold the world over. Available from: http://www.economist.com/node/21558456

The EU climate and policy package,2012 . Available from: http://ec.europa.eu/clima/policies/package/index_en.htm

The Washington Post, 2012, Boosting the economy through natural gas exports. Available online at: http://www.washingtonpost.com/opinions/natural gas-exports-offer-much-to the- economy/2012/03/13/gIQA4WibCS us _story.html

U-tapao C., Gabriel, S.A., Christopher , P.,Ramirez.(2014) A Stochastic MPEC for Sustainable Wastewater Management ,forthcoming .

Uderzo, A. (2010). Exact penalty functions and calmness for mathematical programming under nonlinear perturbations. Nonlinear Analysis , 73, 1596 1609.

Wen, U., & Huang, A. (1996). A Simple Tabu Search Method to Solve the Mixed Integer Linear Bilevel Programming Problem. European Journal of Operational Research , 88, 563-571.

WEO, 2011. "World Energy Outlook" International Energy Agency.

WEO, 2013, World Energy Outlook 2013.www.freeportlng.com

Wood, D. A. (2012). A review and outlook for global LNG trade. *Journal of Natural gas science and Engineering* 9 (2012) 16-27.

Zhaofang, D.(2010). China's gas market outlook, Research institute of Economics and Technology CNPC,Beijing. Available from: http://eneken.ieej.or.jp/data/3561.pdf